

THE UNIVERSITY OF HULL

**A study of the regulation of oestrogen receptor alpha by tissue
factor in breast cancer cells**

being a Thesis submitted for the Degree of Doctor of Philosophy
in the University of Hull

by

Mary Elizabeth Wendy Collier, BSc

February 2008

Abstract

Increased expression of tissue factor (TF) has been associated with invasive forms of breast cancer. In contrast, the expression of oestrogen receptor alpha (ER α) in breast cancer cells is associated with well differentiated breast tumours, with a low invasive potential. The aim of this study was to examine the influence of exogenous TF on the expression of ER α in breast cancer cells, as well as alterations in cell proliferation and invasiveness, and to explore the underlying mechanisms. Incubation of the MCF-7 and T47D breast cancer cell lines with exogenous TF resulted in decreases in the expression of ER α mRNA and protein by a mechanism requiring the interaction of TF with β 1 integrin leading to the activation of the ERK1/2 pathway, but was independent of PAR1 and PAR2 activation. Furthermore, exogenous TF suppressed oestradiol-mediated cell proliferation through a pathway partly mediated through PAR2 activation, and also reversed the inhibitory influence of oestradiol on cell invasion. Exogenous TF also decreased the transcriptional activity of ER α via the classical ERE pathway through a mechanism that involved decreases in the DNA binding activity of ER α to ERE sequences, although the phosphorylation state of serine 118 within ER α was unaffected. Moreover, while TF alone was capable of downregulating the transcriptional activity of AP-1, oestradiol did not affect the transcriptional activity of AP-1. Exogenous TF was shown to bind to the surface of MCF-7 cells by direct interaction with cell surface β 1 integrin which could be disrupted with polyclonal antibodies against TF or β 1 integrin. Furthermore, using computer-aided analysis, a putative binding site for TF within the EGF-4 domain of β 1 integrin was identified which had structural resemblance to the EGF-1 domain of FXa responsible for binding to TF. These data suggest that exogenous TF released from stromal cells interacts with breast cancer cells resulting in the downregulation of ER α which in turn leads to the loss of oestradiol-controlled proliferation and contributes to the progression of breast cancers to an invasive phenotype.

Publications

Abstracts

Collier MEW, Ettelaie C. (2004) Tissue factor modulates the oestrogen response in MCF-7 cells (poster). *Genes & Cancer 2004, 21st meeting*. University of Warwick, UK.

Collier MEW, Li C, Frentzou GA, Ettelaie C. (2007) The influence of tissue factor on oestrogen receptor alpha expression and cell invasion in breast cancer cells (poster). *International Society on Thrombosis and Haemostasis, XXIst congress*. Geneva, Switzerland.

Collier MEW, Ettelaie C. (2007) Alterations in oestradiol-mediated oestrogen receptor alpha activity in breast cancer cells in response to exogenous tissue factor (poster). *Thrombosis and Haemostasis Issues in Cancer, 4th international conference*. Bergamo, Italy.

Presentations

Collier MEW, Ettelaie C. (2007) Alterations in oestradiol-mediated oestrogen receptor alpha activity in breast cancer cells in response to exogenous tissue factor. *Thrombosis and Haemostasis Issues in Cancer, 4th international conference*. Bergamo, Italy.

Papers

Collier MEW, Li C, Ettelaie C. Influence of exogenous tissue factor on oestrogen receptor-alpha expression in breast cancer cells: Involvement of β 1-integrin, PAR2 and MAPK activation. Submitted to *Mol. Cancer Biol.*

Acknowledgments

I would like to thank my supervisor and good friend Dr Camille Ettelaie for her guidance and support throughout this project. I also acknowledge the support of Dr A-M Seymour during this project. I would like to thank my friends Alkistis Frentzou and Chao Li for their help over the last four years. Thanks also to Shenghui Su and Ann Lowry for their help during this project. Finally, I would like to thank my parents and grandparents for their support and encouragement.

To my parents

Table of contents

Abstract	1
Publications	2
Acknowledgments	3
Table of contents	5
List of figures	13
List of tables	17
Abbreviations	18
CHAPTER 1	21
1. General Introduction	22
1.1. Breast cancer	22
1.2. Oestrogen and the oestrogen receptor	24
1.2.1. Oestrogens	24
1.2.2. Oestrogen receptors	25
1.2.3. ER α signalling mechanisms	28
1.3. The role of oestrogen-ER cell signalling in breast cancer	30
1.4. Tissue factor	32
1.4.1. TF structure and biochemistry	32
1.4.2. The role of TF in haemostasis	34
1.4.3. Factor VII	37
1.4.4. Factor X	37
1.5. Non-haemostatic and signalling properties of TF:FVIIa	38
1.5.1. The function of TF as a cell signalling receptor	38
1.5.2. TF signalling through protease activated receptors (PARs)	39
1.5.3. TF signalling through the cytoplasmic domain of TF	41
1.5.4. TF signalling through integrins	41
1.6. Microparticles in cancer	43
1.7. Tissue factor and breast cancer	44
1.8. Aims of the investigation	46

CHAPTER 2	47
2. Materials and Methods	48
2.1. Materials	48
2.2. Methods	53
2.2.1. Culture of breast cancer cell lines	53
2.2.2. Subculture and determination of the number of cells	53
2.2.3. Harvesting of cells for experimental analysis	54
2.2.4. Cryopreservation of cells	54
2.2.5. Adaptation of cells to phenol red-free and low serum medium	54
2.3. Measurement of cell proliferation using the MTS-based colorimetric assay	55
2.4. Flow cytometric determination of cell surface TF antigen and DNA-transfection efficiency	57
2.5. Molecular Biology Techniques	57
2.5.1. Isolation of total RNA from cells	57
2.5.2. Determination of RNA purity and concentration	58
2.5.3. Reverse transcriptase-polymerase chain reaction (RT-PCR)	58
2.5.4. Analysis of DNA by agarose gel electrophoresis	59
2.5.5. Testing of RNA samples for genomic DNA contamination	61
2.6. Estimation of protein concentration using the Bradford assay	62
2.7. SDS-polyacrylamide gel electrophoresis (SDS-PAGE)	62
2.8. Western blot analysis	64
2.9. Measurement of TF activity by the one-stage prothrombin time assay	65
2.10. Bacterial cell culture and plasmid isolation	67
2.10.1. Preparation of LB broth and propagation of <i>Escherichia coli</i> TB-1	67
2.10.2. Isolation of plasmid DNA	67
2.10.3. Determining plasmid DNA purity and concentration	68
2.10.4. Ethanol precipitation of DNA	68
2.10.5. Preparation and transformation of competent bacterial cells	68
2.10.6. Selection of transformed bacteria	69
2.11. Transfection of mammalian cells with plasmid DNA using the Lipofectin reagent	70
2.12. Luciferase assay	70

2.13. Statistical analysis	71
CHAPTER 3	72
3.1. Introduction	73
3.1.1. The role of ER α expression in breast cancer cell proliferation and invasion	73
3.1.2. The association between TF expression and breast cancer invasiveness	74
3.1.3. Aims	75
3.2. Methods	76
3.2.1. Analysis of endogenous TF expression in breast cancer cells	76
3.2.1.1. Analysis of cell surface TF expression by flow cytometry	76
3.2.1.2. Determination of TF activity on cells using the PT assay	76
3.2.2. The influence of TF and oestradiol on cell proliferation	76
3.2.2.1. Examination of the influence of TF and oestradiol on cell proliferation	76
3.2.2.2. Purification of lipids by delipidation of recombinant TF	77
3.2.2.3. The influence of lipids extracted from recombinant TF on cell proliferation	77
3.2.3. Examination of the influence of TF on ER α mRNA expression in breast cancer cells	78
3.2.3.1. Design and optimisation of primers for RT-PCR analysis of ER α and ER β	78
3.2.3.2. Analysis of baseline ER α and ER β mRNA expression using RT-PCR	78
3.2.3.3. Analysis of the influence of TF on ER α mRNA expression using RT-PCR	80
3.2.4. Examination of the influence of TF on ER α protein expression in breast cancer cells	80
3.2.4.1. Analysis of the influence of TF on ER α protein expression by western blot	80

3.2.4.2. Analysis of the influence of TF on ER α protein expression by ELISA	81
3.2.5. Analysis of the long-term influence of TF on ER α mRNA and protein expression	82
3.2.6. Examination of the influence of TF on breast cancer cell invasion	82
3.2.6.1. Influence of TF on cell migration using a Boyden chamber based assay	82
3.2.6.2. Examination of changes in cell morphology in response to exogenous TF	83
3.2.6.3. Influence of TF on cell invasion using collagen type I gels	85
3.3. Results	85
3.3.1. Determination of cell surface TF expression in breast cancer cell lines	85
3.3.2. Analysis of cell proliferation in response to TF and oestradiol	87
3.3.3. Analysis of cell proliferation in response to the lipids extracted from recombinant TF	93
3.3.4. Optimisation of the RT-PCR conditions using the ER α and ER β primers	93
3.3.5. Analysis of baseline expression of ER α and ER β mRNA in breast cancer cells	99
3.3.6. Investigation of the influence of TF on ER α expression in breast cancer cell lines	99
3.3.6.1. Investigation of the influence of TF on the expression of ER α mRNA	99
3.3.6.2. Investigation of the influence of TF on ER α protein expression	103
3.3.6.3. Investigation of the long-term influence of TF on ER α expression	103
3.3.7. Influence of TF on cell migration using a Boyden chamber based assay	110
3.3.8. Examination of changes in cell morphology in response to exogenous TF	110
3.3.9. Influence of TF on cell invasion using collagen type I gels	114
3.4. Discussion	114

CHAPTER 4	123
4.1. Introduction	124
4.1.1. The involvement of ER α activation in breast cancer	124
4.1.2. The classical pathway of the transcriptional activation of ER α	124
4.1.3. Phosphorylation of ER α	126
4.1.4. Aims	128
4.2. Methods	129
4.2.1. Examination of the influence of TF on ER α serine 118 phosphorylation by western blot	129
4.2.2. Examination of the influence of TF on the DNA binding activity of ER α	130
4.2.2.1. Preparation of nuclear extracts	131
4.2.2.2. TransAM ER	131
4.2.3. Examination of the influence of TF on the transcriptional activity of ER α	132
4.2.3.1. Design of the ERE insert	132
4.2.3.2. Preparation of the ERE insert	132
4.2.3.3. Restriction digestion of the pGL3 plasmid	134
4.2.3.4. Removal of 5' phosphates from pGL3 using CIAP	135
4.2.3.5. Ligation of the ERE insert into pGL3	135
4.2.3.6. Determination of transfection efficiency by flow cytometry	136
4.2.4. Examination of the influence of TF on transcriptional activity of ER α using the pGL3-ERE reporter vector	136
4.3. Results	137
4.3.1. Examination of the influence of TF on ER α serine 118 phosphorylation	137
4.3.2. Examination of the influence of TF on ER α DNA binding activity	142
4.3.3. Preparation of an ERE reporter vector	142
4.3.3.1. Optimisation of <i>Mlu</i> I restriction digest of pGL3	142
4.3.3.2. Cloning ERE insert into pGL3	145
4.3.3.3. Optimisation of transfections	145

4.3.4. Examination of the influence of TF on ER α transcriptional activity using the ERE reporter vector	148
4.4. Discussion	153
CHAPTER 5	159
5.1. Introduction	160
5.1.1. AP-1-dependent pathway of ER α transcription	160
5.1.2. Structure and function of activator protein-1	160
5.1.3. Aims	162
5.2. Methods	163
5.2.1. Examination of the influence of exogenous TF on AP-1 activity	163
5.2.1.1. Analysis of AP-1 transcriptional activity by pAP-1-Luc reporter vector transfections	163
5.2.1.2. Analysis of AP-1 DNA binding activity using the TransAM AP-1 kit	164
5.2.3. Cloning of full length ER α	164
5.2.3.1. Design of primers for PCR amplification of full length ER α	166
5.2.3.2. First strand cDNA synthesis using SuperScript II reverse transcriptase	167
5.2.3.3. PCR amplification of ER α cDNA	167
5.2.3.4. Purification of ER α DNA from agarose gels	168
5.2.3.5. Restriction digestion of pEGFP-C3 and the ER α insert	169
5.2.3.6. Ligation of the ER α insert into the pEGFP-C3 plasmid	170
5.3. Results	171
5.3.1. Analysis of the influence of TF and oestradiol on the transcriptional activity of AP-1 using the pAP-1-Luc reporter vector	171
5.3.2. Examination of the influence of TF on the DNA binding activity of AP-1	175
5.3.3. ER α cloning	180
5.3.3.1. PCR amplification of ER α	180
5.3.3.2. Optimisation of <i>Bam</i> H I and <i>Eco</i> R I restriction digest of pEGFP- C3	180
5.3.3.3. Ligation of ER α into pEGFP-C3	184

5.4. Discussion	184
CHAPTER 6	189
6.1. Introduction	190
6.1.1. TF-mediated cell signalling through protease activated receptors	190
6.1.2. The interaction of TF with FVIIa and FXa	191
6.1.3. TF signalling through integrins	191
6.1.4. Aims	193
6.2. Methods	195
6.2.1. Examination of the mechanisms of TF-mediated signalling	195
6.2.1.1. Examination of the expression of PARs in breast cancer cells by RT-PCR	195
6.2.1.2. Examination of the involvement of PARs in TF mediated breast cancer cell proliferation	195
6.2.1.3. Examination of the involvement of PARs, FVIIa, FXa, β 1 integrin and MAPK in the downregulation of ER α expression by exogenous TF	196
6.2.2. Investigation of the interaction of exogenous TF with breast cancer cells	197
6.2.2.1. Preparation of fluorescein-labelled TF	197
6.2.2.2. Examination of the interaction of fluorescein-labelled TF with the cell surface by fluorescence microscopy	197
6.2.3. Identification of receptors involved in the interaction of exogenous TF with the cell surface	198
6.2.3.1. Analysis of β 1 and β 3 integrin expression on the surface of breast cancer cells by fluorescence microscopy	198
6.2.3.2. Co-localisation of TF with β 1 integrin by fluorescence microscopy	198
6.2.3.3. Examination of TF binding to β 1 integrin by co-precipitation	199
6.2.3.4. Visualisation and modification of protein domain structures	200
6.3. Results	200
6.3.1. Examination of the role of PARs and coagulation factors in TF mediated signalling in breast cancer cells	200

6.3.1.1. Examination of the involvement of PARs in TF mediated breast cancer cell proliferation	200
6.3.1.2. Examination of the influence of FVIIa and FXa on ER α expression	201
6.3.1.3. Examination of the involvement of PAR1 and PAR2 in ER α expression	206
6.3.2. Examination of the binding of exogenous TF to the surface of breast cancer cells	206
6.3.2.1. Analysis of fluorescein-labelled TF	206
6.3.2.2. Analysis of fluorescein-labelled TF binding to cell surface by fluorescence microscopy	210
6.3.3. Identification of the receptors involved in the interaction of TF with the cell surface	213
6.3.3.1. Co-localisation of TF with β 1 integrin with TF by fluorescence microscopy	213
6.3.3.2. Analysis of TF binding to β 1 integrin by co-precipitation	217
6.3.3.3. Examination of the involvement of β 1 integrin and the MAPK pathway in TF mediated ER α expression	217
6.3.3.4. Examination of the molecular structure of TF and integrins using Raswin and Alchemy programs	220
6.4. Discussion	224
CHAPTER 7	230
7. General discussion	231
References	240

List of Figures

1.1. Diagram of the mammary gland and structure of 17 β -oestradiol	23
1.2. Arrangement of the structural domains of ER α and ER β	26
1.3. Oestrogen-mediated ER α signalling pathways	29
1.4. Schematic representation of the domains of tissue factor	33
1.5. Coagulation cascade pathways	36
1.6. TF signalling mechanisms	40
2.1. Standard curve for the proliferation assay	56
2.2. Standard curve for Bradford assay	63
2.3. One-step prothrombin time assay standard curve	66
3.1. Schematic representing the set up of the Boyden chamber based migration assay	84
3.2. Analysis of cell surface TF in breast cancer cell lines by flow cytometry	86
3.3. The influence of TF on the rate of MCF-7 proliferation in complete medium	89
3.4. The influence of TF on the rate of MCF-7 proliferation in phenol red-free medium at 24 h	90
3.5. The influence of TF on the rate of MCF-7 proliferation in phenol red-free medium at 48 h	91
3.6. The influence of TF on the rate of MCF-7 proliferation in phenol red-free medium at 72 h	92
3.7. The influence of TF on the rate of T47D proliferation in phenol red-free medium at 24 h	94
3.8. The influence of TF on the rate of T47D proliferation in phenol red-free medium at 48 h	95
3.9. The influence of TF on the rate of T47D proliferation in phenol red-free medium at 72 h	96
3.10. The influence of lipids extracted from TF on MCF-7 proliferation	97
3.11. Optimisation of the ER α primers for RT-PCR	98
3.12. Baseline ER α expression levels in breast cancer cell lines	100

3.13. Short-term influence of TF on ER α mRNA expression in MCF-7 cells	101
3.14. The influence of TF on ER α mRNA expression in MCF-7 and T47D cells	102
3.15. Short-term influence of TF on ER α protein expression in MCF-7 cells	104
3.16. The influence of TF on ER α protein expression as examined by western blot	105
3.17. Standard curve for the ER α ELISA	106
3.18. The influence of TF on ER α protein expression as examined by ELISA	107
3.19. Long-term influence of TF on ER α mRNA expression in MCF-7 cells	108
3.20. Long-term influence of TF on ER α protein expression in MCF-7 cells	109
3.21. MCF-7 cell migration in response to TF in the presence and absence of oestradiol	111
3.22. T47D cell migration in response to TF in the presence and absence of oestradiol	112
3.23. Changes in cell morphology in response to exogenous TF	113
3.24. Collagen gel invasion assays	115
4.1. Phosphorylation sites in ER α	127
4.2. pGL3-promoter vector	133
4.3. The influence of TF on ER α phosphorylation in MCF-7 cells	138
4.4. ER α serine 118 phosphorylation in MCF-7 cells	139
4.5 The influence of TF on ER α phosphorylation in T47D cells	140
4.6. ER α serine 118 phosphorylation in T47D cells	141
4.7. The influence of TF on ER α DNA binding activity in MCF-7 cells	143
4.8. The influence of TF on ER α DNA binding activity in T47D cells	144
4.9. Optimisation of <i>Mlu</i> I restriction digest of pGL3	146
4.10. Optimisation of cell numbers for transfection	147
4.11. Transfection efficiency	149
4.12. Optimisation of time point for ERE transfections	150

4.13. pGL3-ERE reporter vector function in response to oestradiol	151
4.14. The influence of TF on ER α transcriptional activity in MCF-7 cells	152
4.15. The influence of TF on ER α transcriptional activity in T47D cells	154
5.1. Schematic representation of the interactions and functions of AP-1 protein subunits	161
5.2. pEGFP-C3 cloning vector	165
5.3. Optimisation of pAP-1-Luc transfections	172
5.4. The influence of TF on the transcriptional activity of AP-1 in MCF-7 cells	173
5.5. The influence of TF on the transcriptional activity of AP-1 in T47D cells	174
5.6. The influence of TF and oestradiol on AP-1 transcriptional activity	176
5.7. The influence of TF on the DNA binding activity of c-Jun	177
5.8. The influence of TF on the DNA binding activity of c-Fos	178
5.9. The influence of TF on the DNA binding activity of Fra-1	179
5.10. The influence of oestradiol on the DNA binding activity of AP-1 subunits	181
5.11. PCR amplification of ER α using BioTaq DNA polymerase	182
5.12. ER α purified from PCR reaction	183
5.13. Optimisation of pEGFP-C3 restriction digest by <i>Bam</i> H I and <i>Eco</i> R I	185
5.14. Schematic representation of proposed mechanism for TF regulation of ER α -AP-1 transcriptional activation	187
6.1. Structure of the TF:FVIIa:FXa complex	192
6.2. Schematic representation of the structure of β 1 integrin	194
6.3. PAR1 and PAR2 mRNA expression in breast cancer cell lines	202
6.4. The involvement of PAR1 and PAR2 in breast cancer cell proliferation	203
6.5. Examination of the influence of FVIIa and FXa on ER α mRNA expression	204
6.6. Examination of the influence of FVIIa and FXa on ER α protein expression	205
6.7. Examination of the involvement of PARs in ER α mRNA expression	207

6.8. Examination of the involvement of PARs in ER α protein expression	208
6.9. Western blot analysis of fluorescein-labelled TF	209
6.10. Interaction of fluorescein-labelled TF with MCF-7 cells	211
6.11. Optimisation of anti-TF polyclonal antibody concentration to inhibit TF procoagulant activity	212
6.12. Cell surface expression of β 1 and β 3 integrins in breast cancer cells	214
6.13. Co-localisation of exogenous TF with β 1 integrin in MCF-7 cells	215
6.14. Examination of the binding of exogenous TF in the presence of an anti- β 1 integrin antibody	216
6.15. Co-precipitation of TF and β 1 integrin	218
6.16. The role of β 1 integrin and the MAPK pathway in TF-mediated downregulation of ER α expression	219
6.17. Arrangement of the extracellular domain of TF with the C-terminus of β 3 integrin	221
6.18. Comparison of the structures of β 1 integrin EGF-4 and FXa EGF-1	223
7.1. Schematic representation of a proposed mechanism for the control of ER α expression by exogenous TF	234

List of Tables

2.1. RT-PCR program	60
3.1. Primer sequences and conditions for RT-PCR	79
3.2. Procoagulant activity of breast cancer cell lines	88
4.1. Genes controlled by oestrogen and containing ERE regulatory sequences within the promoter DNA regions	125

Abbreviations

°C	Degrees centigrade
μ	Micro
%	Percentage
A	Adenine
A ₂₆₀	Absorption at 260 nm
AF-1	Activation function-1
AP-1	Activator protein-1
ATP	Adenosine triphosphate
bFGF	Basic fibroblast growth factor
bp	Base pair
BSA	Bovine serum albumin
c	Centi
C	Cytosine
CaCl ₂	Calcium chloride
Cdk	Cyclin dependent kinase
cDNA	Complementary deoxyribonucleic acid
CIAP	Calf intestinal alkaline phosphatase
CMV	Cytomegalovirus
CO ₂	Carbon dioxide
dH ₂ O	Distilled water
DMEM	Dulbeco's modified essential medium
DMSO	Dimethyl sulphoxide
DNA	Deoxyribonucleic acid
DNase	Deoxyribonuclease
dNTP	Deoxyribonucleotide triphosphate
DTT	Dithiothreitol
E2	17 β-oestradiol
<i>E. coli</i>	<i>Escherichia coli</i>
EDTA	Ethylenediaminetetraacetic acid
EGF	Epidermal growth factor
EGFP	Enhanced green fluorescent protein
ELISA	Enzyme-linked immunosorbent assay

ER α	Oestrogen receptor alpha
ER β	Oestrogen receptor beta
ERE	Oestrogen response element
ERK1/2	Extracellular signal-regulated kinase 1/2
FCS	Foetal calf serum
FITC	Fluorescein isothiocyanate
Fra	Fos-related antigen
FVII	Factor VII
FVIIa	Activated factor VII
FX	Factor X
FXa	Activated factor FX
g	Gram
g	Gravity
G	Guanine
GAPDH	Glyceraldehyde-3-phosphate dehydrogenase
h	Hour
HRP	Horseradish peroxidase
IgG	Immunoglobulin G
JNK	c-Jun N-Terminal Kinase
KCl	Potassium chloride
L	Litre
Log	Logarithm
M	Molar
m	Milli
mA	Milliamps
MAPK	Mitogen-activated protein kinase
MEM	Minimal essential medium
MgCl ₂	Magnesium chloride
MgSO ₄	Magnesium sulphate
min	Minute
MnCl ₂	Manganese chloride
mol	Mole
mRNA	Messenger ribonucleic acid

NaCl	Sodium chloride
NaOH	Sodium hydroxide
n	Nano
p	Pico
PAR	Protease activated receptor
PBS	Phosphate buffered saline
PE	Phycoerythrin
PI3K	Phosphatidylinositol 3-kinase
PT	Prothrombin time
RGD	Arginine-Glycine-Aspartate
RLU	Relative light unit
RNA	Ribonucleic acid
RNase	Ribonuclease
rpm	Revolutions per minute
RT-PCR	Reverse transcription-polymerase chain reaction
s	Second
SD	Standard deviation
SDS-PAGE	Sodium dodecyl sulphate polyacrylamide gel electrophoresis
T	Thymine
TBE	Tris borate-EDTA
TBST	Tris buffered saline tween 20
TEMED	N,N,N',N'-Tetramethylethylenediamine
TF	Tissue factor
TFPI	Tissue factor pathway inhibitor
TMB	3,3',5,5'-Tetramethylbenzidine
TPA	12- <i>O</i> -tetradecanoylphorbol-13-acetate
TRE	TPA response element
Tris	Tris(hydroxymethyl)aminomethane
U	Unit
UV	Ultra violet
V	Volt
v/v	Volume to volume
w/v	Weight to volume

CHAPTER 1

General Introduction

1. General Introduction

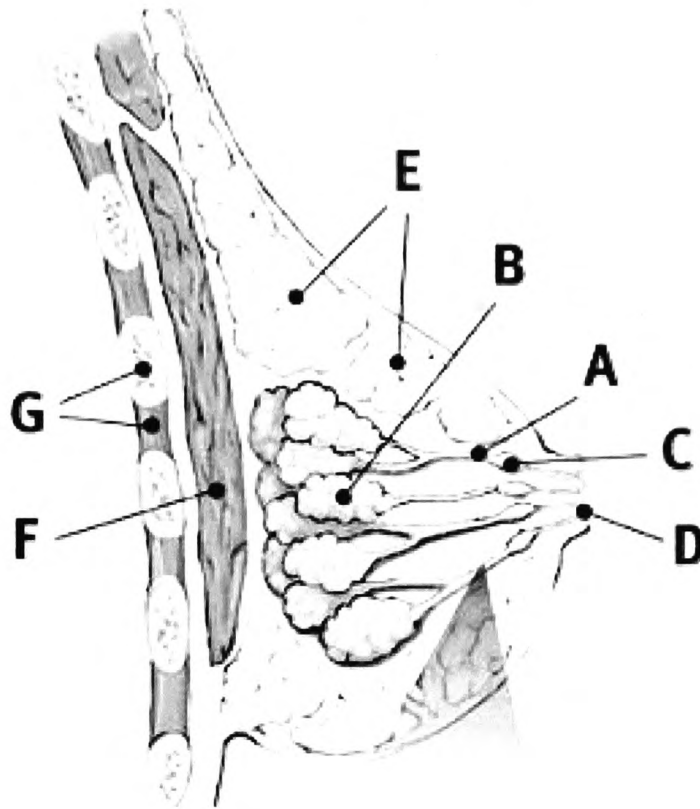
1.1. Breast cancer

Breast cancer is the most common form of malignancy in women in developed countries and accounts for 20% of female cancers in these countries (Cassidy et al 2004). A small percentage (approximately 5%) of breast cancers are hereditary, and attributed to inherited mutations in genes such as BRCA1 and BRCA2 (Futreal et al 1994). However, sporadic forms of breast cancer, which are due to a combination of random genetic alterations and environmental factors, constitute the majority of observed cases. The mammary gland consists of a branching network of ducts which end in lobules termed terminal duct lobuloalveolar units (Fig 1.1A). The lobules are composed of a layer of luminal epithelial cells surrounded by an outer layer of myoepithelial cells which are in contact with the basement membrane. The whole structure is surrounded by fibroblasts and supported by the extracellular matrix (stroma). Histological studies of breast tumours have revealed that about 90% of breast cancers arise from the luminal epithelial cells of the ducts (Santini et al 1996).

The transformation of normal breast epithelial cells into cancerous cells involves the loss of mechanisms that control normal cell proliferation and programmed cell death. This results in increased proliferation of cells which do not respond to normal regulatory signals, resulting in a mass of abnormal cells and the formation of a tumour (Macdonald et al 2004). These benign breast tumours may then develop into malignant tumours that are able to invade surrounding tissues and metastasise to secondary sites, such as the liver, lungs and bone marrow (Price 1990). Recently, a number of mutations in tumour suppressor genes and oncogenes that result in hereditary breast cancers have been identified. However, less is known about the molecular mechanisms that lead to

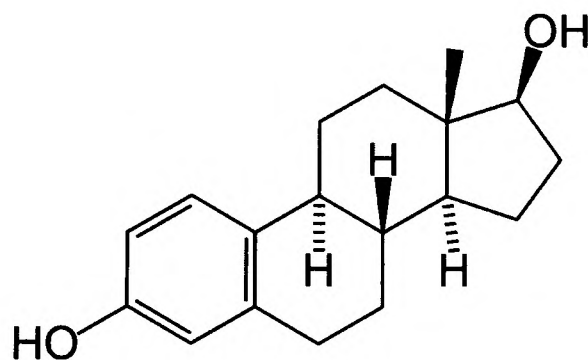
Figure 1.1. Diagram of the mammary gland and structure of 17 β -oestradiol

A.



The mammary gland consists of a branching network of ducts which end in terminal duct lobuloalveolar units. The whole structure is surrounded by an extracellular matrix (stroma) and adipose tissue. A = ducts, B= terminal duct lobuloalveolar units, C= duct, D=duct opening, E= adipose tissue, F= pectoralis major muscle, G= rib cage. Adapted from www.breastcancer.org.

B.



The four ring structure of 17 β -oestradiol. Adapted from Garrett & Grisham (2005).

sporadic breast cancer initiation (oncogenesis) and the transformation of benign to malignant breast cancers (tumorigenesis) (Macdonald et al 2004). A number of risk factors for the development of breast cancer have been identified, including early menarche, late menopause, nulliparity, obesity, and exposure to exogenous oestrogens (Cassidy et al 2004). Moreover, many of these risk factors involve the increased exposure of breast tissue to oestrogens.

1.2. Oestrogen and the oestrogen receptor

1.2.1. Oestrogens

Oestrogens are steroid hormones which have a four ring structure and are synthesised from cholesterol (Fig 1.1B). The three main forms of oestrogen are oestradiol, oestriol and oestrone of which 17 β -oestradiol (E2) is the most abundant and physiologically active form (Behl 2001). This group of steroid hormones controls reproductive processes such as normal mammary gland growth, differentiation and function, as well as the regulation of the menstrual cycle (Anderson et al 1998, Laidlaw et al 1995, Chabbert-Buffet et al 1998). Furthermore, oestrogens have functions in the cardiovascular system, nervous system and in the maintenance of the skeleton (Deroo & Korach 2006, Behl 2001).

The physiological concentration of 17 β -oestradiol in the blood plasma varies during the menstrual cycle and typically ranges between 50 and 1200 pM (Marshall 1995). In non-pregnant, premenopausal women, the main sites of oestrogen production are the ovaries whereas in post-menopausal women oestrogens are produced within the adipose tissue of the mammary gland. In both cases, oestradiol is synthesised from testosterone in a reaction catalysed by the enzyme aromatase. Oestrogens are secreted into the bloodstream and transported to target organs in complex with blood plasma proteins

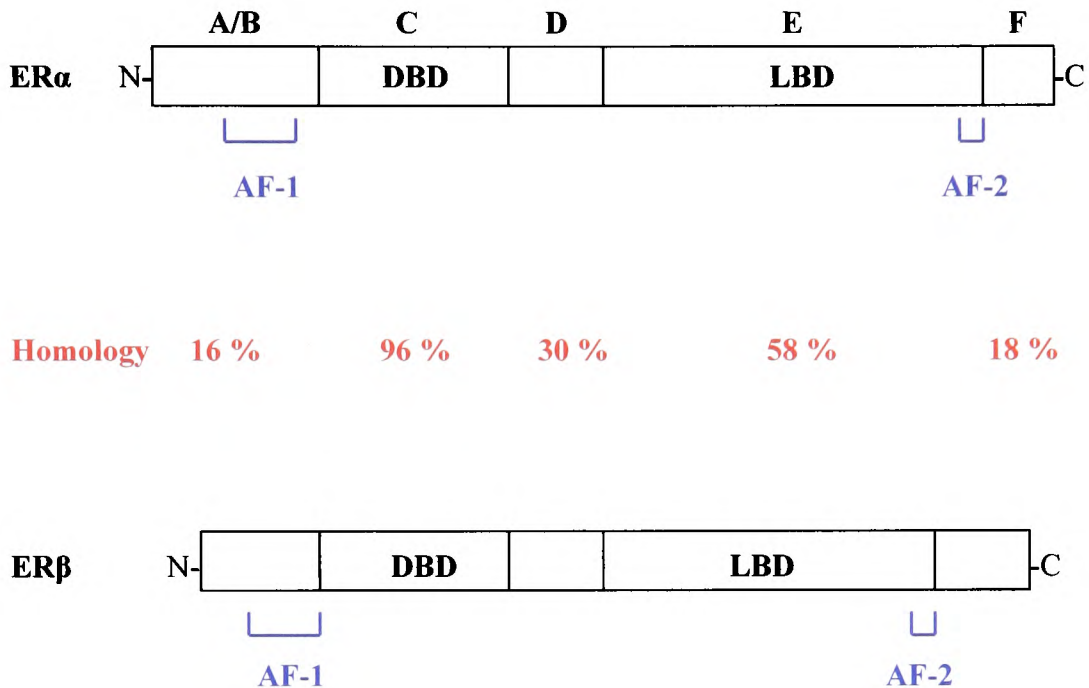
including sex hormone-binding globulin and albumin (Behl 2001), and released at target tissues. Since oestrogens are small, hydrophobic, lipid-soluble molecules, they are able to diffuse directly across the cell membrane and bind to their intracellular receptors, oestrogen receptors (ER), which are located in the cell nucleus.

1.2.2. Oestrogen receptors

Two forms of the oestrogen receptor have been identified and are encoded by separate genes. Oestrogen receptor alpha (ER α) was first cloned by Green et al in 1986. The ER α gene is located on chromosome 6 and encodes a 595 amino acid protein with a molecular mass of 66 kDa. Oestrogen receptor beta (ER β) was identified more recently (Mosselman et al 1996) as a 530 amino acid protein, the gene for which is located on chromosome 14.

Both ER α and ER β belong to the nuclear receptor family and share a large degree of structural homology. Both receptors are composed of six domains (A-F) (Fig 1.2) that have distinct functions. The N-terminus contains domains A and B and includes the N-terminal activation function-1 (AF-1), which modulates the transcriptional activity of ER α in a ligand-independent manner. The adjacent DNA binding domain (DBD) contains two zinc finger motifs which directly interact with specific DNA sequences known as oestrogen response elements (ERE) (Klein-Hitpass et al 1988). This domain is highly conserved between ER α and ER β and they share 96 % homology (Mosselman et al 1996) allowing both types of the receptor to bind to the same DNA response elements. Domain D forms the hinge region of the protein which allows dimerisation and nuclear localisation of the receptor. The ligand binding domain (LBD) of ER is composed of 11 alpha helices which form a pocket for its interaction with 17 β -oestradiol (Kong et al 2003). This domain also interacts with co-activator proteins and

Figure 1.2. Arrangement of the structural domains of ER α and ER β



ER α and ER β are composed of six conserved structural domains (A-F). The A/B domain contains the N-terminal activation function-1 (AF-1). Domain C consists of the DNA binding domain (DBD) and is highly conserved between the two forms of ER. The hinge region (D) allows dimerisation of the receptor. Domain E is the ligand binding domain (LBD) and contains the activation function-2 (AF-2). Percentages of homology observed between the six domains of ER α and ER β are shown in red. Adapted from Platet et al (2004).

contains activation function-2 (AF-2). AF-2 is activated following binding of 17 β -oestradiol to the LBD and regulates transcriptional activation of the receptor (Kong et al 2003). The LBD domain is closely conserved with 58 % homology between the two forms of ER (Mosselman et al 1996). Finally, the C-terminus contains domain F which interacts with co-activator proteins and regulates the transcriptional activity of ER in response to oestradiol (Koide et al 2007). The human ER α gene is composed of 8 exons (Ponglikitmongkol et al 1988) and alternative splicing of the precursor RNA produces variant forms of ER α that lack one or more exons and therefore lack some functional domains of the wild type ER α (Ferro et al 2003). For example, deletion of exon 3 results in an ER α variant that cannot bind to DNA, and deletion of exon 4 or 5 results in a form of ER α that has reduced ability to bind oestradiol since these exons encode parts of the DNA binding domain and ligand binding domains respectively (Leygue et al 2000). The expression of ER α splice variants has been detected both in normal and breast cancer cells and it has been suggested that ER α splice variants interfere with wild type ER α signalling in these cells (Leygue et al 2000).

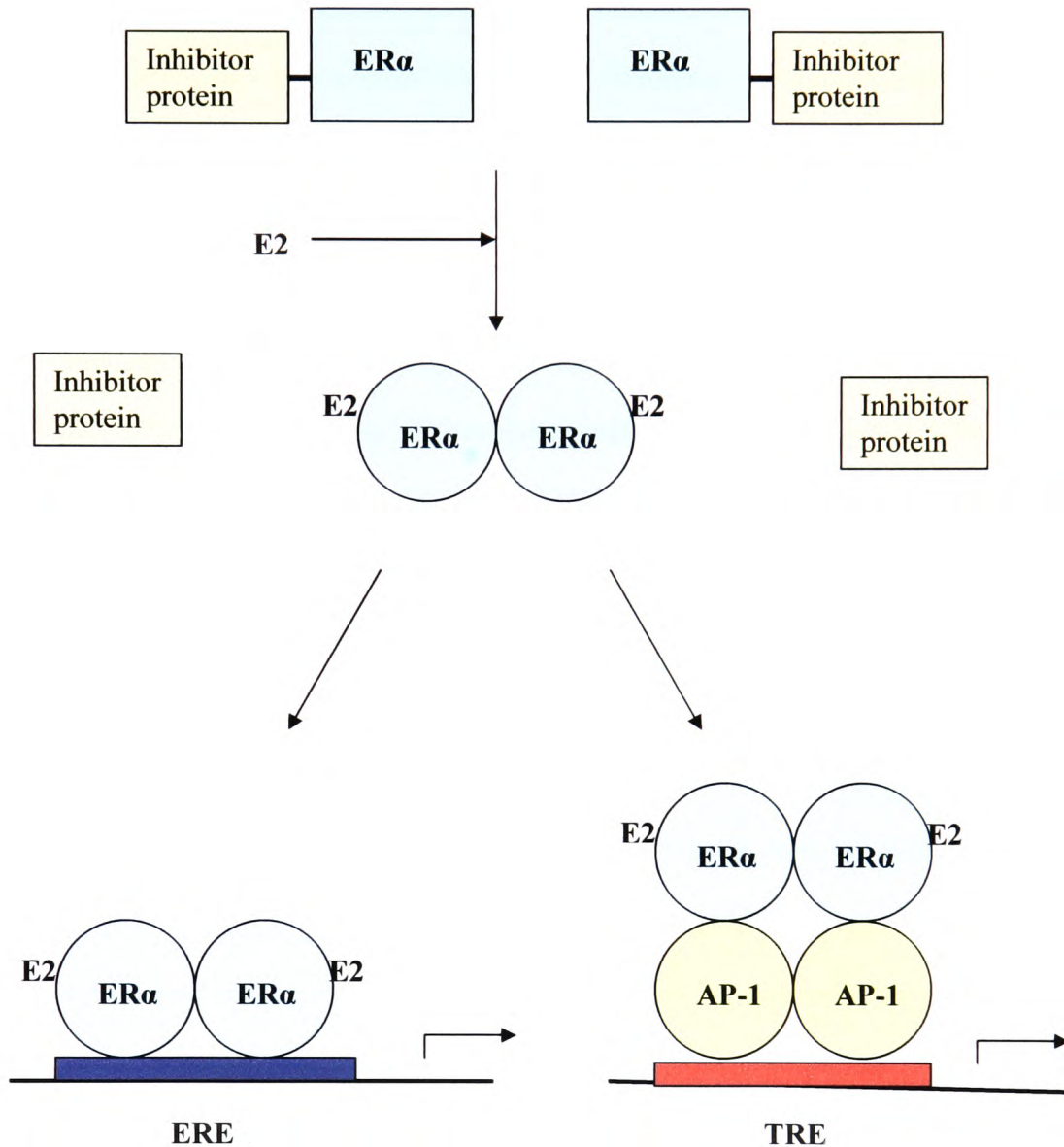
In addition to the structural variations, the two forms of ER have different expression patterns in the body. ER β is more generally expressed and more widely distributed throughout the body than ER α (Taylor & Al-Azzawi 2000, Balfe et al 2004). Moreover, the ratio of ER α to ER β expression varies between different tissues, with higher levels of ER α expressed in the mammary glands and uterus (Gustafsson 1999). In breast tissue, ER α is predominantly expressed in the luminal epithelial cells (Clarke et al 1997). Within cells, ER α is mainly located in the nucleus while a small proportion is found in the cytoplasm and also bound to the inner side of the cell membrane. Since ER is both a receptor and a transcription factor mainly located in the nucleus of cells, ER is

able to regulate gene expression rapidly in response to oestradiol, and induce long-term changes in gene expression.

1.2.3. ER α signalling mechanisms

ER α can modulate gene transcription through four different mechanisms. The classical pathway of ER α transcriptional activation involves the binding of oestrogen to the ligand binding domain of ER α . This results in a conformational change within the receptor, the release of inhibitory proteins, and dimerisation of ER α . The activated ER α dimers then bind to ERE DNA sequences located in the promoter regions of ER α -target genes, resulting in transcription (Fig 1.3). ER α may also regulate gene expression in an ERE-independent manner. In this mechanism, ER α directly binds to other transcription factors, such as activator protein-1 (AP-1) (Teyssier et al 2001) and Sp-1 (Porter et al 1997), which are associated with their own target DNA binding elements (Fig 1.3). In this way, ER α acts as a co-activator protein, increasing the transcriptional activity of the AP-1 or Sp-1 transcription factor complexes and altering the rate of gene transcription. In addition to the two oestradiol-mediated mechanisms, ER α may also be activated in the absence of its ligand through the activation of intracellular signalling pathways in response to extracellular stimuli. For example, it has been demonstrated that the activation of the mitogen-activated protein kinase (MAPK) pathway, in response to growth factors results in the phosphorylation of serine residues within the N-terminal A/B domain of ER α (Chen et al 2002, Kato et al 1995), which in turn increases the transcriptional activity of ER α (Kato et al 1995). Finally, a membrane-bound form of ER α has been identified which is capable of rapidly activating intracellular signalling pathways, such as the MAPK pathway, in response to the binding of oestradiol (Zhang et al 2002). This mechanism has been suggested to involve the interaction of ER α with G protein-coupled receptors at the cell membrane (Albanito et al 2007).

Figure 1.3. Oestrogen-mediated ER α signalling pathways



Oestradiol (E2) enters the nucleus and binds to inactive ER α (squares), resulting in a conformational change within the receptor, the release of inhibitory proteins, and subsequent activation and dimerisation of ER α (circles). In the classical pathway, ER α dimers bind to oestrogen response elements (ERE) upstream of ER α target genes, leading to the initiation of gene transcription. ER α can also act through the ERE-independent pathway by binding to transcription factors such as AP-1 through protein-protein interactions. This binding of ER α to AP-1 then enhances AP-1 mediated transcription through TPA response elements (TRE), which are located upstream of AP-1 target genes.

1.3. The role of oestrogen-ER cell signalling in breast cancer

In normal breast tissue oestrogens regulate the development of the mammary gland by inducing cell proliferation and differentiation (Anderson et al 1998, Laidlaw et al 1995). However, oestrogens also promote breast cancer and many of the risk factors for breast cancer involve increased exposure to oestrogens. It was first shown in the early 1900's that the removal of the ovaries prevents breast cancer and also leads to the regression of existing breast tumours (Beatson 1896). Approximately 70 % of breast tumours express ER α and the majority of breast tumours are derived from ER α positive luminal epithelial cells. Moreover, using ER knock-out mice it has been shown that ER α but not ER β is required for mammary gland development and tumourigenesis (Korach 1994, Krege et al 1998). Among the oestrogen-target genes identified, a number are involved in the regulation of the cell cycle (Prall et al 1998). An outcome of oestrogen-ER α signalling is therefore the increased rate of cell proliferation, as the cells are signalled to enter and progress through the cell cycle (Prall et al 1998). In the early stages of breast cancer, ER α is often overexpressed, leading to increased rates of proliferation in response to oestradiol (Clarke et al 1997). Oestrogen-ER α signalling is therefore thought to have a crucial role in breast cancer initiation by increasing the proliferation rate of the cells. The high rate of cell proliferation in turn increases the risk of spontaneous mutations, and provides an association between the increased rate of cell proliferation and the promotion of tumourigenesis in breast cancer cells.

While benign tumours are often enclosed in a capsule, unable to invade surrounding tissue, malignant tumours have attained the ability to invade the surrounding tissues and metastasise. The ability of cancer cells to migrate and invade surrounding tissues are therefore important events in the progression of breast tumours to malignant forms. Despite the ability of oestrogens to promote cell proliferation and breast cancer growth,

the presence of ER α in breast tumour cells is often associated with the more differentiated, low grade forms of breast tumours (Desombre 1984). These tumours are also less invasive and have a better prognosis for the patient (Godolphin et al 1981). However, ER α expression is often lost during breast cancer progression and one third of breast tumours lack ER α expression (Lapidus et al 1998). ER α negative breast tumours are often less differentiated, more aggressive and invasive, with a poorer prognosis (Desombre 1984). Furthermore, it has been demonstrated that the downregulation of ER α in breast tumours is associated with the progression of breast cancers to more invasive forms of the disease (Thompson et al 1992). In support of these findings, Rochefort et al (1998) demonstrated that ER α -positive breast cancer cell lines are less invasive compared to ER α -negative cell lines both *in vitro* and *in vivo*. In addition, overexpression of ER α in normally invasive, ER α -negative breast cancer cell lines results in reduced invasiveness of these cells (Platet et al 2000, Garcia et al 1992). Therefore, these studies suggest that although ER α -oestradiol cell signalling stimulates the growth of breast tumours, ER α has a protective role against breast tumour cell invasion by regulating cancer cell invasiveness. Furthermore, the presence of functional ER α is clinically important, since it indicates that the breast tumour will respond to treatment with anti-hormone therapies such as Tamoxifen that inhibit ER α activity (Platet et al 2004).

In conclusion, factors involved in regulating ER α expression and activity are crucial in the induction of mechanisms involved in breast cancer progression to invasive forms. Since mutations in ER α are rare (Lapidus et al 1998), the loss of ER α expression in breast tumours is thought to arise from external influences. One significant factor is increased inflammation at the site of breast tumours, which is associated with more invasive tumours with a poor prognosis (Blot et al 2003). An inflammatory protein that

is expressed in breast tumours and is associated with an invasive phenotype is the pro-inflammatory protein tissue factor (TF) (Ueno et al 2000, Vrana et al 1996).

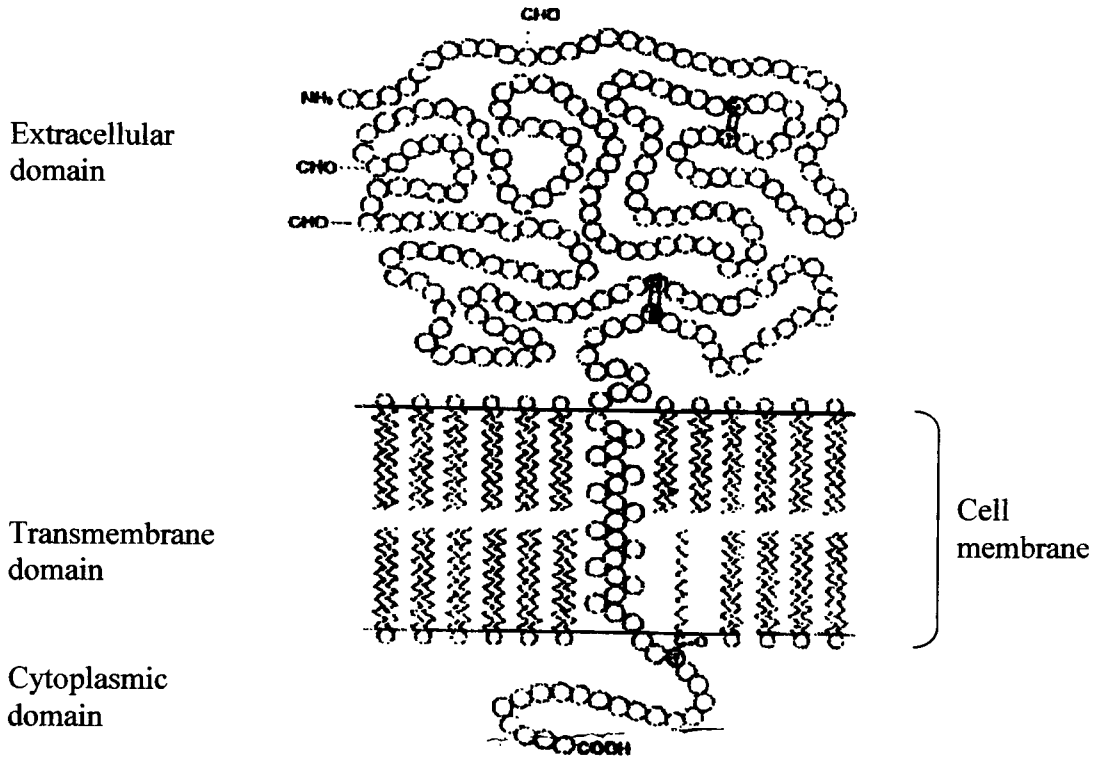
1.4. Tissue factor

1.4.1. TF structure and biochemistry

Tissue factor (TF), also known as CD142, is a 47 kDa transmembrane glycoprotein of 295 amino acids, which is processed after translation into a mature protein of 263 amino acids. TF is a type I integral membrane protein that consists of a large extracellular domain of 219 amino acids, a single hydrophobic membrane-spanning domain of 23 amino acids and a short cytoplasmic domain of 21 amino acids (Fig 1.4) (Morrissey et al 1987). Structurally, TF is similar to class II cytokine receptors such as the interferon- γ receptor (Bazan 1990). Crystallographic studies have shown that the extracellular domain of TF is composed of two fibronectin type III domains, joined at an angle of 120 degrees (Harlos et al 1994). The transmembrane domain of TF is essential for anchoring the molecule to the cell membrane and also for the procoagulant activity of TF. In contrast to cytokine receptors, TF has a small cytoplasmic domain. However, this domain contains three serine residues, two of which (serine 253 and 258) can be phosphorylated (Zioncheck et al 1992).

TF is an early immediate gene composed of 6 exons, located on chromosome 1 (Mackman et al 1989). TF is expressed by cells in response to inflammatory cytokines, growth factors and lipopolysaccharide (Flossel et al 1992, Mackman et al 1993). Following expression, the extracellular domain of TF is glycosylated by post-translational modification at three sites, but this glycosylation is not required for TF function (Paborsky et al 1989). In order to be procoagulantly active, TF requires the

Figure 1.4. Schematic representation of the domains of tissue factor



TF is an integral membrane glycoprotein that consists of 263 amino acids in its mature form. TF has three structural domains; a large extracellular domain of 219 amino acids which is glycosylated (CHO) at three sites and composed of two fibronectin type III domains, a single hydrophobic transmembrane domain that is composed of 23 amino acids and a short cytoplasmic domain of 21 amino acids. Adapted from Spicer et al (1987).

presence of negatively charged phospholipids on the outer side of the cell membrane (Paborsky et al 1991). However, cell surface TF can be encrypted in an inactive form that only becomes functional following cell activation. The mechanism of TF encryption is currently unclear although suggested mechanisms involve asymmetric distribution of negatively charged phospholipids within the inner side of the cell membrane (Bach 2006), sequestering of TF within lipid rafts (Bach 2006) and dimerisation of TF molecules (Roy et al 1991).

In addition to full length TF, an alternatively spliced form of TF (asTF) has been identified (Bogdanov et al 2003). asTF lacks exon 5 and therefore has no transmembrane or cytoplasmic domain but has a unique C-terminus. Due to the lack of a transmembrane domain, asTF is soluble and circulates in the blood stream (Bogdanov et al 2003). Furthermore, asTF has been shown to be released from cells in response to inflammatory cytokines (Szotowski et al 2005). The absence of a transmembrane domain suggests that asTF should have no procoagulant activity, but there are conflicting data on the procoagulant activity of asTF (Censarek et al 2007, Bogdanov et al 2003). In addition, the physiological function of this form of TF is not known.

1.4.2. The role of TF in haemostasis

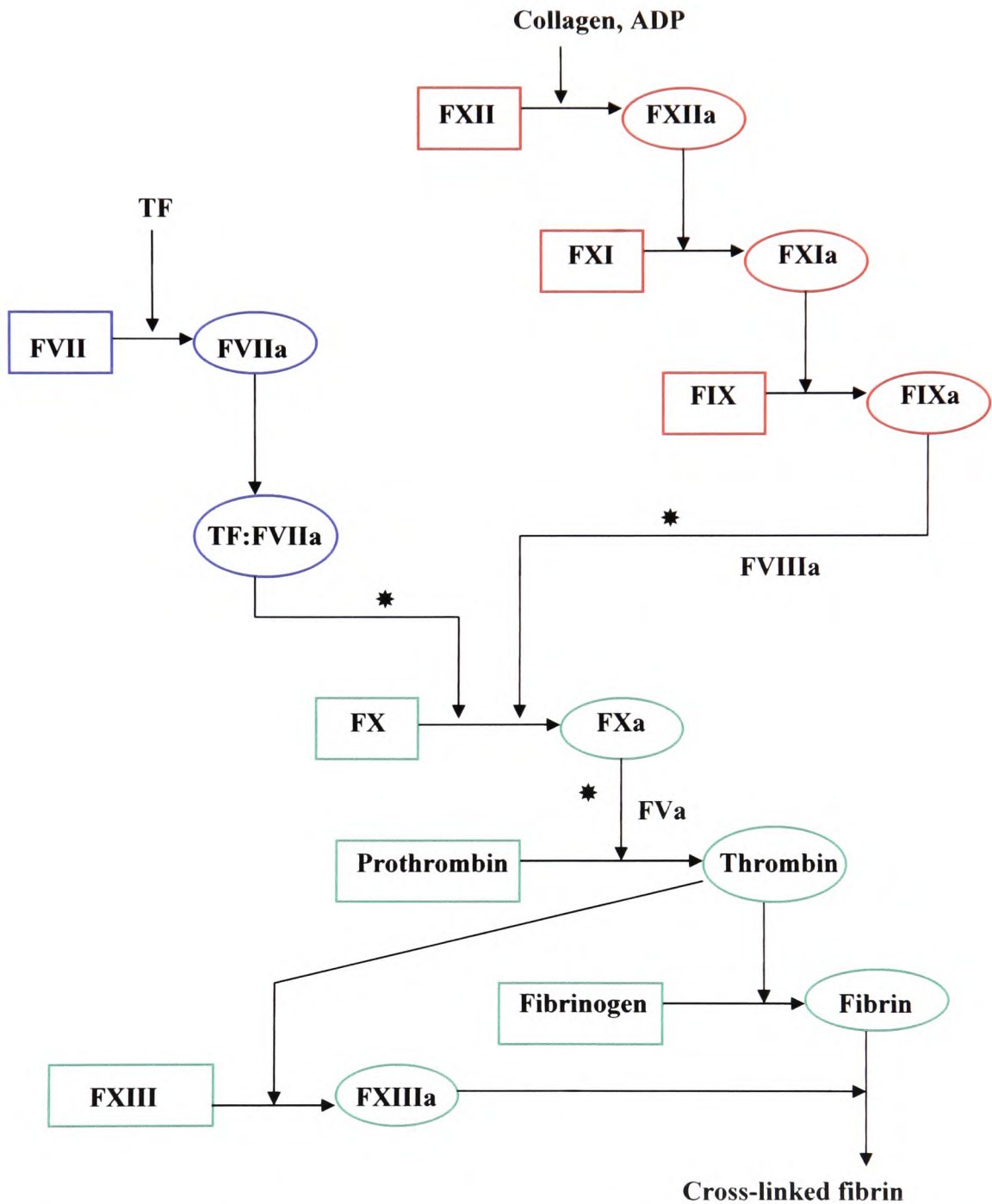
TF has a crucial role in haemostasis as the principal initiator of the extrinsic blood coagulation cascade and functions as a receptor and cofactor for coagulation factor VII (FVII). Many cell types, including epithelial cells of the skin, fibroblasts and astrocytes of the brain, constitutively express TF (Drake et al 1989). Additionally, cells of the intima and adventitia of the vascular wall and cells of the connective tissue surrounding organs constitutively express TF, forming a haemostatic envelope which is activated when vascular integrity is disrupted. In contrast, cells that are in contact with the

bloodstream, principally circulating blood cells and vascular endothelial cells, do not constitutively express TF (Drake et al 1989), although these cells are capable of TF expression upon activation by inflammatory cytokines (Ruf & Edgington 1994).

The coagulation cascade is comprised of two separate pathways which converge at the activation of coagulation factor X (FX) and lead to activation of the common pathway (Fig 1.5). The intrinsic pathway is activated by exposure of the blood stream to negatively charged surfaces such as collagen and leads to FX activation by FIXa in the presence of FVIIIa. The extrinsic pathway of coagulation is activated when blood is exposed to TF from the injured tissue. Circulating FVII within the bloodstream binds to the extracellular domain of membrane bound TF, resulting in the activation of FVII to FVIIa and the formation of a TF:FVIIa complex. The TF:FVIIa complex then activates circulating FX to activated factor Xa (FXa), which in turn converts prothrombin to thrombin. Moreover, the TF:FVIIa complex also activates FIX and therefore feeds back into the intrinsic pathway. Thrombin is a serine protease which digests fibrinogen to fibrin. The fibrin monomers then polymerise, resulting in the formation of a fibrin clot (Fig 1.5). Ultimately, the coagulation mechanism together with platelet activation and aggregation maintains vascular integrity and prevents excessive blood loss through the rapid production of a blood clot at the site of injury.

The physiological inhibitor of the TF:FVIIa complex is a protein known as tissue factor pathway inhibitor (TFPI) (Broze 1995). TFPI contains three protease inhibitor domains, one of which binds to and inhibits FXa. The TFPI:FXa complex then binds to TF:FVIIa on the surface of cells, resulting in the formation of a fully inhibited TF:FVIIa:FXa:TFPI complex, preventing further initiation of the blood coagulation

Figure 1.5. Coagulation cascade pathways



The extrinsic pathway (blue) is activated following injury to blood vessel walls and exposure of TF to FVII in the blood stream. The intrinsic pathway (red) is activated by negatively charged surfaces, such as collagen, in the presence of adenosine diphosphate (ADP). Both pathways lead to the activation of FXa and the common pathway (green), ultimately resulting in the formation of a fibrin clot. (* requires Ca^{2+} ions and phospholipids).

cascade by TF (Broze 1995). Hence, the release of TFPI from endothelial cells into the blood circulation acts as a mechanism of preventing excessive blood coagulation.

1.4.3. Factor VII

Factor VII is a 406 amino acid protein with a molecular mass of 50 kDa (Broze & Majerus 1980). FVII is a vitamin K-dependent serine protease and a member of the trypsin superfamily, which is activated following binding to its receptor and cofactor, TF. FVII circulates in the blood stream at a concentration of 10 nM and a small percentage (1 %) of this is in the active form (FVIIa). FVII is an elongated molecule that consists of a Gla domain, two epidermal growth factor-like domains (EGF domains), and a serine protease domain. The C-terminal Gla domain of FVII contains 10 γ -carboxyglutamic acid residues that allow FVII to bind to the negatively charged phospholipids within the cell membrane via calcium ion bridges. The two EGF domains interact with the extracellular domain of TF and the serine protease domain is responsible for the cleavage of coagulation factor X to its active form (FXa).

1.4.4. Factor X

Factor X (FX) is a vitamin K-dependent serine protease with a molecular weight of 59 kDa. FX is activated by proteolytic cleavage of the heavy chain by either FVIIa or FIXa. Activated FXa consists of two chains that are linked by a disulphide bond. The light chain of FXa contains a Gla domain, which has the same function as the Gla domain of FVIIa. The light chain also contains two EGF domains and the first EGF domain interacts with the extracellular domain of TF (Zhong et al 2002). The heavy chain of FXa contains a serine protease domain, which converts prothrombin to thrombin.

1.5. Non-haemostatic and signalling properties of TF:FVIIa

1.5.1. The function of TF as a cell signalling receptor

In addition to its role in haemostasis, TF has been shown to function as a cell signalling receptor. The first evidence for the role of TF as a cell signalling receptor protein came from a study by Bazan (1990), which showed that TF shares a large degree of structural homology with the class II cytokine receptor family, especially with the interferon- γ receptor. Subsequently, it was demonstrated that the binding of FVIIa to TF results in intracellular calcium ion (Ca^{2+}) oscillations in several cell types (Camerer et al 1996, Rottingen et al 1995). FVIIa binding to TF was also shown to induce tyrosine phosphorylation in monocytes upon formation of the TF:FVIIa complex (Masuda et al 1996), indicating the activation of cell signalling pathways within the cells. This finding was confirmed by the demonstration that TF:FVIIa signalling results in the activation of several intracellular signalling pathways including all three MAPK pathways: extracellular signal-regulated kinase 1/2 (ERK1/2), p38 MAPK and c-Jun N-terminal kinase (JNK) (Poulsen et al 1998, Camerer et al 1999). The TF:FVIIa complex has also been shown to activate the phosphatidylinositol 3-kinase (PI3K) pathway (Versteeg et al 2000). The activation of these pathways by TF:FVIIa signalling has been associated with changes in the expression of many genes including the expression of transcription factors (Camerer et al 2000a, Camerer et al 1999), proinflammatory cytokines (Wang et al 2002), growth factors (Ollivier et al 1998) and proteins involved in cytoskeleton reorganisation and cell migration (Camerer et al 2000a).

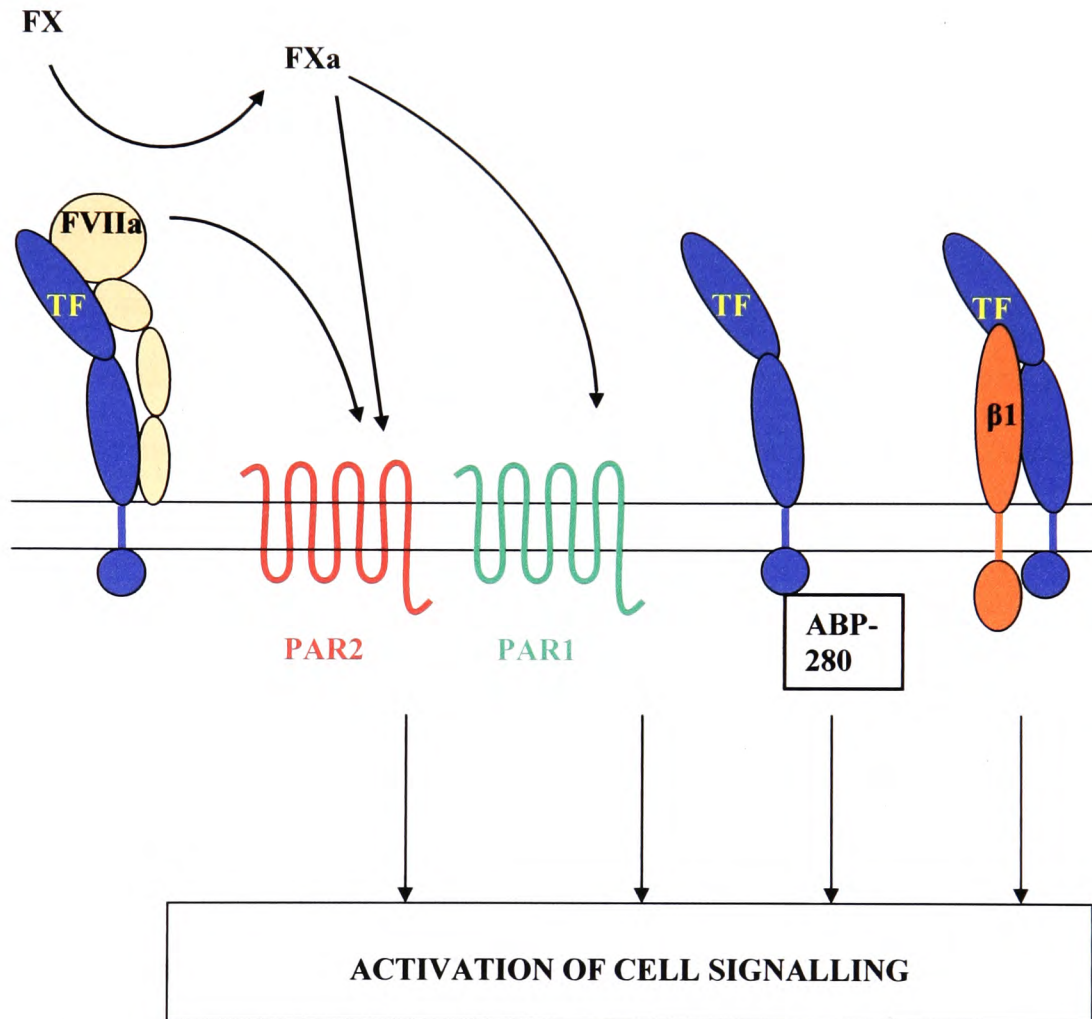
TF has been shown to be essential for embryonic development and TF-deficient mice are known to die following 8 days gestation due to abnormalities in blood vessel formation (Carmeliet et al 1996). In addition, TF influences a number of physiological processes including angiogenesis (Abe et al 1999), cell migration (Jiang et al 2004) and

wound healing (Chen et al 2005). Furthermore, TF signalling has been implicated in pathological conditions such as inflammation (Cunningham et al 1999), tumour angiogenesis (Mueller & Ruf 1998), tumour metastasis (Bromberg et al 1995) and cardiovascular disease (Taubman et al 1997). TF-mediated cell signalling has been suggested to occur via three main mechanisms involving protease-dependent signalling, signal transduction by the cytoplasmic domain of TF, and the binding of TF to other transmembrane receptors such as integrins (Fig 1.6).

1.5.2. TF signalling through protease activated receptors (PARs)

Protease activated receptors (PARs) are G protein-coupled receptors which have seven membrane-spanning regions. PARs are activated by proteolytic cleavage of the N-terminal extracellular domain of the receptor, leading to the formation of a new N-terminus. The new N-terminus then acts as a tethered ligand and binds to the receptor, resulting in the activation of the PAR and the initiation of downstream signalling pathways. To date, four PARs have been identified (PAR 1-4). PAR1 is activated by proteolytic cleavage by FXa and thrombin (Riewald & Ruf 2001) whereas PAR2 is activated by FVIIa, FXa and trypsin (Camerer et al 2000b) and PAR3 and PAR4 are activated by the action of thrombin. The activation of PAR2 by the TF:FVIIa complex and FXa has been shown to result in the induction of MAPK signalling pathways (Morris et al 2006, Jiang et al 2004) and upregulation of the expression of growth factors and proinflammatory cytokines (Morris et al 2006, Hjordtoe et al 2004). PARs also have an important role in the initiation of inflammatory responses since they are activated by serine proteases during tissue injury. PAR activation also leads to the upregulation of the expression of proinflammatory cytokines such as interleukin-8 (IL-8) (Hjordtoe et al 2004). Furthermore, PAR2 signalling results in increased migration and invasion of breast cancer cells (Morris et al 2006, Jiang et al 2004). The formation of

Figure 1.6. TF signalling mechanisms



TF activates cell signalling through three main pathways. In the first mechanism, TF mediated activation of FVIIa and FXa leads to the activation of PAR2 and FXa also activates PAR1. The activation of PARs then leads to the activation of intracellular signalling pathways. TF can signal independently of PARs through the cytoplasmic domain. The cytoplasmic domain of TF binds to actin-binding protein 280 (ABP-280) and leads to reorganisation of the cytoskeleton and cell migration. Finally, TF can directly bind to the $\beta 1$ integrin subunit, resulting in increased cell migration.

the TF:FVIIa complex can also indirectly lead to PAR1 activation through the generation of FXa. The activation of PAR1 by FXa has been demonstrated to lead to the upregulation of the expression of genes involved in angiogenesis and growth (Riewald et al 2001) and also lead to increased tumour metastasis (Bromberg et al 2001).

1.5.3. TF signalling through the cytoplasmic domain of TF

The cytoplasmic domain of TF is small compared to other cytokine receptors and has no intrinsic enzymatic activity. However, this domain of TF is phosphorylated at serine residues 253 and 258 following stimulation of cells with phorbol esters (Zioncheck et al 1992). Serine 253 is phosphorylated by protein kinase C (PKC) following the activation of PAR2 and recruitment of phosphatidylcholine-specific phospholipase C (PC-PLC) (Ahamed & Ruf 2004). This phosphorylation causes a conformational change within the cytoplasmic domain and allows serine 258 phosphorylation by a putative proline directed kinase (Ahamed & Ruf 2004). The cytoplasmic domain of TF has been implicated in tumour metastasis (Bromberg et al 1995), inflammation (Ahamed et al 2007), cell migration (Siegbahn et al 2005), and angiogenesis (Abe et al 1999). Furthermore, a study by Ott et al (1998) demonstrated that the cytoplasmic domain of TF binds to actin-binding protein 280 (ABP-280), a component of the cytoskeleton, independently of FVIIa binding (Fig 1.6). The interaction between TF and ABP-280 results in the reorganisation of the cytoskeleton, cell adhesion and cell migration (Ott et al 1998).

1.5.4. TF signalling through integrins

Integrins are transmembrane adhesion receptors which exist as heterodimers of α and β integrin subunits. The 18 α -subunits and 8 β -subunits combine to form 24 integrin heterodimers. Integrin α and β -subunits have a large extracellular domain, a single

transmembrane spanning domain and a short cytoplasmic domain of between 13 and 70 amino acids. The extracellular domain of integrins binds to components of the extracellular matrix and the cytoplasmic domain is linked to the cytoskeleton. The cytoplasmic domain of integrins has no intrinsic enzymatic activity, but interacts with adapter proteins linked to the cytoskeleton (Brakebusch & Fassler 2005). This connection between the cytoskeleton and extracellular matrix allows cells to transmit signals from the extracellular matrix into the cell and results in the activation of cell signalling pathways such as the ERK1/2, JNK and PI3K pathways (Schwartz 2001, Woodside et al 2001). In addition, the binding of intracellular proteins to the cytoplasmic domain results in changes in the binding affinity of the extracellular domain. This 'inside-out' activation of integrins allows cells to respond to their surrounding environment and to regulate cell processes including cell adhesion, cell migration, proliferation and differentiation (Woodside et al 2001). Integrin heterodimers bind specific components of the extracellular matrix including fibronectin, laminin, vitronectin and collagen. In addition, integrins are activated by the binding of divalent cations such as Mg^{2+} and Mn^{2+} (Humphries 1996). Furthermore, the extracellular domain of integrins has also been shown to be capable of associating with cell membrane receptors including the urokinase receptor (uPAR) and epidermal growth factor receptor (Brown 2002).

The earliest evidence for an association between TF and integrins came from a study where membrane vesicles released from smooth muscle cells were shown to contain TF and this was co-localised with the $\beta 1$ integrin subunit (Schechter et al 2000). TF was then shown to mediate cell migration through interactions with the $\alpha 3\beta 1$ integrin heterodimer (Dorfleutner et al 2004). The induction of cell migration was shown to be dependent on both the extracellular domain of TF and the phosphorylation of the cytoplasmic domain

of TF and it was suggested that the extracellular domain of TF contains a putative integrin-binding site (Dorfleutner et al 2004). Recently, cell surface TF has been shown to directly bind to the $\beta 1$ integrin subunit (Versteeg et al 2008). Furthermore, disrupting this interaction using specific monoclonal antibodies against the extracellular domain of TF was shown to inhibit the growth of breast tumours (Versteeg et al 2008). However, neither the structure of the TF- $\beta 1$ integrin complex nor the signalling mechanisms initiated by the complex have been elucidated. Moreover, the mechanisms that induce the formation of the TF-integrin complex or terminate its function remain unknown.

1.6. Microparticles in cancer

Microparticles are small (0.1-1 μm) membrane vesicles that are released from cells following cell activation and during apoptosis. These vesicles are composed of a phospholipid bilayer rich in the negatively charged phospholipid phosphatidylserine. In addition to the phospholipid component, microparticles contain proteins such as adhesion proteins derived from the activated cells. Furthermore, it has been shown that these microparticle proteins can be transferred to other cell types by incorporation of the microparticles into the cell membrane (Scholz et al 2002, Rauch et al 2000). Microparticles often possess procoagulant activity which is primarily due to the presence of TF (Morel et al 2004). Furthermore, TF-bearing microparticles are the major source of blood-borne TF (Yu & Rak 2004): Microparticles may be released from cancer cells (Yu & Rak 2004), endothelial cells, platelets (Schloz et al 2002) and leucocytes (Rauch et al 2000). Moreover, elevated levels of microparticles are associated with pathological conditions including cancer, cardiovascular disease, sepsis and inflammation (Morel et al 2004). Due to the procoagulant activity of TF-containing microparticles, elevated levels of circulating microparticles have been associated with

the increased risk of thrombosis associated with these pathological conditions (Zwicker et al 2007).

Increased levels of circulating TF-containing microparticles have been detected in breast cancer patients compared to normal healthy patients (Tesselaar et al 2007). As well as increasing the risk of thrombosis, elevated levels of microparticles during cancer have been shown to influence cellular functions. For example, Janowska-Wieczorek et al (2005) demonstrated that incubation of lung cancer cells with microparticles resulted in increased metastasis and angiogenesis in lung tumours. Furthermore, incubation of breast cancer cells with platelet-derived microparticles has been shown to result in the transfer of platelet-derived proteins to the cancer cells, activation of MAPK signalling pathways and increased invasiveness of the breast cancer cells (Janowska-Wieczorek et al 2006). These studies indicate that far from being inactive cell debris, cell-derived microparticles contribute to the progression of cancer by transferring proteins between cell types, activating intracellular signalling pathways and influencing cell functions.

1.7. Tissue factor and breast cancer

The association between cancer and thrombosis was first recognised by Trousseau in 1865 and TF has been identified as a main cause of the hypercoagulation frequently observed in cancer patients (Rickles & Falanga 2001). Increased expression of TF has been detected in many types of solid tumours including breast cancer (Callander et al 1992). A number of studies have reported increased expression of TF in aggressive/invasive breast tumours. Contrino et al (1996) correlated TF expression and tumour histological grade, and higher levels of TF have been observed in malignant breast tumours compared to benign forms of the disease. It has also been shown that

breast cancer cells derived from aggressive breast cancers express high levels of TF, whereas cells from benign breast cancers have little to no TF expression (Hu et al 1994).

In addition to increases in tumour cell-derived TF, analysis of TF distribution within breast tumours demonstrated higher levels of TF in the tumour stroma. Tumour stroma is a connective tissue framework that surrounds the tumour cells and is composed of extracellular matrix components such as collagen and fibronectin, macrophages, fibroblasts and new blood vessels (Dvorak 1986). Vrana et al (1996) showed that the higher levels of TF in breast tumour stroma arose from increased TF expression by the infiltrating macrophages and fibroblasts. Furthermore, the appearance of these TF-positive stromal cells within breast tumours correlated with the progression of the breast tumours to an invasive phenotype (Vrana et al 1996). Moreover, Contrino et al (1996) detected functional TF in vascular endothelial cells within invasive but not benign breast tumours. In addition, Lwaleed et al (1999) showed that increased TF expression in monocytes was associated with greater tumour grade and poorer prognosis, while others have reported increased plasma concentrations of TF in breast cancer patients compared to controls (Ueno et al 2000). Together these studies highlight the importance of TF-positive stromal cells in breast cancer progression. The presence of inflammation in the locality of the tumour is also a feature of invasive forms of breast cancer and is often associated with a poor prognosis (Blot et al 2003). Furthermore, infiltration of the tumour stroma by macrophages in an inflammatory-type response is often observed in aggressive tumours. Monocytes-macrophages and endothelial cells are known to express high levels of TF in response to inflammatory cytokines (Grignani & Maiolo 2000). Therefore, leukocytes recruited to the site of the tumour are a potential source of TF in the vicinity of breast tumours. In support of this, Blot et al (2003) reported that incubation of monocytes with breast tumour cells resulted in increased TF expression in

both cell types, suggesting a possible paracrine signalling mechanism between tumour cells and the infiltrating monocytes leading to up-regulation of TF expression. Therefore, far from being an innate component of tumours, the tumour stroma has been shown to actively promote tumour growth and progression, as infiltrating inflammatory cells and fibroblasts release inflammatory molecules that directly affect the tumour cells (Ben-Baruch 2003, Blot et al 2003). Collectively, the evidence from these studies suggests that increased TF levels both in the tumour stroma and tumour cells at the site of a breast tumour in response to inflammation in the vicinity of the tumour may be a determining factor in the progression from benign to invasive forms of breast cancer.

1.8. Aims of the investigation

The aims of this investigation were to examine the influence of TF on breast cancer cells and to elucidate the mechanism for the interaction of exogenous TF with the cell surface. Factors that alter ER α expression and function in breast cancer cells are important to the understanding of the mechanisms involved in the loss of responsiveness to oestrogen and progression of tumours to more invasive forms. The main objectives were as follows.

- To examine the influence of exogenous TF on ER α expression in breast cancer cell lines and the influence of TF on oestradiol-mediated cell proliferation and invasion.
- To investigate the influence of TF on ER α activity through the classical ERE pathway and ER α phosphorylation.
- To examine the influence of TF on ER α activity through the AP-1 dependent pathway.
- To investigate the interactions of exogenous TF with the cell surface and the resultant signalling mechanisms that lead to the regulation of ER α expression and cellular proliferation.

CHAPTER 2

Materials and Methods

2.1. Materials

Abcam, Cambridge, UK

Anti-human FVIIa antibody

Active Motif, Rixensart, Belgium

ER α ELISA kit, nuclear extract kit, phosphatase inhibitors, recombinant human ER α , TransAM AP-1 kit, TransAM ER kit

Amersham Biosciences, Little Chalfont, UK

GFX PCR DNA and gel band purification kit, high-range rainbow molecular weight protein marker, Ready-To-Go PCR beads, Ready-To-Go RT-PCR beads

Autogen Bioclear, Calne, UK

Mouse monoclonal anti-human β 1 integrin PE-conjugated antibody, mouse monoclonal anti-human β 3 integrin PE-conjugated antibody

Axis-Shield Diagnostics Ltd, Dundee, UK

Mouse monoclonal anti-human TF FITC-conjugated antibody, recombinant human factor VIIa, recombinant human factor Xa

BD Biosciences, Oxford, UK

Becton Dickinson FACSCalibur flow cytometer, CellQuest software program, 8 well cultureslides, Falcon FACS tubes, pEGFP-C3 vector, rat tail collagen type 1

BDH Laboratories Supplies, Poole, UK

Bromophenol blue, glycerol, MgCl₂, sodium acetate, NaOH

Beckman Coulter, High Wycombe, UK

Mouse monoclonal anti-human PAR1 antibody (WEDE15)

Berthold Technologies Ltd, St Albans, UK

Junior LB 9509 luminometer, luminometer tubes

Bioline Ltd, London, UK

BioTaq DNA polymerase, molecular grade agarose, HyperLadder II (50-2000 bp), PCR Ranger DNA ladder (50-1000 bp)

BioRad Laboratories Inc, Hemel Hempstead, UK

Nitrocellulose membrane

Calbiochem/Merck Chemicals, Nottingham, UK

HBTU, mouse monoclonal anti-human TF antibody, Triton X-100

Dade Behring, Liederbach, Germany

Recombinant truncated human tissue factor Innovin reagent

Developmental Studies Hybridoma Bank University of Iowa, Iowa City, USA

Mouse anti-human β 1 integrin antibody (AIIB2)

Fermentas Inc, Glen Burnie, USA

GeneRuler 1 kb DNA ladder

Fisher Scientific, Loughborough, UK

Glycine, NaCl, Tris base

Flowgen, Ashby de la Zouch, UK

ProtoFLOW acrylamide solution, ProtoFLOW resolving buffer, ProtoFLOW stacking buffer, TEMED, electrophoresis tank

Gibco Invitrogen Corporation, Paisley, UK

Enzyme-free cell dissociation buffer, kanamycin sulphate, lipofectin reagent, low melting point agarose, OptiMEM I reduced serum medium, phosphate buffered saline (PBS), phenol red-free MEM, phenol red-free RPMI, SOC medium, SuperScript II reverse transcriptase

GlaxoWellcome Research and Development, Stevenage, UK

Raswin version 6 program

Greiner Bio-One Ltd, Stonehouse, UK

12 well culture plates, 24 well culture plates, T25, T75 and T150 cell culture flasks

Helena Laboratories, Sunderland, UK

Cascade M coagulometer, normal human plasma

Lab Vision Corporation, Runcorn, UK

Rabbit polyclonal anti-human β 1 integrin antibody

Leica Microsystems, Milton Keynes, UK

Leitz Laborlux S fluorescence microscope

LGC-ATCC, Teddington, UK

MCF-7, MDA-MB-231, T47D and ZR-75-1 human breast cancer cell lines

Media Cybernetics, Wokingham, UK

Cool Snap-Pro camera, Image-Pro Plus Version 5.1.2.

MP Biomedicals, Cambridge, UK

Serum replacement media

MWG-Biotech AG, Ebersberg, Germany

β -actin primers, ER α primers, ER β primers, ERE DNA sequences

Nikon, Kingston-upon-Thames, UK

Nikon TMS inverted microscope

Promega Corporation, Southampton, UK

Anti-mouse alkaline phosphatase-conjugated antibody, 100 \times BSA, calf intestinal alkaline phosphatase (CIAP), cell lysis buffer (5 \times), CellTiter 96 AQueous One Solution reagent, luciferase substrate (Luciferin), pGL3-promoter vector, protease inhibitor cocktail, restriction enzymes (*Bam*H I, *Eco*R I, *Mlu* I), Tris-borate EDTA (TBE) buffer, TMB stabilised substrate for horse radish peroxidase, Western blue stabilized substrate for alkaline phosphatase, Wizard Plus Minipreps DNA purification system

PromoCell, Heidelberg, Germany

Foetal calf serum (FCS)

R&D Systems, Abingdon, UK

Escherichia coli TB-1 strain

Santa Cruz Biotechnology Inc, Heidelberg, Germany

Donkey anti-goat alkaline phosphatase-conjugated antibody, donkey anti-goat HRP-conjugated antibody, goat anti-human GAPDH HRP-conjugated antibody, goat anti-human phospho-serine 118 ER α antibody, goat anti-mouse HRP-conjugated antibody, goat anti-rabbit IgG FITC-conjugated antibody, goat anti-rabbit HRP-conjugated antibody, mouse monoclonal anti-human ER α antibody, mouse monoclonal anti-human PAR1 antibody (ATAP2), mouse monoclonal anti-human PAR2 antibody (SAM11), rabbit polyclonal anti-human TF antibody

Scientific Laboratory Supplies Ltd, Hessle, UK

CO₂ incubator

Sigma Chemical Company Ltd, Poole, UK

Absolute ethanol, ammonium persulphate, antibiotic/antimycotic solution, basic fibroblast growth factor, Bradford reagent, CaCl₂, carbenicillin disodium salt, chloroform, collagen type IV, dioctadecyl-3, 3, 3', 3'-tetramethylindocarbocyanine perchlorate (DiI), dimethyl sulphoxide (DMSO), N, N-Diisopropylethylamine (DIPEA), DMEM medium, DNase/RNase free water, ethanolamine, fluorescein, glutaraldehyde, isopropanol, L-alanyl-L-glutamine (Glutamax), 2 \times Laemmli's buffer, LB agar, LB broth, lipid free BSA, minimum essential medium Eagle (MEM), 10 \times MEM, MnCl₂, molecular weight marker (27,000-180,000 Da), 17 β -oestradiol, PBS tablets, p-nitrophenyl chloroformate-activated agarose, RGD peptide, RPMI medium, sodium bicarbonate, sodium dodecyl sulphate (SDS), SYBR Green I, 12-O-tetradecanoylphorbol-13-acetate (TPA), Tween 20, TRI reagent, trypsin/EDTA solution

Stratagene, Amsterdam, The Netherlands

pAP-1-Luc PathDetect reporter vector, Herculase enhanced DNA polymerase, *Pfu* DNA polymerase, T4 DNA ligase

Syngene, Cambridge, UK

GeneSnap imaging system and GeneTool analysis program

TCS CellWorks Ltd, Buckingham, UK

DMSO freeze medium

Techne Incorporated, Cambridge, UK

Techgene PCR thermal cycler

Tocris Bioscience, Bristol, UK

MAPK inhibitor PD98059

Tripos Associates Inc, St Louis, USA

Alchemy III program

UVP Ltd, Cambridge, UK

UV transilluminator

VWR International Ltd, Lutterworth, UK

Boyden chambers (8 μm pore size), RNase Away

Weber Scientific International Ltd, Teddington, UK

Haemocytometer

Wissenschaftliche Software, Freberg, Germany

Basepair primer design program

WPA, Cambridge, UK

WPA lightwave UV/Vis diode-array spectrophotometer

Yorkshire Bioscience, York, UK

dNTP mix

2.2. Methods

2.2.1. Culture of breast cancer cell lines

All cells were cultured under sterile conditions and all reagents pre-warmed to 37°C. The human breast carcinoma cell line MCF-7 was cultured in T75 (75 cm²) flasks with minimum essential medium (MEM) supplemented with 2 mM Glutamax I (L-alanyl-L-glutamine), 10 % (v/v) foetal calf serum (FCS) and 1 % (v/v) antibiotic (penicillin (5 units/ml), streptomycin (5 µg/ml) and amphotericin (25 ng/ml)). The human breast cancer cell lines T47D and ZR-75-1 were cultured in RPMI medium supplemented as above. The human breast cancer cell line MDA-MB-231 was cultured in DMEM medium supplemented as above. Cells were incubated at 37°C under 5 % (v/v) CO₂ atmosphere and supplemented every 3 days by replacing 3 ml of culture medium with fresh medium.

2.2.2. Subculture and determination of the number of cells

Cells were subcultured when approximately 80 % confluent. Medium was removed from the flask and the cells washed with 8 ml of phosphate buffered saline (PBS) (pH 7.2) to remove all traces of medium. Trypsin/EDTA (5 mg/ml porcine trypsin, 2 mg/ml EDTA) (5 ml) was added to the flask and the cells incubated for approximately 3 min at 37°C to detach the cells. The flask was then tapped firmly to release the cells and the trypsin, which can be detrimental to cells, neutralized by adding 5 ml of complete medium. The cell suspension was transferred to a 20 ml Sterilin tube and centrifuged at 400 g for 5 min to pellet the cells. The medium was carefully removed to avoid disrupting the pellet and the cells resuspended in 5 ml of fresh medium. To determine the number of cells, 20 µl of cell suspension was loaded onto a haemocytometer and the number of cells in five 1 mm² squares counted. The density of cells per ml was then calculated as the average number of cells counted per mm² × dilution factor × 10⁴. To

start new cultures, 10^6 cells were added to T75 flasks containing 10 ml of medium and incubated at 37°C.

2.2.3. Harvesting of cells for experimental analysis

Cells were trypsinised and cell numbers determined as described in section 2.2.2. An appropriate volume of medium containing the required number of cells was placed in a centrifuge tube and the cells pelleted by centrifugation at 400 g for 5 min. The cells were washed by resuspension in PBS (1 ml), centrifuged at 12,000 rpm (9,000 g) for 3 min in a microcentrifuge and the supernatant removed. The cell pellet was stored at -70°C until required.

2.2.4. Cryopreservation of cells

Cells were trypsinised and cell density determined as described in section 2.2.2. Cells were then resuspended in DMSO freeze medium (5 ml) and aliquoted into cryotubes at a density of 10^6 cells/tube. The cryotubes were placed in a freezing chamber and gradually cooled down at a rate of -1°C/min overnight to -70°C. The cells were then transferred to liquid nitrogen for long-term storage. To start new cultures from frozen cells, the cells were thawed at 37°C and immediately placed in T75 flasks containing 10 ml of pre-warmed medium.

2.2.5 Adaptation of cells to phenol red-free and low serum medium

Cell culture medium contains the pH indicator phenol red (phenolsulfonphthalein), which has been shown to have oestrogenic properties (Berthois et al 1986). Furthermore, FCS is a possible source of oestrogens in culture medium. In order to observe the effects of oestrogen on breast cancer cells, cells were adapted to phenol red-free medium and 1 % (v/v) FCS over four days prior to experiments using 17 β -oestradiol, in order to reduce the concentration of oestrogens in the culture medium.

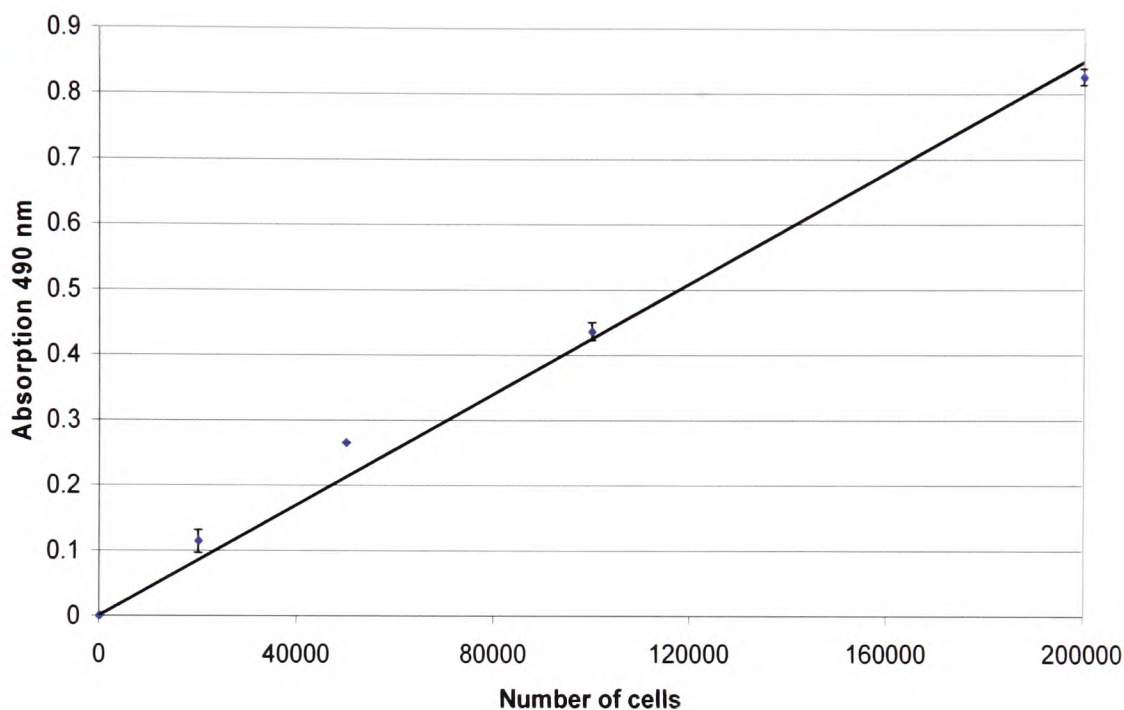
Cells were gradually adapted to 1 % (v/v) FCS by reducing the percentage of FCS in medium from 10 % (v/v) to 5 % (v/v) and finally 1 % (v/v) FCS over four days.

2.3. Measurement of cell proliferation using the MTS-based colorimetric assay

The CellTiter 96 AQueous One Solution reagent contains a tetrazolium compound (3-(4,5-dimethylthiazol-2-yl)-5-(3-carboxymethoxyphenyl)-2-(4-sulphophenyl)-2H-tetrazolium (MTS)), which is reduced to a coloured formazan product by NADH and NADPH produced by dehydrogenase enzymes in metabolically active cells. The amount of formazan produced is therefore proportional to the number of viable cells. Following incubation of cells with the reagent the number of viable cells is determined by measuring the quantity of formazan product by measuring absorption at 490 nm.

Cells (5×10^4) were seeded out into 12 well plates and incubated at 37°C for 2 h to allow the cells to adhere. Following treatment of cells for 24-72 h, the medium was then carefully removed from each well. In order to determine the rate of proliferation, medium (500 μ l) and CellTiter 96 AQueous One Solution Reagent (40 μ l) were added to each well, including one well with no cells used as a blank. The cells were incubated at 37°C for 1 h, until a colour change was observed. 240 μ l of medium from each sample was then transferred to a plastic cuvette, diluted with 560 μ l distilled water and absorptions measured at 490 nm against the blank sample using a spectrophotometer. A standard curve was prepared by preparing serial dilutions of MCF-7 cells ranging from 0 to 2×10^5 cells in 500 μ l of medium and seeding out into a 12 well plate. The plate was incubated at 37°C for 2 h to allow the cells to adhere without any proliferation. CellTiter 96 AQueous One Solution Reagent (40 μ l) was added to each well and the cells incubated for a further 1 h until a colour change was observed. The proliferation assay was then carried out as above for each sample in order to construct a standard curve of cell number against absorption at 490 nm (Fig 2.1).

Figure 2.1. Standard curve for the proliferation assay



MCF-7 cells ($0-2 \times 10^5$) were seeded out into 12 well plates in 500 μ l of medium. Following 2 h incubation at 37°C, 40 μ l of the CellTiter proliferation reagent was added to each well. Absorptions of the samples were measured at 490 nm and a standard curve of cell number against absorption at 490 nm constructed. Data represents the mean value of two experiments measured in duplicate \pm SD.

2.4. Flow cytometric determination of cell surface TF antigen and DNA-transfection efficiency

Flow cytometry is a procedure for measuring physical and chemical characteristics of cells as they pass through a laser light. The instrument measures particle size and granularity as well as the presence of fluorescent groups. The fluorescent groups may be a fluorescent protein or alternatively, a fluorescent-conjugated antibody used to label specific cell antigens. Using this technique, the density of fluorescent groups per cell, as well as the proportion of positive cells may be determined. The FL1 detection wavelength (530 nm) excites green fluorescent tags. In order to determine cell surface TF expression, cells (5×10^5) were harvested, washed three times in PBS (1 ml) and resuspended in 100 μ l of PBS. The cells were then incubated with the mouse monoclonal FITC-conjugated anti-human TF antibody (2 μ g/ml) or a goat anti-rabbit IgG FITC-conjugated antibody (4 μ g/ml) for 30 min in the dark. The cells were then centrifuged at 12,000 rpm for 3 min in a microcentrifuge and the antibody solution removed. The cells were washed three times in PBS (1 ml) to remove unbound antibody and then resuspended in PBS (300 μ l) and transferred to polypropylene FACS tubes. Alternatively, cells transfected with pEGFP-C3 were analysed directly. Cells were analysed on a Becton Dickinson FACSCalibur flow cytometer by recording 10,000 events and fluorescence on the FL1 channel. A gate was set to contain approximately 3% of events from unlabelled or untransfected cells, and mean fluorescence and maximum fluorescence determined using the CellQuest software.

2.5. Molecular Biology Techniques

2.5.1. Isolation of total RNA from cells

The total RNA isolation (TRI) system was used to isolate RNA from cells. In order to prevent degradation of RNA, all work surfaces were cleaned with RNase Away to eliminate ribonucleases (RNase). Previously harvested cells were thawed at room

temperature, lysed in 200 μ l of TRI reagent by repeated pipetting and incubated at room temperature for 5 min. Chloroform (40 μ l) was added to each tube, vortexed for 15 s and the samples allowed to stand for 10 min at room temperature. The samples were centrifuged at 12,000 rpm for 15 min in a microcentrifuge to form two visible layers, and the clear aqueous upper phase was carefully transferred to a fresh RNase-free 1.5 ml eppendorf tube. To precipitate the RNA, isopropanol (100 μ l) was added to each sample, mixed by vortexing and incubated at -20°C for 1 h. In order to pellet the RNA, the samples were centrifuged at 12,000 rpm for 10 min in a microcentrifuge. The supernatant was removed and the RNA pellet washed with 200 μ l of 75 % (v/v) ethanol. The RNA pellet was resuspended in 60 μ l RNase-free water and the samples stored at -70°C until required.

2.5.2. Determination of RNA purity and concentration

The concentration of RNA in the samples was determined by measuring the absorption of each sample at 260 nm using a spectrophotometer. The spectrophotometer was calibrated using 54 μ l of distilled water in a quartz micro-cuvette as a blank. 6 μ l of RNA sample was then added to the cuvette and the sample mixed by pipetting. The absorption at 260 nm was measured and the concentration of RNA calculated as follows:

$$\text{RNA concentration } (\mu\text{g/ml}) = \text{Absorption (260 nm)} \times 40 \times \text{dilution factor}$$

The 260:280 ratio was used to determine the purity of RNA in each sample, with a ratio above 1.3 indicating RNA of sufficient purity for subsequent RT-PCR analysis.

2.5.3. Reverse transcriptase-polymerase chain reaction (RT-PCR)

Each RNA sample was amplified with ER α and ER β primers as well as with β -actin primers as a reference. β -actin, a house-keeping gene is constitutively expressed in cells

and hence is commonly used as a reference. Primers were reconstituted in RNase-free water to give a final concentration of 100 pmol/ μ l. Using the calculated RNA concentrations, an appropriate volume of each RNA solution containing 0.3 μ g of RNA was diluted in RNase free water to a final volume of 147 μ l. 49 μ l of this solution, containing 0.1 μ g of RNA, was placed into three separate RT-PCR tubes. Mixed forward and reverse primers (100 pmol) for ER α , ER β and β -actin primers were then in turn added to separate tubes to make up the volume in each tube to 50 μ l. Semi-quantitative RT-PCR was carried out with each RNA sample to convert RNA to cDNA and then amplify the cDNA using Ready-To-Go RT-PCR beads. When made up to a final volume of 50 μ l each bead contained 2 units of *Taq* DNA polymerase, 10 mM Tris-HCl (pH 9), 60 mM KCl, 1.5 mM MgCl₂, 200 μ M of each dNTP, Moloney Murine Leukemia Virus reverse transcriptase, RNAGuard ribonuclease inhibitor and stabilisers including RNase/DNase free BSA. The RT-PCR program was carried out as shown in table 2.1.

2.5.4. Analysis of DNA by agarose gel electrophoresis

A 2 % (w/v) agarose gel was prepared by dissolving 1 g of agarose in 50 ml of TBE buffer (89 mM Tris-borate pH 8.3, 89 mM boric acid, 2 mM EDTA), and heating in a microwave until dissolved. The electrophoresis tray was prepared by sealing the ends with masking tape and placing combs with an appropriate number of wells into the electrophoresis tray. The gel was mixed and poured into the electrophoresis tray, allowed to cool down at room temperature for 20 min and then placed at 4°C for 30 min to solidify. When the gel had set, the comb was removed and the gel placed in an electrophoresis tank and covered with TBE buffer. Samples were prepared for electrophoresis by mixing 10 μ l of RT-PCR amplified DNA with 2 μ l of loading dye

Table 2.1. RT-PCR program

Number of cycles	Temperature	Time	Step
1	42°C	30 min	Conversion of RNA to cDNA
	95°C	5 min	Degradation of RNA
18-30	95°C	1 min	Denature DNA strands
	58/59°C	1 min	Primers anneal
	72°C	1 min	Extension by <i>Taq</i> polymerase
1	72°C	10 min	Final extension
N/A	4°C	Hold	Final hold

The number of amplification cycles and annealing temperature used for the PCR step were optimised for each primer set.

(10 % (w/v) glycerol, 0.1 % (w/v) bromophenol blue, 89.9 % (v/v) TBE buffer pH 8.3) and 1 μ l of SYBR Green I. Additionally, a DNA marker was prepared by mixing 5 μ l of PCR Ranger DNA marker and 1 μ l of SYBR Green I. The DNA markers and samples were in turn loaded into separate wells and electrophoresis carried out at 100 V until the bromophenol blue band was 1 cm from the end of the gel. Following separation of the DNA, the bands were visualised with a UV transilluminator and recorded using the GeneSnap imaging system. mRNA expression was analysed by comparing the intensity of the bands to β -actin for each sample using the GeneTool program.

2.5.5. Testing of RNA samples for genomic DNA contamination

In order to ensure that the RT-PCR products were representative of DNA amplified from RNA only, the RNA samples were routinely checked for genomic DNA contamination by carrying out a PCR reaction with the RNA samples. During this procedure, RNA samples free of genomic DNA would produce no PCR product, since the RNA template would be destroyed during the first denaturing step at 95°C. Genomic contamination of the RNA samples would result in PCR products visible when examined by agarose electrophoresis. PCR reactions were set up using Ready-To-Go PCR beads. Each bead contains 2.5 units of PuReTaq DNA polymerase, 10 mM Tris-HCl (pH 9), 50 mM KCl, 1.5 mM MgCl₂, 200 μ M of each dNTP, stabilizers, and BSA when reconstituted with 25 μ l of DNase free water. 0.1 μ g of RNA sample and 100 pmol of β -actin forward and reverse primer mix were added to the PCR tube and the volume made up to 25 μ l using DNase free water. The samples were denatured at 95°C for 5 min followed by PCR for 1 min at 95°C, 1 min at 58°C and 1 min at 72°C for 18 cycles. Samples were analysed by 2 % (w/v) agarose gel electrophoresis and viewed on a UV transilluminator. On no occasion when the RNA samples were tested were any

bands detected, indicating that there was no genomic DNA contamination in the samples and the RT-PCR products were representative of DNA amplified from RNA.

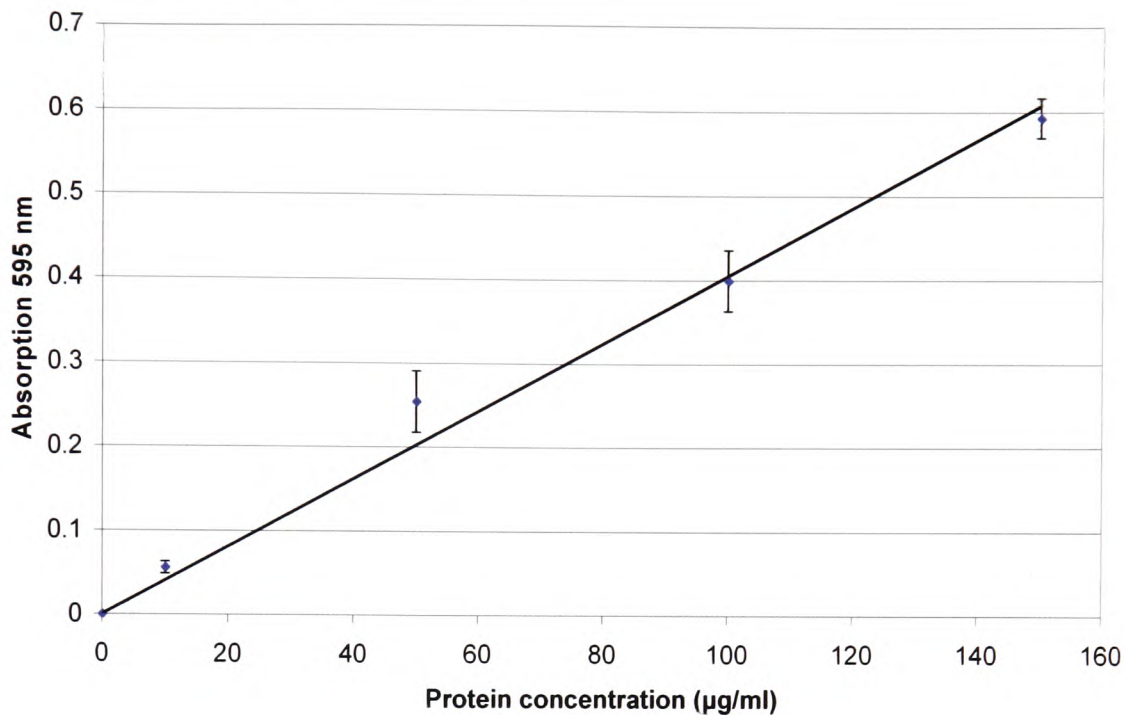
2.6. Estimation of protein concentration using the Bradford assay

Cell samples were resuspended in 200 μ l of Laemmli's buffer (62.5 mM Tris-HCl pH 6.8, 10 % (w/v) glycerol, 5 % (w/v) 2-mercaptoethanol, 2 % (w/v) SDS, 0.002 % (w/v) bromophenol blue) and lysed by repeated pipetting. The samples were heated at 99°C for 5 min and diluted in distilled water for the assay. Additionally, standards of a range of known protein concentrations (0, 10, 50, 100 and 150 μ g/ml) were prepared by serial dilutions of lipid-free BSA in distilled water. The Bradford reagent was prepared by diluting the stock reagent with distilled water (1:1 v/v). Standards and samples (100 μ l) were placed into individual 1 ml plastic cuvettes and Bradford reagent (900 μ l) added to each cuvette. The samples were allowed to develop for 10 min and the absorption of the samples measured at 595 nm using a spectrophotometer. The absorption values of the standards were used to construct a standard curve (Fig 2.2) of absorption at 595 nm against protein concentration and used to determine protein concentrations of the samples.

2.7. SDS-polyacrylamide gel electrophoresis (SDS-PAGE)

A 12 % (v/v) polyacrylamide gel was prepared by mixing 4 ml of acrylamide solution (30 % (w/v) acrylamide, 0.8 % (w/v) bis-acrylamide), 2.6 ml of resolving buffer (1.5 M Tris-HCl pH 8.8, 0.4 % (w/v) SDS), 3.3 ml of distilled water and 50 μ l of 10 % (w/v) ammonium persulphate. The solution was gently mixed and de-gased for 2 min under a vacuum. Tetramethylethylenediamine (TEMED) (10 μ l) was then added to start

Figure 2.2. Standard curve for Bradford assay



A range of protein concentration standards (0-150 µg/ml) was prepared by serial dilutions of BSA in distilled water. 100 µl of each sample was placed in a separate plastic cuvette in duplicate and the diluted Bradford reagent (900 µl) added. Samples were allowed to develop for 10 min and the absorptions measured at 595 nm using a spectrophotometer. The data represents a typical standard curve \pm SD that was prepared on each occasion.

polymerisation and the solution was poured in between the electrophoresis plates in a gel caster. A layer of butanol was placed on top of the gel to ensure that the gel was level and the gel was allowed to polymerise for at least 1 h. A 4 % (v/v) stacking gel was prepared by mixing 0.65 ml of acrylamide solution, 1.3 ml of stacking buffer (0.5 M Tris-HCl pH 6.8, 0.4 % (w/v) SDS), 3 ml of distilled water and 50 μ l of 10 % (w/v) ammonium persulphate. The solution was gently mixed and de-gased under a vacuum for 2 min. TEMED (10 μ l) was added and the gel was poured on top of the polymerised lower gel. A comb was placed into the gel and the gel allowed to polymerise for 1.5 h. The gel was then placed in the electrophoresis tank and covered with electrophoresis buffer (25 mM Tris-HCl pH 8.3, 192 mM glycine, 0.035 % (w/v) SDS). A set of molecular weight protein markers (10 μ l) was loaded into the first well followed by the protein samples loaded into subsequent wells. Electrophoresis was carried out at 100 V for 1.5 h until the bromophenol blue band had reached approximately 1 cm from the end of the gel. The separated proteins were transferred onto nitrocellulose filter as follows. The gel was placed in between blotting paper and nitrocellulose filter soaked in transfer buffer (20 mM Tris-HCl pH 8.3, 150 mM glycine, 20 % (v/v) methanol), placed in the transfer tank and transferred at 16 mA overnight, at 4°C.

2.8. Western blot analysis

Following the transfer of proteins onto nitrocellulose membrane, the membrane was blocked with Tris-buffered Saline Tween 20 buffer (TBST) (20 mM Tris-HCl pH 8, 150 mM NaCl, 0.05 % (v/v) Tween 20) for 2 h and then incubated with the mouse monoclonal ER α antibody diluted in TBST (0.2 μ g/ml final concentration) for 1.5 h at room temperature. The membrane was washed twice in distilled water for 5 min each and then incubated with an anti-mouse IgG alkaline phosphatase-conjugated secondary antibody diluted in TBST (0.1 μ g/ml final concentration) for 1.5 h at room temperature. The membrane was washed twice in distilled water for 5 min each and developed with

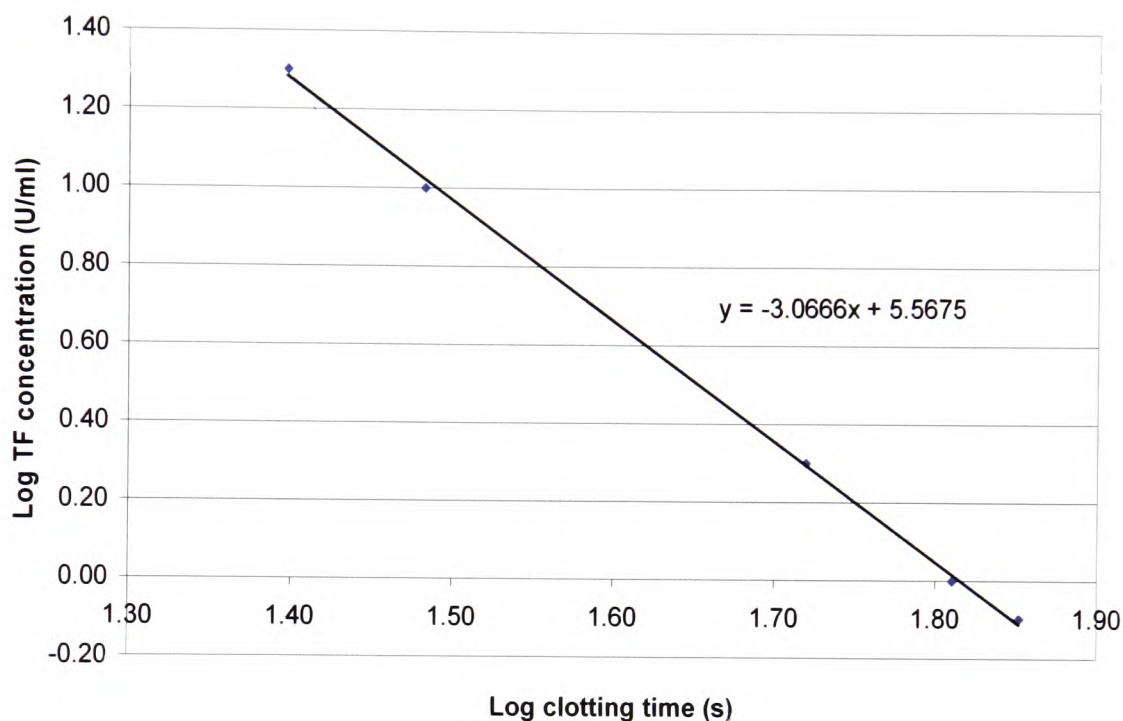
Western Blue stabilised substrate for alkaline phosphatase. Subsequently, the membrane was washed twice in distilled water for 5 min each and then probed with a goat polyclonal HRP-conjugated GAPDH antibody diluted in TBST (0.1 µg/ml final concentration) for 1.5 h at room temperature. The membrane was washed twice with distilled water for 5 min each and developed using 3,3',5,5 tetramethylbenzidine (TMB)-stabilised substrate for HRP. The membrane was then photographed under white light using the GeneSnap program and ERα expression analysed by comparing the intensity of the bands to GAPDH for each sample using the GeneTool program.

2.9. Measurement of TF activity by the one-stage prothrombin time assay

Cells were harvested and 4×10^5 , 8×10^5 or 10^6 cells placed into three separate 1.5 ml microfuge tubes. The cells were pelleted by centrifugation at 12,000 rpm for 3 min in a microcentrifuge, the medium removed and the cells washed with PBS (1 ml). The cells were then resuspended in PBS (100 µl). Prior to testing, all reagents, cuvettes and pipette tips were warmed up to 37°C. 25 mM CaCl₂ (100 µl) was added to a cuvette in the Cascade M coagulometer, followed by cell suspension (100 µl). Following equilibration for 30 s, normal human plasma (100 µl) was added which also triggered the timing mechanism automatically. The clotting time for each sample was recorded by the coagulometer. A standard curve was prepared using Innovin recombinant human truncated tissue factor (TF) dissolved in distilled water (10 ml), and serial dilutions prepared of 0,1, 2, 10 and 20 U/ml, where the recombinant TF stock solution was taken to have 1000 arbitrary units/ml. The TF activity of the diluted TF solutions was measured as above, converted to log values and used to prepare a standard curve of TF concentration against clotting time. TF concentrations were determined using the following equation derived from the standard curve (Fig 2.3):

$$\text{Log [TF] (U/ml)} = -3.0666 \times \log \text{ clotting time} + 5.5675$$

Figure 2.3. One-stage prothrombin time assay standard curve



Serial dilutions of the recombinant human TF Innovin reagent (0-20 U/ml) were prepared in distilled water and the clotting times of the samples measured using the PT assay to construct a standard curve of clotting time against TF concentration. Data represents the average of two experiments measured in duplicate.

2.10. Bacterial cell culture and plasmid isolation

2.10.1. Preparation of LB broth and propagation of *Escherichia coli* TB-1

LB broth was prepared by dissolving LB broth powder (6.25 g) in de-ionised water (250 ml) and autoclaving. *E. coli* strain TB-1 was propagated overnight in 50 ml of LB broth at 37°C with gentle agitation.

2.10.2. Isolation of plasmid DNA

Plasmid DNA from bacterial cells was extracted and isolated using the Wizard Plus Miniprep DNA purification system as follows. 3 ml of bacterial cell suspension was centrifuged at 2,500 g for 5 min and the supernatant removed. The bacteria were resuspended in 200 µl of resuspension buffer (50 mM Tris pH 7.5, 10 mM EDTA, 100 µg/ml RNase A). Cell lysis solution (0.2 M NaOH, 1 % SDS) (200 µl) was added and mixed by inverting the tube. Neutralisation solution (1.32 M potassium acetate pH 4.8) (200 µl) was added, mixed and the lysate centrifuged at 12,000 rpm for 5 min in a microcentrifuge to pellet the cell debris. For each miniprep, a 3 ml syringe barrel was attached to a minicolumn connected to a vacuum manifold. 1 ml of DNA purification resin was added to the column. The cell lysate was mixed with the resin and the solution cleared through, retaining the resin in the column. The column was washed with 2 ml of wash buffer (80 mM potassium acetate, 8.3 mM Tris-HCl pH 7.5, 40 µM EDTA, 55 % ethanol) and cleared through under vacuum as before. The minicolumn was then placed into a 1.5 ml tube and residual ethanol removed by centrifugation at 12,000 rpm for 2 min in a microcentrifuge. 50 µl of DNase free water was added to the minicolumn and incubated for 1 min. The plasmid DNA was then eluted from the column by centrifugation at 12,000 rpm for 1 min in a microcentrifuge.

2.10.3. Determining plasmid DNA purity and concentration

To determine the purity of the eluted plasmid DNA, the samples were analysed on a 1 % (w/v) agarose gel, prepared by dissolving 0.5 g agarose in 50 ml of TBE buffer. The plasmid DNA samples were prepared for electrophoresis and electrophoresis carried out as described in section 2.5.5. The bands were visualized and inspected using a UV transilluminator. The concentration of plasmid DNA in each sample was determined by measuring the absorption of a 1 in 10 dilution of the DNA at 260 nm against a water blank. The concentration of DNA was then calculated as:

$$\text{DNA concentration } (\mu\text{g/ml}) = \text{Absorbance (260 nm)} \times 50 \times \text{dilution factor}$$

DNA purity was determined by measuring the 260:280 ratio, with a ratio above 1.3 indicating DNA of sufficient purity.

2.10.4. Ethanol precipitation of DNA

The DNA solution was mixed with sodium acetate (5 M) pH 5.2, and 100 % (v/v) ethanol at a ratio of 1:1:4 (v/v/v) and incubated at -20°C for 30 min. The sample was then centrifuged at 12,000 rpm for 20 min in a microcentrifuge and the pellet washed with 200 μl of 75 % (v/v) ethanol. The sample was centrifuged at 12,000 rpm for 10 min and the ethanol removed. The pellet was dried and resuspended in DNase free water (50 μl).

2.10.5. Preparation and transformation of competent bacterial cells

E.coli strain TB-1 was incubated overnight at 37°C in 50 ml of LB broth. The cells were then chilled on ice for 30 min and pelleted by centrifugation at 2,500 g for 20 min. The cells were resuspended in 20 ml of ice-cold trituration buffer (100 mM CaCl_2 , 70 mM

MgCl₂, 40 mM sodium acetate) pH 7.4, and diluted to 50 ml with trituration buffer. The cells were then incubated on ice for 45 min, centrifuged at 1,800 g for 10 min and resuspended in 5 ml of fresh trituration buffer. 80 % (w/v) glycerol (750 µl) was added gradually with gentle stirring, and the competent cells divided into 0.2 ml aliquots and stored at -70°C until use. In order to transform the competent cells with plasmid DNA, DMSO (3 µl) was added to 200 µl of competent cells, mixed and 100 µl of the cell suspension transferred into two 0.2 ml microfuge tubes. Plasmid DNA (20 ng) was added to one tube and the other used as a negative control. The cells were incubated on ice for 30 min and then heat shocked at 42°C for 2 min on a heating block. The samples were cooled to 4°C for 1 min, 100 µl of SOC medium added, and the samples incubated at 37°C for 1 h to allow the expression of the antibiotic resistance gene encoded within the plasmid.

2.10.6. Selection of transformed bacteria

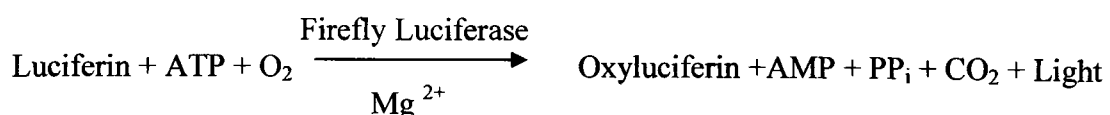
To prepare agar/antibiotic plates, LB agar was prepared by dissolving LB agar powder (3.5 g) in de-ionised water (100 ml) and autoclaving. The agar was cooled to 50°C and an appropriate antibiotic added. LB agar antibiotic plates were then prepared by pouring approximately 20 ml of LB agar into separate Petri dishes and allowing the liquid to set. The plates were sealed and stored at 4°C until use. To select the transformed bacterial cells, bacterial suspension (20 µl) was spread out onto antibiotic-LB agar plates using a sterile glass pipette, and incubated at 37°C overnight. Following the incubation, colonies were removed from the plates using a sterile pipette tip and transferred to 10 ml of LB broth. The bacteria were then incubated at 37°C for 24 h. The bacterial cells were pelleted by centrifuging at 2,500 g for 15 min and resuspended in 5 ml of LB broth containing 1 % (w/v) glycerol. The cells were then aliquoted and stored at -70°C until use.

2.11. Transfection of mammalian cells with plasmid DNA using the Lipofectin reagent

Lipofectin reagent is an anionic lipid-based reagent which can encapsulate the plasmid DNA into liposomes that readily fuse with the cell membrane and release the plasmid into the cell cytoplasm. Prior to transfection, cells (4×10^5 /well) in 0.5 ml of complete medium were seeded out into a 12 well plate and incubated at 37°C for 24 h. The medium was then removed from each well and the cells washed with PBS (1 ml). OptiMEM 1 reduced serum medium (800 μ l) with no antibiotic was then added to each well. For each transfection, solution A was prepared by diluting 1 μ g of plasmid DNA for each of the plasmids in turn in OptiMEM 1 medium (100 μ l). Solution B was prepared by diluting Lipofectin reagent (10 μ l) in OptiMEM 1 reduced serum medium (100 μ l) for each sample. The two solutions were allowed to stand at room temperature for 30 min and then mixed together and allowed to stand at room temperature for a further 15 min. Lipid-DNA complexes were then added to the corresponding wells and incubated at 37°C for 6 h. Following transfection, the medium was removed and the cells washed with 1 ml of PBS. Medium (1 ml) was then added to each well and the cells incubated at 37°C for 16 h.

2.12. Luciferase assay

In order to measure transcriptional activation in the cells, resultant luciferase activity was developed by adding the luciferase substrate (luciferin) to the cell lysates as described below. Luciferase converts luciferin to oxyluciferin and the reaction produces light, which is measured and used to determine transcription factor activity in the samples.



The medium was removed and the cells washed with PBS (1 ml). Lysis buffer (25 mM Tris-phosphate pH 7.8, 2 mM DTT, 2 mM 1,2-diaminocyclohexane-N,N,N',N'-tetraacetic acid, 10 % (w/v) glycerol, 1 % (v/v) Triton X-100) was prepared with distilled water and allowed to equilibrate to room temperature. Lysis buffer (200 μ l) was then added to the cells and left for 1 min. The cells were lysed by pipetting, and each sample transferred to a 1.5 ml microfuge tube and kept on ice. The samples were vortexed for 15 s and centrifuged at 12,000 rpm for 15 s in a microcentrifuge to pellet the cell debris. The supernatant from each sample was transferred to a fresh 1.5 ml microfuge tube and kept on ice. The luciferase substrate was equilibrated to room temperature and 100 μ l added to each luminometer tube. 20 μ l of cell lysate was added to the luciferase substrate, the sample mixed and the luciferase activity of each sample measured over 5 min using a Junior LB 9509 luminometer.

2.13. Statistical analysis

The data are shown as the mean of experiments \pm standard deviation (SD). The statistical package for the social sciences (SPSS) was used for statistical analysis of the results. Significance was determined using one-way ANOVA and p values < 0.05 were taken as significant.

CHAPTER 3

The influence of exogenous tissue factor on the expression of ER α in breast cancer cells

3.1. Introduction

3.1.1. The role of ER α expression in breast cancer cell proliferation and invasion

Oestradiol-ER α signalling results in the increased rate of cell proliferation of ER α -positive cells by upregulating the expression and activity of proteins involved in the cell cycle such as cyclin D and cyclin dependent kinases (Foster et al 2001, Prall et al 1998). In breast tissue, increased rates of cellular proliferation in response to oestrogens can promote the initiation of breast cancer and also the growth of existing breast tumours (Clarke et al 1997). However, the presence of ER α in breast tumours has been associated with more differentiated, less invasive tumours, with a better prognosis for the patient (Godolphin et al 1981). Furthermore, the loss of ER α is associated with the progression of breast tumours to a less differentiated, invasive phenotype and oestradiol-independent growth (Thompson et al 1992, Desombre 1984). Therefore, it has been suggested that ER α may have a protective function against cell invasion and consequently the rate of cancer metastasis. During the progression of tumours from benign to malignant forms, cancer cells acquire the ability to degrade the surrounding extracellular matrix and migrate through basement membranes, allowing cancer cells to metastasise to secondary sites (Knowles & Selby 2005). The ability of cancer cells to invade surrounding tissues is the first step in this process and involves the loss of cell to cell adherence, rearrangement of the cytoskeleton and the production of enzymes to degrade the extracellular matrix (Knowles & Selby 2005). Several studies have reported an anti-invasive function for ER α in breast cancer cells. Initially it was observed that ER α positive breast cancer cell lines are less invasive than ER α negative cells both *in vitro* and *in vivo* (Thompson et al 1992). In addition, treatment of ER α -positive cells with oestrogen was shown to reduce cell invasiveness whereas anti-oestrogens increased cell invasiveness (Rochefort et al 1998). Furthermore, transfection of functional ER α into

highly invasive, ER α -negative breast cancer cell lines results in reduced invasiveness in these cells (Platet et al 2000, Garcia et al 1992). The oestradiol-ER α complex downregulates the transcription of specific genes that promote cell invasion such as the matrix metalloproteinases (MMPs), which degrade the extracellular matrix (Nilsson et al 2007, Lu et al 2006). Furthermore, the oestradiol-ER α complex upregulates the expression of anti-proteases such as α 1-anti-chymotrypsin, which inhibit matrix degradation (Rocheffort et al 2001). Therefore, understanding the mechanisms by which ER α expression is downregulated will elucidate some of the processes that occur during the progression of breast tumours to more invasive, oestrogen-independent phenotypes. Among the signalling pathways known to influence ER α expression are the MAPK pathways. One such cell signalling pathway is the ERK1/2 pathway (Creighton et al 2006, Kronblad et al 2005), the induction of which has been shown to downregulate ER α in breast cancer cells (Holloway et al 2004, Oh et al 2001). In addition, the transcriptional enhancer region upstream of the ER α gene contains an AP-1 response element (Tang et al 1997), which positively regulates ER α expression through the activation of the JNK signalling pathway (Huang et al 2006).

3.1.2. The association between TF expression and breast cancer invasiveness

The association between increased expression of TF and more invasive breast tumours is well established (Contrino et al 1996, Vrana et al 1996). Furthermore, overexpression of TF in breast cancer cell lines results in increased invasiveness in these cells *in vitro* (Kato et al 2005). TF has been shown to promote breast cancer cell migration through the formation of the TF:FVIIa:FXa complex which activates PAR2 and downstream signalling pathways (Hjortoe et al 2004, Jiang et al 2004). Furthermore, the ability of TF to induce breast cancer metastasis *in vivo* may be inhibited using a specific anti-TF monoclonal antibody (Ngo et al 2007).

3.1.3. Aims

Recombinant truncated TF was used in this investigation to represent soluble or microparticle-derived TF that is released from infiltrating stromal cells in the vicinity of the tumour. Initially, the influence of exogenous TF on breast cancer cell proliferation and invasion in the presence and absence of 17 β -oestradiol was examined. The recombinant human truncated TF used in this investigation constitutes the active component of the Innovin reagent and consists of the extracellular domain and transmembrane domain of TF (amino acids 1-242) but lacks the cytoplasmic domain. Furthermore, in the Innovin reagent TF is incorporated into phospholipid vesicles (60:20:20 phosphatidylcholine: phosphatidylserine: phosphatidylethanolamine) for optimal procoagulant activity. Therefore, to confirm that the influence of the Innovin reagent arose from the TF protein and not the lipid component, the influence of the lipid component on cell proliferation was examined. Subsequently, the influence of exogenous TF on ER α expression was investigated. The main objectives of the study were as follows.

- To establish the influence of exogenous TF on the proliferation of ER α -positive breast cancer cells
- To confirm that the function was due to the TF component of the Innovin reagent
- To examine the influence of exogenous TF on ER α expression in breast cancer cells
- To examine the influence of exogenous TF on the invasiveness of ER α -positive breast cancer cells

3.2. Methods

3.2.1. Analysis of endogenous TF expression in breast cancer cells

3.2.1.1. Analysis of cell surface TF expression by flow cytometry

MCF-7, T47D, ZR-75-1 and MDA-MB-231 human breast cancer cells (5×10^5 each) were harvested, washed twice with PBS (1 ml) and resuspended in PBS (100 μ l) containing the mouse monoclonal anti-human TF FITC-conjugated antibody (2 μ g/ml final concentration). Parallel sets of cells were incubated with a goat anti-rabbit IgG FITC-conjugated antibody (4 μ g/ml final concentration) as negative controls. Cells were incubated for 30 min at 4°C in the dark, washed and resuspended with PBS (300 μ l) and analysed by flow cytometry as described in the general methods section 2.4.

3.2.1.2. Determination of TF activity on cells using the PT assay

MCF-7, T47D, ZR-75-1 and MDA-MB-231 cells were harvested and washed with PBS (1 ml). Cell numbers were determined and serial dilutions of cells (4×10^5 , 8×10^5 and 10^6) were prepared in PBS (100 μ l) in duplicate. The clotting time of each sample was determined using the PT assay as described in the general methods section. TF activity (units/ml) of the samples was determined from the previously prepared standard curve (Fig 2.3). The calculated concentrations of TF were used to determine TF activity per 10^6 cells.

3.2.2. The influence of TF and oestradiol on cell proliferation

3.2.2.1. Examination of the influence of TF and oestradiol on cell proliferation

17 β -oestradiol (50 mg) was reconstituted in a minimal volume of absolute ethanol and incubated at 50°C until completely dissolved. The solution was then diluted in PBS by

drop-wise addition to 0.1 μM oestradiol which was used as a stock solution. MCF-7 or T47D cells (5×10^4) were seeded out into 12 well plates in complete medium and incubated with the recombinant human truncated TF Innovin reagent (0-500 nM) in the presence and absence of oestradiol (0-1000 pM) for 24 h. The rate of cell proliferation was determined using the MTS based assay (section 2.3). The study was then repeated over 24, 48 and 72 h using phenol red-free medium supplemented with 1 % FCS to reduce the oestrogenic influence of phenol red or serum-derived oestrogens.

3.2.2.2. Purification of lipids by delipidation of recombinant TF

The recombinant TF reagent was dissolved in ice-cold chloroform (25 ml) for 2 h on a rolling platform. Methanol (25 ml) was added and incubated at -20°C for 2 h to precipitate proteins, and the solution was then centrifuged at 500 *g* for 10 min. The supernatant was transferred to a conical flask attached to a rotary evaporator in a water bath at 40°C and incubated for 2 h until the chloroform had evaporated. The lipids were then freeze-dried to ensure the removal of chloroform and then resuspended in 10 ml of phenol red-free MEM to the original concentration in the Innovin reagent and kept under nitrogen. The lipids were also supplemented with 1 % (w/v) BSA in order to buffer the lipids, as in the original Innovin reagent.

3.2.2.3. The influence of lipids extracted from recombinant TF on cell proliferation

MCF-7 cells (5×10^4) were seeded out into 12 well plates in phenol red-free medium supplemented with 1 % FCS and incubated with lipids (diluted to the same concentrations as the Innovin reagent used) extracted from recombinant TF for 24 h. Following 24 h incubation, cell proliferation was measured using the MTS-based assay as before.

3.2.3. Examination of the influence of TF on ER α mRNA expression in breast cancer cells

3.2.3.1. Design and optimisation of primers for RT-PCR analysis of ER α and ER β

The full length cDNA sequences for ER α and ER β were obtained from published sequences on PubMed (Green et al 1986, Mosselman et al 1996). Primers were designed for both genes using the Basepair program. Ideally, primers should be 18 to 24 bp in length and have a GC content of 40 to 60 %. The expected DNA fragment sizes were 511 bp for ER α , 456 bp for ER β designed using Basepair program, and 460 bp for the β -actin primer set. In addition, a set of published ER β primers (Kurebayashi et al 2000) with an expected fragment size of 346 bp were used.

The primer sets for ER α and ER β designed using the Basepair program were optimised for RT-PCR by carrying out RT-PCR with RNA isolated from MCF-7 cells over a range of annealing temperatures of 50-60°C and number of cycles of amplification. In order to optimise the number of amplification cycles, six reactions were set up with RT-PCR beads and the primers as described in the general methods section 2.5.3. A tube was removed after 21 cycles and subsequently after every second cycle up to 31 cycles, and the RT-PCR products analysed by 2 % (w/v) agarose gel electrophoresis. The annealing temperatures and number of amplification cycles of the primer sets are shown in table 3.1.

3.2.3.2. Analysis of baseline ER α and ER β mRNA expression using RT-PCR

MCF-7, T47D, ZR-75-1 and MDA-MB-231 cells (5×10^5) were harvested and total RNA was isolated. The quantity and purity of each RNA sample was determined as described in the general methods section. Three RT-PCR reactions were set up with each RNA sample and the ER α , ER β , and β -actin primers added to separate tubes and the RT-PCR reactions

Table 3.1. Primer sequences and conditions for RT-PCR

Gene	Primer sequence	Temp. (°C)	No. of cycles
ER α	For: 5'-TCA GAT AAT CGA CGC CAG G-3' Rev: 5'-GGC TCA GCA TCC AAC AAG G-3'	59	25
ER β	For: 5'-GCA GTC AAT CCA TCT TAC C-3' Rev: 5'- TTA CAT CCT TCA CAC ACG ACC-3'	N/A	N/A
ER β (Kurebayashi et al 2000)	For: 5'-TCA CAT CTG TAT GCG GAA CC-3' Rev: 5'-CGT AAC ACT TCC GAA GTC GG-3'	58	30
β -actin	For: 5'-CCA GAG CAA GAG AGG CAT CC-3' Rev: 5'-CTG TGG TGG TGA AGC TGT AG-3'	58	18

carried out as before. The RT-PCR products were examined by agarose gel electrophoresis and images recorded using the GeneSnap program.

3.2.3.3. Analysis of the influence of TF on ER α mRNA expression using RT-PCR

MCF-7 and T47D cells (2×10^5) were seeded out into 12 well plates and incubated with recombinant TF (0-500 nM) for 24 h. The cells were then harvested and total RNA isolated from the cell samples. The samples were amplified by RT-PCR using the ER α and β -actin primer sets and the products examined by agarose gel electrophoresis. Images were recorded using the GeneSnap program and ER α expression compared to β -actin using the GeneTool program.

3.2.4. Examination of the influence of TF on ER α protein expression in breast cancer cells

3.2.4.1. Analysis of the influence of TF on ER α protein expression by western blot

MCF-7 and T47D cells (2×10^5) were seeded out into 12 well plates and incubated with recombinant TF (0-500 nM) for 24 h. The cells were then harvested, lysed in Laemmli's buffer (200 μ l) and protein concentrations estimated using the Bradford assay as described in the general methods section 2.6. Protein samples were separated using 12 % (w/v) SDS-PAGE and transferred onto nitrocellulose membranes as described in the general methods section 2.7. The membranes were then probed for ER α and GAPDH with appropriate antibodies as described in the general methods section 2.8. Images were recorded using the GeneSnap program and ER α expression was compared to GAPDH using the GeneTool program.

3.2.4.2. Analysis of the influence of TF on ER α protein expression by ELISA

A commercial sandwich ELISA kit (NR Sandwich ER α ELISA) was used to measure ER α protein levels. MCF-7 or T47D cells (2×10^5) were seeded out into 12 well plates and treated with recombinant TF (0-500 nM) for 24 h. The cells were then harvested and whole cell extracts prepared using the Nuclear Extract Kit as follows. Cells were lysed in 50 μ l of complete lysis buffer (lysis buffer (composition not revealed), 10 mM DTT, 1 % (v/v) protease inhibitors). The samples were vortexed for 10 s, incubated on ice for 10 min on a rocking platform at 100 rpm and finally vortexed for a further 30 s to ensure complete cell lysis. The cell debris was pelleted by centrifugation at 14,000 rpm for 10 min in a microcentrifuge. The supernatant was then transferred to a 1.5 ml tube and protein concentrations of the samples determined using the Bradford assay.

10 μ g of protein from each cell sample was added to separate wells in the ELISA plate in duplicate and incubated for 1 h at room temperature on a rocking platform at 100 rpm. The wells were washed three times with wash buffer (200 μ l) and then incubated with the supplied rabbit anti-human ER α antibody, diluted 1:400 in diluent buffer (50 μ l), for 1 h at room temperature. The wells were then washed three times with wash buffer (200 μ l) and incubated with the supplied anti-rabbit HRP-conjugated secondary antibody diluted 1:1000 in diluent buffer (50 μ l) for 1 h at room temperature. Finally, the wells were washed four times with 200 μ l of wash buffer and developed with the supplied HRP substrate solution (100 μ l) for 9 min in the dark. The reactions were terminated with 0.5 M sulphuric acid (100 μ l) and the absorptions measured at 450 nm with a reference at 620 nm using an Anthos 2010 microplate reader. To prepare a standard curve, serial dilutions of recombinant ER α protein were prepared in diluent buffer. 50 μ l of each sample was added to wells in

duplicate to give final concentrations of 0, 31.25, 62.5, 125, 250, 500, 1000 and 2000 ng/ml of ER α protein. The ELISA was carried out alongside the samples as described above. The standard curve of ER α protein concentration against absorption at 450 nm was prepared and used to convert absorption values from the unknown samples into ER α protein concentrations.

3.2.5. Analysis of the long-term influence of TF on ER α mRNA and protein expression

MCF-7 cells were cultured in three T75 flasks in complete MEM (12 ml) supplemented with recombinant TF (0-500 nM). The cells were supplemented with fresh medium every 3 days and recombinant TF as above. Samples of cells were harvested from each flask over a period of 5 weeks as follows. The cells were subcultured every 7 days and two sets of cells (10^6) from each flask were removed, washed with PBS and pelleted in 1.5 ml eppendorf tubes and stored at -70°C until required. The remainder of the cells were cultured under the above conditions and harvested periodically. RNA was isolated from the cell samples and analysed by RT-PCR using ER α and β -actin primers as described in section 2.5.3. ER α protein levels were examined by SDS-PAGE and western blot for ER α and GAPDH as described in section 2.8.

3.2.6. Examination of the influence of TF on breast cancer cell invasion

3.2.6.1. Influence of TF on cell migration using a Boyden chamber based assay

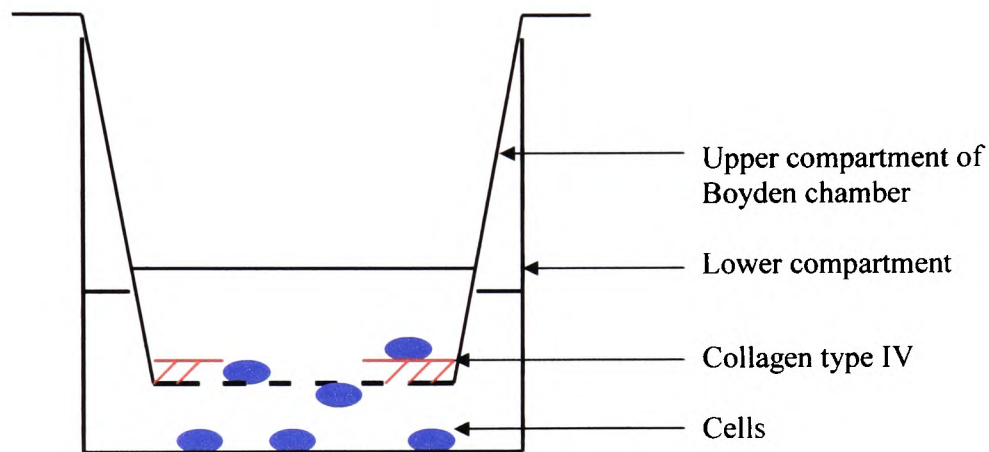
A Boyden chamber method based on the migration of cells across a collagen type IV membrane was used to examine the influence of TF on cell invasion. Boyden chambers with 8 μm pore size were placed in the wells of a 24 well plate and coated with 50 μl collagen type IV (1 mg/ml (w/v)) by incubation at 37°C for 12 h. Following the incubation,

excess collagen solution was removed and MCF-7 or T47D cells (2×10^5) were seeded out into the upper compartment of each Boyden chamber in phenol red-free medium (250 μ l) supplemented with 1 % (v/v) FCS. Oestradiol (250 pM) was added to the medium in the upper chamber in parallel with control samples without oestradiol. Phenol red-free medium (250 μ l) supplemented with TF (0-500 nM) was added to the lower compartment (Fig 3.1). The cells were incubated at 37°C for 24 h to allow migration through the collagen barrier. Following 24 h incubation, cells on the upper side of the filter were removed using a cotton swab and discarded. The volume of the medium in the lower chamber was measured and adjusted to 500 μ l with medium. CellTiter 96 AQueous One Solution reagent (40 μ l) was added to the lower compartment and the empty Boyden chambers placed back into the wells. The cells were then incubated for 5 h at 37°C, until a colour change was observed. The absorption of each sample (240 μ l) was then measured at 490 nm and the number of cells that had migrated across the filter determined using the previously prepared standard curve (Fig 2.1).

3.2.6.2. Examination of changes in cell morphology in response to exogenous TF

MCF-7 cells (2×10^4) were seeded out into 8 well cultureslides in MEM medium containing 1 % FCS and incubated at 37°C for 24 h. The cells were treated with TF (0-500 nM) or basic fibroblast growth factor (bFGF) (30 ng/ml) as a positive control (Johnston et al 1995) and incubated at 37°C for 48 h. The cells were then washed with PBS and fixed with 3 % (v/v) glutaraldehyde for 20 min at room temperature. The cells were washed three times with PBS and incubated at 37°C for 15 min with the cell membrane stain 1, 1'-Dioctadecyl-3, 3, 3', 3'-tetramethylindocarbocyanine perchlorate (DiI) at a final

Figure 3.1. Schematic representing the set up of the Boyden chamber based migration assay.



Boyden chambers with pores (8 μm) were placed into 24 well plates and coated with type IV collagen. Cells (2×10^5) were placed in the upper chamber containing medium with oestradiol (0-250 pM). The lower compartment containing medium was supplemented with TF (0-500 nM) and the cells incubated for 24 h to allow cells to migrate across the filter. Cells in the upper compartment were removed and the CellTiter reagent placed in the lower compartment. The number of migrated cells was determined by measuring absorption of the samples at 490 nm.

concentration of 10 µg/ml. The cells were then washed three times with PBS and visualised using a CoolSnap Pro camera attached to a Leitz Laborlux S fluorescence microscope. Images were processed using the Image-Pro Plus Version 5.1.2.

3.2.6.3. Influence of TF on cell invasion using collagen type I gels

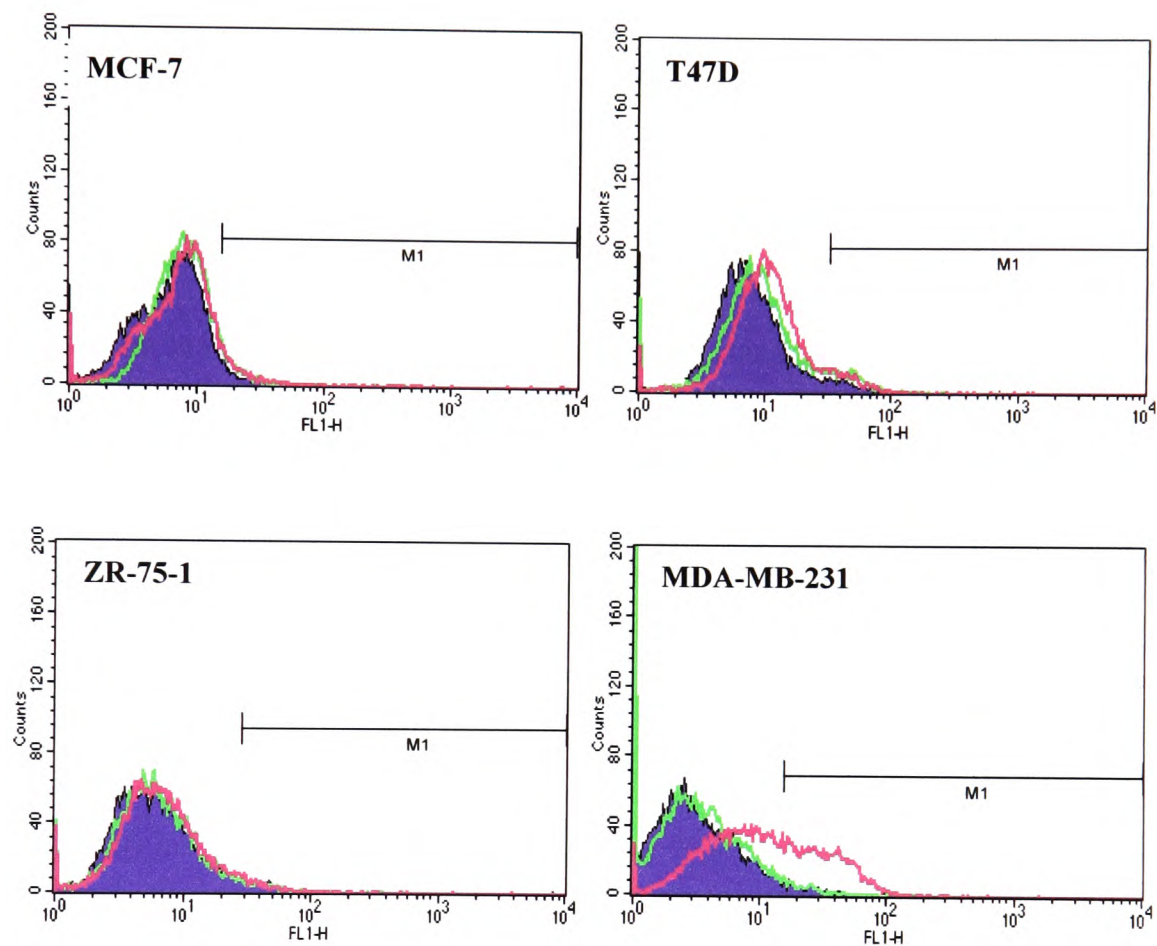
A collagen solution was prepared by mixing rat tail collagen type I (4.66 mg/ml in 0.02 M acetic acid (w/v)) mixed with appropriate amounts of 10× sterile MEM to produce a range of collagen concentrations (0.28-0.38 % (w/v)) and neutralised with 1 M sterile NaOH. The collagen solutions (0.5 ml) were placed in individual wells in a 24 well plate and incubated at 37°C overnight to allow the collagen to solidify. Cells (10^4) were seeded out onto the collagen gels in 0.5 ml complete MEM and incubated at 37°C for 24 h to allow adherence. The cells were supplemented with TF (0-500 nM) and examined daily using a light microscope. The cells were supplemented with fresh medium and test reagents every 3 days up to 7 days.

3.3. Results

3.3.1. Determination of cell surface TF expression in breast cancer cell lines

The expression of cell surface TF in four breast cancer cell lines was examined by flow cytometry using a monoclonal anti-human TF FITC-conjugated antibody. 10,000 events were measured and a gate set to contain 3 % of unlabelled cells. 7.2 % of MCF-7 cells, 6.5 % of T47D cells, 3.7 % of ZR-75-1 cells and 35.4 % of MDA-MB-231 cells were in this region (Fig 3.2). In addition, TF procoagulant activity on the surface of each cell line was measured using the PT assay, since there is often disparity between TF antigen and

Figure 3.2. Analysis of cell surface TF in breast cancer cell lines by flow cytometry



Cells (5×10^5) were labelled with an anti-TF FITC-conjugated antibody or a goat anti-rabbit FITC-IgG control antibody for 30 min in the dark. The cells were then washed three times in PBS (1 ml), resuspended in PBS (300 μ l) and analysed on a FACSCalibur flow cytometer. 10,000 events were measured and a gate was set to contain 3 % of unlabelled cells. The mean fluorescence and number of fluorescent events was measured and analysed using the CellQuest software program. Area = untreated cells, red line = anti-human TF FITC-conjugated antibody, green line = FITC-IgG control.

procoagulant activity in tumour cells. The TF procoagulant activities of the breast cancer cells mirrored TF antigen expression, with MCF-7 cells having no detectable procoagulant activity and MDA-MB-231 cells showing high TF activity (Table 3.2). ZR-75-1 cells exhibited very low procoagulant activity, while T47D cells had slightly higher procoagulant activity. These data indicate that MCF-7, T47D and ZR-75-1 cells express little to no TF, while MDA-MB-231 cells express high levels of TF.

3.3.2. Analysis of cell proliferation in response to TF and oestradiol

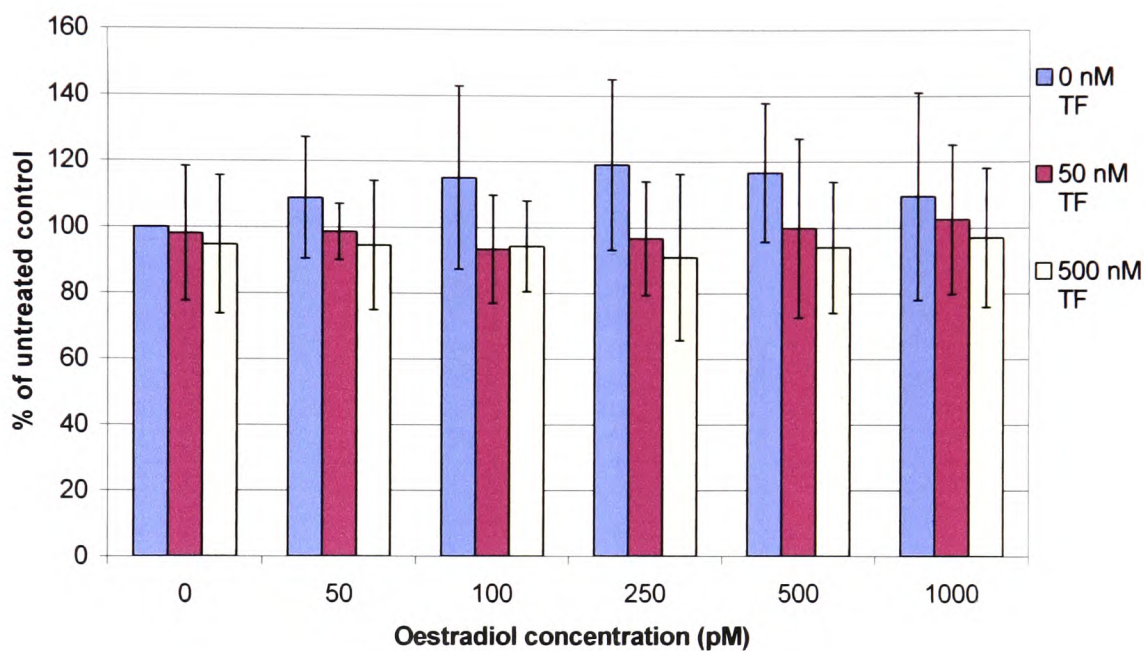
Incubation of MCF-7 cells with TF (50 and 500 nM), in culture medium containing phenol red and 10 % (v/v) FCS, had no detectable influence on the proliferation rate of MCF-7 cells at 24 h post-treatment (Fig 3.3). Furthermore, the addition of oestradiol (50-1000 pM) resulted only in small increases in the rate of cell proliferation. The addition of TF (50 and 500 nM) together with oestradiol (100-500 pM) appeared to interfere with the oestradiol-mediated cell proliferation, but the differences were not significant (Fig 3.3). Since the pH indicator phenol red, which is present in culture medium, is known to have oestrogenic properties the assay was repeated in phenol red-free culture medium containing 1 % (v/v) FCS in order to reduce the amount of oestrogens in the medium. Measurement of the response of MCF-7 cells to TF (50 nM) indicated increased rates of proliferation over 24 to 48 h (Fig 3.4 & 3.5). Examination of the influence of TF (500 nM) showed no detectable effect on cell proliferation at 24 h, but appeared to inhibit MCF-7 cell proliferation rates between 48 and 72 h compared to the untreated control (Fig 3.5 & 3.6). The addition of oestradiol (100-500 pM) to MCF-7 cells seemed to induce proliferation when examined over 24 to 72 h, and was largely unaffected by the addition of 50 nM TF. However, the appearance of a trend was observed in which the addition of a combination of TF (500 nM) with a range of concentrations of oestradiol (100-500 pM) seemed to reduce the rate of

Table 3.2. Procoagulant activity of breast cancer cell lines

Breast cancer cell line	Clotting time (s)			TF (U/10⁶ cells)
	4 × 10⁵ cells	8 × 10⁵ cells	10⁶ cells	
MCF-7	No clot	No clot	No clot	0
ZR-75-1	No clot	98.5 ± 8.5	90 ± 1.4	0.39
T47D	No clot	No clot	64.7 ± 2.4	1.04
MDA-MB-231	38.2 ± 1.6	31.4 ± 3.6	27.7 ± 2.9	14.2

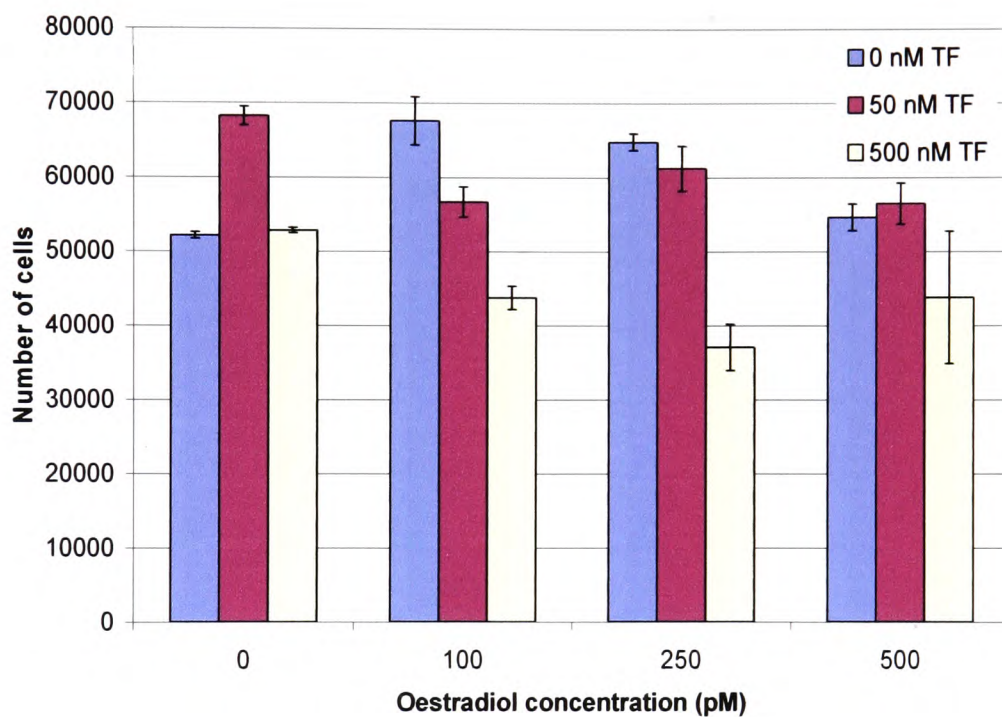
Breast cancer cells were harvested and serial dilutions of the cells (4×10^5 , 8×10^5 and 10^6) were prepared in PBS (100 μ l) in duplicate. The PT assay was carried out with each sample and the clotting time recorded using a Cascade M coagulometer. Clotting times were converted to units of TF activity using a standard curve prepared with a range of concentrations of recombinant TF. The calculated concentrations of TF were then used to determine TF activity per 10^6 cells. The data represents the average of two independent experiments \pm SD.

Figure 3.3. The influence of TF on the rate of MCF-7 proliferation in complete medium



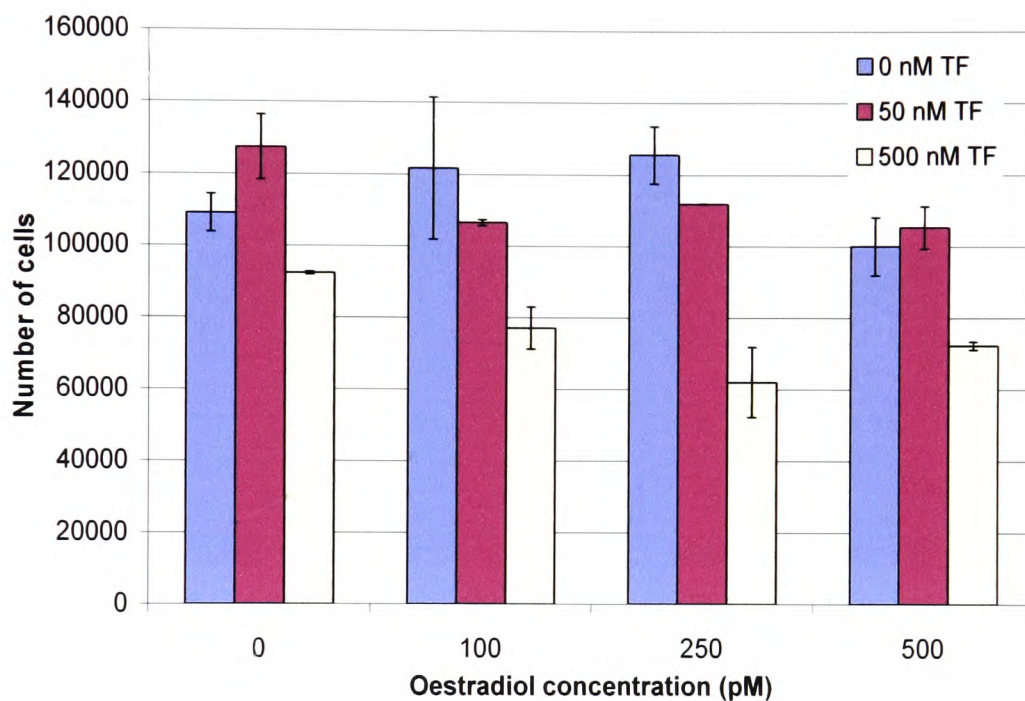
MCF-7 cells (5×10^4) were seeded out into 12 well plates and treated with recombinant TF (0-500 nM) and oestradiol (0-1000 pM). The rate of proliferation was measured at 24 h post-treatment using the MTS-based assay and cell numbers determined using the standard curve. The data is representative of eight individual experiments \pm SD.

Figure 3.4. The influence of TF on the rate of MCF-7 proliferation in phenol red-free medium at 24 h



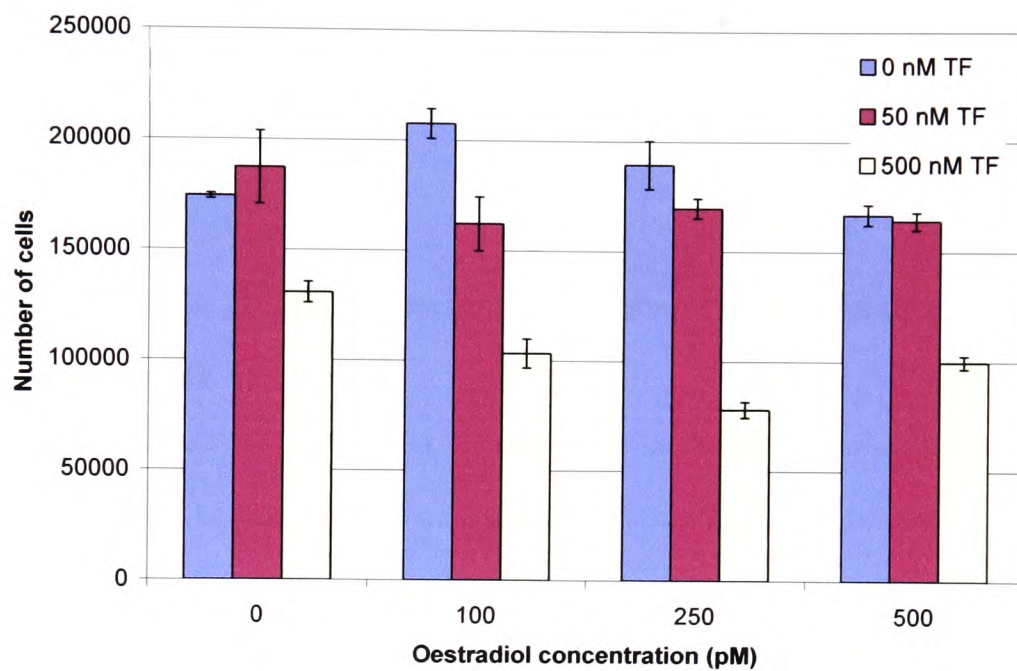
MCF-7 cells were (5×10^4) were seeded out into 12 well plates and treated with recombinant TF (0-500 nM) and oestradiol (0-500 pM). The rate of proliferation was measured at 24 h post-treatment using the MTS-based assay. The data is representative of two independent experiments \pm SD.

Figure 3.5. The influence of TF on the rate of MCF-7 proliferation in phenol red-free medium at 48 h



MCF-7 cells (5×10^4) were seeded out into 12 well plates and treated with recombinant TF (0-500 nM) and oestradiol (0-500 pM). The rate of proliferation was measured at 48 h post-treatment using the MTS-based assay. The data is representative of two independent experiments \pm SD.

Figure 3.6. The influence of TF on the rate of MCF-7 proliferation in phenol red-free medium at 72 h



MCF-7 cells (5×10^4) were seeded out into 12 well plates and treated with recombinant TF (0-500 nM) and oestradiol (0-500 pM). The rate of proliferation was measured at 72 h post-treatment using the MTS-based assay. The data is representative of two independent experiments \pm SD.

MCF-7 cell proliferation, with maximal suppression observed in the presence of 250 pM oestradiol. Incubation of T47D cells with TF (0-500 nM) and oestradiol (0-500 pM) appeared to have little influence on cell proliferation following 24 h (Fig 3.7). However, T47D cells incubated with oestradiol (100-250 pM) exhibited an increased tendency to proliferate when measured at 48 h (Fig 3.8). The inclusion of TF (500 nM) together with oestradiol (250 pM) appeared to reduce the rate of T47D cell proliferation at 48 and 72 h (Fig 3.8 & 3.9).

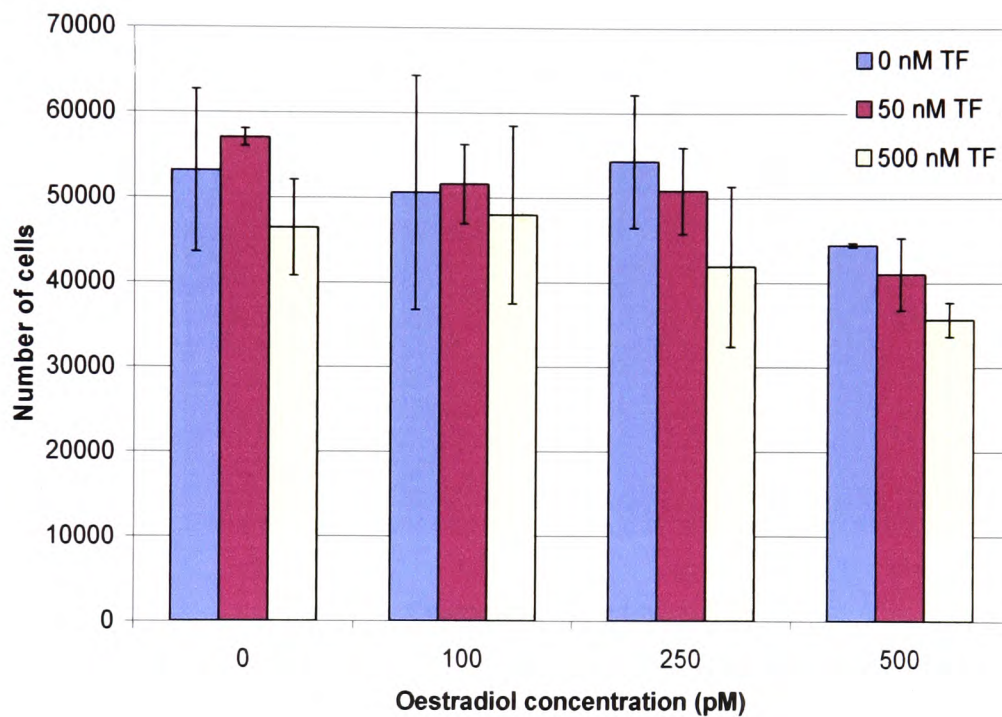
3.3.3. Analysis of cell proliferation in response to the lipids extracted from recombinant TF

Lipids extracted from recombinant TF were tested for residual TF using the PT assay, and were shown to be free from any procoagulant activity. The influence of the lipids on cell proliferation was examined using the MTS-based assay. Incubation of MCF-7 cells with lipids alone (diluted $\times 100$ and $\times 10$) had no measurable effect on cell proliferation over 24 h (Fig 3.10). Furthermore, the addition of lipids (diluted $\times 100$ and $\times 10$) together with oestradiol (250 pM) slightly reduced the rate of proliferation, but not to the same extent as recombinant TF (500 nM) with oestradiol (250 pM) (Fig 3.4), indicating that the contribution of the TF-associated lipids to the suppression of oestradiol induced proliferation is minimal.

3.3.4. Optimisation of the RT-PCR conditions using the ER α and ER β primers

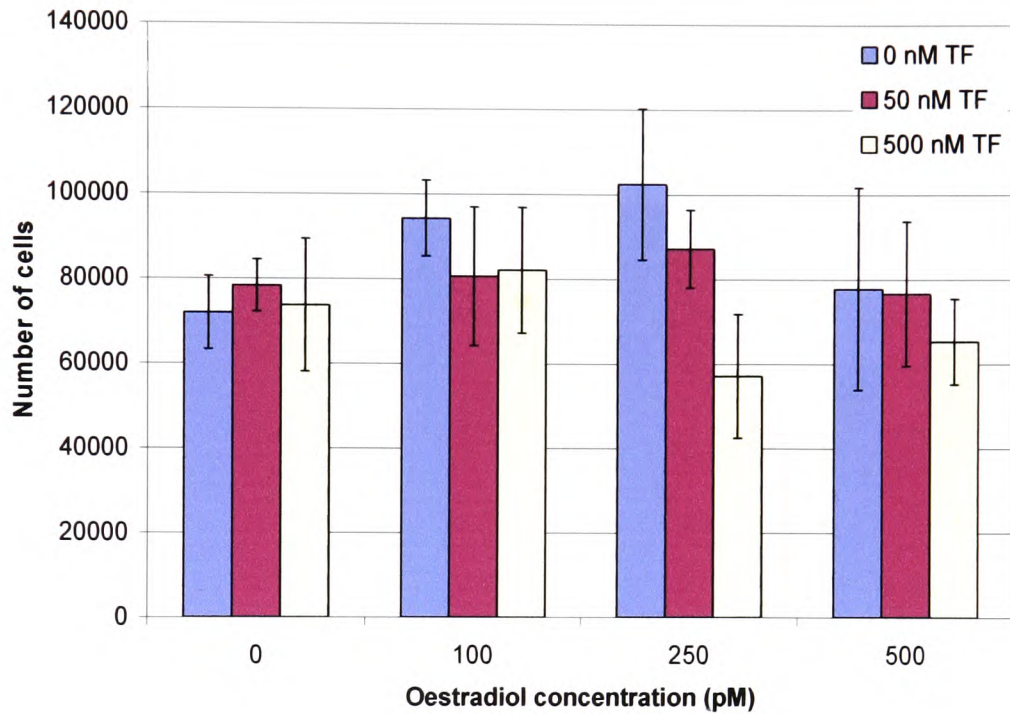
The annealing temperature and number of cycles of amplification for the ER α and ER β primer sets, designed using the BasePair program, were optimised for RT-PCR. The optimal annealing temperature and number of cycles of amplification for the ER α primers were determined as 59°C and 25 cycles respectively (Fig 3.11). A range of annealing

Figure 3.7. The influence of TF on the rate of T47D proliferation in phenol red-free medium at 24 h



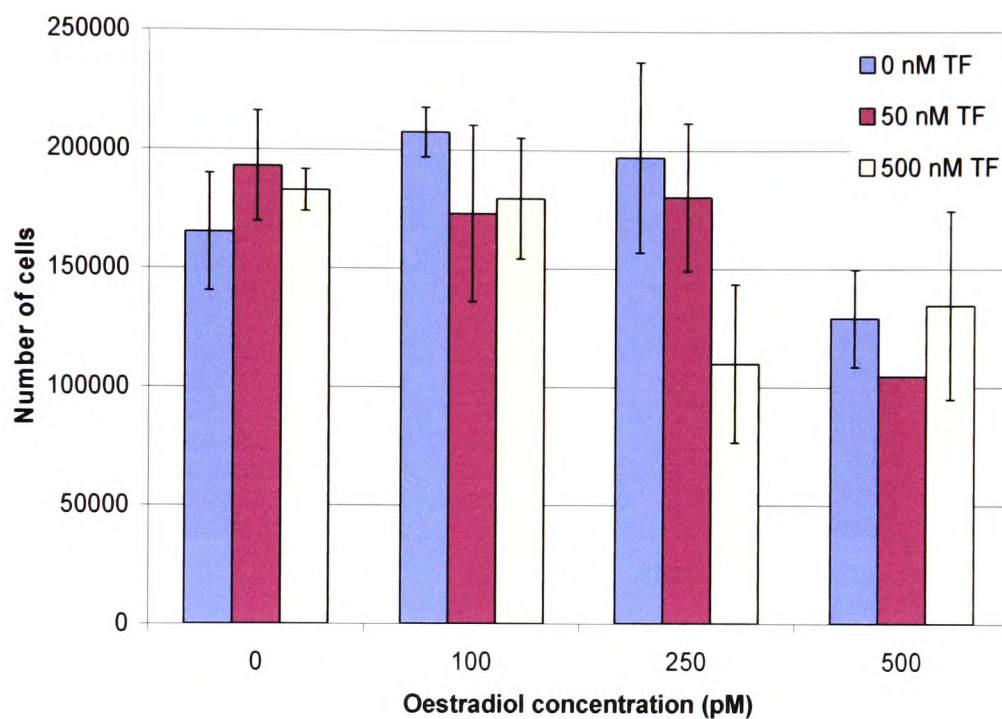
T47D cells (5×10^4) were seeded out into 12 well plates and treated with recombinant TF (0-500 nM) and oestradiol (0-500 pM). The rate of proliferation was measured at 24 h post-treatment using the MTS-based assay. The data is representative of two independent experiments \pm SD.

Figure 3.8. The influence of TF on the rate of T47D proliferation in phenol red-free medium at 48 h



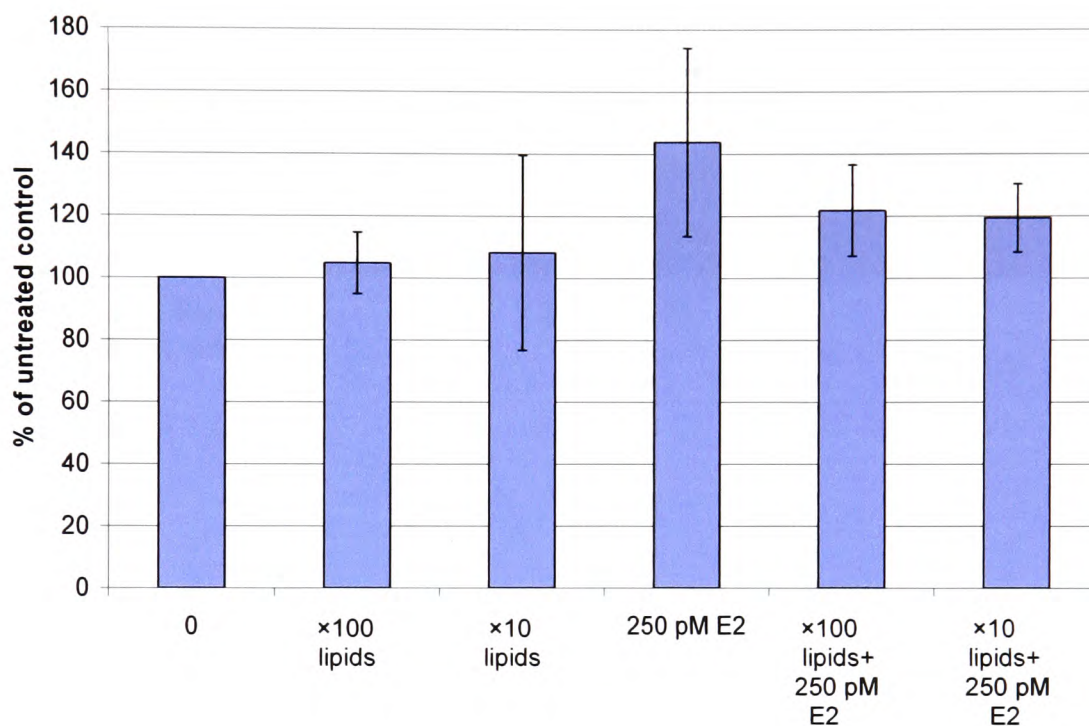
T47D cells (5×10^4) were seeded out into 12 well plates and treated with recombinant TF (0-500 nM) and oestradiol (0-500 pM). The rate of proliferation was measured at 48 h post-treatment using the MTS-based assay. The data is representative of two independent experiments \pm SD.

Figure 3.9. The influence of TF on the rate of T47D proliferation in phenol red-free medium at 72 h



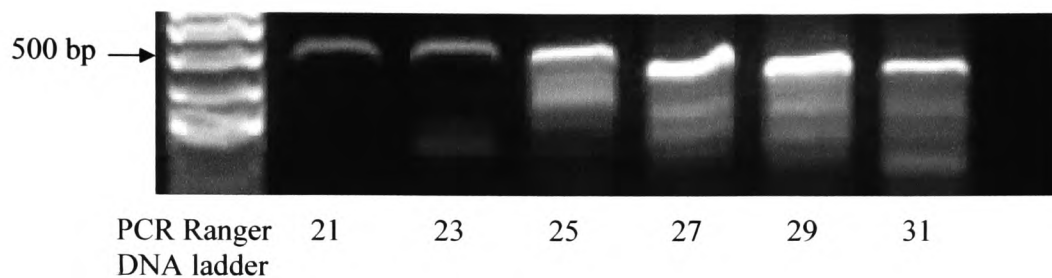
T47D cells (5×10^4) were seeded out into 12 well plates and treated with recombinant TF (0-500 nM) and oestradiol (0-500 pM). The rate of proliferation was measured at 72 h post-treatment using the MTS-based assay. The data is representative of two independent experiments \pm SD.

Figure 3.10. The influence of lipids extracted from TF on MCF-7 proliferation



MCF-7 cells were treated with lipids extracted from recombinant TF (diluted ×100 and ×10) and oestradiol (0-250 pM). The rate of proliferation was measured at 24 h post-treatment using the MTS-based assay. The data is representative of five independent experiments in duplicate ± SD.

Figure 3.11. Optimisation of the ER α primers for RT-PCR



RNA was isolated from MCF-7 cells and six reactions set up using Ready-to-go RT-PCR beads and the ER α primers. RT-PCR was carried out for 31 cycles amplification with an annealing temperature of 59°C. A tube was removed every two cycles starting from cycle 21 and the RT-PCR products analysed by 2 % (w/v) agarose gel electrophoresis and images taken using the GeneSnap program.

temperatures was used to optimise the ER β amplification reaction using the designed ER β primers, but no observable bands were obtained with any of the test conditions. Therefore, a second set of published ER β primers were tested according to the published conditions (Kurebayashi et al 2000). However, no detectable bands were obtained using the procedure and therefore it was presumed that MCF-7 cells do not express this protein.

3.3.5. Analysis of baseline expression of ER α and ER β mRNA in breast cancer cells

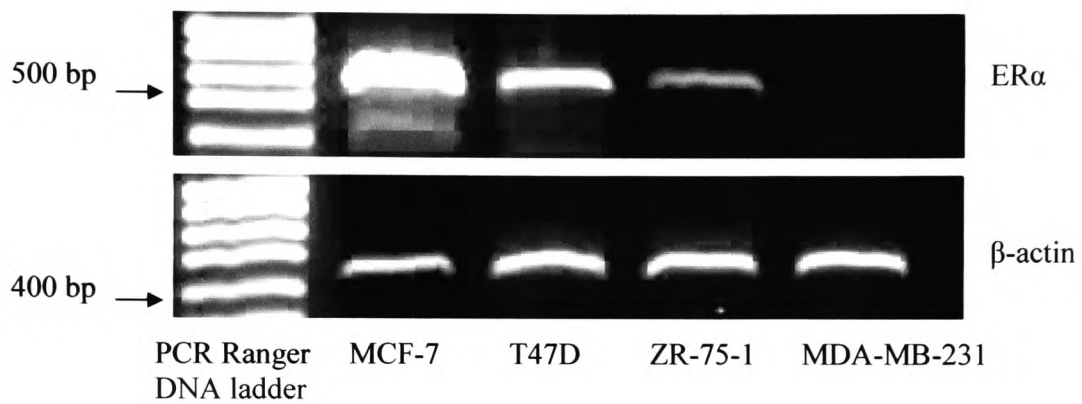
Baseline expression of ER α and ER β mRNA in four breast cancer cell lines was examined by RT-PCR. MCF-7 cells expressed the highest levels of ER α , while T47D cells had lower levels of ER α (Fig 3.12). ZR-75-1 cells expressed very low levels of ER α and MDA-MB-231 had no detectable ER α . No ER β bands were detected using either set of primers in any of the breast cancer cell lines tested and therefore it was assumed that these cells do not express this protein.

3.3.6. Investigation of the influence of TF on ER α expression in breast cancer cell lines

3.3.6.1. Investigation of the influence of TF on the expression of ER α mRNA

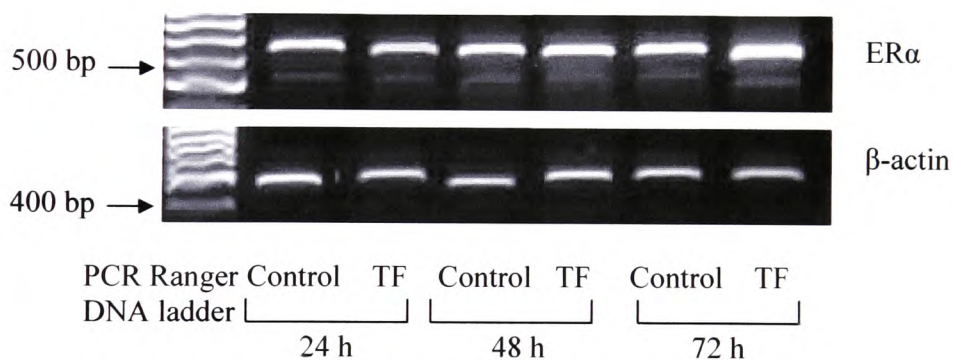
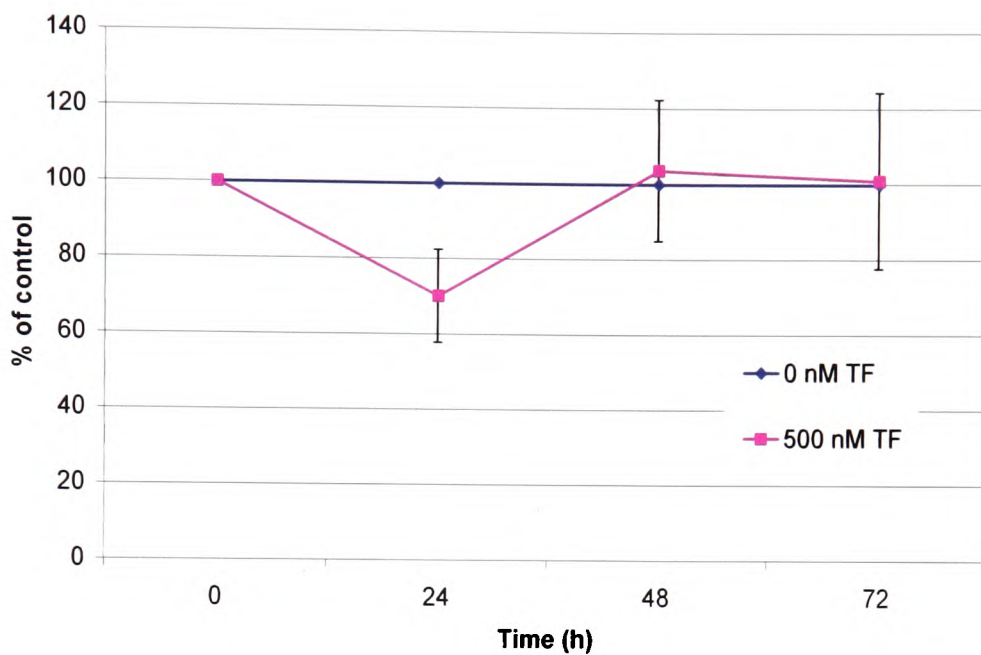
MCF-7 and T47D cells were used to examine the influence of TF on ER α expression, as these cells were shown to express high levels of ER α but had little to no TF. The influence of TF on ER α expression in MCF-7 cells was initially examined over 72 h. The expression of ER α mRNA in MCF-7 cells appeared to follow a trend in which the initial decrease at 24 h incubation was normalised by 48 h post-treatment with TF (500 nM) (Fig 3.13.). Furthermore, the decrease in ER α mRNA expression seemed to be TF concentration dependent, with 25 % and 36 % reductions in ER α mRNA expression observed on incubation with 50 and 500 nM TF respectively (Fig 3.14). Incubation of T47D cells with

Figure 3.12. Baseline ER α expression levels in breast cancer cell lines



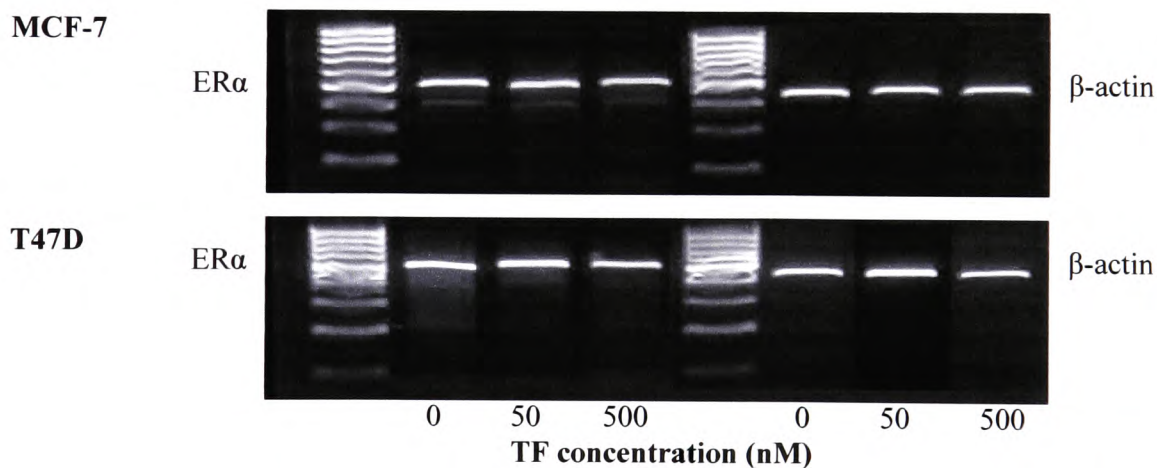
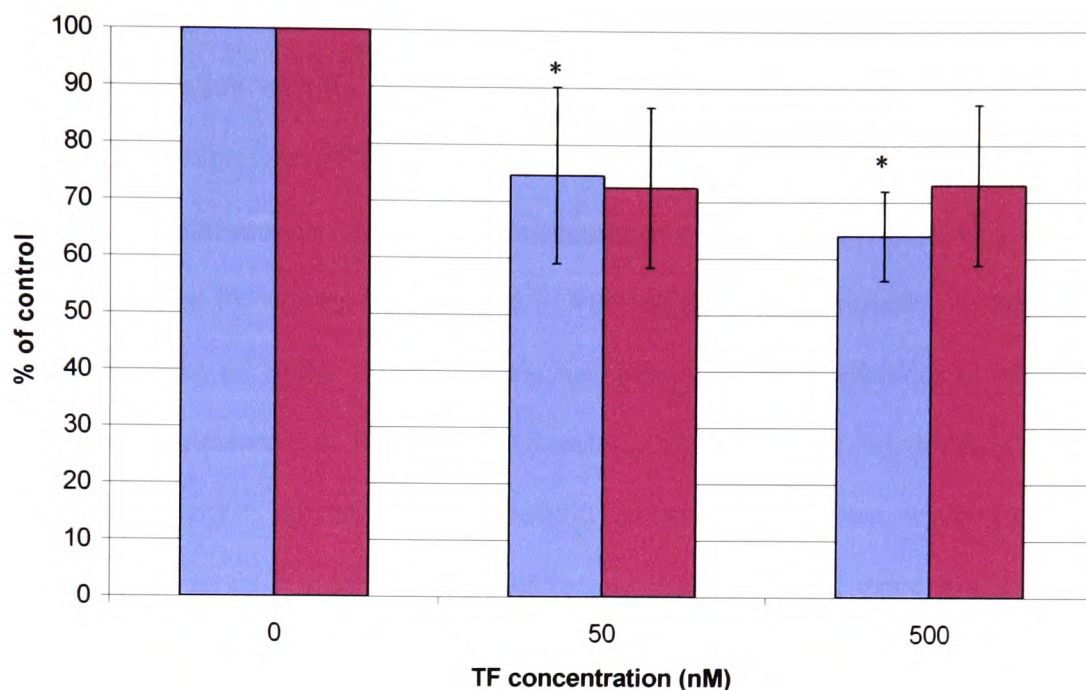
RNA was isolated from breast cancer cells (5×10^5) and RT-PCR carried out using Ready-to-go RT-PCR beads and the ER α primers. The DNA products were separated by 2 % (w/v) agarose gel electrophoresis and visualised under UV light.

Figure 3.13. Short-term influence of TF on ER α mRNA expression in MCF-7 cells



MCF-7 cells (2×10^5) were incubated with recombinant TF (0 or 500 nM) and harvested at intervals over 72 h. RNA was isolated from the samples and ER α amplified by RT-PCR. The products were examined using agarose gel electrophoresis, images recorded using the GeneSnap program and ER α expression compared to β -actin using the GeneTool program. Data represent the average of two independent experiments \pm SD.

Figure 3.14. The influence of TF on ER α mRNA expression in MCF-7 and T47D cells



MCF-7 or T47D cells (2×10^5) were incubated with TF (0-500 nM) for 24 h, total RNA isolated and ER α mRNA expression examined by RT-PCR. DNA products were examined by agarose gel electrophoresis and images recorded using the GeneSnap program. ER α expression was compared to β -actin using the GeneTool program. Data represent the average of five independent experiments for MCF-7 cells (blue) and two independent experiments for T47D cells (red) \pm SD. * $p < 0.05$ vs. untreated control for MCF-7 cells.

TF (50 and 500 nM) showed similar trends in reductions in ER α mRNA expression at 24 h.

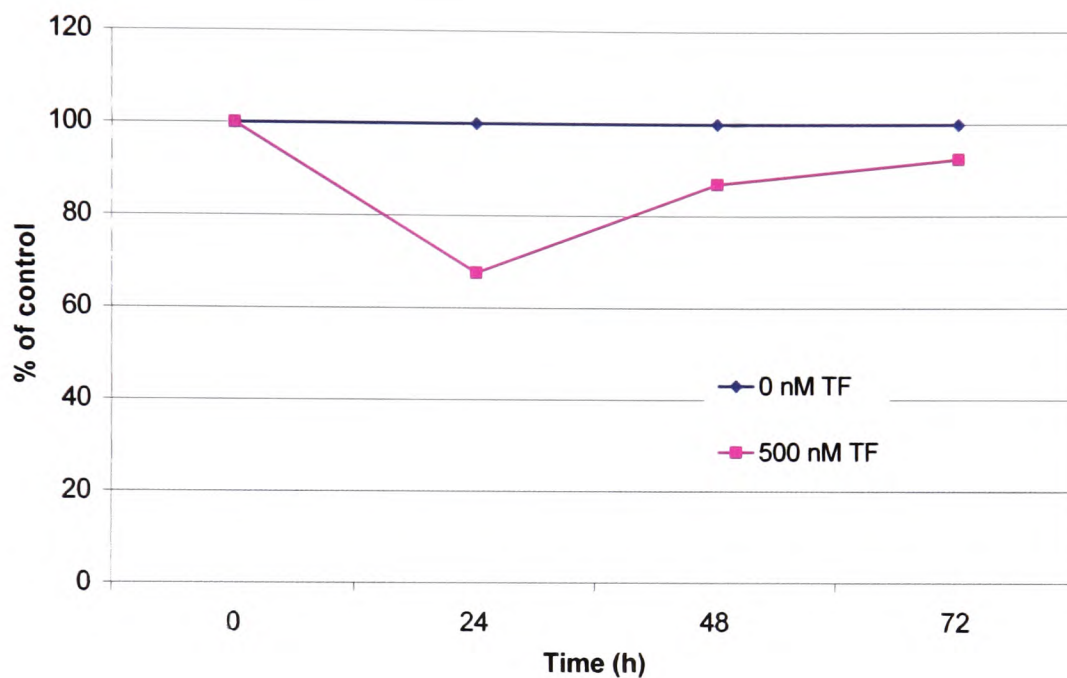
3.3.6.2. Investigation of the influence of TF on ER α protein expression

The downregulation of ER α mRNA expression was reflected in the level of protein expressed. The expression of ER α protein in MCF-7 cells appeared to follow a similar trend in which the initial decrease in ER α protein expression at 24 h post-treatment with TF (500 nM) as measured by western blot, seemed to increase to levels comparable to that of the control sample by 48 h (Fig 3.15). Similarly, incubation of T47D cells with TF (500 nM) resulted in the reduction of ER α protein expression at 24 h (Fig 3.16). Moreover, since western blot analysis results are only semi-quantitative, the protein levels were also measured using an ELISA for ER α , and interpreted from a standard curve prepared using recombinant human ER α (Fig 3.17). The data obtained by the ELISA showed reductions in ER α protein expression of 20 % and 50 % in MCF-7 and T47D cells respectively, following 24 h incubation with TF (500 nM) (Fig 3.18).

3.3.6.3. Investigation of the long-term influence of TF on ER α expression

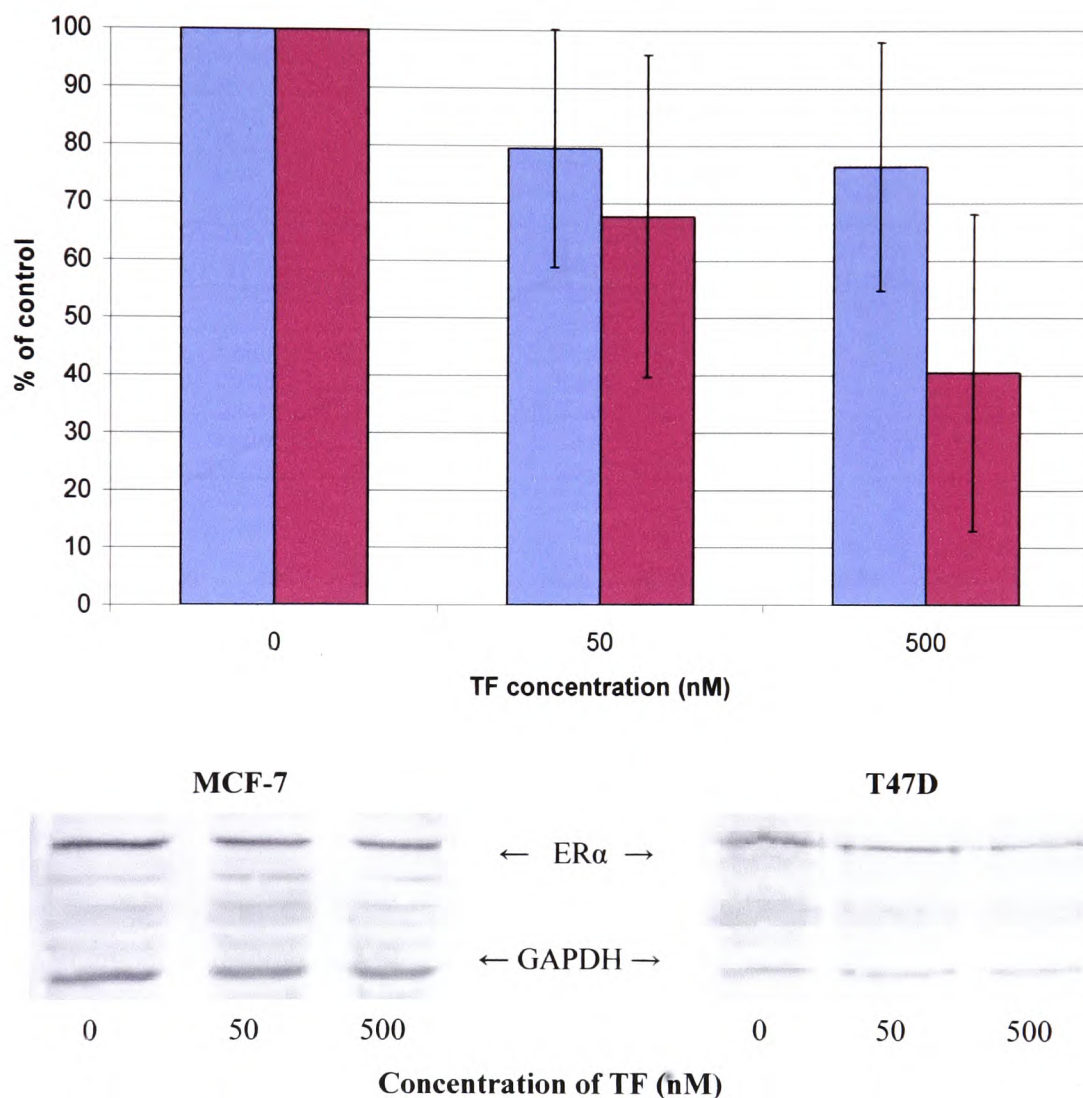
MCF-7 cells were incubated with recombinant TF (0-500 nM), which was supplemented every 3-4 days for 5 weeks. Cell samples were collected every 7 days and ER α expression measured by RT-PCR and western blot. In general, the presence of TF (50 and 500 nM) appeared to result in the downregulation of ER α mRNA expression compared to control cells. Moreover, the decrease in ER α mRNA expression seemed to be progressive and reached 50 % of the control by day 28 (Fig 3.19). The downregulation of ER α mRNA was reflected in the level of protein expression, which decreased to 40 % by 21 days incubation with TF (500 nM) (Fig 3.20), although the trend observed was less consistent. Furthermore, due to the nature of the experiment the analysis was carried out using only one set of cells.

Figure 3.15. Short-term influence of TF on ER α protein expression in MCF-7 cells



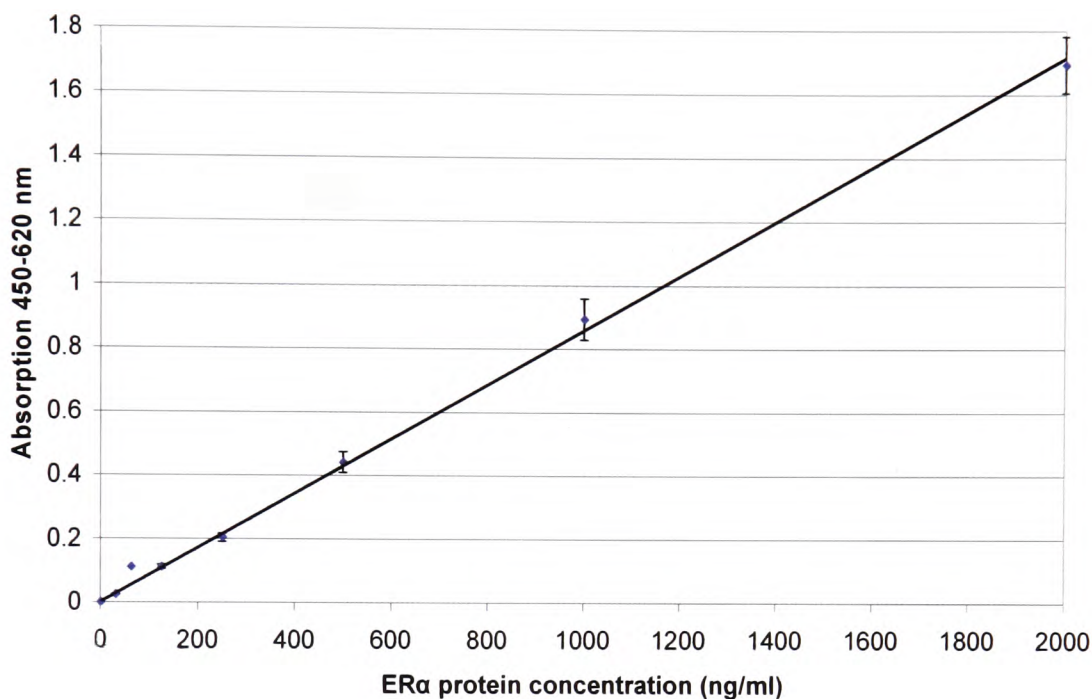
MCF-7 cells (2×10^5) were incubated with recombinant TF (0 or 500 nM) and harvested at intervals over 72 h. The cells were lysed and proteins separated by 12 % (w/v) SDS-PAGE. The proteins were transferred onto nitrocellulose membranes and probed for ER α and GAPDH. Images were recorded using the GeneSnap program and ER α compared to GAPDH using the GeneTool program. The data are from one experiment.

Figure 3.16. The influence of TF on ER α protein expression as examined by western blot



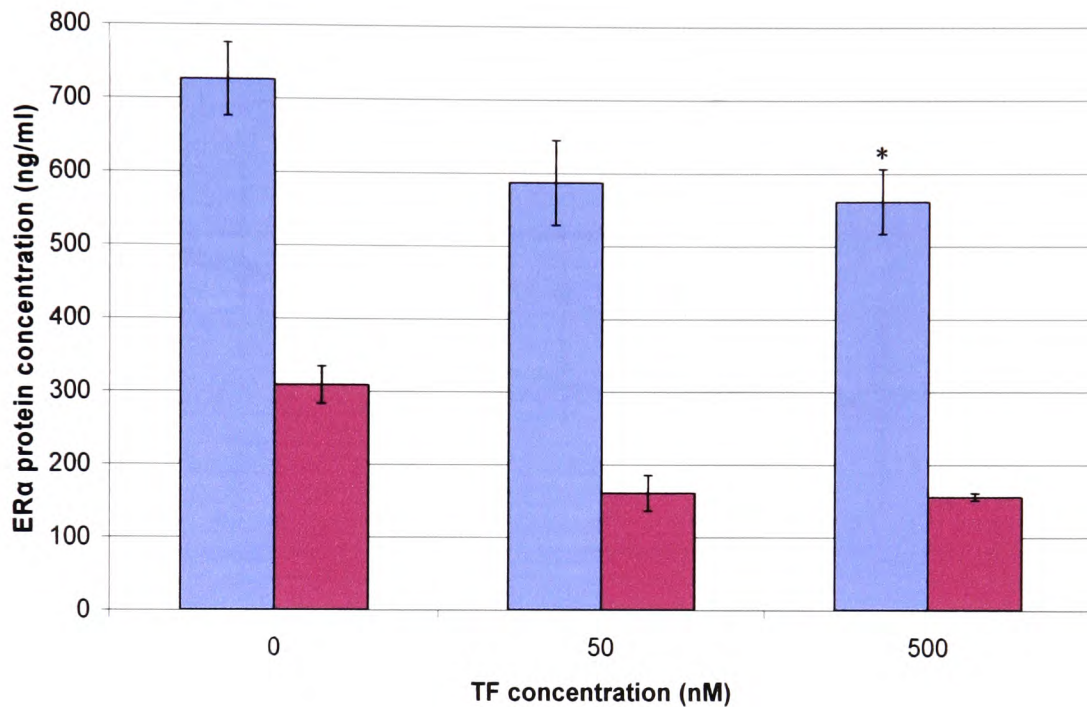
MCF-7 or T47D cells (2×10^5) were incubated with TF (0-500 nM) for 24 h, the cells lysed and protein separated by 12 % (w/v) SDS-PAGE. Proteins were transferred onto nitrocellulose membranes and probed for ER α and GAPDH. ER α expression was compared to GAPDH using the GeneTool program. MCF-7 cells = blue, T47D cells = red. Data represent the average of five independent experiments for MCF-7 cells (blue) and three independent experiments for T47D cells (red) \pm SD.

Figure 3.17. Standard curve for the ER α ELISA



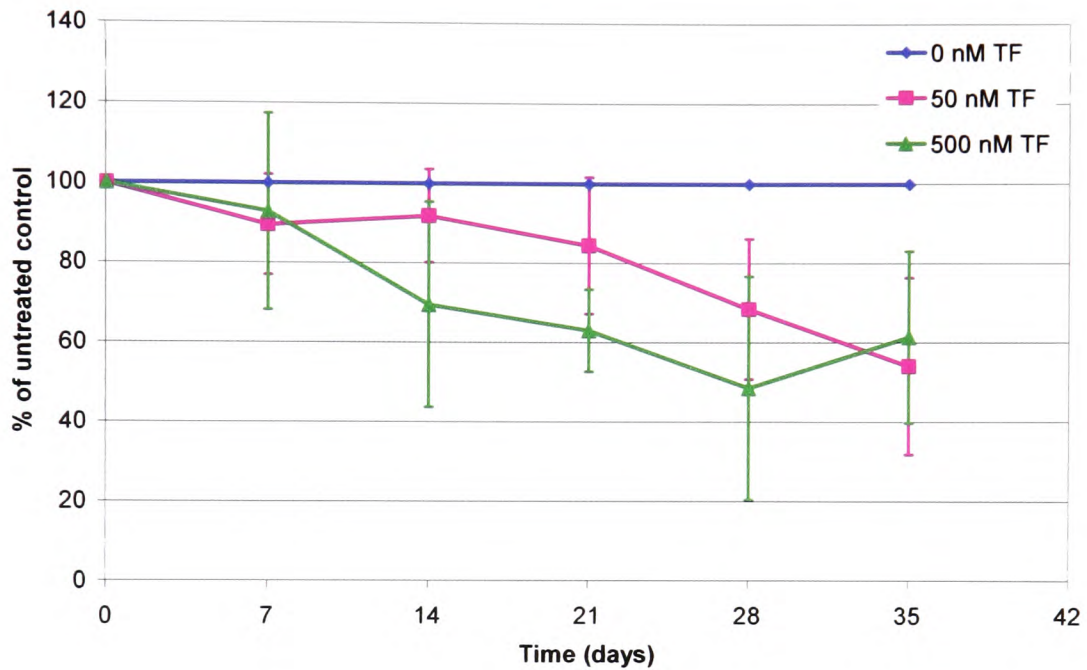
Serial dilutions of recombinant ER α protein were prepared to give a range of concentrations (0-2000 ng/ml). 50 μ l of each diluted sample was added to wells in duplicate and the ELISA carried out using the rabbit anti-human ER α antibody. The absorption of the samples was measured at 450 nm with a reference of 620 nm and the standard curve constructed. Data is representative of one experiment in duplicate \pm SD. A new standard curve was prepared for each experiment.

Figure 3.18. The influence of TF on ER α protein expression as examined by ELISA



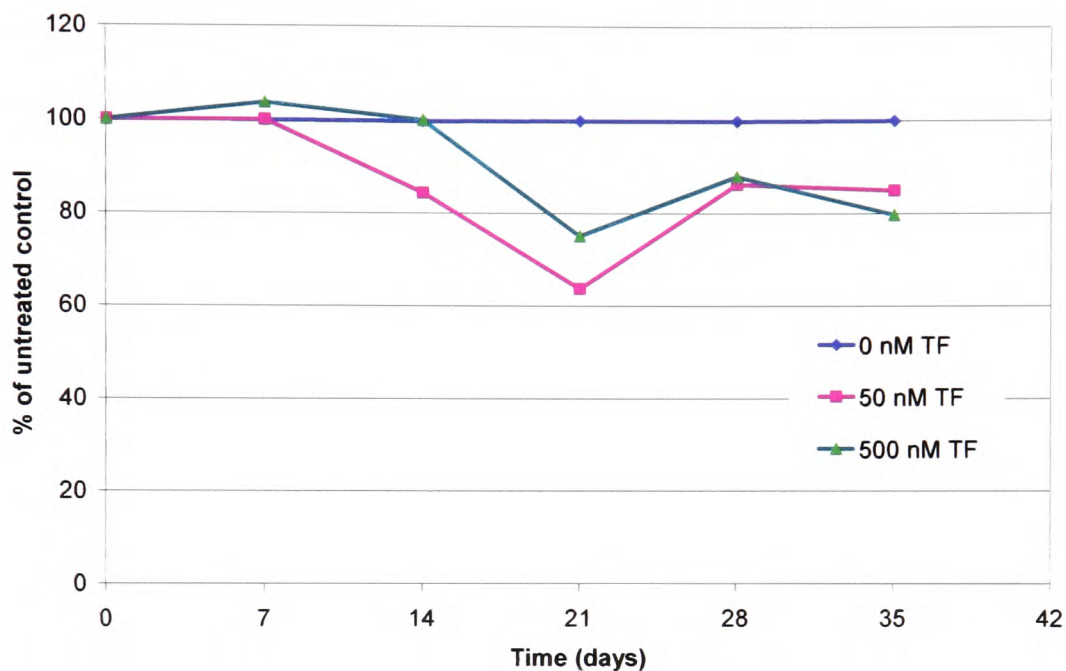
MCF-7 or T47D cells (2×10^5) were incubated with TF (0-500 nM) for 24 h, harvested and protein concentrations determined using the Bradford assay. Each sample containing 10 μ g of protein was placed in the wells of the ELISA plate in duplicate and probed for ER α protein. Absorptions were measured at 450 nm with a reference at 620 nm using an Anthos 2010 microplate reader. Absorption values were converted to protein concentrations using the standard curve prepared with recombinant ER α protein. Data represent the average of three independent experiments for MCF-7 cells (blue) and two independent experiments for T47D cells (red) \pm SD. * $p < 0.05$ vs. untreated control for MCF-7 cells.

Figure 3.19. Long-term influence of TF on ER α mRNA expression in MCF-7 cells



MCF-7 cells were cultured in T75 flasks and supplemented with recombinant TF (50 and 500 nM) every three days over five weeks. The samples were subcultured every 7 days and samples collected for RT-PCR analysis of ER α mRNA expression. Data represents one experiment analysed by RT-PCR in duplicate \pm SD.

Figure 3.20. Long-term influence of TF on ER α protein expression in MCF-7 cells



MCF-7 cells were cultured in T75 flasks and supplemented with recombinant TF (50 and 500 nM) every three days over five weeks. The samples were subcultured every 7 days and samples collected for western blot analysis of ER α protein expression. Data represents one experiment.

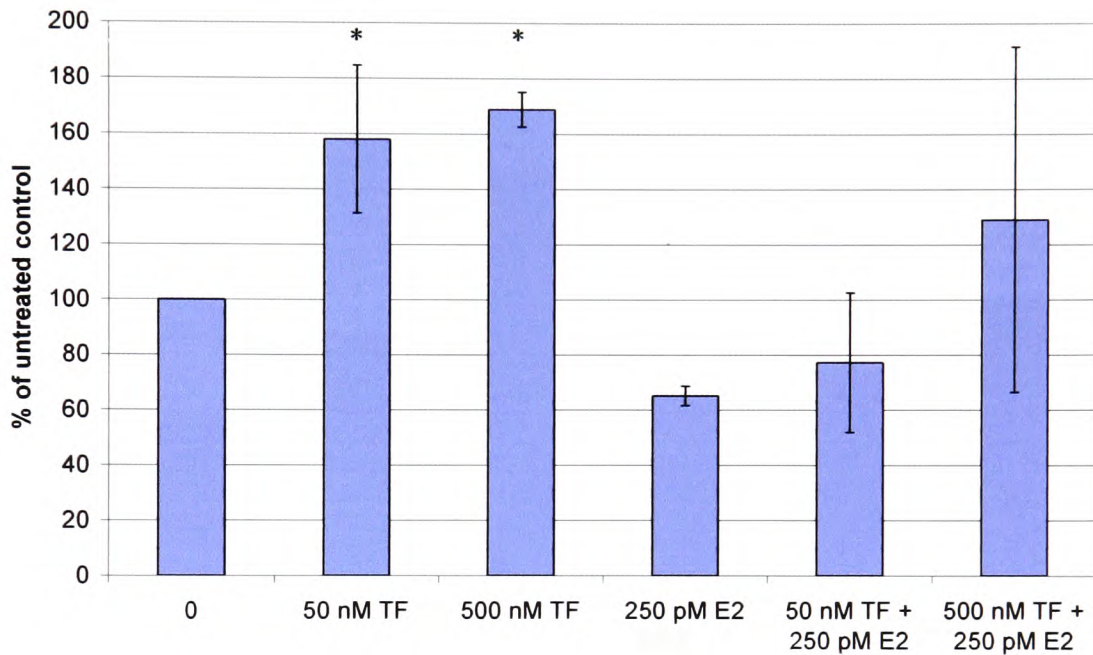
3.3.7. Influence of TF on cell migration using a Boyden chamber based assay

A Boyden chamber based invasion/migration assay was used to examine the influence of TF on breast cancer cell invasion in the presence and absence of oestradiol. In order to reach the lower chamber, the cells must digest the collagen type IV barrier and actively migrate across the filter. The TF was placed in the lower chamber and the number of cells that had migrated across the filter determined using the MTS-based assay. The rate of MCF-7 cell migration across the filter increased when TF (50 and 500 nM) was placed in the lower chamber by 59 % and 70 % respectively (Fig 3.21). Furthermore, the addition of oestradiol (250 pM) to the upper chamber containing the cells inhibited MCF-7 cell migration by 38 % of that of the untreated control. The addition of TF (50 nM) together with oestradiol (250 pM) had no significant effect on migration compared to cells treated with oestradiol alone. However, the addition of a higher concentration of TF (500 nM) together with oestradiol (250 pM) increased the mean rate of cell migration over that of oestradiol treated cells. Similarly, the addition of TF (50 and 500 nM) increased the rate of T47D cell migration across the filter (Fig 3.22). The addition of oestradiol (250 pM) to the upper chamber containing the cells had no effect on cell migration compared to the untreated control. The addition of TF (50 nM) to the lower chamber also had no effect on rates of cell migration in the presence of oestradiol (250 pM). However, the addition of TF (500 nM) together with oestradiol (250 pM) resulted in increased rates of T47D cell migration.

3.3.8. Examination of changes in cell morphology in response to exogenous TF

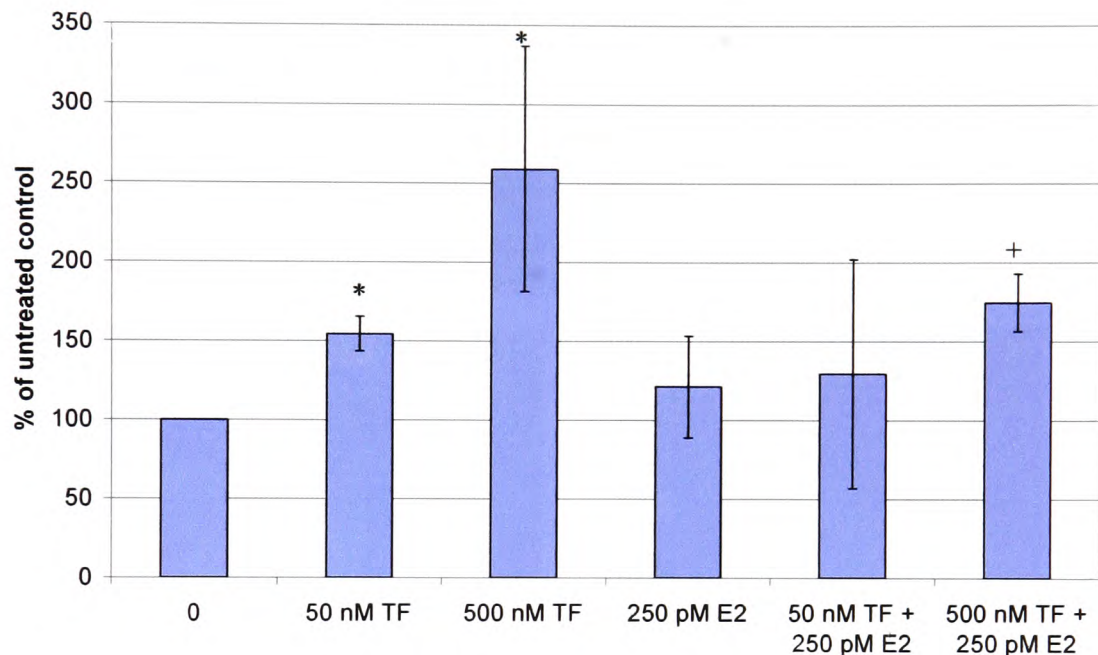
Incubation of MCF-7 cells with TF (500 nM) appeared to result in the formation of sheet-like extensions of the cell membrane (lamellipodia) which were not present in the untreated cells (Fig 3.23). This was also observed in cells treated with bFGF (30 ng/ml). bFGF was

Figure 3.21. MCF-7 cell migration in response to TF in the presence and absence of oestradiol



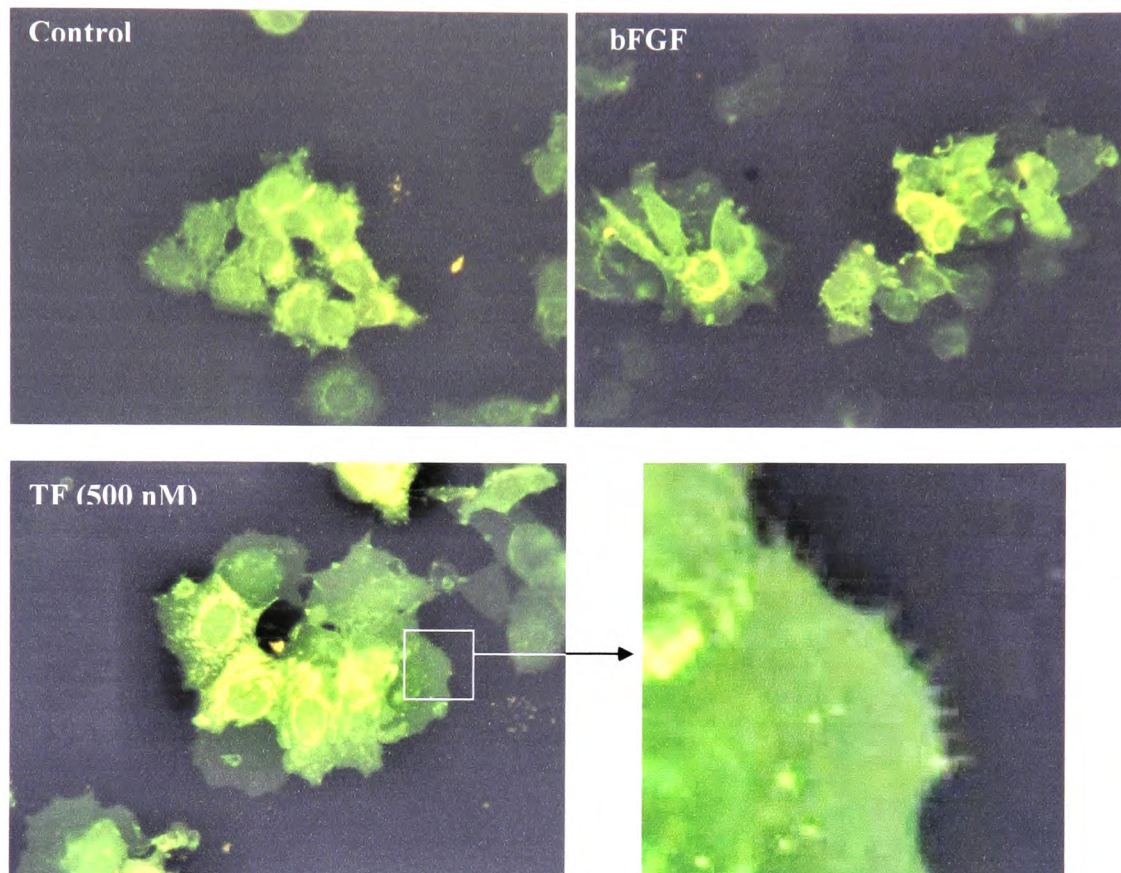
MCF-7 cells (2×10^5) were seeded out in phenol red free medium supplemented with 1 % (v/v) FCS into Boyden chambers coated with collagen type IV. The upper compartment containing the cells was supplemented with oestradiol (E2) (250 pM), and the lower compartment supplemented with TF (0-500 nM). The cells were incubated at 37°C for 24 h to allow migration across the collagen barrier. Following incubation, the cells on the upper side of the filter were removed and the number of migrated cells determined using the CellTiter proliferation reagent. Data is representative of four independent experiments \pm SD. Average number of cells migrated: untreated control = 3600 cells, 500 nM TF = 6100 cells. * $p < 0.05$ vs. untreated control.

Figure 3.22. T47D cell migration in response to TF in the presence and absence of oestradiol



T47D cells (2×10^5) were seeded out in phenol red free medium supplemented with 1 % (v/v) FCS into Boyden chambers coated with collagen type IV. The upper compartment containing the cells was supplemented with oestradiol (E2) (250 pM), and the lower compartment supplemented with TF (0-500 nM). The cells were incubated at 37°C for 24 h to allow migration across the collagen barrier. Following incubation, the cells on the upper side of the filter were removed and the number of migrated cells determined using the CellTiter proliferation reagent. Data is representative of four independent experiments \pm SD. Average number of cells migrated: untreated control = 2900 cells, 500 nM TF = 6800 cells. * $p < 0.05$ vs. untreated control. + $p < 0.05$ vs. oestradiol treated control.

Figure 3.23. Changes in cell morphology in response to exogenous TF



MCF-7 cells were adapted to medium containing 1 % (v/v) FCS and seeded out into 8 well cultureslides. The cells were treated with TF (500 nM) or bFGF (30 ng/ml) as a positive control and incubated at 37°C for 48 h. The cells were fixed with 3 % (v/v) glutaraldehyde and then incubated with the membrane stain DiI for 15 min. The cells were washed with PBS and visualised using a CoolSnap Pro camera attached to a Leitz Laborlux S fluorescence microscope. Images were processed using the Image-Pro Plus Version 5.1.2. Data are representative of two independent experiments. (Magnification $\times 25$).

used as a positive control as it is known to induce changes in cell morphology associated with cell migration (Johnson et al 1995). Furthermore, in the close up of cells treated with TF, microspikes (filopodia) are visible at the edge of the cell membrane.

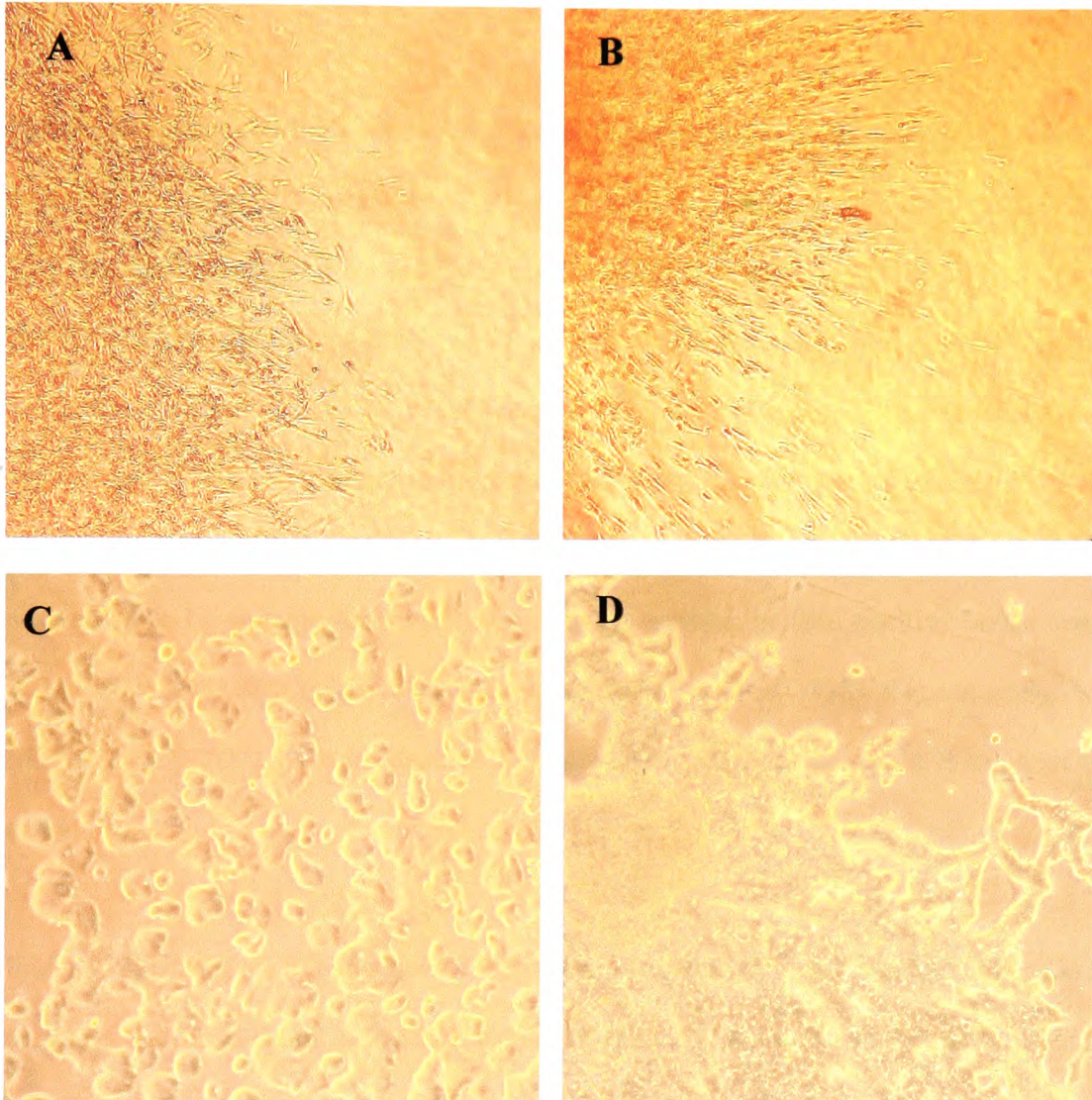
3.3.9. Influence of TF on cell invasion using collagen type I gels

A procedure for an invasion assay was devised in order to observe the influence of TF on the rate of cell invasion into a surrounding collagen I matrix. Initially, a range of collagen I concentrations (0.28-0.38 % (w/v)) were used with the highly invasive breast cancer cell line MDA-MB-231 and invasion was recorded over 7 days. Optimal rate of invasion was observed with 0.28 % (w/v) collagen I gels (Fig 3.24). However, no accurate invasion could be measured with MCF-7 cells as the cells formed colonies which overgrew into the gel. Consequently, it was not possible to measure the change in the rate of invasion in response to TF and the assay was not further employed.

3.4. Discussion

Increased TF expression within the stroma surrounding breast tumours has been associated with aggressive/invasive forms of breast cancer (Vrana et al 1996). In contrast, the expression of ER α is associated with more differentiated, less invasive tumours. In this section of the investigation, the influence of exogenous truncated TF on breast cancer cell proliferation and invasion and the expression of ER α was examined. The recombinant TF used in this investigation represents the soluble or microparticle-derived TF, released by infiltrating stromal cells such as macrophages and fibroblasts within the vicinity of tumour cells in response to inflammatory mediators. Furthermore, the concentrations of TF used throughout this investigation represent TF concentrations observed during mild

Figure 3.24. Collagen gel invasion assays



MCF-7 or MDA-MB-231 cells (10^4) were seeded out onto collagen I gels (0.28 % (w/v)) in medium (500 μ l) and incubated at 37°C. The cells were examined daily under a light microscope. Following 24 h and 7 days incubation, images were taken using a CoolSnap Pro camera. **A** = MDA-MB-231 cells at 24 h, **B** = MDA-MB-231 cells at 7 days, **C** = MCF-7 cells at 24 h, **D** = MCF-7 cells at 7 days. Data are representative of six independent experiments. (Magnification $\times 10$).

pathological conditions (50 nM TF) and severe pathological conditions (500 nM TF) (Watanabe et al 1999).

The breast cancer cell lines MCF-7 and T47D expressed little to no surface TF antigen as determined by flow cytometry (Fig 3.2) or TF activity as shown by the PT assay (Table 3.2). In addition, both of these cell lines expressed ER α but not ER β . The breast cancer cell line ZR-75-1 expressed low levels of TF as well as low levels of ER α , while MDA-MB-231 cells expressed high levels of cell surface TF and exhibited no ER α expression. Both MCF-7 and T47D cell lines have frequently been used in the past as models for breast cancer cells with a low invasive potential (Rocheffort et al 1998, Thompson et al 1992) and are known to be suitable for investigating the progression of ER α positive breast cancer cells to invasive, ER α negative phenotypes (Schiemann et al 1998). Consequently, both MCF-7 and T47D cells were deemed as appropriate cell lines and used throughout this study.

Initially, the influence of exogenous TF on the proliferation of breast cancer cell lines in the presence and absence of oestradiol was investigated. Cells cultured in culture medium containing phenol red and 10 % FCS showed little alterations in the rate of proliferation in response to oestradiol (50-1000 pM) (Fig 3.3). The lack of change in the rate of proliferation following the addition of oestradiol was due to the oestrogenic influence of the medium pH indicator phenol red (Berthois et al 1986) and oestrogenic compounds in FCS, hence masking the effects of the addition of physiological concentrations of oestradiol. Therefore, all subsequent assays using oestradiol were performed in phenol red-free medium. However, the cells did not respond to oestradiol in the total absence of FCS. The lack of cell response to oestrogen in the absence of serum has been reported previously and

is suggested to be as a result of the lack of albumin (Germain & Harbrioux 1993) or other unknown serum-derived factors (Ruedl et al 1990) which act as carrier proteins for oestrogen. To overcome this, the medium was supplemented with 1 % FCS to permit the transport of oestradiol to the cells.

Another issue requiring confirmation prior to performing these studies arose from the fact that the recombinant TF component of the Innovin reagent used in this investigation is incorporated into phospholipid vesicles for optimal procoagulant activity. To confirm that any observed effects of the Innovin reagent on cells arose from the TF apoprotein and not the lipid component, any influence of the lipids derived from the Innovin reagent on cell proliferation was examined. The lipids extracted from the Innovin reagent were found to have no procoagulant activity when examined by the PT assay, confirming the absence of residual TF. Moreover, the addition of lipids alone had no measurable influence on MCF-7 cell proliferation (Fig 3.10). The addition of the Innovin reagent-derived lipids together with oestradiol (250 pM) resulted in a small decrease in the rate of proliferation compared to cells treated with oestradiol alone. However, this lowering in the rate of proliferation was not comparable to the decreases observed in the presence of the complete TF Innovin reagent (500 nM) together with oestradiol (250 pM). This indicates that the lipid component of the Innovin reagent does not have a significant effect on the cells and also the lipids do not sequester sufficient amounts of oestradiol to account for the decreases in proliferation observed with the Innovin reagent.

Next, the influence of oestradiol on cell proliferation was examined in order to ensure oestradiol stimulated cell proliferation in the cells and determine optimal oestradiol concentration. Incubation of cells with oestradiol (100-500 pM) appeared to increase the

rate of cell proliferation in both cell lines with the maximal proliferation rate observed with 100-250 pM oestradiol (Fig 3.4 & 3.8), which is in agreement with previous reports that physiological concentrations of oestradiol stimulate the proliferation of ER α -positive breast cancer cells (Prall et al 1998, Anderson et al 1998, Laidlaw et al 1995). However, the rate of proliferation of T47D cells in response to oestradiol increased at a later time point than MCF-7 cells, possibly due to the slower growth rate of these cells or lower levels of ER α expression. Examination of the influence of exogenous TF on oestradiol-induced cell proliferation revealed an appearance of a trend in which a high concentration of TF (500 nM) appeared to suppress oestradiol-induced cell proliferation in MCF-7 cells and to a lesser extent in T47D cells, possibly due to a downregulation of ER α expression in the cells. Alternatively, the suppression of oestradiol-mediated proliferation by exogenous TF may be due to the increased rate of apoptosis. Prolonged arrest of the progression through the cell cycle, during cell division often results in apoptosis of the cells (Johnson & Walker 1999). Furthermore, it has previously been shown that high concentrations of exogenous TF inhibit components of the cell cycle, leading to cell cycle arrest and apoptosis (Pradier & Ettelaie 2007). Since oestradiol promotes ER α -positive cells to enter the cell cycle (Prall et al 1998), it is possible that the suppression of oestradiol-mediated proliferation observed in this investigation is due to the inhibition of specific cell cycle proteins by exogenous TF, leading to the arrest of the cell cycle and subsequent apoptosis.

In the absence of oestradiol, incubation of MCF-7 cells with a low concentration of exogenous TF (50 nM) appeared to increase the rates of proliferation following 24 h incubation (Fig 3.4), whereas incubation with a high concentration of TF (500 nM) seemed to reduce the rate of MCF-7 cell proliferation measured at 48 and 72 h. These differential influences of exogenous TF on cell proliferation depending on the concentration of TF have

been previously reported in endothelial cells (Pradier & Ettelaie 2007). Furthermore, the addition of TF (500 nM) alone did not reduce the rate of proliferation to the same extent as the combination of 500 nM TF and oestradiol, which may be explained by fewer cells entering the cell cycle in the absence of oestradiol, and therefore fewer cells undergoing apoptosis.

The ability of cells to respond to oestradiol depends on the presence of ER α . Therefore, in order to identify the underlying mechanism involved in the reduction in oestradiol-mediated proliferation by exogenous TF, the influence of TF on ER α expression was examined next. A trend was observed in which incubation of MCF-7 and T47D cells with TF (50 and 500 nM) resulted in decreases in the expression of ER α mRNA and protein at 24 h (Fig 3.14 & 3.18), which then normalised at 72 h post-treatment (Fig 3.13 & 3.15), indicating that single exposure of cells to exogenous TF may have a short-term influence on ER α expression. Since ER α is required for cells to respond to oestradiol, this downregulation in ER α expression may partly account for the suppression of oestradiol-mediated cell proliferation in these cell lines in the presence of a high concentration of TF (500 nM). Moreover, since breast cancer cells *in vivo* would be exposed to a continuous level of exogenous TF released from stromal cells over period of time, the cumulative influence of continuous exposure to exogenous TF on ER α expression over 5 weeks was examined. Exposure of MCF-7 cells to continuous levels of TF (500 nM) for 28 days appeared to result in a cumulative decrease in the expression of ER α mRNA by 50 % (Fig 3.19), which was also reflected as a 40 % decrease in protein expression following 21 days incubation compared to the untreated control (Fig 3.20). Despite the limited number of times that this experiment was repeated these results may indicate the role of exogenous TF as a factor involved in the depletion of ER α expression in breast cancer cells. Breast cancer

cells derived from aggressive tumours often lack ER α expression but express high levels of TF (Hu et al 1994) indicating that TF may have a role in ER α downregulation. One possible mechanism by which exogenous TF may influence ER α expression is the activation of the MAPK ERK1/2 signalling pathway, since previous studies have shown that the activation of the ERK1/2 pathway by growth factors results in the downregulation of ER α expression in breast cancer cells (Oh et al 2001, Creighton et al 2006). Moreover, the TF:FVIIa complex has been shown to be capable of initiating the activation of signalling pathways including the ERK1/2 pathway (Ettelaie et al 2007, Sorensen et al 1999), leading to changes in gene expression (Camerer et al 2000a, Camerer et al 1999, Pendurthi et al 1997). It is therefore possible that the incubation of breast cancer cells with exogenous TF results in the activation of signalling pathways such as the ERK1/2 pathway leading to the downregulation of ER α expression. In conclusion, TF may suppress oestradiol-mediated cell proliferation, which may in part involve the downregulation of ER α , reducing the responsiveness of cells to oestradiol. Furthermore, it is possible that TF may suppress oestradiol-mediated proliferation by inducing apoptosis in cells stimulated to enter the cycle by oestradiol, although this requires further investigation.

Next the influence of exogenous TF on breast cancer cell invasiveness was examined. A frequently used *in vitro* procedure involving the migration of cells across a collagen IV coated Boyden chamber was employed to assess the rate of cell invasion in response to exogenous TF. In this assay, cells must degrade the collagen IV barrier and actively migrate across the barrier towards the stimulus (Rocheffort et al 1998). Since collagen IV is a major component of the basement membrane which surrounds blood vessels, this assay represents an *in vitro* measurement of the ability of cancer cells to cross blood vessel basement membranes and metastasis. Addition of TF (50 or 500 nM) to the lower chamber increased

the rate of MCF-7 and T47D invasion across the barrier in a concentration-dependent manner (Fig 3.21 & 3.22). Previously, the induction of smooth muscle cell migration towards TF has been demonstrated (Sato et al 1996), suggesting that TF acts as a chemokine promoting cell migration along the TF concentration gradient. Furthermore, cell surface TF has been shown to enhance migration through mechanisms that involve TF binding to FVIIa and subsequent PAR activation (Jiang et al 2004), as well as through interactions of the cytoplasmic domain of TF with specific intracellular proteins resulting in cytoskeletal reorganisation (Ott et al 1998). Since the exogenous TF used in the present study is devoid of the cytoplasmic domain, the ability of this TF to induce cell migration may be attributed to the interaction with FVIIa present in the small concentration of serum included in the medium and the subsequent activation of PARs on the surface of the examined cells. Furthermore, in the presence of TF (500 nM), MCF-7 cells appeared to form sheet-like extensions of the cell membrane known as lamellipodia as well as microspikes termed filopodia at the edge of the cell membrane (Fig 3.23). These structures are formed following reorganisation of the actin cytoskeleton in response to external stimuli and are required for cell migration as they contain adhesion molecules that attach to the substratum and pull the cell along (Yamaguchi et al 2005). These data are in agreement with those previously reported by Versteeg et al (2000), showing the induction of lamellipodia and filopodia formation in fibroblasts by TF:FVIIa signalling. The formation of migratory structures in breast cancer cells in the presence of TF also supports the data from the Boyden chamber invasion assay, demonstrating that TF induces breast cancer cell invasion. In contrast, the addition of oestradiol (250 pM) to the upper chamber containing the cells inhibited MCF-7 cellular invasion, which is in agreement with several previous studies which show that oestradiol inhibits invasion of ER α -positive cells (Platet et al 2000, Rochefort et al 1998, Garcia et al 1992). However, the ability of oestradiol (250 pM) to

inhibit cell invasion was reversed by the inclusion of a high concentration of TF (500 nM) to the lower chamber, resulting in increased average rates of cell invasion in both MCF-7 and T47D cells. The increase in the rate of invasion following incubation with TF in the presence of oestradiol may in part be explained by the downregulation of ER α in the presence of exogenous TF. In addition, an invasion assay employing collagen I gels was used to further investigate the influence of TF on cellular invasion. In this assay, the highly invasive MDA-MB-231 cell line was shown to invade through the collagen I gels in the absence of any external stimuli (Fig 3.24). However, MCF-7 cells were not able to invade through even the lowest concentration of collagen I gels. Therefore, since the purpose of the assay was to examine the influence of TF on ER α -positive cells, the assay was not deemed suitable and no longer employed in the studies.

In summary, a trend was observed in which the exposure of breast cancer cells to high concentrations of TF appeared to result in a reduction in oestradiol-mediated cell proliferation below that of the untreated cells, possibly through the downregulation of ER α expression in the breast cancer cells and/or by increasing the rate of cell apoptosis. Moreover, incubation of breast cancer cells with exogenous TF reversed the anti-invasive effect of oestradiol and enhanced the rate of cell invasion, as well as inducing the formation of lamellipodia and filopodia which are required for cell migration. These observations may be partly explained by the downregulation of ER α , particularly as the long-term incubation of MCF-7 cells with TF (500 nM) resulted in a progressive suppression of ER α expression. In conclusion, high levels of TF, detected in the stroma of invasive breast cancers (Vrana et al 1996, Contrino et al 1996) may alter the response of ER α -positive breast cancer cells to oestradiol and contribute to the progression of breast cancer cells to an invasive, oestradiol-independent phenotype.

CHAPTER 4

The influence of exogenous TF on ER α activity through
the ERE pathway

4.1. Introduction

4.1.1. The involvement of ER α activation in breast cancer

The presence of functional ER α in breast tumours has been associated with well differentiated, less invasive breast tumours and is indicative of a good prognosis. These properties are largely due to oestradiol-ER α mediated regulation of the transcription of genes involved in cell proliferation, differentiation, migration and invasion, some of the more prominent of which are shown in table 4.1. Furthermore, the detection of functional ER α in breast tumours is predictive of the response of breast cancers to anti-hormone therapies such as Tamoxifen that inhibit ER α activity.

4.1.2. The classical pathway of the transcriptional activation of ER α

Transcriptional activation of ER α through the classical mechanism involves the binding of the oestradiol-ER α complex to specific DNA sequences known as oestrogen response elements (ERE), which are located within upstream promoter regions of ER α -regulated genes (Klein-Hitpass et al 1988). The consensus ERE DNA sequence is a 13 bp palindromic sequence with three variable bases (N) in the middle: 5'-GGTCANNNTGACC-3'. Many of the genes controlled by ER α have imperfect ERE sequences which vary by a few nucleotides. The binding affinity of ER α for these ERE sequences decreases with the amount of variation compared to the consensus ERE DNA sequence. This permits transcription of ER α -target genes at different rates and magnitudes in response to oestradiol (Gruber et al 2004). In the absence of its ligand 17 β -oestradiol, ER α is normally sequestered in the nucleus as an inhibited complex with heat shock protein 90 (hsp90) (Smith & Toft 1993). The binding of 17 β -oestradiol to the ligand binding domain of ER α results in a conformational change within the receptor, which leads to the release of hsp90 and induces receptor

Table 4.1. Genes controlled by oestrogen and containing ERE regulatory sequences within the promoter DNA regions

Gene *	Function	Reference
c-myc	Proliferation	Dubik & Shiu 1992
Progesterone receptor	Response to progesterone	Petz & Nardulli 2000
Transforming growth factor- α (TGF- α)	Proliferation	El-Ashry et al 1996
Vascular endothelial growth factor (VEGF)	Angiogenesis Vascular permeability	Mueller et al 2000
c-Fos	Proliferation Differentiation	Weisz & Rosales 1990
pS2	Proliferation Differentiation Cell survival	Berry et al 1989

* Genes upregulated by 17 β -oestradiol.

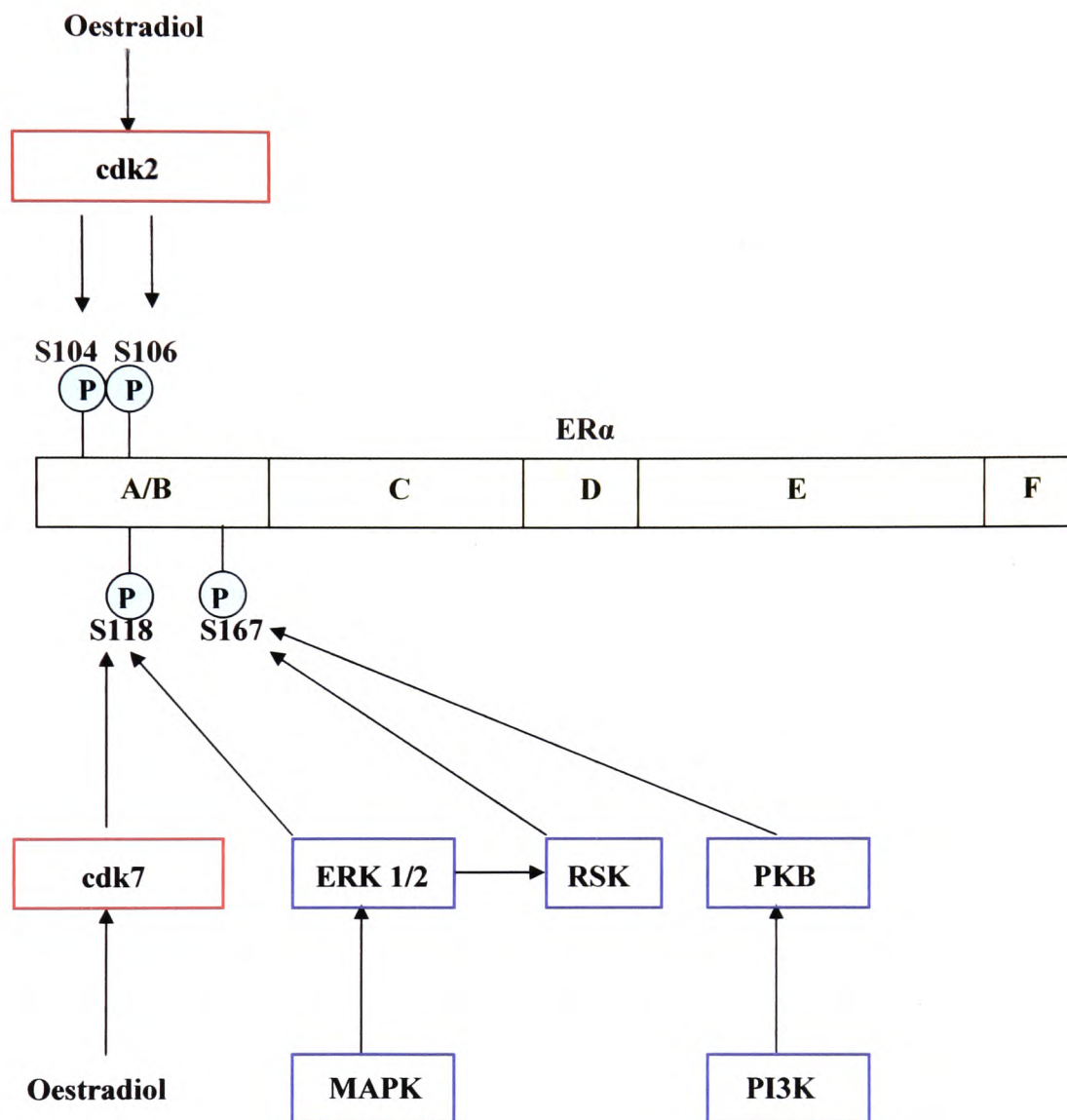
dimerisation. Furthermore, ER α may be phosphorylated at several sites following the binding of oestradiol (Chen et al 2000, Rogatsky et al 1999). These conformational changes upon ligand binding allow the DNA binding domain of ER α to interact with ERE DNA sequences. This in turn promotes the recruitment of coactivator proteins and RNA polymerase II to the DNA, leading to the formation of the transcription initiation complex and subsequent transcriptional activation from ERE promoters. Subsequently, ER α is ubiquitinated and then degraded by proteasomes within 45 minutes of binding to the DNA (Reid et al 2003). This rapid turnover of ER α allows cells to respond rapidly to small alterations in oestradiol levels.

4.1.3. Phosphorylation of ER α

Phosphorylation of proteins is a common mechanism used to alter protein functions, such as DNA binding activity, protein dimerisation and transcriptional activity. ER α is known to be regulated by phosphorylation at multiple sites, mediated through both oestradiol-dependent and oestradiol-independent signalling pathways (Chen et al 2002, Ali et al 1993) (Fig 4.1). The main phosphorylation sites in ER α are serine residues 104, 106, 118 and 167, which are located within the N-terminus AF-1 domain of the receptor (Rogatsky et al 1999, Joel et al 1998, Chen et al 2002). Serine 167 is phosphorylated following the activation of MAPK pathways, phosphatidylinositol 3-kinase (PI3K) and ribosomal S6 kinase (RSK), but not by oestradiol (Joel et al 1998, Campbell et al 2001). Conversely, serines 104 and 106 are phosphorylated only in response to oestradiol through the activation of cyclin-dependent kinase 2 (cdk2) (Rogatsky et al 1999).

An important regulatory phosphorylation site in ER α is on serine 118, the phosphorylation of which is essential for full activity of the AF-1 domain of ER α (Ali et

Figure 4.1. Phosphorylation sites in ER α



ER α has several phosphorylation sites that can be phosphorylated by oestradiol-dependent and/or oestradiol-independent pathways. The main phosphorylation sites in ER α are serine residues 104, 106, 118 and 167, located in the N-terminus trans-activation-1 (AF-1) region of the receptor. Serine 104, 106 and 118 are phosphorylated in response to oestradiol binding to the receptor. Serine 118 is also phosphorylated by the activation of the MAPK pathway. Serine 167 is phosphorylated by the activation of the MAPK and PI3K pathways, but is not phosphorylated in response to oestradiol. PKB = protein kinase B, RSK = ribosomal s6 kinase.

al 1993). Serine 118 is rapidly phosphorylated by cyclin-dependent kinase 7 (cdk7) following the binding of oestradiol to ER α (Chen et al 2000). Cdk7 is part of the general transcription factor TFIID. On ER α binding to ERE sequences and the formation of the pre-initiation complex, which consists of RNA polymerase II and general transcription factors including TFIID, cdk7 phosphorylates ER α on serine 118 (Chen et al 2000). In addition, phosphorylation of serine 118 can occur through an oestradiol-independent pathway, by the extracellular signal-regulated kinase 1/2 (ERK 1/2) pathway, which occurs by the activation of this pathway by growth factors (Chen et al 2002, Kato et al 1995). The phosphorylation of ER α serine 118 by either pathway results in enhanced ER α dimerisation and recruitment of co-activator proteins, and results in increased ER α transcriptional activity from ERE DNA sequences (Dutertre & Smith 2003). The functional importance of serine 118 phosphorylation has been demonstrated by alanine substitution of serine 118, which resulted in decreases in ER α transcriptional activity in response to both oestradiol and growth factors (Kato et al 1995). In contrast, mutation of serine 118 to glutamic acid to substitute for phosphoserine, resulted in a 150 % increase in ER α transcriptional activity compared to wild type ER α (Ali et al 1993). Phosphorylated ER α has been detected in breast tumour samples, and studies have correlated the phosphorylation of serine 118 with well differentiated tumours and a better prognosis (Murphy et al 2004, Sarwar et al 2006). Furthermore, the oestradiol-independent pathways of ER α activation have been suggested as a mechanism for the resistance of some ER α positive breast tumours to anti-hormone therapies (Campbell et al 2001, Sarwar et al 2006).

4.1.4. Aims

Functional ER α is essential for oestradiol-controlled proliferation and invasion and response to anti-hormone therapies. The results obtained in the previous chapter

demonstrate that exogenous TF can suppress oestradiol-mediated proliferation and overcome the anti-inhibitory effect of oestradiol on cell invasion, providing a regulatory mechanism in oestradiol-mediated pathways. However, the transcriptional activity of ER α is regulated at several levels including phosphorylation of the receptor, alterations in DNA binding activity, recruitment of coactivator proteins to the promoter and rates of ER α degradation. TF is known to initiate the activation of various cell signalling pathways which lead to changes in rates of gene transcription. Therefore, the aim of this part of the investigation was to examine the influence of exogenous TF on the transcriptional activity of ER α through the ERE promoter. The main objectives were as follows.

- To examine the influence of exogenous TF on serine 118 phosphorylation within ER α .
- To examine the influence of exogenous TF on the DNA binding activity of ER α to ERE DNA sequences.
- To construct an ERE luciferase reporter vector and test and optimise its suitability for measuring ER α activity.
- To examine the influence of exogenous TF on the transcriptional activity of ER α using the constructed ERE reporter vector.

4.2. Methods

4.2.1. Examination of the influence of TF on ER α serine 118 phosphorylation by western blot

Cells were cultured in T25 flasks and adapted to phenol red-free medium supplemented with 1 % (v/v) FCS. When approximately 60 % confluent, the cells were incubated with recombinant TF (0-500 nM) in the presence and absence of oestradiol (250 pM) and

harvested at intervals over 120 min. The cells were then washed with 2 ml of PBS/ phosphatase inhibitors and the cells detached using enzyme-free cell dissociation buffer (1.8 ml) to prevent further activation of cell signalling pathways by trypsin. The cell suspension for each sample was transferred to a 1.5 ml tube and the cells pelleted by centrifugation at 12,000 rpm for 3 min in a microcentrifuge. The cells were then lysed in Laemmli's buffer (100 μ l) and protein concentrations of the samples determined using the Bradford assay. Proteins were separated by 12 % (w/v) SDS-PAGE and transferred onto nitrocellulose membranes as described in the general methods section. Membranes were probed using a goat anti-human ER α phospho-serine 118 antibody diluted in TBST (0.2 μ g/ml final concentration) for 1 h at room temperature, followed by a donkey anti-goat HRP-conjugated antibody diluted in TBST (0.1 μ g/ml final concentration) and then developed using TMB stabilised substrate for HRP. Images were recorded using the GeneSnap imaging system and the antibodies then removed from the membranes by incubation in high salt TBST (20 mM Tris-HCl pH 8, 1 M NaCl, 0.05 % (v/v) Tween) at 4°C overnight. Membranes were then washed in distilled water and probed for total ER α as described in the general methods section. Images were recorded and phospho-serine 118 ER α compared to total ER α using the GeneTool program.

4.2.2. Examination of the influence of TF on the DNA binding activity of ER α

ER α DNA binding activity was examined using the TransAM ER kit, an ELISA based method which consists of wells coated with the ERE consensus sequence. Active ER α in the cell extract binds to the ERE sequence and is subsequently detected using an ER α antibody.

4.2.2.1. Preparation of nuclear extracts

Cells were cultured in T75 cell culture flasks and adapted to phenol red-free medium supplemented with 1 % (v/v) FCS. When approximately 60 % confluent, the cells were treated with TF (0-500 nM) in the presence and absence of oestradiol (250 pM) and harvested at intervals over 120 min. Nuclear extracts were prepared using the Nuclear Extract kit. The composition of the reagents in the kit were not disclosed by the company, Active Motif. Cells were washed with PBS/phosphatase inhibitors (5 ml) and a further 3 ml of PBS/phosphatase inhibitors then added to the flask. The cells were gently scraped off the flask, transferred to a 15 ml tube and pelleted by centrifugation at 400 g for 5 min. The cells were resuspended in the hypotonic buffer (500 μ l) and incubated on ice for 15 min. The detergent solution (25 μ l) was added and the cells vortexed for 10 s followed by centrifugation at 12,000 rpm for 30 s in a microcentrifuge. The nuclear pellet was resuspended in the lysis buffer (50 μ l), vortexed for 10 s and incubated on ice on a rocking platform for 30 min. The extract was vortexed for 30 s and then centrifuged at 12,000 rpm for 10 min in a microcentrifuge. The supernatant (nuclear fraction) was retained and protein concentrations of the samples were determined using the Bradford assay.

4.2.2.2. TransAM ER

Complete binding buffer (40 μ l) was added to each well. Protein from each nuclear extract sample (8 μ g) diluted in complete lysis buffer to a final volume of 10 μ l was added to the wells in duplicate and incubated for 1 h on a rocking platform at 100 rpm at room temperature. The wells were washed three times with wash buffer (200 μ l) and then incubated with the supplied ER α antibody diluted 1:1000 in antibody binding buffer (100 μ l) for 1 h at room temperature. The wells were then washed three times with wash buffer (200 μ l) and incubated with the HRP-conjugated secondary antibody

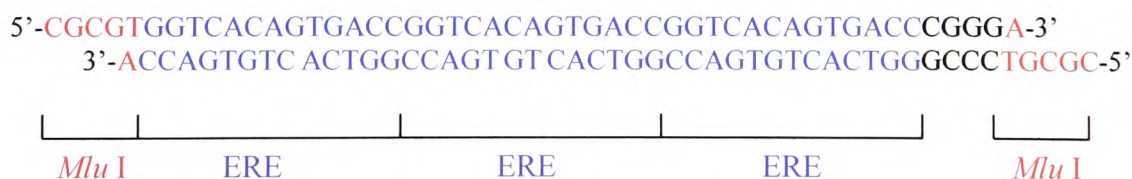
diluted 1:1000 in antibody binding buffer (100 μ l) for 1 h at room temperature. Finally, the wells were washed four times with wash buffer (200 μ l) and developed using the HRP substrate solution (100 μ l) for 5 min in the dark. The reactions were terminated using 0.5 M sulphuric acid (100 μ l) and the absorptions measured using a plate reader at 450 nm with a reference of 620 nm using an Anthos 2010 microplate reader.

4.2.3. Examination of the influence of TF on the transcriptional activity of ER α

ER α transcriptional activity was examined using a luciferase reporter vector constructed by cloning the ERE consensus sequence for ER α into the pGL3-promoter vector (Fig 4.2) upstream of the luciferase gene. Following transfection of this reporter vector into cells, ER α transcriptional activity can be determined by measuring the luciferase activity of the cell lysates.

4.2.3.1. Design of the ERE insert

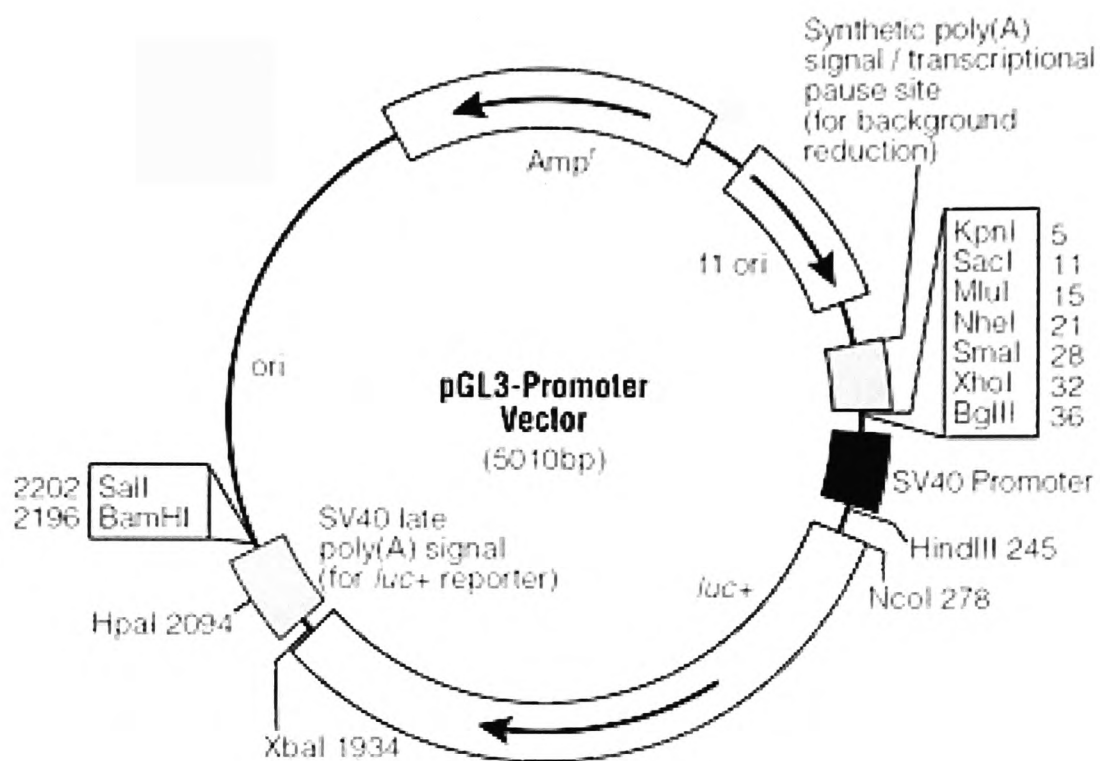
Forward and reverse DNA sequences were designed to contain three tandem ERE sequences flanked by the *Mlu* I restriction site to allow the production of 5' overhangs for the ligation of the insert into the digested pGL3 vector. Additionally, the ERE sequences were synthesised with 5' phosphate groups to allow the ligation of the insert into the dephosphorylated pGL3 vector.



4.2.3.2. Preparation of the ERE insert

Before ligation into the vector, the ERE construct was prepared by annealing the forward and reverse sequences. Forward and reverse ERE sequences (500 pmol each)

Figure 4.2. pGL3-promoter vector



The pGL3 promoter vector contains a multiple cloning site where enhancer elements can be cloned into the vector upstream of the luciferase gene. The SV40 promoter permits transcription of the luciferase gene in mammalian cells upon activation of the upstream enhancer element. The vector has a constitutively-expressed ampicillin resistance gene (Amp^r) for selection and propagation in bacterial cells. Image taken from www.promega.com.

were mixed with annealing buffer (6 mM Tris-HCl pH 7.5, 6 mM MgCl₂, 100 mM NaCl, 1 mM DTT) and made up to a final volume of 100 µl with distilled water. The reaction was incubated at 95°C for 10 min and then gradually cooled to room temperature at a rate of -1°C/30 s.

4.2.3.3. Restriction digestion of the pGL3 plasmid

The incubation time required for the *Mlu* I enzyme to completely digest the pGL3 plasmid was optimised by examining digested samples at intervals up to 3 h. Following optimisation, restriction digestion reactions were set up to contain *Mlu* I (10 U), restriction enzyme buffer (6 mM Tris-HCl pH 7.9, 6 mM MgCl₂, 150 mM NaCl, 1 mM DTT), BSA (0.1 mg/ml) and pGL3 (100 µg/ml) and made up to 20 µl with distilled water. The reactions were incubated at 37°C for 1 h and the plasmid then purified from the reaction mix using the GFX DNA purification kit as follows.

GFX columns contain a glass fibre matrix that binds DNA, allowing plasmid DNA to be extracted from reactions. A GFX column was placed in a collection tube and capture buffer (500 µl) added to the GFX column. The reaction mixture containing the plasmid was added to the GFX column, mixed by repeated pipetting and then centrifuged at 13,000 rpm for 1 min in a microcentrifuge and the flow-through discarded. Wash buffer (500 µl) was added to the GFX column and centrifuged at 13,000 rpm for 1 min in a microcentrifuge. The GFX column was transferred to a 1.5 ml tube and distilled water (50 µl) added to the top of the glass fibre matrix in the GFX column. The column was incubated at room temperature for 1 min and then centrifuged at 13,000 rpm for 1 min in a microcentrifuge to elute the DNA from the column.

4.2.3.4. Removal of 5' phosphates from pGL3 using CIAP

Following restriction digest of pGL3, the 5' phosphate groups were removed from the digested plasmid using calf intestinal alkaline phosphatase (CIAP) to prevent the vector from self-annealing. A reaction was set up containing plasmid solution (40 μ l), CIAP reaction buffer (50 mM Tris-HCl pH 9.3, 1 mM MgCl₂, 0.1 mM ZnCl₂, 1 mM spermidine), CIAP (0.01 U) and made up to a final volume of 50 μ l with distilled water and incubated at 37°C for 30 min. A further 0.01 units of CIAP was then added and incubated for another 30 min at 37°C. This further addition of CIAP was carried out as CIAP is known to be inhibited by inorganic phosphate generated during the reaction. The vector was then purified from the reaction mix using the GFX kit as described above. The quantity of pGL3 was determined by measuring absorption at 260 nm and purity assessed by 1 % (w/v) agarose gel electrophoresis.

4.2.3.5. Ligation of the ERE insert into pGL3

Ligation reactions were set up containing T4 DNA ligase (4 U), ligase buffer (50 mM Tris-HCl pH 7.5, 7 mM MgCl₂, 1 mM DTT), ATP (1 mM) and digested, CIAP treated pGL3 and the ERE insert at molar ratios of 1:100, 1:1000, 1:5000 and 1:10,000 (plasmid:insert) and made up to a final volume of 20 μ l with distilled water. The reactions were incubated overnight at 4°C, 2 days at 4°C or 2 h at 23°C. Competent *E.coli* TB-1 were then transformed with each ligation mix in turn (10 μ l) as described in the general methods section. Transformed bacterial cells (20 μ l) were selected by plating out on carbenicillin-agar plates (100 μ g/ml) and incubated overnight at 37°C. Colonies were transferred and grown in LB broth (50 ml) at 37°C overnight and plasmids extracted using the miniprep plasmid isolation procedure as described in the general methods section. Plasmids were sequenced externally (Yorkshire Biosciences)

using the following forward primer which binds a short distance (50 bp) upstream of the multiple cloning site of pGL3:

5'-CTAGCAAAATAGGCTGTCCCC-3'

4.2.3.6. Determination of transfection efficiency by flow cytometry

Transfection efficiency was determined by transfecting cells with the pEGFP-C3 mammalian expression vector, which encodes enhanced green fluorescent protein (EGFP), and measuring the expression of green fluorescence by flow cytometry. MCF-7 cells (4×10^5) were seeded out into 12 well plates and transfected with 1 μ g of the pEGFP-C3 vector using the Lipofectin reagent as described in the general methods section. Following 24 h incubation to allow the expression of EGFP, the cells were harvested, washed twice in PBS (1 ml) and then resuspended in PBS (300 μ l). The cells were examined by flow cytometry as described in the general methods section 2.4.

4.2.4. Examination of the influence of TF on transcriptional activity of ER α using the pGL3-ERE reporter vector

Cells (4×10^5) were seeded out into 12 well plates and incubated at 37°C overnight. The cells were then transfected with pGL3-ERE (1 μ g) using the Lipofectin reagent. Following incubation for 6 h, the cells were washed with PBS (1 ml) and phenol red-free medium (1 ml) containing 1 % (v/v) FCS added to each well, and incubated at 37°C overnight. The cells were then treated with recombinant TF (0-500 nM) in the presence and absence of oestradiol (250 pM) for 8 h. The cells were lysed and luciferase activity measured by adding luciferase substrate (100 μ l) to cell lysate (20 μ l) and measuring light emitted using a luminometer as described in the general methods section.

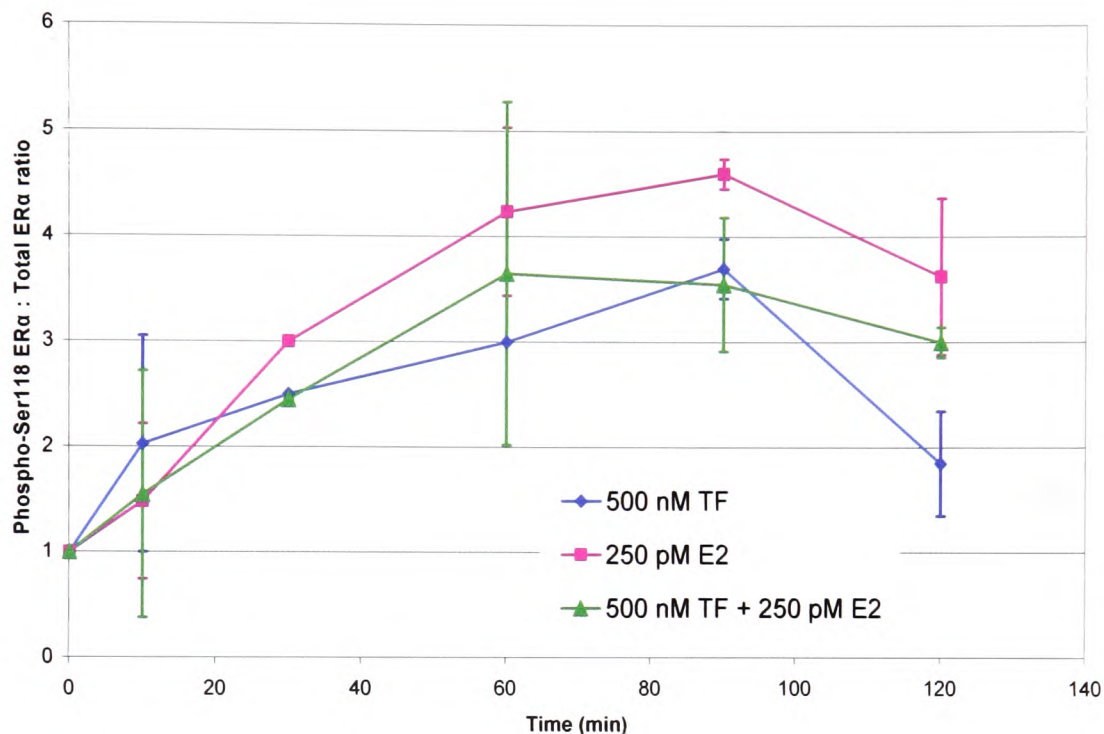
4.3. Results

4.3.1. Examination of the influence of TF on ER α serine 118 phosphorylation

Incubation of MCF-7 cells with oestradiol (250 pM) resulted in a 4.5 fold increase in ER α serine 118 phosphorylation at 90 min post-treatment (Fig 4.3 & 4.4). The addition of TF (500 nM) alone resulted in increased ER α phosphorylation, also peaking at 90 min post-treatment, although the increase in phosphorylation was at a lower magnitude compared to that observed with oestradiol. The addition of TF (500 nM) together with oestradiol (250 pM) also resulted in increased ER α serine 118 phosphorylation.

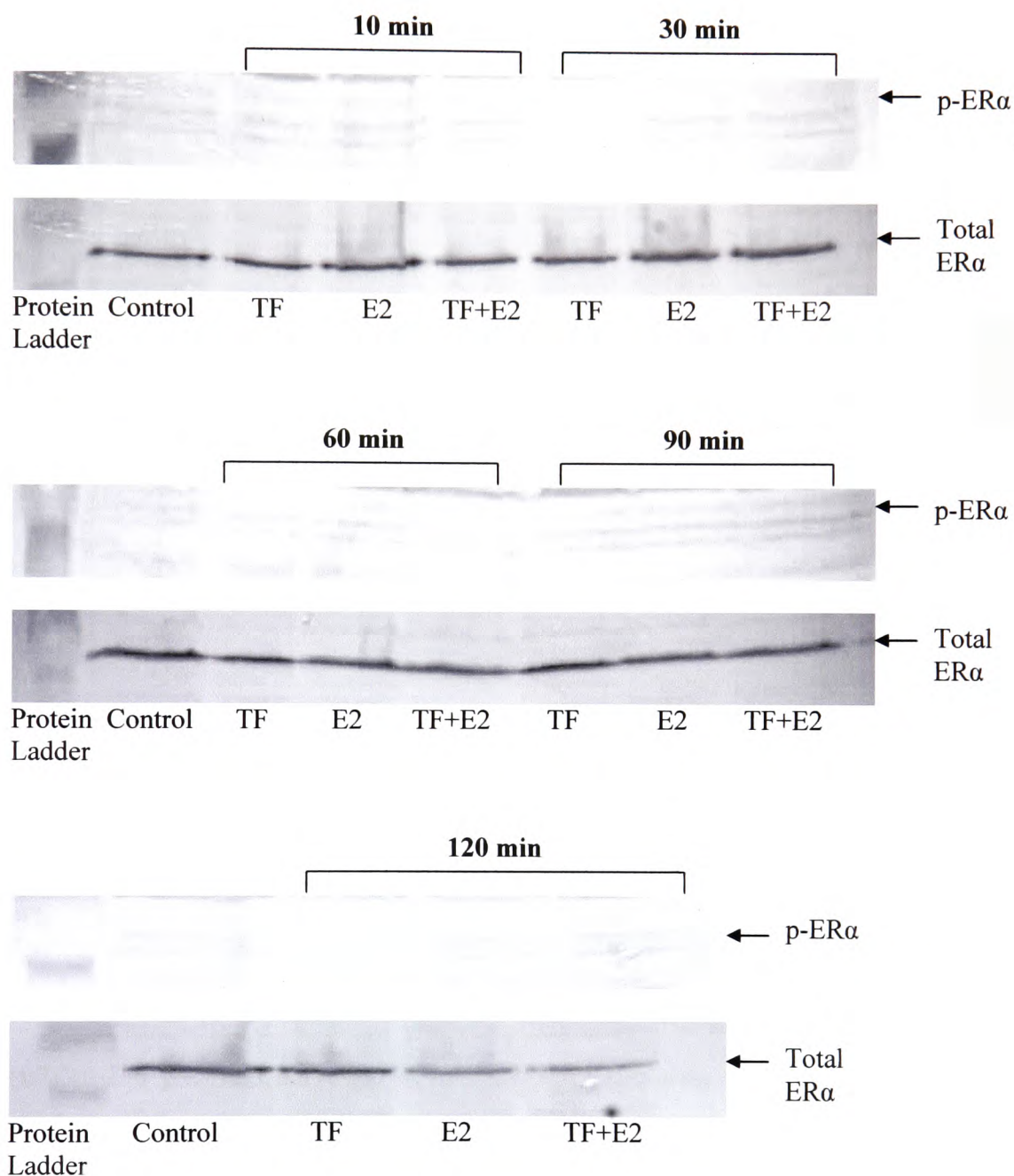
Incubation of T47D cells with oestradiol (250 pM) resulted in a small increase in ER α serine 118 phosphorylation, peaking at 90 min post-treatment (Fig 4.5). However, the level of ER α phosphorylation in T47D cells in response to oestradiol (250 pM) was neither as rapid nor as pronounced compared to that in MCF-7 cells (Fig 4.6). Moreover, the addition of TF (500 nM) alone resulted in a small increase in ER α phosphorylation, reaching a maximum at 60 min post-treatment. Furthermore, the combination of TF (500 nM) and oestradiol (250 pM) produced no detectable difference in ER α phosphorylation compared to those observed with the individual components alone. However, due to the low levels of ER α serine 118 phosphorylation in these cells, the phospho-ER α bands for some samples were difficult to detect and subject to errors. Therefore, the measured changes in ER α phosphorylation were not deemed to be reliable.

Figure 4.3. The influence of TF on ER α phosphorylation in MCF-7 cells



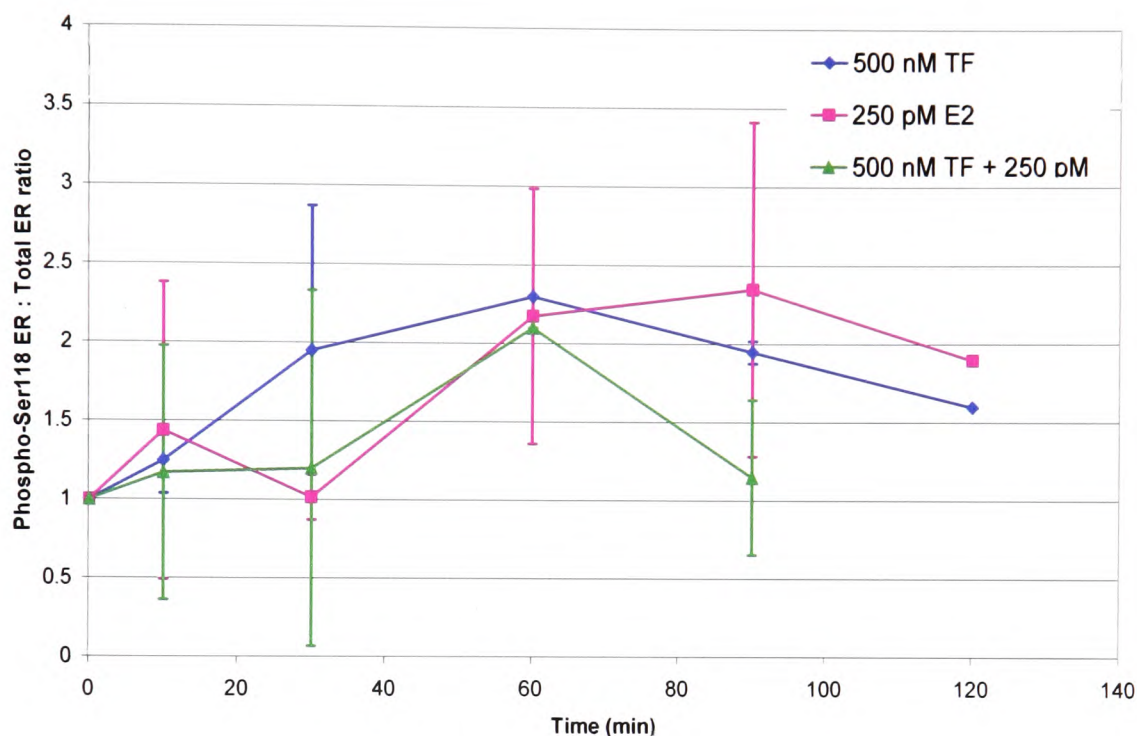
MCF-7 cells were cultured in T25 flasks and adapted to phenol red-free medium containing 1 % (v/v) FCS. The cells were treated with TF (0-500 nM) and oestradiol (E2) (0-250 pM) and harvested at intervals over 120 min. The cells were lysed in Laemmli's buffer, and proteins separated by SDS-PAGE. Proteins were transferred onto nitrocellulose membranes and then probed for phosphorylated serine 118 ER α using a goat anti-human ER α phospho-serine 118 antibody. The membranes were then probed for total ER α using a mouse anti-human ER α antibody, and images recorded using the GeneSnap program. The ratio of phosphorylated ER α to total ER α was calculated using the GeneTool program. Data represent the average of two independent experiments \pm SD.

Figure 4.4. ER α serine 118 phosphorylation in MCF-7 cells



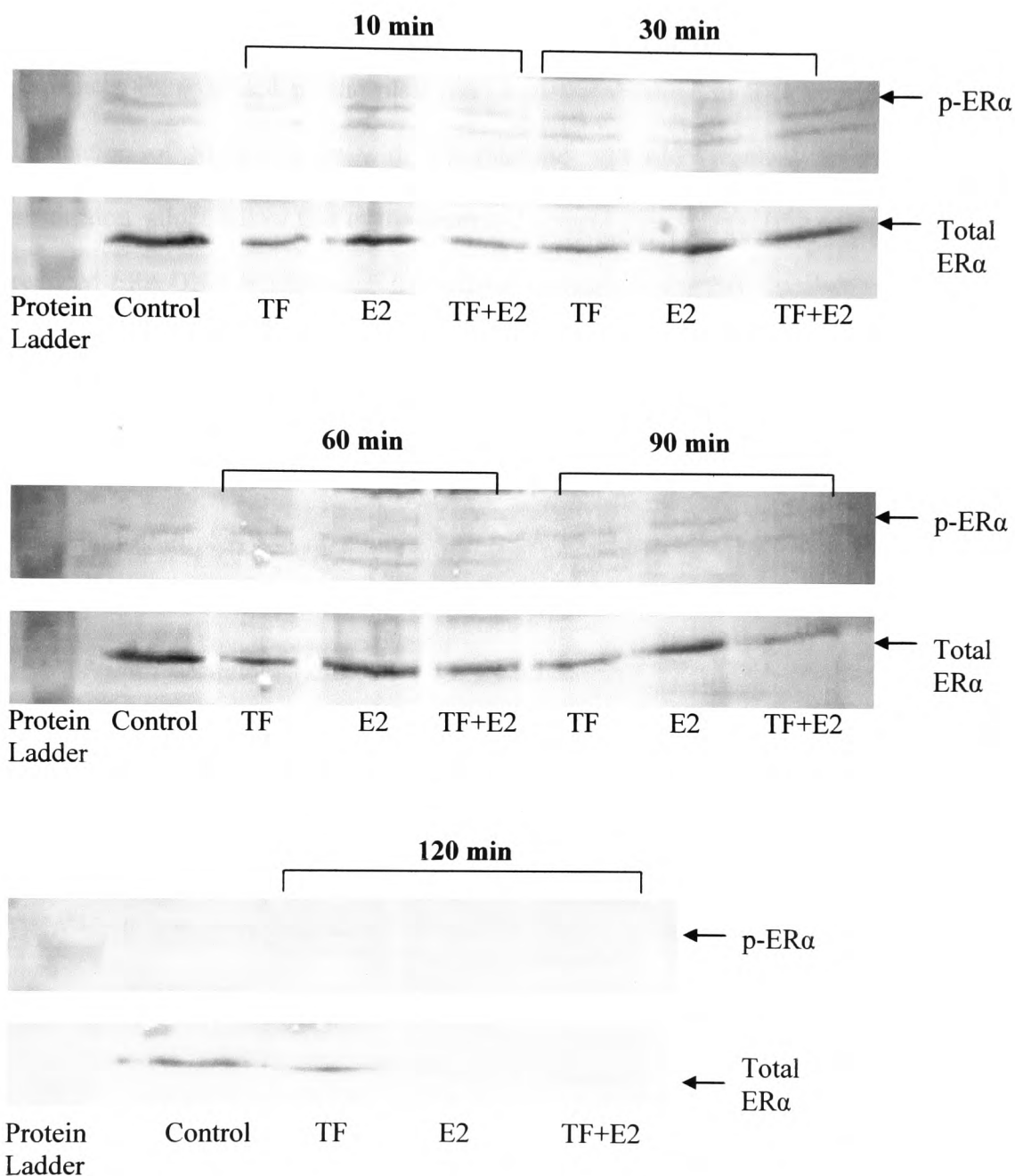
MCF-7 cells were treated with exogenous TF (500 nM) in the presence or absence of oestradiol (250 pM). The cells were then lysed in Laemmli's buffer, and proteins separated by SDS-PAGE. Proteins were transferred onto nitrocellulose membranes and probed for phosphorylated serine 118 ER α using a goat anti-human ER α phospho-serine 118 antibody. The membranes were then probed for total ER α using a mouse anti-human ER α antibody, and images recorded using the GeneSnap program.

Figure 4.5 The influence of TF on ER α phosphorylation in T47D cells



T47D cells were cultured in T25 flasks and adapted to phenol red-free medium containing 1 % (v/v) FCS. The cells were treated with TF (0-500 nM) and oestradiol (E2) (0-250 pM) and harvested at intervals over 120 min. The cells were lysed in Laemmli's buffer, and proteins separated by SDS-PAGE. Proteins were transferred onto nitrocellulose membranes and then probed for phosphorylated serine 118 ER α using a goat anti-human ER α phospho-serine 118 antibody. The membranes were then probed for total ER α using a mouse anti-human ER α antibody, and images recorded using the GeneSnap program. The ratio of phosphorylated ER α to total ER α was calculated using the GeneTool program. Data represent the average of two independent experiments \pm SD.

Figure 4.6. ER α serine 118 phosphorylation in T47D cells



T47D cells were treated with exogenous TF (500 nM) in the presence or absence of oestradiol (250 pM). The cells were then lysed in Laemmli's buffer, and proteins separated by SDS-PAGE. Proteins were transferred onto nitrocellulose membranes and probed for phosphorylated serine 118 ER α using a goat anti-human ER α phospho-serine 118 antibody. The membranes were then probed for total ER α using a mouse anti-human ER α antibody, and images recorded using the GeneSnap program.

4.3.2. Examination of the influence of TF on ER α DNA binding activity

The DNA binding activity of ER α was examined using the TransAM ER kit. This is an ELISA-based method in which active ER α in cell samples binds to synthetic ERE DNA sequences immobilised on the plate, and is detected using an ER α specific antibody. Incubation of MCF-7 cells with TF (50 and 500 nM) resulted in reductions in absorption values below that of the untreated control over 90 min (Fig 4.7A), indicating reduced ER α DNA binding activity in these samples. In contrast, incubation of MCF-7 cells with oestradiol (250 pM) resulted in a rapid increase in ER α DNA binding activity, peaking at 30 min post-treatment, and subsequently decreasing to untreated control levels by 120 min (Fig 4.7B). The addition of a combination of TF (50 nM) and oestradiol (250 pM) had no additional influence on oestradiol-mediated DNA binding activity of ER α compared to that of oestradiol alone. In contrast, the inclusion of 500 nM TF with oestradiol (250 pM) resulted in reduced ER α DNA binding activity in MCF-7 cells below that of the untreated control at 90 min post-treatment (Fig 4.7B).

Incubation of T47D cells with TF (50 and 500 nM) also resulted in the reduction in ER α DNA binding activity over 90 min (Fig 4.8A). However, incubation of T47D cells with oestradiol (250 pM) had no measurable effect on ER α DNA binding activity over the tested period (Fig 4.8B), and remained unaffected by the inclusion of TF.

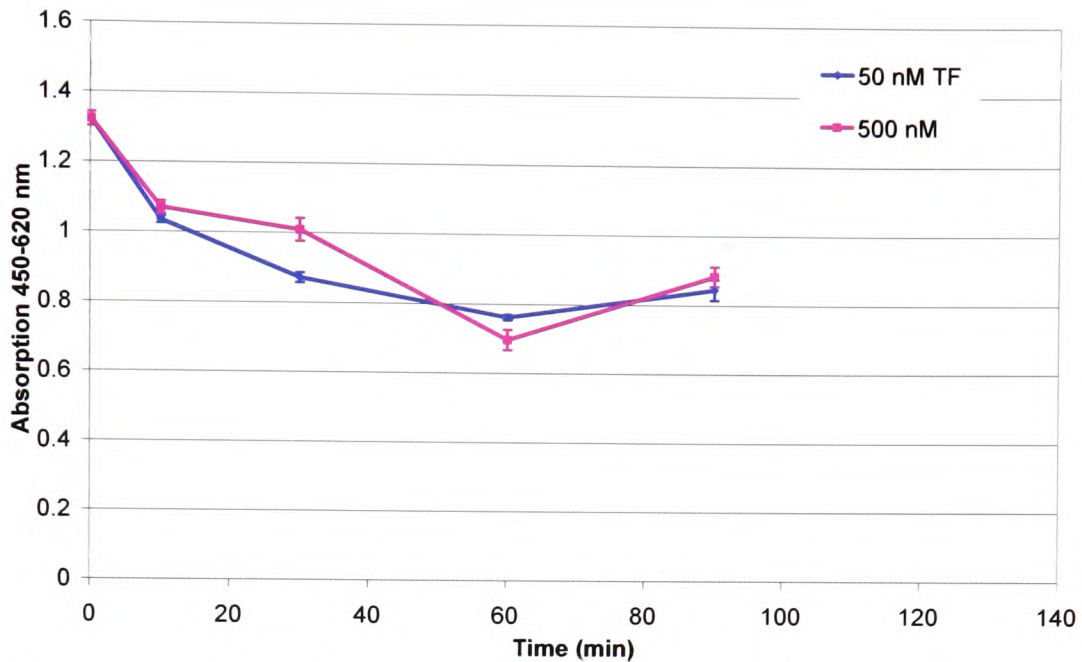
4.3.3. Preparation of an ERE reporter vector

4.3.3.1. Optimisation of *Mlu* I restriction digest of pGL3

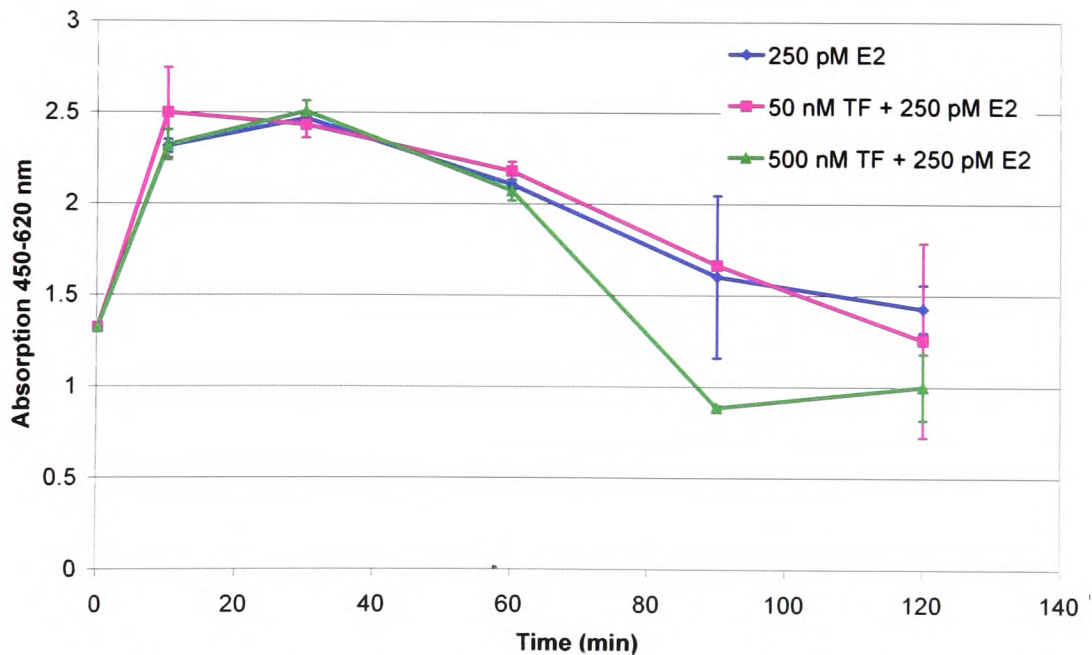
The pGL3-promoter vector was digested using the *Mlu* I restriction enzyme in order to produce 5' overhangs to allow the cloning of the ERE insert into the vector. The incubation time required for the *Mlu* I enzyme to completely digest the pGL3 plasmid was optimised by examining pGL3 samples digested by *Mlu* I at 37°C over 1-3 h.

Figure 4.7. The influence of TF on ER α DNA binding activity in MCF-7 cells

A.



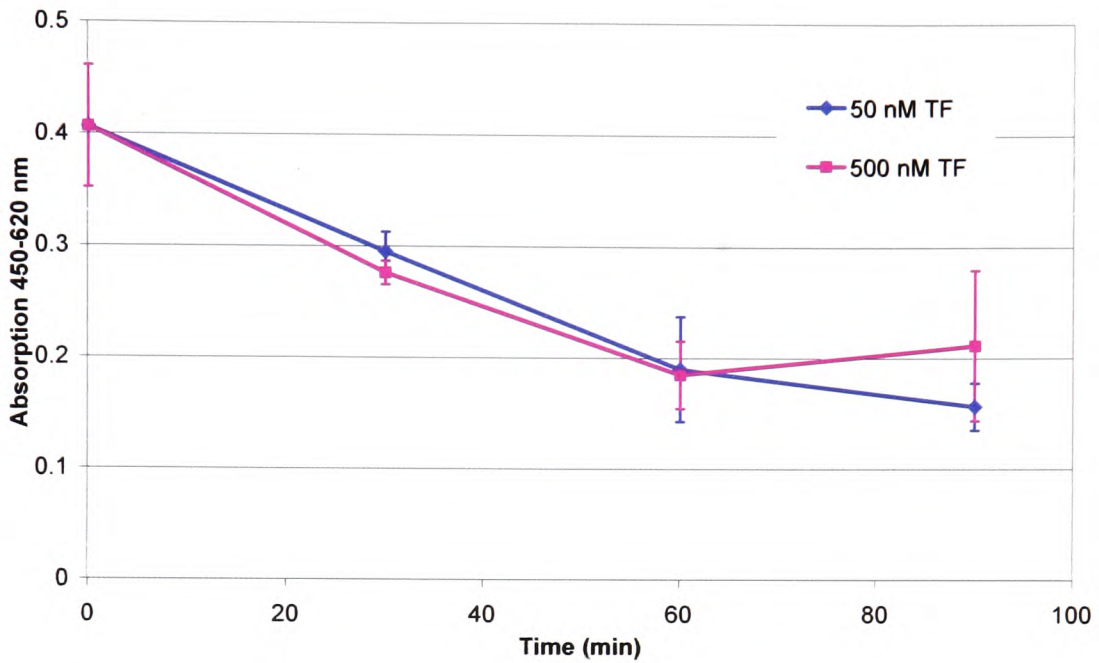
B.



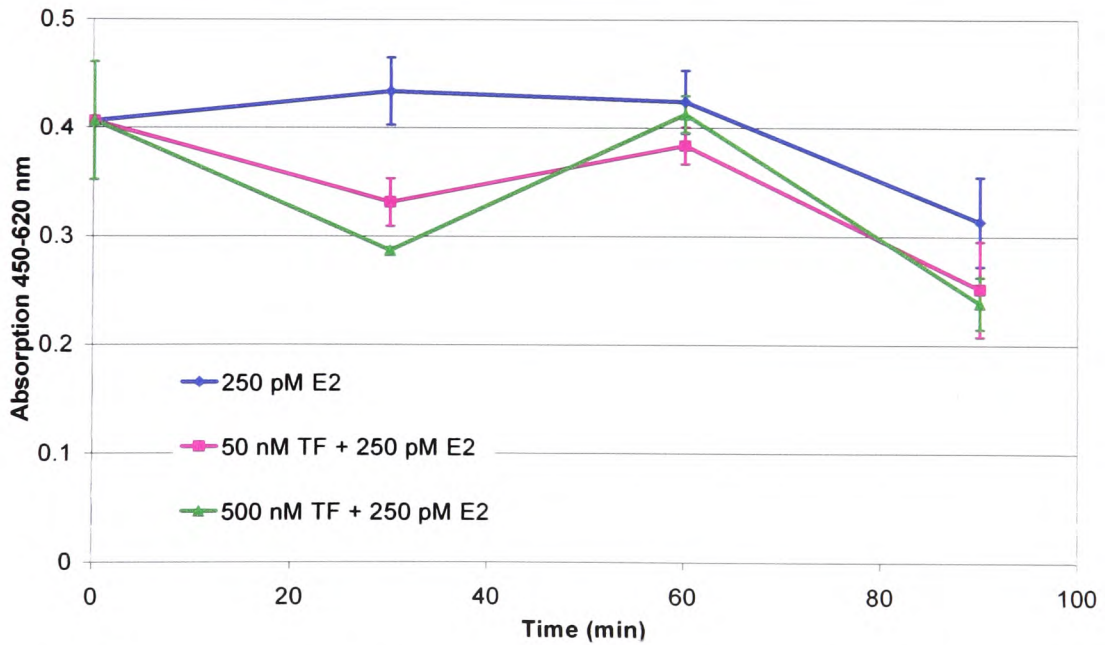
MCF-7 cells were cultured in T75 flasks and adapted to phenol red-free medium containing 1 % (v/v) FCS. The cells were treated with TF (0-500 nM) in the absence (A) and presence (B) of oestradiol (250 pM) and then harvested at intervals (0-120 min). Nuclear extracts were purified and the ability of ER α to bind to the ERE DNA sequence was examined using the TransAM ER α kit. Data represent the average of two experiments measured in duplicate \pm SD.

Figure 4.8. The influence of TF on ER α DNA binding activity in T47D cells

A.



B.



T47D cells were cultured in T75 flasks and adapted to phenol red-free medium containing 1 % (v/v) FCS. The cells were treated with TF (0-500 nM) in the absence (A) and presence (B) of oestradiol (250 pM) and then harvested at intervals (0-120 min). Nuclear extracts were purified and the ability of ER α to bind to the ERE DNA sequence was examined using the TransAM ER α kit. Data represent the average of two experiments measured in duplicate \pm SD.

Complete restriction digest of the plasmid results in linearisation of the plasmid, which is visible as one band. pGL3 digestion by *Mlu* I was achieved after 1 h incubation at 37°C (Fig 4.9).

4.3.3.2. Cloning ERE insert into pGL3

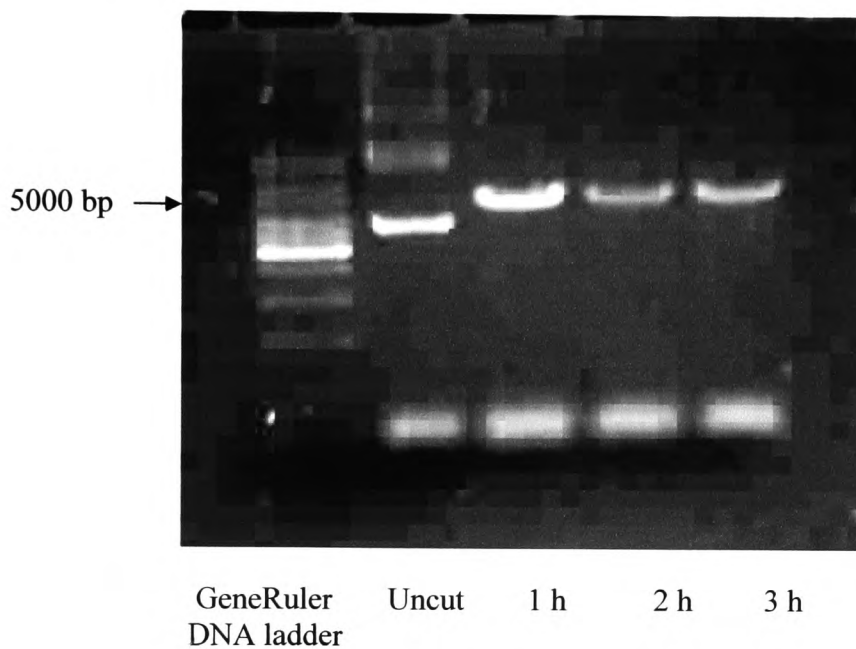
A range of molar ratios of the pGL3 plasmid and ERE insert were ligated by incubation over a range of durations and at different temperatures. Positive clones were selected using carbenicillin-agar plates and plasmids were purified from the bacteria and sent for sequencing by Yorkshire Biosciences. The sequencing results showed that two of the positive clones had the ERE insert but in reverse. One positive clone, ligated overnight at 4°C with a 1:1000 plasmid:insert molar ratio, contained the ERE insert in the correct orientation.

4.3.3.3. Optimisation of transfections

To ensure efficient transfection of the cells the optimal cell number was estimated by transfecting a range of MCF-7 cell populations (10^5 - 6×10^5) with the pCMV-Luc plasmid. The pCMV-Luc plasmid contains the luciferase gene under the control of the cytomegalovirus (CMV) promoter and is capable of constitutively expressing luciferase when transfected into mammalian cells. Following transfection, the cells were incubated at 37°C for 20 h to allow expression of the luciferase gene, and luciferase activity was then measured. Luciferase activity increased in proportion with the number of cells up to a maximum of 650,000 relative light units (RLU) with 4×10^5 cells (Fig 4.10). In comparison, the background count for untransfected cells was 1086 RLU.

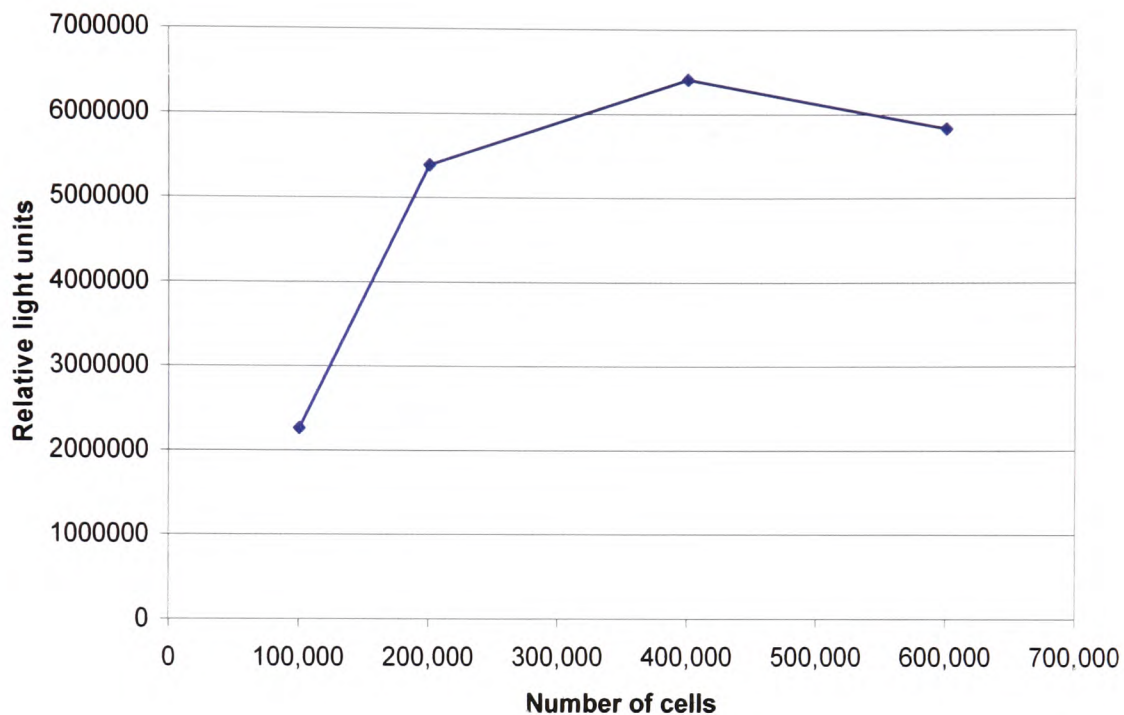
The transfection efficiency was assessed by transfection of MCF-7 cells with the pEGFP-C3 expression vector, which constitutively expresses enhanced green

Figure 4.9. Optimisation of *Mlu* I restriction digest of pGL3



Reactions were set up containing the pGL3-promoter vector and the *Mlu* I restriction enzyme and incubated at 37°C for 1-3 h. The restriction products were then examined alongside the undigested plasmid using 1 % (w/v) agarose gel electrophoresis and images recorded using the GeneSnap program.

Figure 4.10. Optimisation of cell numbers for transfection



MCF-7 cells (10^5 - 6×10^5) were seeded out into 12 well plates and transfected with the pCMV-Luc plasmid, which constitutively expresses luciferase. The cells were incubated at 37°C for 20 h to allow expression of the luciferase gene. The cells were then lysed and the luciferase activity of the cell lysates measured using a Junior LB 9509 luminometer. The data are from one experiment.

fluorescent protein (EGFP). Transfection efficiency was determined by measuring 10,000 events and calculating the percentage of cells expressing green fluorescence using a flow cytometer. A gate was set to contain 7 % of untransfected cells. The average percentage of transfected cells in this area, indicating the transfection efficiency, was 27.4 % above that of the untransfected control cells (Fig 4.11).

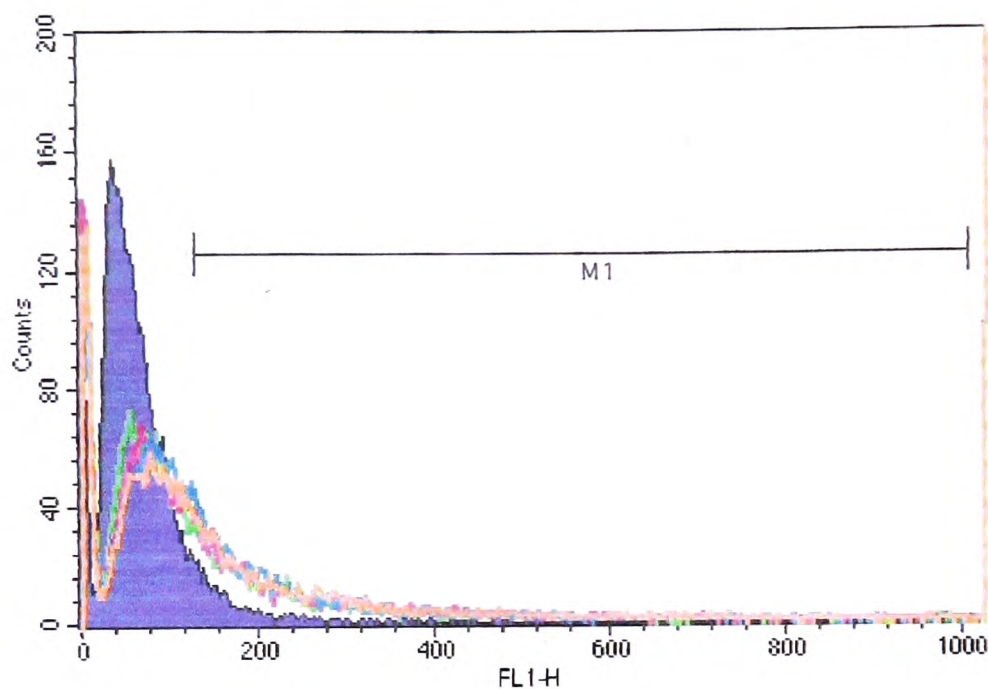
In order to determine the optimal duration of incubation required for maximal response to oestradiol, MCF-7 cells (4×10^5) transfected with the pGL3-ERE reporter vector were treated with oestradiol (0 or 250 pM) and luciferase activities were measured at 4, 8, 16 and 24 h post-treatment. The greatest difference in luciferase activity between oestradiol treated and untreated cells was observed at 8 h post-treatment (Fig 4.12). Moreover, by 24 h incubation the expression of luciferase became independent of oestradiol.

In addition to the duration of incubation, the sensitivity of the pGL3-ERE reporter vector to oestradiol (0-1000 pM) was assessed in transfected MCF-7 cells. The luciferase activity in response to oestradiol increased in a concentration dependent manner up to a maximal value with 500 pM oestradiol (Fig 4.13).

4.3.4. Examination of the influence of TF on ER α transcriptional activity using the ERE reporter vector

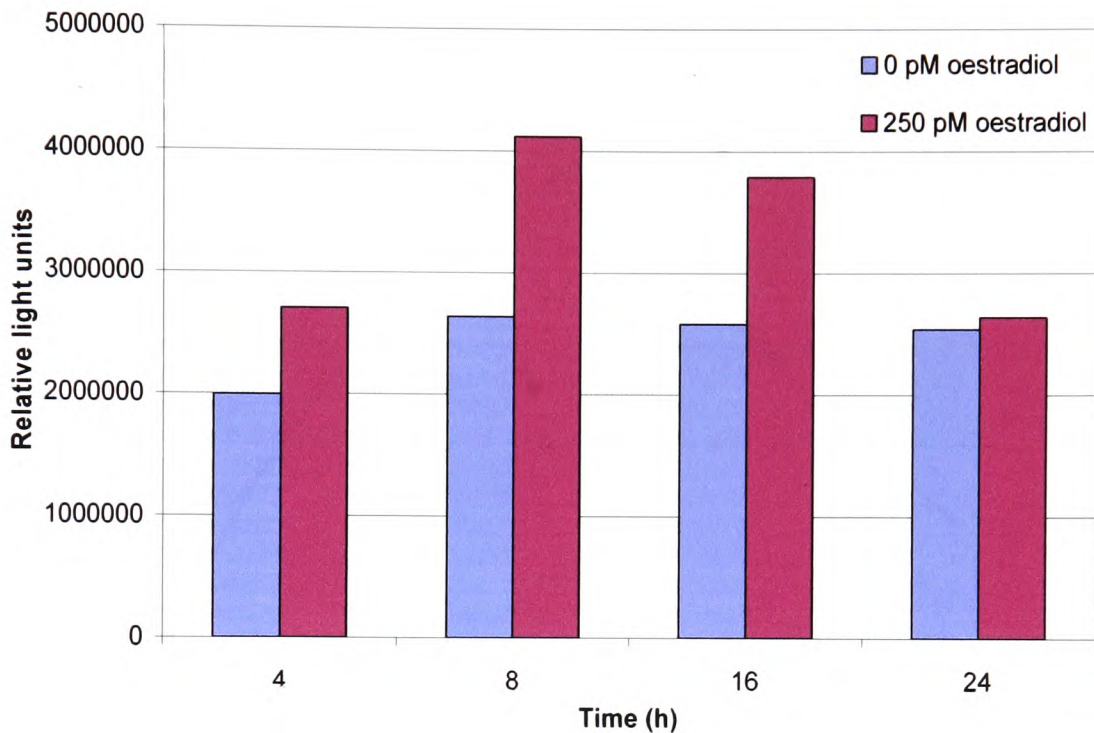
The addition of oestradiol (250 pM) alone resulted in increased luciferase activity above that of the untreated control (Fig 4.14). The addition of recombinant TF (50 and 500 nM) alone had no significant effect on ER α transcriptional activity in MCF-7 cells. However, inclusion of TF (50 and 500 nM) with oestradiol (250 pM) reduced the luciferase activity below that of cells incubated with oestradiol (250 pM) alone.

Figure 4.11. Transfection efficiency



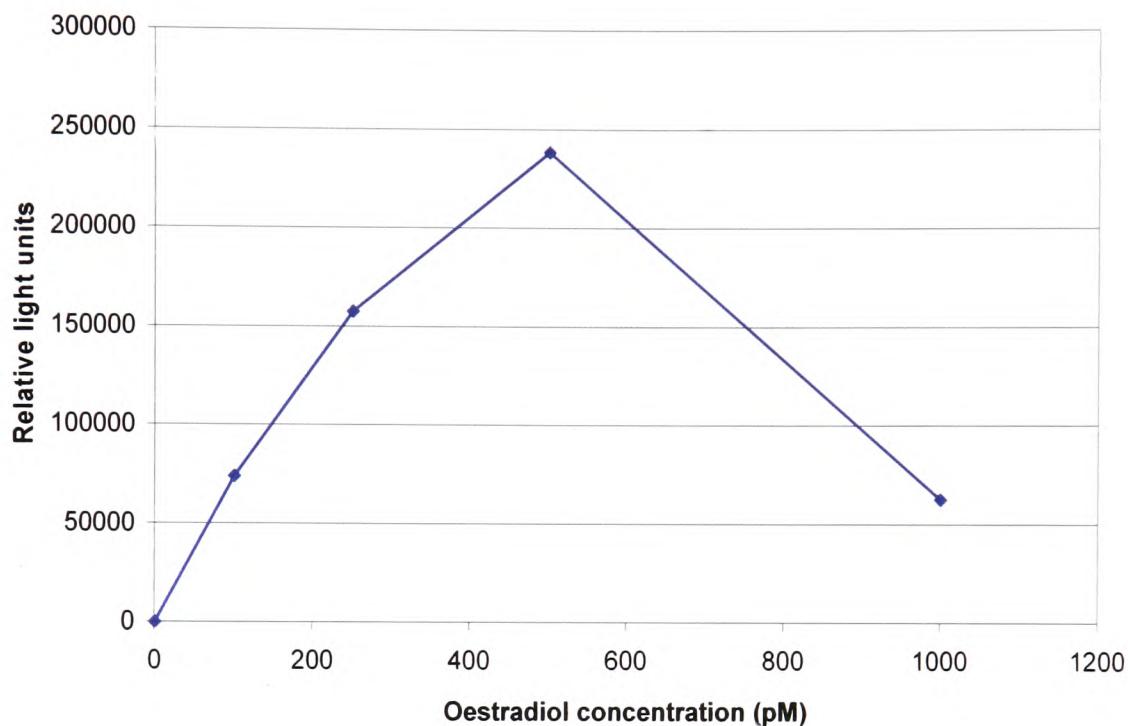
MCF-7 cells (4×10^5) were seeded out into 12 well plates and transfected with the pEGFP-C3 vector. The cells were incubated at 37°C for 24 h to allow the expression of the enhanced green fluorescent protein (EGFP) gene. The cells were then harvested, washed twice in PBS (1 ml) and resuspended in PBS ($300 \mu\text{l}$). Cells were examined by flow cytometry using a FACSCalibur flow cytometer. A gate was set to contain 7 % of untransfected cells and 10,000 events were recorded for each sample. The transfection efficiency was determined by measuring the number of fluorescent green events. The data is representative of two independent experiments. Area = untransfected cells. Green, red, blue and orange lines represent four separate sets of cells each transfected with pEGFP-C3.

Figure 4.12. Optimisation of time point for ERE transfections



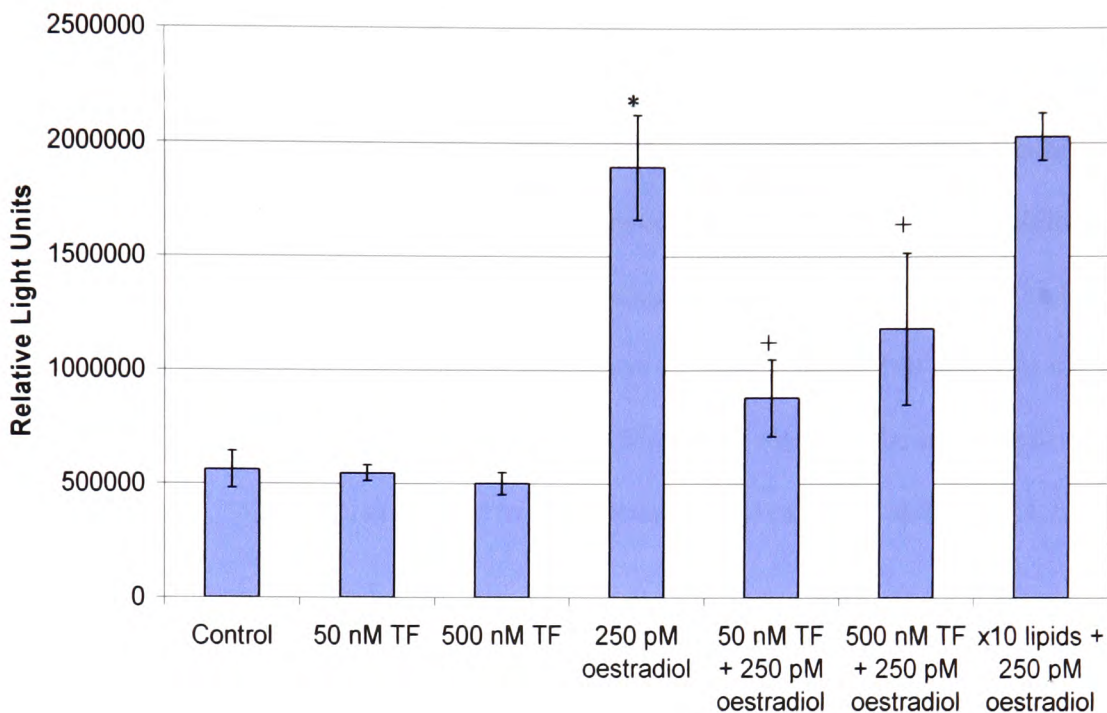
MCF-7 cells (4×10^5) were seeded out into 12 well plates and transfected with the pGL3-ERE reporter vector using the Lipofectin reagent. The cells were then placed in phenol red-free medium containing 1 % (v/v) FCS, treated with oestradiol (0 or 250 pM) and incubated at 37°C. The cells were harvested at intervals over 24 h and the luciferase activities of the cell lysates measured using a Junior LB 9509 luminometer. The data are from one experiment.

Figure 4.13. pGL3-ERE reporter vector function in response to oestradiol



MCF-7 cells (4×10^5) were seeded out into 12 well plates and transfected with the pGL3-ERE reporter vector. The cells were treated with oestradiol (0-1000 pM) and incubated at 37°C for 8 h. The cells were then lysed and luciferase activity measured using a Junior LB 9509 luminometer. Background luciferase activity was subtracted from the samples. The data are from one experiment.

Figure 4.14. The influence of TF on ER α transcriptional activity in MCF-7 cells



MCF-7 cells (4×10^5) were seeded out into 12 well plates and transfected with the pGL3-ERE reporter vector. The cells were then placed in phenol red-free medium containing 1 % FCS and treated with recombinant TF (0-500 nM) in the presence or absence of oestradiol (250 pM). Furthermore, a set was incubated with lipids diluted $\times 10$ (containing 1 % (w/v) BSA) extracted from recombinant TF together with oestradiol (250 pM). The cells were incubated at 37°C for 8 h, lysed and luciferase activities of the cell lysates measured using a Junior LB 9509 luminometer. Data represents the average of six independent experiments measured in duplicate \pm SD.

* $p < 0.05$ vs. the untreated control. + $p < 0.05$ vs. oestradiol treated cells.

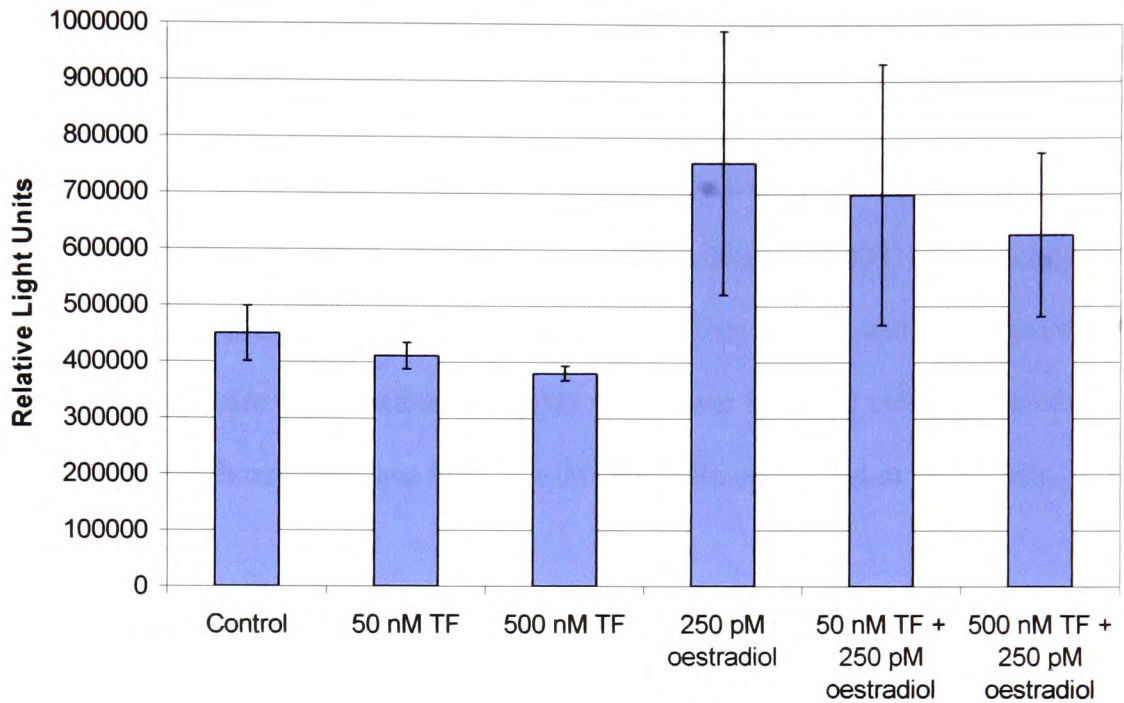
Furthermore, addition of the lipids (containing 1 % (w/v) BSA) extracted from recombinant TF (500 nM) had no detectable effect on oestradiol-mediated ER α transcriptional activation in MCF-7 cells.

Incubation of T47D cells with TF (500 nM) appeared to result in a small decrease in ER α transcriptional activity compared to the untreated control (Fig 4.15). The addition of oestradiol (250 pM) led to an increase in luciferase activity, although this was not as pronounced as observed in MCF-7 cells (Fig 4.14). Inclusion of TF (50 and 500 nM) together with oestradiol (250 pM) resulted in a downward trend in the transcriptional activity of ER α in T47D cells compared to cells treated with oestradiol alone (Fig 4.15).

4.4. Discussion

The data obtained in chapter 3 demonstrate the suppression of ER α expression on exposure of breast cancer cells to exogenous TF. In this part of the study, the hypothesis that exogenous TF may also suppress normal oestradiol-ER α signalling was examined. The addition of oestradiol (250 pM) to MCF-7 and T47D cells resulted in increases in the DNA binding activity of ER α to ERE sequences, peaking at 30 min post-treatment (Fig 4.7B & 4.8B). Since steroid receptors such as ER α bind to DNA when in an active form (Gross & Yee 2002), this increase in the DNA binding of ER α may indicate increases in the activity of ER α in response to oestradiol. Furthermore, oestradiol (250 pM) increased the rate of phosphorylation of ER α on serine 118 in both MCF-7 and T47D cells, peaking at 90 min post-treatment (Fig 4.3 & 4.5). These results are also in agreement with previous studies which have shown that the binding of ER α to ERE promoters in response to oestradiol results in phosphorylation on serine 118 by cdk7, a component of the transcription initiation complex (Ito et al 2004, Chen et al 2000). In addition, oestradiol (250 pM) increased the transcriptional activity of ER α from the

Figure 4.15. The influence of TF on ER α transcriptional activity in T47D cells



T47D cells (4×10^5) were seeded out into 12 well plates and transfected with the pGL3-ERE reporter vector. The cells were then placed in phenol red-free medium containing 1 % FCS and treated with recombinant TF (0-500 nM) in the presence or absence of oestradiol (250 pM). The cells were incubated at 37°C for 8 h, lysed and luciferase activities of the cell lysates measured using a Junior LB 9509 luminometer. Data represents the average of three independent experiments measured in duplicate \pm SD.

ERE promoter above that observed in the untreated control (Fig 4.14 & 4.15). Together, these data are in agreement with previous studies which have shown that oestradiol enhances ER α DNA binding and serine 118 phosphorylation, resulting in the increased transcriptional activity of ER α and increased expression of genes under the control of ERE promoters (Ito et al 2004, Ali et al 1993). Following transcription, ER α is degraded by the ubiquitin-proteasome pathway, allowing cells to respond rapidly to small changes in levels of oestradiol (Valley et al 2005, Reid et al 2003). Interestingly, levels of ER α phosphorylation at serine 118, DNA binding activity and transcriptional activation in response to oestradiol (250 pM) were lower in T47D cells compared to MCF-7 cells, which may be due to the lower levels of ER α expression in T47D cells.

The influence of oestradiol on cellular processes ultimately arises from the ability of oestradiol-ER α complexes to regulate the transcription of oestradiol-target genes (Gross & Yee 2002). Therefore, the activation or inhibition of oestradiol-mediated transcriptional activity must include the regulation of ER α . In this section, the influence of exogenous TF on ER α activity, in the presence of oestradiol was examined. Comparison of the DNA binding activity of ER α in response to oestradiol (250 pM) showed no variation on inclusion of TF (500 nM) for the first 60 min (Fig 4.7B). This is likely to be due to the rapid activation of ER α by oestradiol, leading to binding of ER α to ERE sequences. Furthermore, there was no difference in the level of phosphorylation of ER α on serine 118 (Fig 4.3), indicating that exogenous TF has no influence on oestradiol-mediated serine 118 phosphorylation. However, at 90 min post-treatment, the DNA binding activity of ER α , in MCF-7 cells treated with TF (500 nM), appeared to be reduced compared to that of the cells treated with oestradiol (250 pM) alone. In contrast, the phosphorylation state of serine 118 was not altered. These alterations in the DNA binding ability of ER α seemed to be paralleled in the suppression of oestradiol-mediated

increases in the transcriptional activity of ER α from the ERE promoter in the presence of exogenous TF (500 nM) (Fig 4.14 & 4.15). Therefore, it is possible that TF-induced signalling inhibits another step essential for ER α -mediated transcriptional activity. For example, the recruitment of coactivator proteins to the ERE promoter is prerequisite for the transcriptional activity of the oestradiol-ER α complex, and it has been shown that inhibition of these coactivators also inhibits ER α transcriptional activity (Higashimoto et al 2007). Furthermore, ER α contains multiple phosphorylation sites (Fig 4.1), the phosphorylation of which are known to modulate ER α activity (Lannigan 2003) but were not explored here. In contrast, incubation of cells with lipids extracted from the Innovin reagent together with oestradiol had no measurable effect on oestradiol-mediated increases in ER α transcriptional activity (Fig 4.14), confirming that the changes in the transcriptional activity of ER α in the presence of the Innovin reagent were due to the TF apoprotein. Furthermore, any influence of the TF-associated lipids through the sequestration of oestradiol was discounted. In conclusion, exogenous TF reduced oestradiol-mediated ER α transcriptional activity, possibly through a mechanism independent of the regulation of serine 118 phosphorylation.

To further investigate the mechanism by which TF influences ER α activity, the outcome of the incubation of cells with TF, in the absence of oestradiol, on ER α activation was examined. Therefore, the influence of exogenous TF on the phosphorylation, DNA binding activity and ER α -mediated expression from the ERE promoter was measured. Addition of TF (50 and 500 nM) alone appeared to reduce ER α DNA binding below baseline activity of the untreated control in both MCF-7 and T47D cells (Fig 4.7A & 4.8A). However, incubation of MCF-7 cells with TF (500 nM) alone also seemed to induce serine 118 phosphorylation. TF is known to activate the MAPK signalling pathway through the activation of PAR2 (Morris et al 2006, Poulsen et al 1998).

Therefore, it is possible that the addition of exogenous TF may result in the activation of the MAPK ERK1/2 pathway, which directly phosphorylates serine 118 within ER α (Chen et al 2002, Kato et al 1995). These results are contradictory since MAPK-induced phosphorylation of ER α serine 118 has previously been shown to increase ER α transcriptional activity (Kato et al 1995), whereas in this study, TF alone appeared to increase the phosphorylation of serine 118 but reduce the DNA binding activity of ER α . Furthermore TF alone had no effect on ER α transcriptional activity. One possible explanation for this discrepancy could be the activation of other signalling pathways known to be initiated by TF, which in turn regulate the phosphorylation of other residues within ER α necessary for activation of the receptor. For example, phosphorylation of serine 236 in the DNA binding domain of ER α has been shown to inhibit dimerisation and DNA binding of ER α in the absence of oestradiol (Chen et al 1999). Furthermore, it has been reported that serine 118 phosphorylation is involved in controlling the rate of ER α degradation as well as the initiation of transcription (Valley et al 2005).

In summary, although TF (500 nM) alone was shown to increase the rate of phosphorylation of ER α at serine 118 while reducing the DNA binding activity, this appeared to have no influence on the transcriptional activity of ER α . In contrast, the addition of TF (50 and 500 nM) together with oestradiol (250 pM) resulted in a decrease in DNA binding of ER α and a reduction in transcriptional activity from the ERE promoter, through a mechanism that appears to be independent of the phosphorylation state of serine 118. Therefore, in this investigation exogenous TF signalling was capable of interfering with oestradiol-mediated transcriptional activity of ER α from ERE promoters. Many ER α target genes are involved in the regulation of breast cancer cell proliferation and invasion in response to oestradiol. Therefore, in conclusion, the

downregulation of ER α transcriptional activity in the presence of exogenous TF may suppress oestradiol-mediated cell proliferation, which may also lead to the development of an oestradiol-independent cell phenotype and increased invasiveness. However, in addition to the classical ERE-dependent pathway, the oestradiol-ER α complex can also regulate the transcription of genes containing other response elements, such as AP-1 promoters (Philips et al 1993) and this is considered next.

CHAPTER 5

The influence of exogenous TF on ER α activity through
the AP-1-dependent pathway

5.1. Introduction

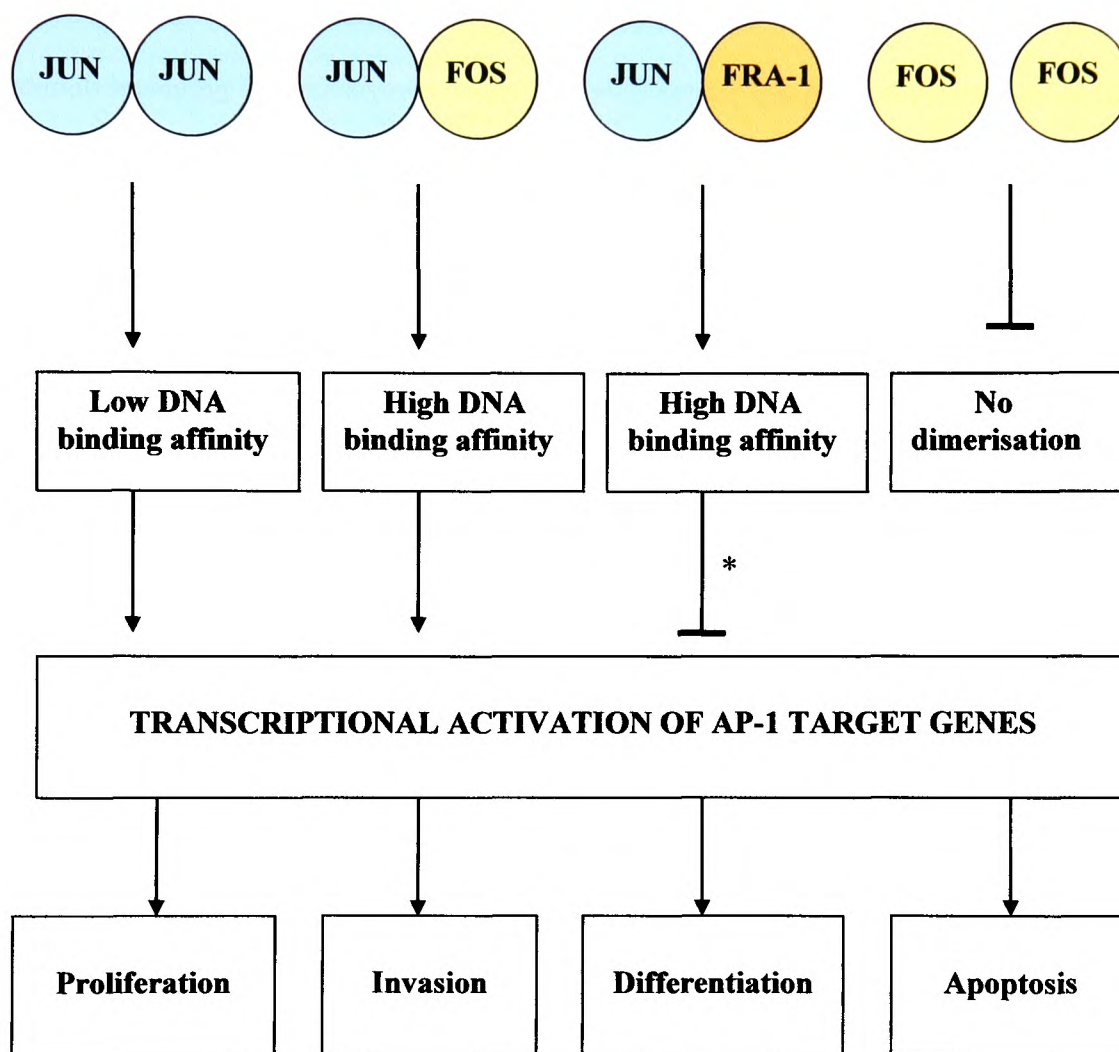
5.1.1. AP-1-dependent pathway of ER α transcription

In the classical pathway of ER α transcriptional activity, the oestradiol-ER α complex binds to ERE promoters, resulting in increased transcriptional activity of oestradiol-responsive genes. However, it has been shown that oestradiol can also modulate the expression of genes that do not have ERE promoters, but contain binding sites for other transcription factors such as AP-1 (Philips et al 1993, Umayahara et al 1994). Incubation of ER α -positive breast cancer cells with oestradiol has been shown to result in the enhanced transcriptional activity of AP-1 and lead to the expression of genes regulated by AP-1 (Philips et al 1993). Furthermore, it has been demonstrated that ER α does not need to bind to DNA in order to alter the transcriptional activation of these genes (Jakacka et al 2001). Instead, ER α directly binds to transcription factors such as AP-1, which are already associated with their own DNA binding elements (Teyssier et al 2001) (Fig 1.3). These protein-protein interactions between AP-1 and ER α at AP-1 promoters stabilise the transcription initiation complex. In this way ER α acts as a coactivator protein, enhancing the activity of the AP-1 complex and increasing the rate of transcription of AP-1 controlled genes (Teyssier et al 2001). Genes that contain AP-1 promoters and are upregulated by oestradiol-ER α include growth factors (Umayahara et al 1994), and genes that are inhibited include those involved in cell invasion such as matrix metalloproteinases (Lu et al 2006, Crowe & Brown 1999).

5.1.2. Structure and function of activator protein-1

AP-1 is a dimeric transcription factor that principally consists of the protein subunits Jun and Fos (Fig 5.1). The Jun family of proteins includes c-Jun, JunB and JunD, and the Fos family of proteins includes c-Fos, FosB, FosD and fos-related antigen-1 (Fra-1)

Figure 5.1. Schematic representation of the interactions and functions of AP-1 protein subunits



AP-1 is a dimeric transcription factor which is composed of Jun and Fos protein subunits. Jun subunits include c-Jun, JunB and JunD. Jun proteins can form homodimers, and can also form heterodimers with the Fos proteins c-Fos, FosB, Fra-1 or Fra-2. The combination of Jun or Fos subunits determines the DNA binding affinity and transcriptional activation of AP-1. The activation of AP-1 leads to gene transcription and regulates cellular processes that are important both in normal and cancerous cells. Adapted from Latchman (1998). * Negative regulator of transcription.

and fos-related antigen-2 (Fra-2). Jun proteins can form homodimers, and can also form heterodimers with Fos proteins, whereas Fos can only form heterodimers (Fig 5.1) (Latchman 1998). Jun and Fos are immediate early genes that are present in cells in an inactive form. The activation of intracellular pathways in response to extracellular stimuli including inflammatory cytokines, growth factors and phorbol esters such as 12-*O*-tetradecanoylphorbol-13-acetate (TPA), leads to Jun and Fos phosphorylation and activation (Karin et al 1997, Adler et al 1992). An example of this is the predominant AP-1 subunit, c-Jun, which is activated by phosphorylation at serine residues 63 and 73 by the JNK pathway (Dunn et al 2002). Jun-Jun or Jun-Fos dimers regulate gene transcription by binding to specific DNA sequences termed TPA-response elements (TRE) with a consensus sequence of 5'-TGA(C/G)TCA-3' (Karin et al 1997). Furthermore, different combinations of Jun and Fos subunits confer different functions on the AP-1 complex, for example, Jun-Fos heterodimers have a greater DNA binding affinity than Jun-Jun homodimers, and the presence of Fra-1 in AP-1 dimers often suppresses the transcriptional activity of AP-1 (Fig 5.1) (Yoshioka et al 1995). Through altering the expression of genes, AP-1 regulates many cellular processes including cell proliferation, cell differentiation and apoptosis (Ludes-Meyers et al 2001, Bamberger et al 1999). Furthermore, AP-1 has been implicated in the oncogenic transformation and increased growth of breast cancer cells (Liu et al 2002). In particular, the increased expression and activity of the c-Jun and Fra-1 AP-1 subunits is associated with more invasive, aggressive breast tumours (Belguise et al 2005, Smith et al 1999).

5.1.3. Aims

In chapter 3 and 4, exogenous TF was shown to reduce oestradiol-mediated proliferation and suppress the anti-invasive effect of oestradiol. Furthermore, incubation of breast cancer cells with exogenous TF resulted in the downregulation of ER α and

reduced oestradiol-mediated transcriptional activity through the ERE pathway. In this section, the main objectives were as follows.

- To examine the influence of exogenous TF on the transcriptional activity of ER α through the AP-1 dependent pathway
- To clone the ER α gene into a mammalian expression vector and mutate serine 118 to aspartic acid to produce a constitutively active form of ER α and subsequently, overexpress the wild type and mutated ER α in breast cancer cells and determine whether the influence of exogenous TF on oestradiol-mediated proliferation and invasion arises from the downregulation of ER α expression and/or inhibition of its activity.

5.2. Methods

5.2.1. Examination of the influence of exogenous TF on AP-1 activity

5.2.1.1. Analysis of AP-1 transcriptional activity by pAP-1-Luc reporter vector transfections

The pAP-1-Luc reporter vector contains the luciferase gene under the control of 7 consecutive TRE promoters. Transfection of the plasmid into mammalian cells allows AP-1 transcriptional activity to be determined by measuring luciferase activity of the cell lysates. Cells (4×10^5) were seeded out into 12 well plates and transfected with 1 μ g of the pAP-1-Luc reporter vector using the Lipofectin reagent as described in the general methods section 2.11. Following transfection, the cells were treated with TF (0-500 nM) and oestradiol (250 pM) as described in the results section. The cells were then lysed and the luciferase activities measured by adding luciferase substrate (100 μ l) to cell extract (20 μ l) and measuring light emitted on a luminometer as described in section 2.12.

5.2.1.2. Analysis of AP-1 DNA binding activity using the TransAM AP-1 kit

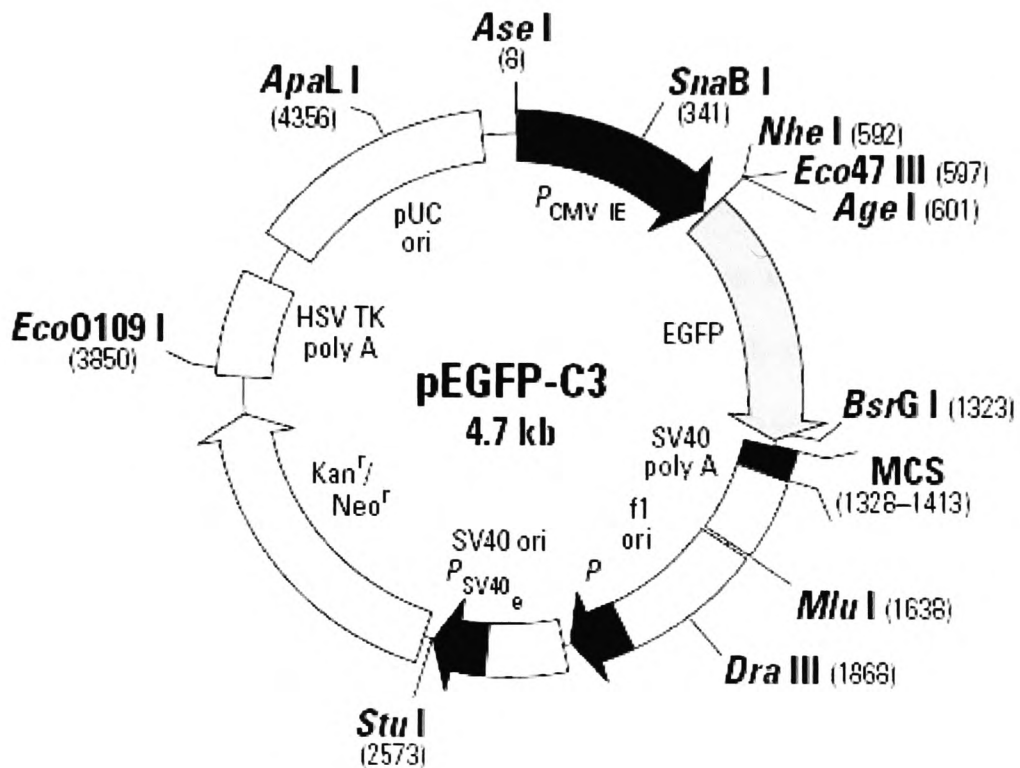
An ELISA-based TransAM AP-1 kit was used to investigate the influence of TF on the DNA binding activity of AP-1 subunits. The TransAM AP-1 kit is an ELISA based method, which consists of wells coated with oligonucleotides containing the TRE AP-1 DNA binding consensus sequence. Active AP-1 in the cell extract binds to this sequence and individual AP-1 subunits are detected using antibodies against c-Jun, JunB, JunD, FosB, Fra-1 and Fra-2.

Cells were cultured in T75 flasks to approximately 60 % confluence and then treated with TF (0-500 nM) for 20 and 40 min. The cells were then harvested and nuclear extracts were prepared using the nuclear extract kit as described previously (section 4.2.2.1). Protein concentrations were determined using the Bradford assay as described in the general methods. TransAM AP-1 was carried out as described in section 4.2.2.2 using 8 µg of protein from each sample. Control nuclear extract (5 µg) from cells stimulated with TPA (supplied) was used as a positive control for AP-1 activation. Furthermore, wells containing no nuclear extract were used as a negative control. The plates were probed using the supplied phospho-serine 73 c-Jun antibody diluted 1:500 in antibody binding buffer or the JunB, JunD (phospho-serine 100), c-Fos, FosB, Fra-1 and Fra-2 antibodies diluted 1:1000 in antibody binding buffer. The absorptions of the samples were measured at 450 nm with a reference of 620 nm using an Anthos 2010 microplate reader.

5.2.3. Cloning of full length ERα

The pEGFP-C3 vector (Fig 5.2) is a mammalian expression vector into which a gene of interest may be cloned into the multiple cloning site downstream of the gene for enhanced green fluorescent protein (EGFP). Transfection of the vector into mammalian

Figure 5.2. pEGFP-C3 cloning vector



The pEGFP-C3 mammalian expression vector encodes the enhanced green fluorescent protein (EGFP) gene upstream of a multiple cloning site (MCS). Cloning a gene of interest into this vector results in the expression of the gene in tandem with the EGFP protein at the N-terminus. The kanamycin resistance gene (Kan^r) allows selection of transformed bacteria, whereas the geneticin resistance gene (Neo^r) permits the selection of mammalian cells transfected with the vector. Image taken from www.stratagene.com.

cells results in the expression of a hybrid protein consisting of the gene of interest with EGFP attached to the N-terminus. The expression of the hybrid protein permits detection by fluorescence microscopy or flow cytometry.

5.2.3.1. Design of primers for PCR amplification of full length ER α

Primers for the PCR of full length ER α were designed from the published ER α cDNA sequence (Green et al 1986) using the BasePair program. The restriction sites for *EcoR* I and *BamH* I were included in the primers to permit the production of 5' overhangs for the ligation of the gene into the digested vector. Furthermore, the use of two different restriction sites ensures that the gene is inserted unidirectionally into the plasmid in the correct orientation. The forward primer was designed to start 16 bp upstream of the start codon of the ER α gene and include 18 bp of coding sequence (see below). Additionally, an *EcoR* I restriction site was incorporated into the 16 bp non-coding sequence. The 10 bp sequence preceding the restriction enzyme site was included to ensure efficient restriction digestion. The reverse primer was designed to include the stop codon and 17 bp of coding sequence which included a *BamH* I restriction site incorporated after the stop codon, followed by another 10 bp.

Forward primer: 5'-CCCGCGGC**GAATTC**CCATG**ACCATGACCCTCCAC**-3'

EcoR I Start codon ER α cDNA

Reverse primer: 5'-GGAAGCCAG**GGATCC**TCAG**ACTGTGGCAGGGA**-3'

BamH I Stop codon ER α cDNA

5.2.3.2. First strand cDNA synthesis using SuperScript II reverse transcriptase

The reverse transcription step was carried out using mRNA isolated from MCF-7 cells and SuperScript II reverse transcriptase. A reaction was set up with RNA (0.5 µg), dNTP mix (10 mM each) and reverse cloning primer (100 pmol) and made up to a final volume of 12 µl with RNase/DNase-free water. The reaction was incubated at 65°C for 5 min and then quickly chilled on ice. First strand buffer (50 mM Tris-HCl pH 8, 75 mM KCl, 3 mM MgCl₂) and 2 µl of 0.1 M DTT were added to the reaction and incubated at 42°C for 2 min. SuperScript II reverse transcriptase (200 U) was added to the reaction and made up to a final volume of 20 µl using RNase/DNase-free water. The reaction was incubated at 42°C for 50 min and the enzyme then deactivated by heating at 70°C for 15 min.

5.2.3.3. PCR amplification of ERα cDNA

PCR of full length ERα was optimised using different MgCl₂ concentrations (1-4 mM) and three DNA polymerase enzymes (*Pfu* DNA polymerase, BioTaq DNA polymerase and Herculase enhanced DNA polymerase).

The PCR mix for the amplification of ERα cDNA using BioTaq DNA polymerase, contained the template cDNA (100 ng), dNTP mix (4 mM), forward and reverse cloning primers (50 pmol each), PCR buffer (16 mM (NH₄)₂SO₄, 67 mM Tris-HCl pH 8.8, 0.01 % Tween-20), MgCl₂ (3 mM) and BioTaq DNA polymerase (2.5 U) and was made up to 50 µl with RNase/DNase-free water. The DNA was denatured at 95°C for 5 min, followed by 30 cycles of amplification carried out as 1 min at 95°C, 1 min 45 s at 58°C and 3 min at 72°C. Final extension was carried out at 72°C for 10 min. The PCR products with an expected size of 1785 bp were analysed by 1 % (w/v) agarose gel electrophoresis and viewed under UV light using a transilluminator.

The PCR mix for the amplification of ER α cDNA using *Pfu* DNA polymerase, contained the template cDNA (100 ng), dNTP mix (0.8 mM), forward and reverse cloning primers (50 pmol each), PCR buffer (20 mM Tris-HCl pH 8.8, 2 mM MgSO₄, 10 mM KCl, 10 mM, (NH₄)₂SO₄, 0.1 % Triton X-100, 0.1 mg/ml nuclease-free BSA) and *Pfu* DNA polymerase (5 U) and was made up to 100 μ l with RNase/DNase-free water. The DNA was denatured at 95°C for 45 s, followed by 30 cycles of amplification carried out as 45 s at 95°C, 45 s at 58°C and 4 min at 72°C. Final extension was carried out at 72°C for 10 min. The PCR products were analysed by 1 % (w/v) agarose gel electrophoresis.

The PCR mix for the amplification of ER α cDNA using Herculase DNA polymerase, contained the template cDNA (100 ng), dNTP mix (0.8 mM), forward and reverse cloning primers (12.5 pmol each), PCR buffer (5 μ l) and Herculase DNA polymerase (2.5 U) and was made up to 50 μ l with RNase/DNase-free water. The DNA was denatured at 95°C for 2 min, followed by 30 cycles of amplification carried out as 30 s at 95°C, 30 at 58°C and 2 min at 72°C. Final extension was carried out at 72°C for 10 min.

5.2.3.4. Purification of ER α DNA from agarose gels

ER α DNA was isolated from the PCR reactions mix using the GFX DNA purification kit as follows. The products of PCR amplification were separated on a 0.75 % (w/v) low melting point agarose gel to separate and identify the transcript for full length ER α . The bands were visualised under UV light and the 1785 bp band for ER α quickly excised from the gel using a scalpel. The gel slice was transferred to a pre-weighed 1.5 ml tube, weighed again and 10 μ l of capture buffer added for every 10 mg of the gel. The gel was then vortexed and incubated at 60°C for 10 min until dissolved. The solution was

transferred into a GFX column in a collection tube and incubated at room temperature for 1 min, followed by centrifugation at 13,000 rpm for 30 s in a microcentrifuge. The flow through was discarded and wash buffer (500 μ l) added to the column. The column was centrifuged at 13,000 rpm for 30 s in a microcentrifuge and then transferred to a 1.5 ml tube. Distilled water (50 μ l) was added to the glass fibre matrix of the GFX column and incubated at room temperature for 1 min. The DNA was then eluted from the column by centrifugation at 13,000 rpm for 1 min in a microcentrifuge.

5.2.3.5. Restriction digestion of pEGFP-C3 and the ER α insert

Both the pEGFP-C3 plasmid and the ER α sequence contain the *EcoR* I and *BamH* I restriction enzyme sites which allow the production of 5' overhangs and permit the ligation of the insert into the plasmid. Initially, the duration of incubation for both *EcoR* I and *BamH* I to achieve full digestion of pEGFP-C3 was optimised by examining digested samples at intervals up to 3 h. Following optimisation, restriction digestion reactions were set up containing *EcoR* I (10 U), restriction enzyme buffer (90 mM Tris-HCl pH 7.5, 10 mM MgCl₂, 50 mM NaCl), BSA (0.1 mg/ml) and pEGFP-C3 or the ER α insert (30 μ l) and incubated at 37°C for 1 h. The plasmid and insert were purified from the reaction mix using the GFX PCR purification kit as previously described. Restriction digest reactions were then set up with *BamH* I (10 U), restriction enzyme buffer (6 mM Tris-HCl pH 7.5, 6 mM MgCl₂, 100 mM NaCl, 1 mM DTT), BSA (0.1 mg/ml) and pEGFP-C3 or ER α insert (30 μ l) and incubated at 37°C for 3 h. The plasmid and insert were purified from the reaction mix using the GFX PCR product kit and resuspended in distilled water (50 μ l). The quantity of both the pEGFP-C3 plasmid and ER α insert DNA were determined by measuring absorption at 260 nm as described before, and the purity of the DNA was confirmed by 1 % (w/v) agarose gel electrophoresis.

5.2.3.6. Ligation of the ER α insert into the pEGFP-C3 plasmid

Ligation reactions containing T4 DNA ligase (4 U), ligase buffer (50 mM Tris-HCl pH 7.5, 7 mM MgCl₂, 1 mM DTT), ATP (1 mM) and the digested pEGFP-C3 plasmid and ER α insert were set up at molar ratios of 1:1, 1:3 and 1:5 (plasmid:insert), as well as a negative control with no insert. A volumetric description of the components is shown below. The reactions were made up to 20 μ l with distilled water and incubated at 4°C overnight, 4°C for 2 days or 23°C for 2 h. Competent *E.coli* TB-1 were transformed with each ligation mix (10 μ l) in turn as described before (section 2.10.5). Transformed bacterial cells (20 μ l) were selected by plating out on kanamycin agar plates (45 μ g/ml) and incubated overnight at 37°C. Colonies were removed, grown in LB broth (50 ml) at 37°C overnight and plasmids extracted using the miniprep plasmid isolation procedure.

Reaction components	Plasmid : insert ratio			Neg control
	1:1	1:3	1:5	
pEGFP-C3 (176 μ g/ml)	5 μ l	5 μ l	4 μ l	5 μ l
ER α insert (137 μ g/ml)	2.5 μ l	7.5 μ l	10 μ l	-
10 \times ligase buffer	2 μ l	2 μ l	2 μ l	2 μ l
ATP (10 mM)	2 μ l	2 μ l	2 μ l	2 μ l
T4 DNA ligase	1 μ l	1 μ l	1 μ l	1 μ l
dH ₂ O	7.5 μ l	2.5 μ l	1 μ l	10 μ l

5.3. Results

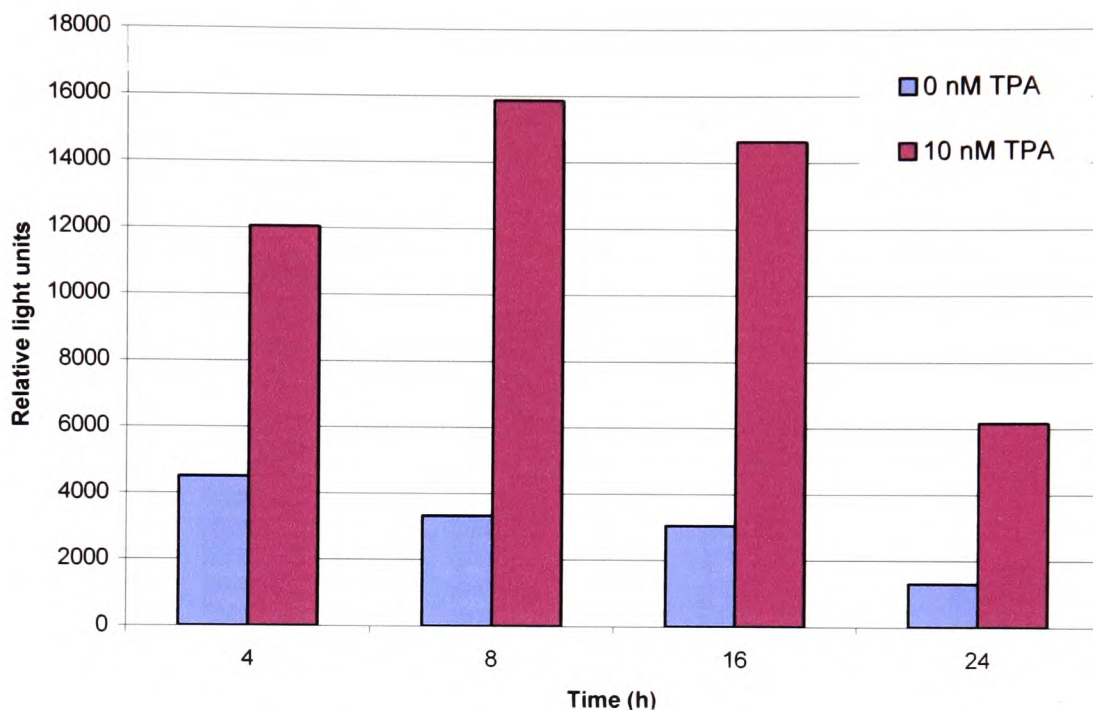
5.3.1. Analysis of the influence of TF and oestradiol on the transcriptional activity of AP-1 using the pAP-1-Luc reporter vector

In order to determine the optimal duration of incubation required for maximal AP-1 activation, MCF-7 cells (4×10^5) were transfected with the pAP-1-Luc reporter vector. The cells were then treated with TPA (0 or 10 nM) to induce the phosphorylation and activation of AP-1 (Adler et al 1992). Luciferase activities in the transfected samples were measured at 4, 8, 16 and 24 h post-treatment. The maximal difference in luciferase activity between TPA treated and untreated cells was observed at 8 h post-treatment (Fig 5.3).

Following the optimisation step, alterations in the transcriptional activity of AP-1 in response to TF (0-500 nM), in MCF-7 and T47D cells was examined. Cells previously transfected with the pAP-1-Luc reporter vector, were incubated with TF (0-500 nM) in the presence of 10 % FCS. Incubation of MCF-7 cells with TF (50 and 500 nM) resulted in a TF concentration dependent decrease in AP-1 transcriptional activity compared to the untreated sample at 8 h post-treatment (Fig 5.4). The incubation of T47D cells with TF (50 and 500 nM) also appeared to result in a downward trend in luciferase activity below that of the untreated control (Fig 5.5), although the difference between the luciferase activity of untreated cells and untransfected cells was smaller than that observed in MCF-7 cells, indicating that T47D cells contain lower levels of active AP-1.

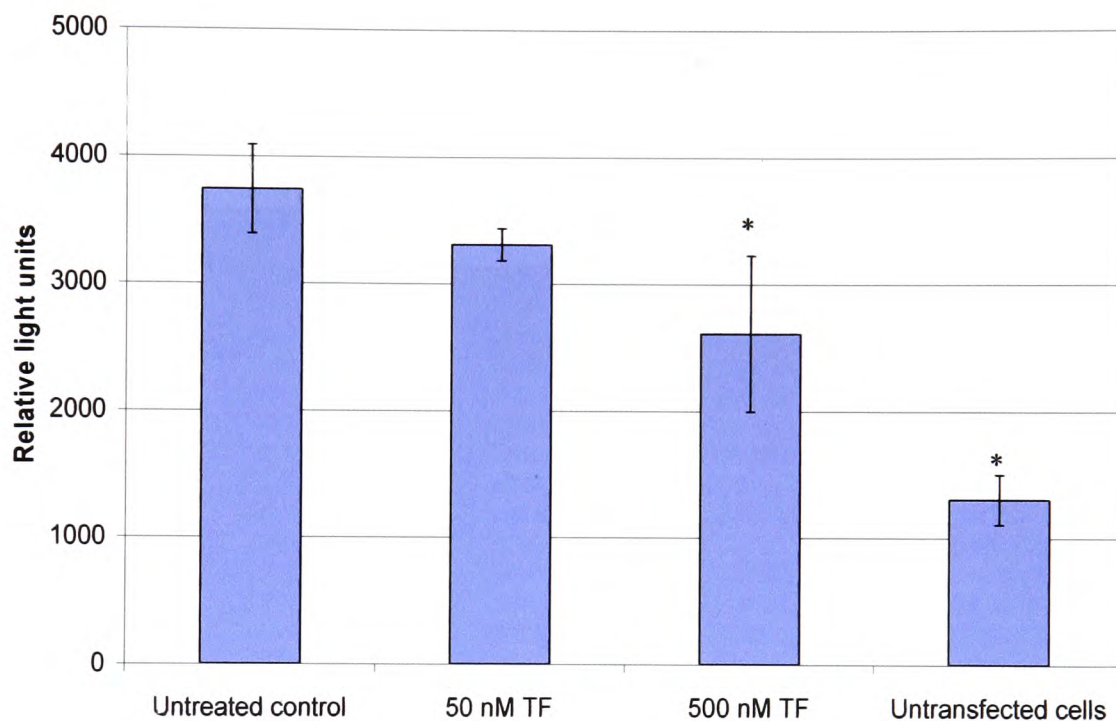
In the subsequent experiments, alterations in the transcriptional activity of AP-1 in response to TF in the presence of oestradiol were examined. These studies were carried out in MCF-7 cells, since these cells exhibited higher levels of AP-1 activity compared

Figure 5.3. Optimisation of pAP-1-Luc transfections



MCF-7 cells (4×10^5) were seeded out into 12 well plates and transfected with the pAP-1-Luc reporter vector using the Lipofectin transfection reagent. The cells were treated with TPA (0 or 10 nM) and lysed at 4, 8, 16 and 24 h post-treatment. The luciferase activities of the cell samples were measured using a Junior LB 9509 luminometer. The data are from one experiment.

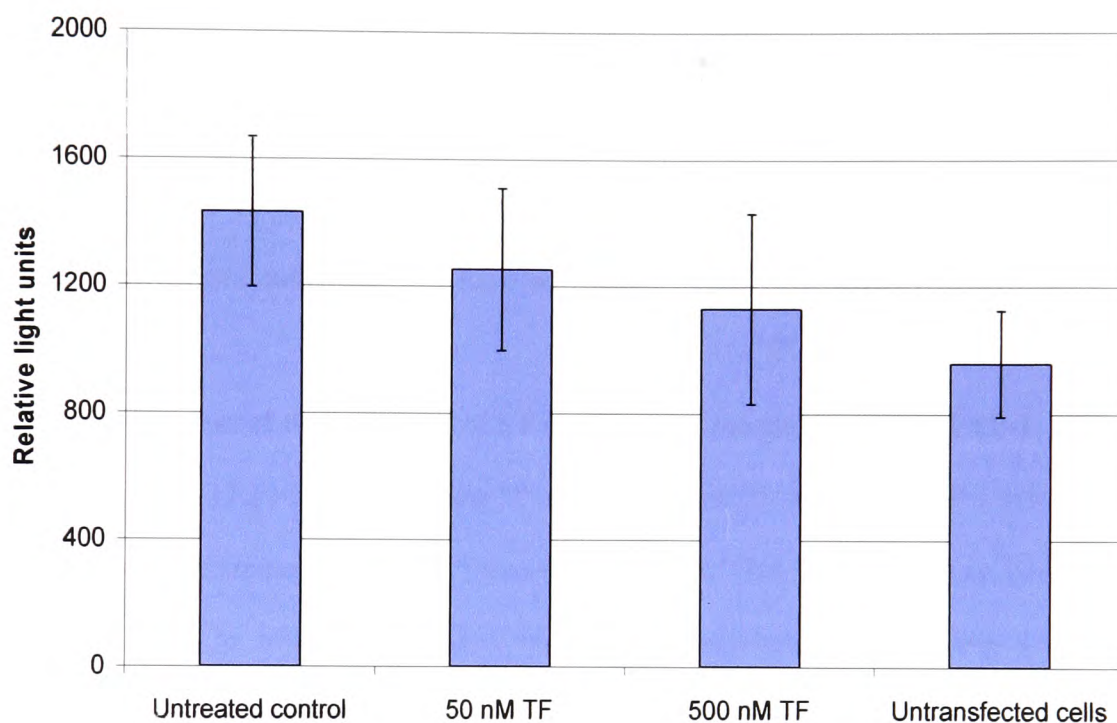
Figure 5.4. The influence of TF on the transcriptional activity of AP-1 in MCF-7 cells



MCF-7 cells (4×10^5) were seeded out into 12 well plates and transfected with the pAP-1-Luc reporter vector. The cells were placed in medium supplemented with 10 % FCS and treated with TF (0-500 nM), alongside an untransfected set of cells to determine the background count. The cells were lysed following 8 h incubation at 37°C, and luciferase activities of the cell samples measured using a Junior LB 9509 luminometer. The data represent the average of three independent experiments measured in duplicate \pm SD.

* $p < 0.05$ vs. the untreated control.

Figure 5.5. The influence of TF on the transcriptional activity of AP-1 in T47D cells



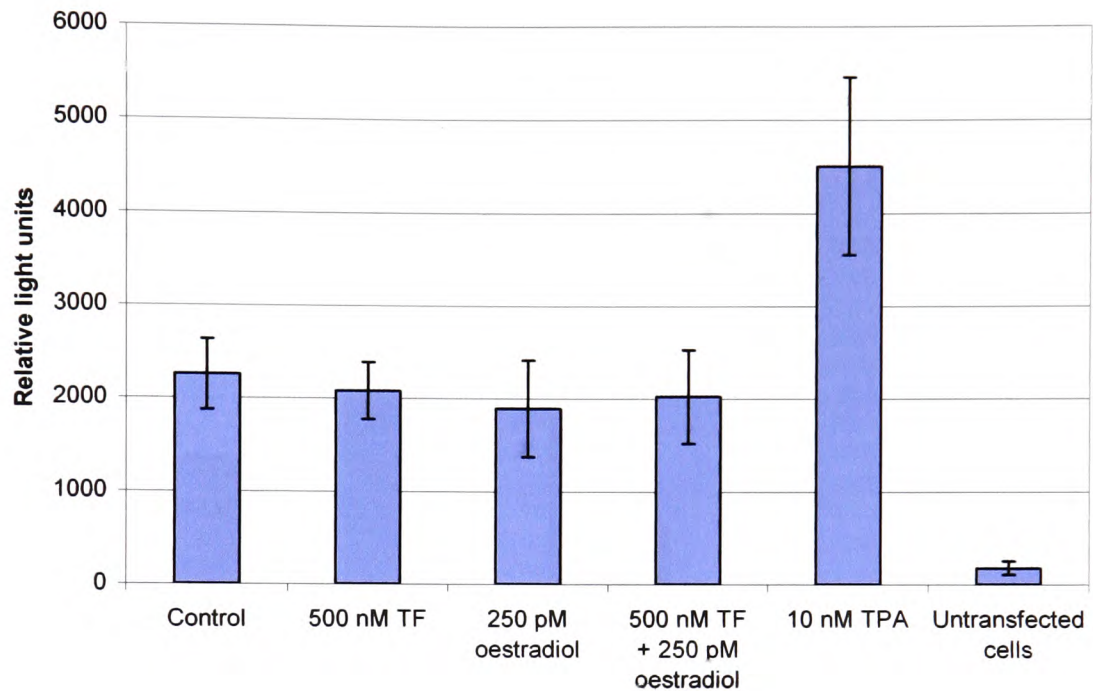
T47D cells (4×10^5) were seeded out into 12 well plates and transfected with the pAP-1-Luc reporter vector. The cells were placed in medium supplemented with 10 % FCS and treated with TF (0-500 nM), alongside an untransfected set of cells to determine the background count. The cells were lysed following 8 h incubation at 37°C, and luciferase activities of the cell samples were measured using a Junior LB 9509 luminometer. Data represent the average of two independent experiments measured in duplicate \pm SD.

to T47D cells. Following transfection with the pAP-1-Luc reporter vector, MCF-7 cells were adapted to phenol red-free medium containing 1 % FCS over 24 h, and then treated with TF (500 nM), oestradiol (250 pM) or TPA (10 nM) for 8 h. The incubation of MCF-7 cells with either TF (500 nM) or oestradiol (250 pM) alone, in phenol red-free/low-serum medium had no measurable influence on AP-1 activity in MCF-7 cells (Fig 5.6). Furthermore, the combination of oestradiol (250 pM) and TF (500 nM) had no additional effect on luciferase activity compared to the untreated cells. Incubation of MCF-7 cells with TPA (10 nM) resulted in increased luciferase activity above that of the untreated control, indicating that AP-1 was functional in these cells.

5.3.2. Examination of the influence of TF on the DNA binding activity of AP-1

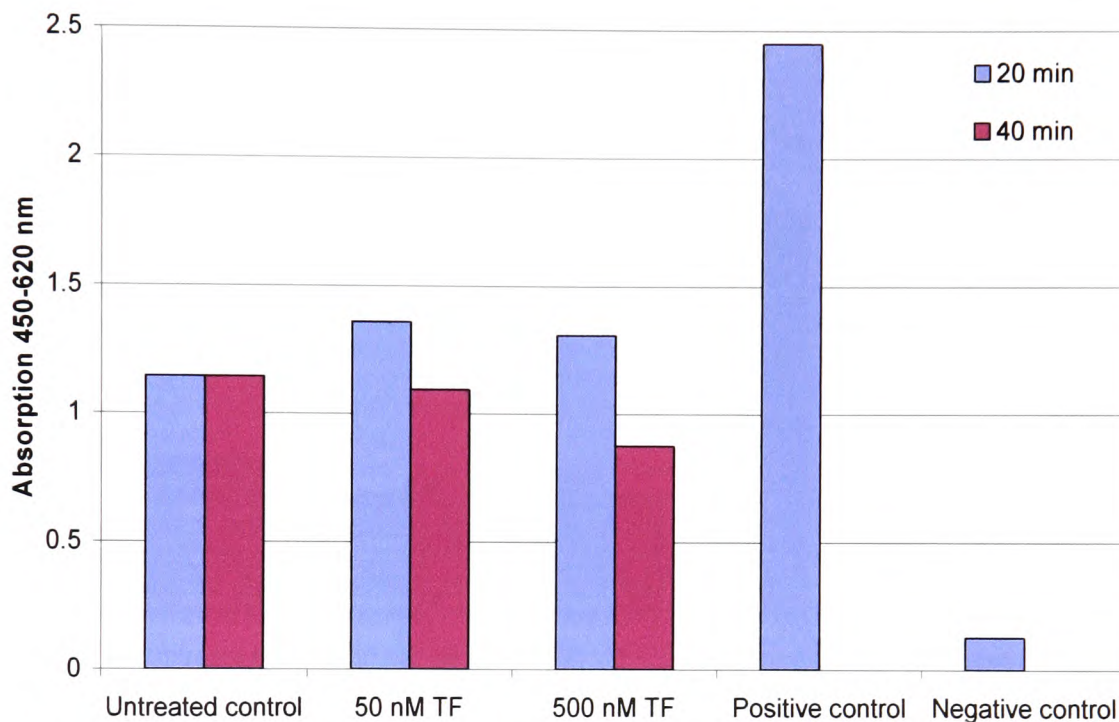
The influence of TF (0-500 nM) on the DNA binding activity of a set of AP-1 subunits was separately examined using the TransAM AP-1 kit. This kit employs an ELISA-based procedure in which active AP-1 binds to oligonucleotides containing a TRE binding sequence. Individual AP-1 protein subunits are then detected using specific antibodies to c-Jun, JunB, JunD, c-Fos, FosB, Fra-1 and Fra-2. Using this procedure, the influence of TF (0-500 nM) on the DNA binding activities of the AP-1 subunits c-Jun, JunB, JunD, c-Fos, FosB, Fra-1 and Fra-2 over 40 min was examined in MCF-7 cells in the presence of 10 % FCS. The nuclear extract from cells stimulated with TPA (supplied with the kit) was used as a positive control. The high levels of c-Jun DNA binding activity detected in this control confirmed the suitability of this procedure (Fig 5.7). Measurement of the DNA binding activity of c-Jun on stimulation with TF (50 nM) indicated a possible increase at 20 min post-treatment. In contrast, 500 nM TF seemed to reduce the DNA binding activity of c-Jun by 40 min (Fig 5.7). Incubation of MCF-7 cells with TF (50 and 500 nM) appeared to have no measurable influence on the DNA binding activities of either c-Fos (Fig 5.8) or Fra-1 (Fig 5.9).

Figure 5.6. The influence of TF and oestradiol on AP-1 transcriptional activity



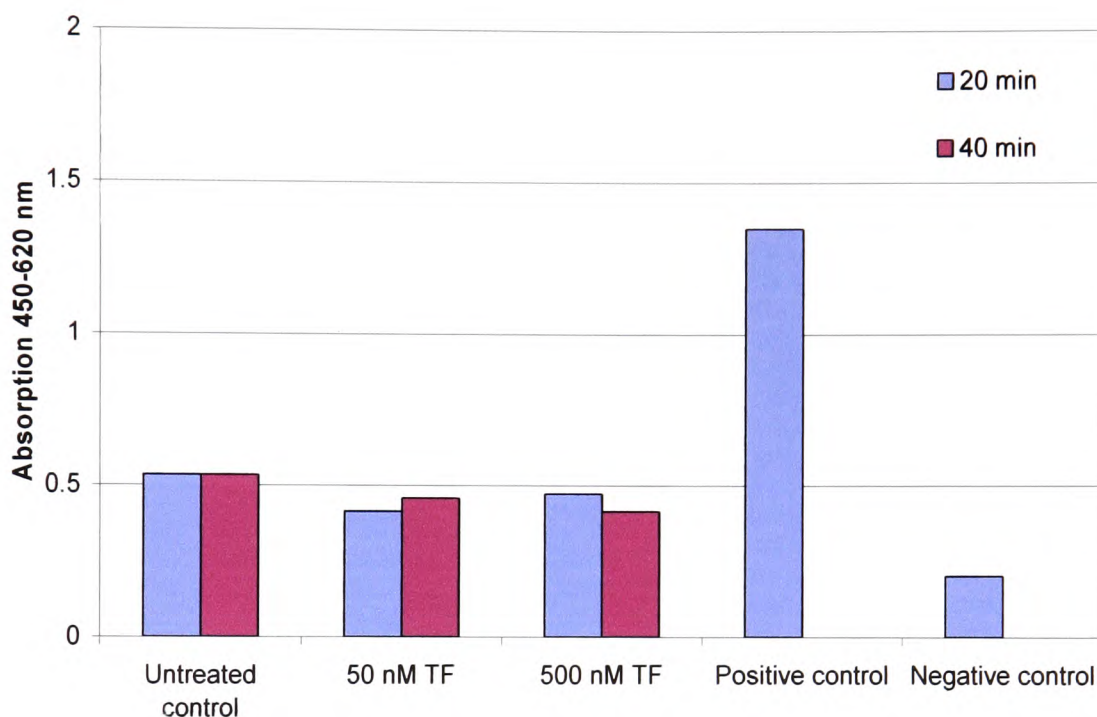
MCF-7 cells (4×10^5) were transfected with the pAP-1-Luc reporter vector and adapted to phenol red-free medium containing 1 % FCS. The cells were treated with TF (500 nM), oestradiol (250 pM) or TPA (10 nM) and incubated at 37°C for 8 h. The cells were then lysed and the luciferase activities of the samples measured using a Junior LB 9509 luminometer. The data represents the average of two independent experiments carried out in duplicate and measured in duplicate \pm SD.

Figure 5.7. The influence of TF on the DNA binding activity of c-Jun



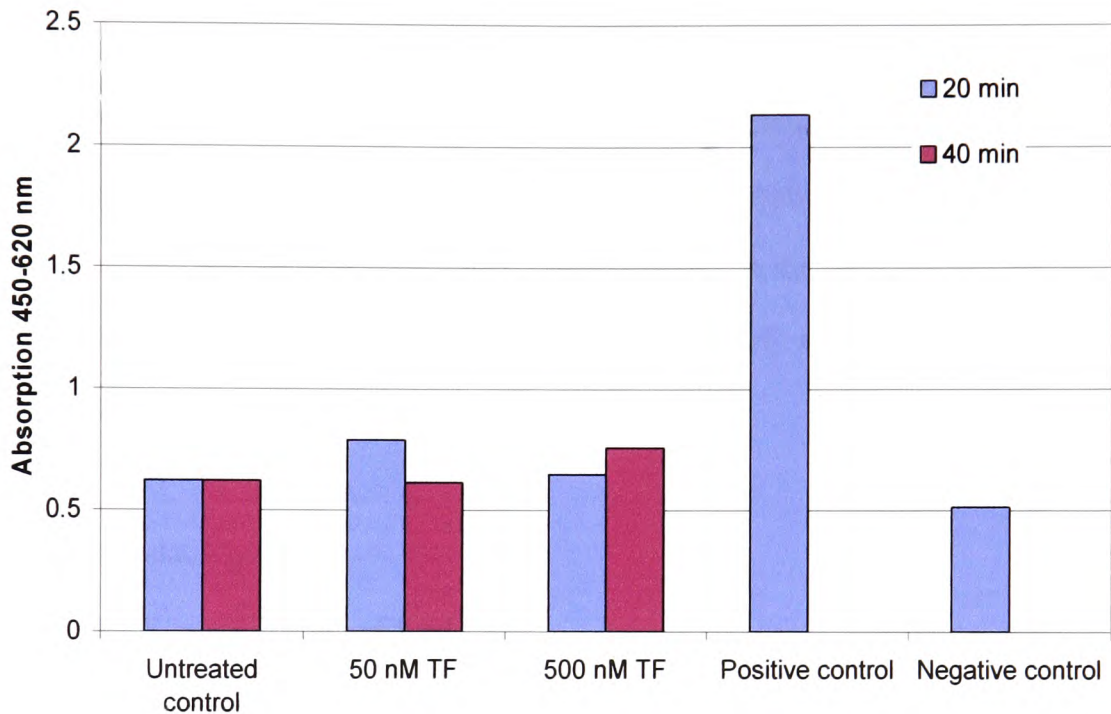
MCF-7 cells were cultured in T75 flasks and treated with TF (0-500 nM) when approximately 60 % confluent. The cells were harvested at 20 and 40 min and nuclear extracts prepared. The protein concentration in each sample was determined using the Bradford assay following which the DNA binding activity of c-Jun in the samples was determined using the TransAM AP-1 kit and using a specific phospho-serine 73 c-Jun antibody. The positive control sample contained 5 μ g of nuclear extract from cells stimulated with TPA, while the negative control contained no nuclear extract. The data are from one experiment.

Figure 5.8. The influence of TF on the DNA binding activity of c-Fos



MCF-7 cells were cultured in T75 flasks and treated with TF (0-500 nM) when approximately 60 % confluent. The cells were harvested at 20 and 40 min and nuclear extracts prepared. The protein concentration in each sample was determined using the Bradford assay following which the DNA binding activity of c-Fos in the samples was determined using the TransAM AP-1 kit and using a specific c-Fos antibody. The positive control sample contained 5 μ g of nuclear extract from cells stimulated with TPA, while the negative control contained no nuclear extract. The data are from one experiment.

Figure 5.9. The influence of TF on the DNA binding activity of Fra-1



MCF-7 cells were cultured in T75 flasks and treated with TF (0-500 nM) when approximately 60 % confluent. The cells were harvested at 20 and 40 min and nuclear extracts prepared. The protein concentration in each sample was determined using the Bradford assay following which the DNA binding activity of Fra-1 in the samples was determined using the TransAM AP-1 kit and using a specific Fra-1 antibody. The positive control sample contained 5 μ g of nuclear extract from cells stimulated with TPA, while the negative control contained no nuclear extract. The data are from one experiment.

Furthermore, TF (50 and 500 nM) appeared to have no measurable effect on the DNA binding activities of the AP-1 subunits, Jun D, FosB and Fra-2, over 40 min (results not shown).

In order to examine the influence of oestradiol on the DNA binding activity of AP-1, MCF-7 cells were adapted to phenol red-free medium containing 1 % (v/v) FCS and incubated with oestradiol (0 or 250 pM) for 10 min. Incubation of MCF-7 cells with oestradiol (250 pM) seemed to have no measurable effect on the DNA binding activities of the following AP-1 subunits; c-Jun, JunB, JunD and FosB, at 10 min post-treatment (Fig 5.10).

5.3.3. ER α cloning

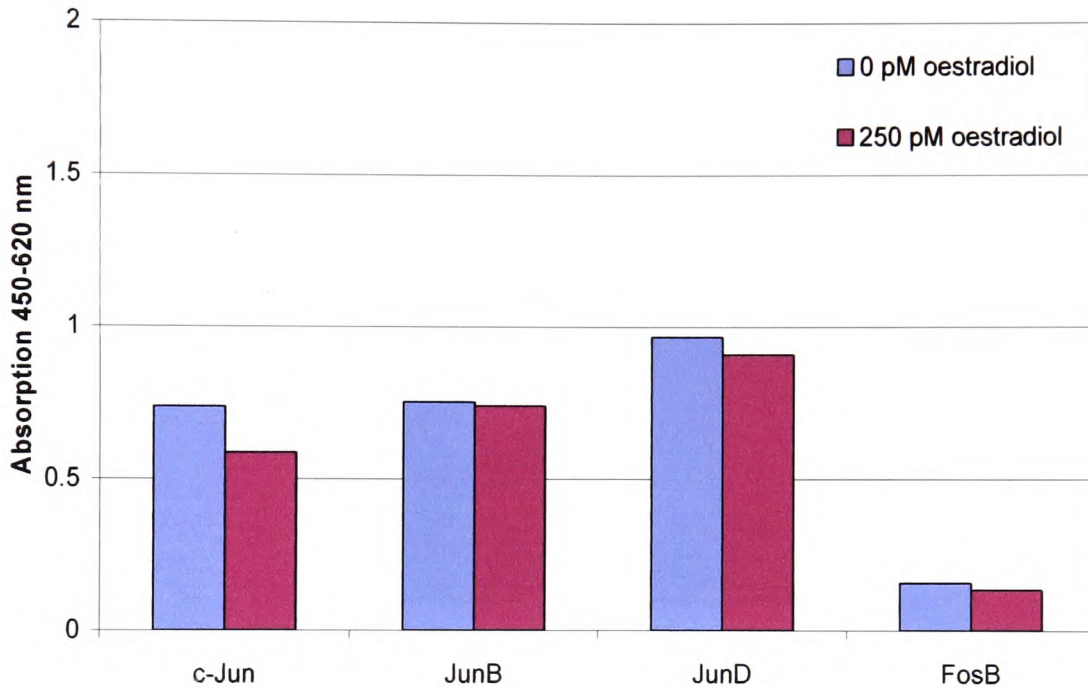
5.3.3.1. PCR amplification of ER α

Three different DNA polymerase enzymes were tested for suitability for the PCR amplification of ER α cDNA. Furthermore, a range of MgCl₂ concentrations (1-4 mM) were used at various annealing temperatures to optimise the PCR amplification reaction of ER α . A band at approximately 1800 bp corresponding to full length ER α was amplified using BioTaq DNA polymerase in the presence of 3 mM MgCl₂ carried out at an annealing temperature of 58°C (Fig 5.11). The ER α PCR product was then purified from the spurious amplification bands using the GFX DNA purification kit to obtain one clear band at 1800 bp (Fig 5.12). PCR amplification of ER α using *Pfu* DNA polymerase and Herculase DNA polymerase did not amplify full length ER α at any annealing temperature or MgCl₂ concentration tested.

5.3.3.2. Optimisation of *Bam*H I and *Eco*R I restriction digest of pEGFP-C3

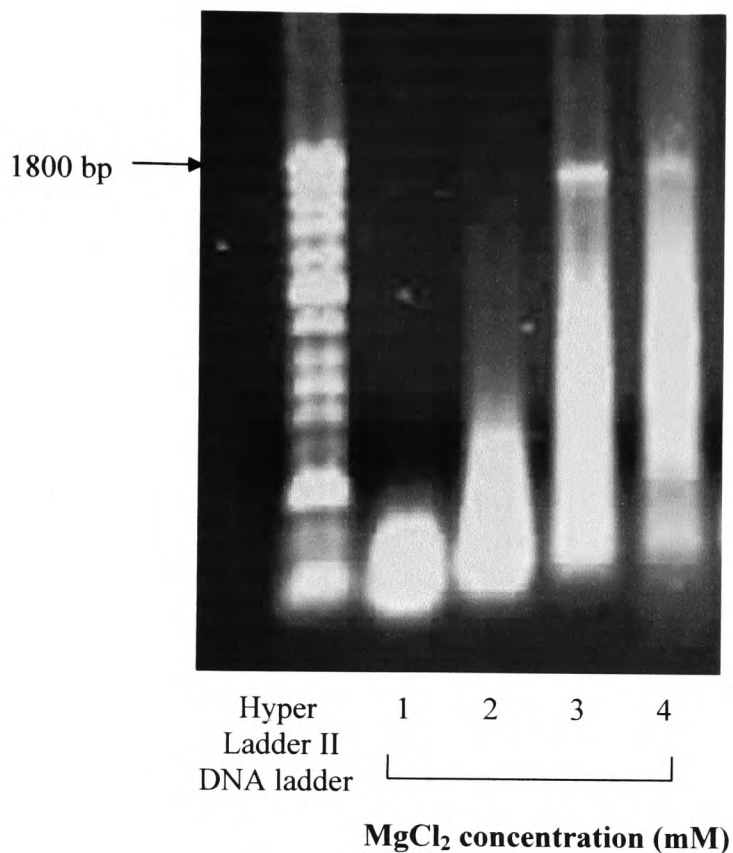
The EGFP-C3 plasmid was digested using the *Bam*H I and *Eco*R I restriction enzymes in order to produce 5' overhangs to allow unidirectional cloning of ER α into the

Figure 5.10. The influence of oestradiol on the DNA binding activity of AP-1 subunits



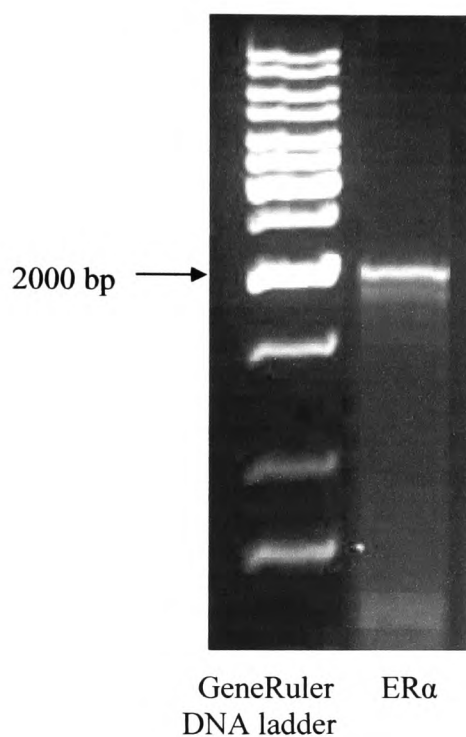
MCF-7 cells cultured in T75 flasks were adapted to phenol red-free medium containing 1 % (v/v) FCS and treated with oestradiol (0 or 250 pM) for 10 min. The cells were then harvested and nuclear extracts prepared. The protein concentration in each sample was determined using the Bradford assay and the DNA binding activity of AP-1 subunits determined using the TransAM AP-1 with specific antibodies for c-Jun, JunB, JunD and FosB. The data are from one experiment.

Figure 5.11. PCR amplification of ER α using BioTaq DNA polymerase



PCR reactions were set up containing cDNA (100 ng) previously amplified from MCF-7 RNA, BioTaq DNA polymerase (2.5 U) and a range of MgCl₂ concentrations (1-4 mM). PCR amplification of ER α was carried out with an annealing temperature of 58°C for 30 amplification cycles. The PCR products were analysed by 1 % (w/v) agarose gel electrophoresis and viewed under UV light using a transilluminator.

Figure 5.12. ER α purified from PCR reaction



The PCR products amplified using BioTaq DNA polymerase were separated on a 0.75 % (w/v) low melting point agarose gel. A band at approximately 1800 bp corresponding to ER α was excised from the gel and purified using the GFX PCR purification kit. The purified ER α PCR product was then examined by 1 % agarose gel electrophoresis.

plasmid. The incubation times required for the restriction enzymes to completely digest pEGFP-C3 were optimised by examining pEGFP-C3 samples digested by *Bam*H I and *Eco*R I individually at 37°C over 1-3 h and examining the restriction products by agarose gel electrophoresis. pEGFP-C3 was digested by *Bam*H I after incubation at 37°C for 3 h, while *Eco*R I required incubation at 37°C for 1 h (Fig 5.13).

5.3.3.3. Ligation of ER α into pEGFP-C3

A range of ligation conditions were tested in order to clone ER α into the pEGFP-C3 vector, including a range of plasmid:insert molar ratios, different temperatures and different durations of incubation. However, no positive clones were obtained under any of these conditions.

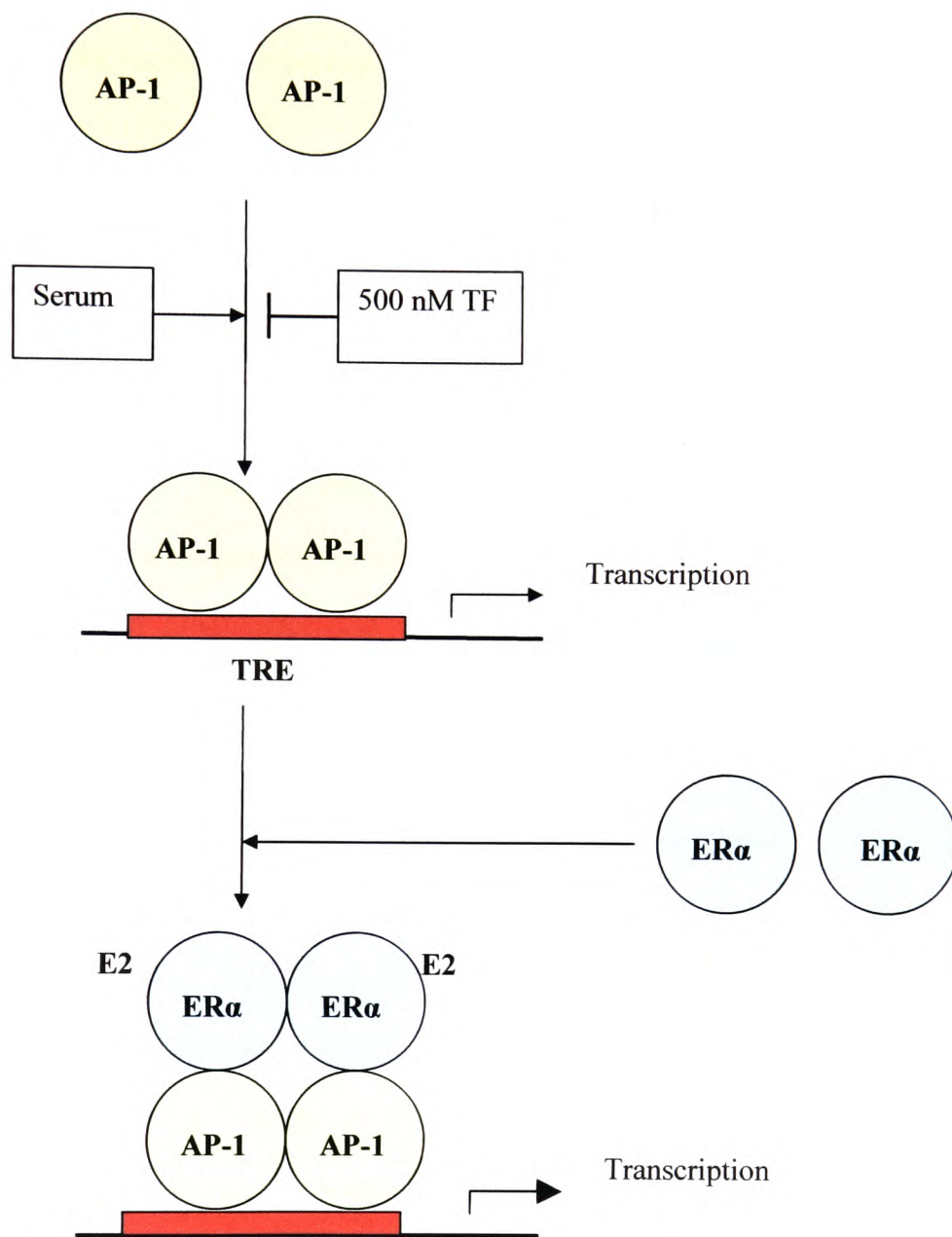
5.4. Discussion

The aim of this investigation was to examine the influence of exogenous TF on the transcriptional activity of ER α , mediated through the AP-1-dependent pathway. Incubation of MCF-7 cells with exogenous TF (50 and 500 nM) resulted in reductions in the transcriptional activity of AP-1 in the presence of 10 % FCS (Fig 5.4) and a similar trend was observed in T47D cells (Fig 5.5). These results are in contrast to previous studies that have shown that TF signalling results in the activation of the JNK pathway (Camerer et al 1999) which is known to directly phosphorylate and activate c-Jun (Dunn et al 2002). However, differential responses of cells to TF concentrations are likely and were reported in chapter 3. In fact, measurement of the DNA binding activity of c-Jun in the presence of TF (50 nM) indicated a possible increase, while 500 nM TF seemed to reduce the DNA binding activity of c-Jun (Fig 5.7), which was reflected in the decreased transcriptional activity of AP-1 in the luciferase assay (Fig 5.4). Since c-Jun is strongly associated with cell proliferation (Liu et al 2002), the contrasting

influences of exogenous TF on cell proliferation observed in chapter 3 may be due to differential influences of exogenous TF on c-Jun DNA binding activity, although this requires further investigation.

Following establishment of the ability of TF to modulate AP-1 transcriptional activity, any ability of exogenous TF to interfere with oestradiol-mediated AP-1 activity was explored. The levels of active AP-1 in MCF-7 cells were found to be suppressed in low-serum medium (Fig 5.6) compared to that observed in the presence of 10 % FCS (Fig 5.4). Furthermore, exogenous TF (500 nM) seemed to have no measurable influence on AP-1 transcriptional activity under these conditions (Fig 5.6). Moreover, the addition of oestradiol (250 pM) appeared to have no effect on AP-1 transcriptional activity, although in agreement with previous studies, oestradiol (250 pM) did not seem to affect the binding activity of Jun or Fos proteins to TRE DNA sequences (Fig 5.10) (Chen et al 1996). However, increased transcriptional activity from AP-1 response elements on treatment of ER α -positive cells with oestradiol has been previously reported (Philips et al 1993, Umayahara et al 1994). The addition of TPA (10 nM) stimulated AP-1 transcriptional activity in MCF-7 cells in low serum, confirming that these cells contained functional AP-1 (Fig 5.6). However, since AP-1 has to be recruited to DNA before ER α binds (Fig 1.3), and oestradiol (250 pM) did not appear to affect AP-1 DNA binding (Fig 5.10), the lack of response to oestradiol may be attributed to the repression of AP-1 binding to TRE sequences in the presence of low serum (Fig 5.14). This obstacle may be overcome by using charcoal-stripped FCS, which does not contain oestrogens but still has serum to permit AP-1 activation, to examine the effect of addition of oestradiol on the transcriptional activity of AP-1. However, since incubation of cells with exogenous TF (500 nM) appeared to result in reduced DNA binding activity of c-Jun, this may by default indirectly suppress any oestradiol-mediated AP-1

Figure 5.14. Schematic representation of proposed mechanism for TF regulation of ER α -AP-1 transcriptional activation



The presence of serum increases AP-1 DNA binding activity, allowing ER α to bind to the AP-1 complex and increase transcriptional activation from TRE promoters. A high concentration of TF (500 nM) suppresses AP-1 binding to TRE promoters and may therefore indirectly prevent oestradiol-ER α transcriptional activity through the AP-1-dependent pathway.

transcription by reducing AP-1/c-Jun binding to TRE DNA sequences (Fig 5.14). In effect, in the absence of functional AP-1 at TRE promoters, ER α would not be able to mediate transcription through the AP-1-dependent pathway (Fig 5.14). However, due to the limited number of experiments in this part of the study further investigations would be needed to confirm this.

The aim of the final part of the investigation was to clone ER α into a mammalian expression vector and mutate serine 118 to aspartic acid to mimic phospho-serine 118 and therefore produce a constitutively active form of ER α (Ali et al 1993). By overexpression of the wild type or mutated ER α in MCF-7 cells, it would have been possible to explore and determine whether the influence of exogenous TF on oestradiol-mediated cell proliferation and invasion arises from the downregulation of ER α expression and/or activity. Although the ER α gene was amplified by PCR using *Taq* DNA polymerase (Fig 5.12), ligation of the gene into the pEGFP-C3 mammalian expression vector was not possible under any of the tested conditions and due to time limits was not continued further.

In conclusion, incubation of breast cancer cells with exogenous TF resulted in decreases in the transcriptional activity of AP-1 and possibly the DNA binding activity of the c-Jun protein. However, the possible ability of oestradiol to alter the transcriptional activity of AP-1 is dependent on other activating factors present in serum (Fig 5.14).

CHAPTER 6

Investigation of the mechanism of exogenous TF
signalling in breast cancer cells

6.1. Introduction

In the previous chapters, exogenous TF was shown to induce changes in ER α expression and activity, as well as oestradiol-mediated cell proliferation and invasion. However, the mechanism by which exogenous TF interacts with the cell surface and initiates these cellular changes has not been explored. Since the exogenous TF used in this investigation lacks the cytoplasmic domain, signalling by this domain can be ruled out. Therefore, the main mechanisms by which the extracellular domain of TF can initiate cell signalling are through protease activated receptors (PARs) and integrins.

6.1.1. TF-mediated cell signalling through protease activated receptors

One known mechanism by which TF can initiate cell signalling pathways is through the activation of protease activated receptors 1 and 2. PAR1 is activated by the cleavage of the N-terminus of the receptor by FXa and thrombin downstream of TF in the coagulation cascade (Riewald & Ruf 2001), whereas PAR2 may be activated by both FXa and FVIIa following the formation of the TF:FVIIa complex (Camerer et al 2000b). Proteolytic cleavage of PARs leads to the activation of G-proteins which subsequently induce intracellular signalling pathways such as the ERK1/2 and PI3K pathways (Riewald & Ruf 2001), resulting in changes in the expression of genes encoding for growth factors and proinflammatory cytokines (Liu & Mueller 2006, Hjortoe et al 2004). A number of outcomes arising from TF:FVIIa signalling, including Ca²⁺ oscillations, induction of the MAPK pathway and alterations in patterns of gene expression are mediated through the activation of PARs, and do not involve the cytoplasmic domain of TF (Sorensen et al 1999, Poulsen et al 1998). Furthermore, activation of PARs has been shown to lead to reorganisation of the cytoskeleton and cell migration through the induction of the PI3K pathway and the small GTPase Rac (Versteeg et al 2000). Both PAR1 and PAR2 are known to participate in promoting

tumour cell migration and metastasis (Bromberg et al 2001), and both the TF:FVIIa complex and FXa have been shown to induce breast cancer cell migration through the activation of PAR2 (Morris et al 2006). Furthermore, activation of both PAR1 and PAR2 promotes tumour cell growth and proliferation (Versteeg et al 2008, Yin et al 2003). PARs are essential mediators by which the TF:FVIIa:FXa complex can initiate cell signalling pathways leading to changes in gene expression and cell morphology.

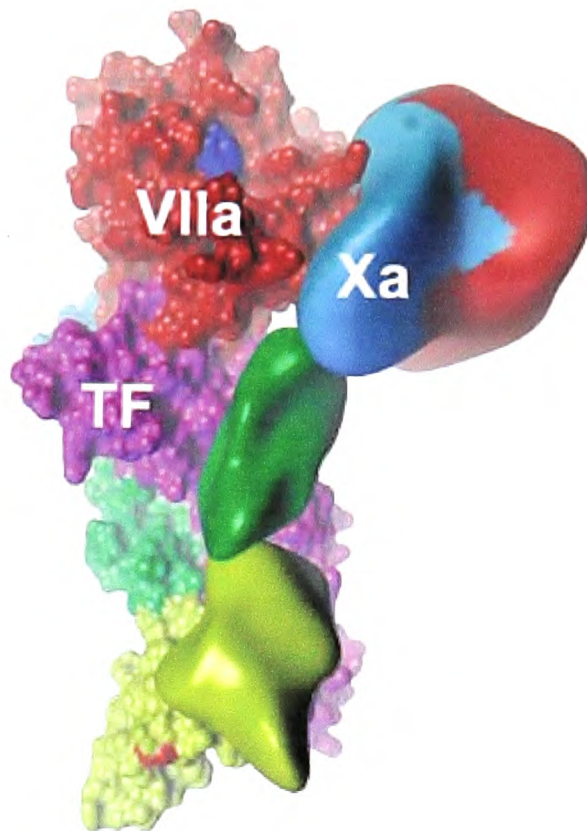
6.1.2. The interaction of TF with FVIIa and FXa

The extracellular domain of TF consists of two fibronectin type III domains (Harlos et al 1994), which interact with the coagulation factors FVIIa and FXa to form a tertiary complex (Fig 6.1). FVIIa and FXa are composed of a single Gla domain followed by two tandem epidermal growth factor (EGF) domains and an N-terminus serine protease domain. All four domains of FVIIa are involved in the interaction with the two fibronectin domains of the extracellular domain of TF (Banner et al 1996). In addition, the first EGF domain (EGF-1) in the C-terminus of FXa is known to bind to the first fibronectin domain of TF (Fig 6.1) (Zhong et al 2002). Mutagenesis studies have identified the amino acids Asp48, Glu51, Ser52, Asn57, Phe76, Asn80 and Glu82 within the EGF-1 domain of FXa as residues essential for binding to TF (Zhong et al 2002). In addition, residues Arg200 and Lys201 within the first fibronectin domain of TF have been shown to interact with the EGF-1 domain of FXa (Manithody et al 2007).

6.1.3. TF signalling through integrins

Recently it has been shown that TF can mediate changes in cell migration and proliferation by interacting with the integrin family of adhesion molecules (Dorfleutner et al 2004, Versteeg et al 2008). The integrin family of cell surface receptors link the extracellular matrix to the cytoskeleton, allowing cells to respond to their surroundings

Figure 6.1. Structure of the TF:FVIIa:FXa complex



The extracellular domain of TF (purple) forms a complex with FVIIa and FXa. Both FVIIa and FXa contain a C-terminal Gla domain (yellow), followed by an EGF-1 domain (green), an EGF-2 domain (blue) and a serine protease domain (red). FVIIa uses all four domains to bind to TF, whereas the EGF-1 domain of FXa binds to the extracellular domain of TF. Adapted from Ruf et al (2003).

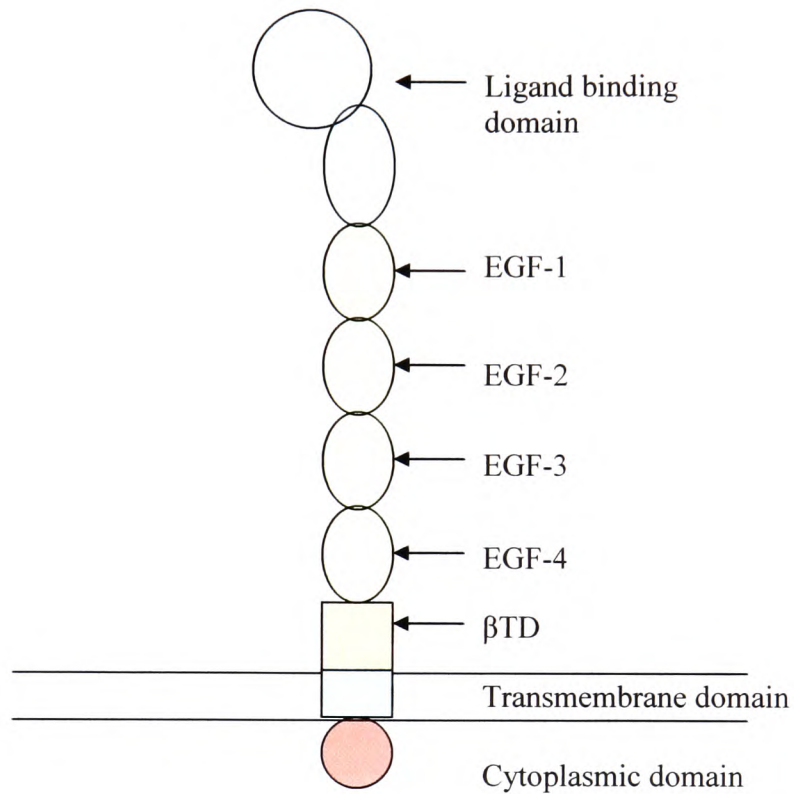
and controlling cellular processes including cell adhesion, migration and proliferation (Woodside et al 2001). Integrins bind to components of the extracellular matrix including fibronectin, laminin and collagens through short sequences within the ligands, such as the arginine-glycine-aspartate (RGD) sequence (Brakebusch & Fassler 2005). The binding of integrins to ligands, as well as the binding of divalent cations such as Mn^{2+} and Mg^{2+} , results in the activation of integrins (Humphries 1996). Integrins exist as heterodimers of α and β subunits. The $\beta 1$ integrin subunit is an elongated molecule of 130 kDa that has a small cytoplasmic domain, a single transmembrane domain and a large extracellular domain (Fig 6.2). The extracellular domain of $\beta 1$ integrin consists of a proximal membrane domain termed the β TD domain followed by four epidermal growth factor domains termed EGF-4 to EGF-1 in ascending order away from the cell membrane, and a ligand-binding domain (Fig 6.2) (Xiong et al 2001). TF has been shown to mediate changes in cell migration and gene expression by interacting with integrins (Dorfleitner et al 2004, Versteeg et al 2008). Furthermore, TF has been shown to directly bind to the $\beta 1$ integrin subunit in both keratinocytes and breast cancer cells (Versteeg et al 2008). However, the mechanism by which TF binds to the integrin subunit is unknown and has not been previously explored.

6.1.4. Aims

In the previous chapters, the influence of exogenous TF on ER α expression and activity and breast cancer proliferation and invasion was examined. However, the mechanisms by which exogenous TF interacts with the cell surface and promotes these cellular changes have not been examined. The main objectives of this chapter were:

- To examine the interaction of exogenous TF with the surface of breast cancer cells
- To explore the possible role of integrins in exogenous TF binding to the cell surface

Figure 6.2. Schematic representation of the structure of $\beta 1$ integrin



The $\beta 1$ integrin subunit is an elongated molecule composed of a large extracellular domain, a single transmembrane domain and a small cytoplasmic domain. The extracellular domain consists of a membrane-proximal domain termed the β TD domain, followed by four EGF domains and a ligand binding domain. Adapted from Luo et al (2007).

- To investigate the involvement of PARs in TF mediated cell signalling in breast cancer cells and elucidate the associated mechanisms in the control of ER α expression and cell proliferation.

6.2. Methods

6.2.1. Examination of the mechanisms of TF-mediated signalling

6.2.1.1. Examination of the expression of PARs in breast cancer cells by RT-PCR

Total RNA was isolated from MCF-7, T47D and MDA-MB-231 cells (10^6 each) and amplified by RT-PCR using published primers specific for PAR1 and PAR2 (Jiang et al 2004) shown below. PCR was carried out with an annealing temperature of 56°C and for 29 amplification cycles. The DNA products were examined by agarose gel electrophoresis and images recorded using the GeneSnap program. The expected band sizes were 850 bp for PAR1 and 503 bp for PAR2.

PAR 1 forward: 5'-TGT ACG CCT CTA TCT TGC TCA TGA C-3'

PAR 1 reverse: 5'-GCA GGT ATG CAA GTC GTA CAT CTG-3'

PAR 2 forward: 5'-TGA GCA GCT CTT GGT GGG AGA CAT-3'

PAR 2 reverse: 5'-ACT CAA TAG GAG GTC TTA ACA GTG G-3'

6.2.1.2. Examination of the involvement of PARs in TF mediated breast cancer cell proliferation

MCF-7 cells (2.5×10^4) were seeded out into 24 well plates in phenol red-free medium supplemented with 1 % (v/v) FCS and treated with combinations of recombinant TF (500 nM), 17 β -oestradiol (250 pM), PAR agonist peptides (SFLLRN for PAR1 and SLIGRL for PAR2) (20 μ M each), or pre-incubated with the PAR1 inhibitory

antibodies ATAP2 and WEDE15 (25 µg/ml each), the PAR2 inhibitory antibody SAM11 (25 µg/ml) or a rabbit polyclonal anti-human TF antibody (100 µg/ml), as described in the results. The cells were incubated for 24 h at 37°C and cell proliferation examined using the MTS-based assay described in the general methods section 2.3.

6.2.1.3. Examination of the involvement of PARs, FVIIa, FXa, β1 integrin and MAPK in the downregulation of ERα expression by exogenous TF

MCF-7 cells (2×10^5) were seeded out into 12 well plates in medium supplemented with 1 % (v/v) FCS and incubated at 37°C overnight. The cells were then washed four times with PBS (1 ml), medium containing 2 % (v/v) serum replacement medium added to each well and the cells incubated for 3 h at 37°C. The cells were then treated with combinations of TF (50 and 500 nM), FVIIa (5 nM) and FXa (10 nM) as described in the results section. Similar samples were incubated with PAR1 and PAR2 inhibitory antibodies (25 µg/ml) prior to the addition of TF (500 nM), or treated with PAR1 and PAR2 agonist peptides (20 µM). In addition, cells were pre-incubated with a rabbit polyclonal anti-human β1 integrin antibody (5.3 µg/ml) or a β1 integrin inhibitory antibody (AIIB2) (50 µg/ml). Finally, samples were incubated with an ERK1/2 MAPK inhibitor PD98059 (50 µM) in the presence or absence of TF (500 nM). Following 24 h incubation at 37°C the cells were harvested and total RNA isolated and analysed by RT-PCR as described in section 2.5.3. Alternatively, whole cell extracts were prepared using the nuclear extract kit, and levels of ERα protein expression analysed using the ERα ELISA as described in section 3.2.4.2.

6.2.2. Investigation of the interaction of exogenous TF with breast cancer cells

6.2.2.1. Preparation of fluorescein-labelled TF

Fluorescein molecules were coupled to recombinant TF by the catalysis of carboxamide bond formation between COO^- groups on fluorescein molecules and free NH_3^+ groups on TF using the reagents O-(benzotriazol-1-yl)-N,N,N',N'-tetramethyluronium hexafluorophosphate (HBTU) and N, N-diisopropylethylamine (DIPEA). Recombinant TF (0.5 g) was dissolved in distilled water (10 ml) containing HBTU (0.1 M). To initiate the reaction, a fluorescein solution (25 μmol) containing DIPEA (0.1 M) was added to the TF/HBTU solution and incubated for 2 h at room temperature with stirring. Excess fluorescein was removed by stepwise dialysis, first in PBS (5 L) at 4°C for 2 h. The PBS was then replaced with fresh PBS (5 L) and incubated at 4°C, overnight. The dialysis step was repeated until all excess fluorescein had been removed. The presence of TF was determined by 12 % (w/v) SDS-PAGE, followed by western blot analysis for TF using a mouse monoclonal anti-human TF antibody (0.5 $\mu\text{g}/\text{ml}$ final concentration). The activity of the fluorescein-labelled TF was confirmed by measuring the procoagulant activity using the PT assay as described in section 2.9.

6.2.2.2. Examination of the interaction of fluorescein-labelled TF with the cell surface by fluorescence microscopy

MCF-7 cells (5×10^4) were seeded out into 8 well cultureslides in medium (300 μl) and incubated at 37°C overnight. Fluorescein-labelled TF solution (5 μl) was added to the wells at intervals up to 60 min. The cells were then washed three times with PBS (500 μl) and fixed with glutaraldehyde (3 % (v/v)) for 20 min at room temperature in the dark. The cells were washed three times with PBS (500 μl) and viewed using a Leitz

Leitz Laborlux S fluorescence microscope. Images were recorded and analysed using Image-Pro Plus Version 5.1.2.

6.2.3. Identification of receptors involved in the interaction of exogenous TF with the cell surface

6.2.3.1. Analysis of $\beta 1$ and $\beta 3$ integrin expression on the surface of breast cancer cells by fluorescence microscopy

MCF-7 or T47D cells (5×10^4) were seeded out into 8 well culture slides in medium (300 μ l) and incubated at 37°C overnight. The cells were washed three times with PBS (500 μ l) and fixed with glutaraldehyde (3 % (v/v)) as before. The cells were then washed three times with PBS (500 μ l) and incubated with anti-human $\beta 1$ integrin or $\beta 3$ integrin phycoerythrin (PE)-conjugated antibodies (0.1 μ g/ml final concentration) for 1 h in the dark. Finally, the cells were washed three times with PBS (500 μ l) and viewed using a Leitz Laborlux S fluorescence microscope. Images were recorded and processed using Image-Pro Plus Version 5.1.2.

6.2.3.2 Co-localisation of TF with $\beta 1$ integrin by fluorescence microscopy

MCF-7 cells (5×10^4) were seeded out into 8 well culture slides in medium (300 μ l) and incubated at 37°C overnight. Fluorescein-labelled TF solution (5 μ l) was added to the wells and incubated at 37°C for 15 min. The cells were then washed twice with PBS (500 μ l) and fixed with glutaraldehyde (3 % (v/v)) as before. The cells were washed three times with PBS and incubated with the $\beta 1$ integrin PE-conjugated antibody (0.1 μ g/ml final concentration) for 1 h in the dark. The cells were washed three times with PBS (500 μ l) and visualised using a Leitz Laborlux S fluorescence microscope. Images were recorded and analysed using Image-Pro Plus Version 5.1.2.

In a separate experiment, MCF-7 cells (5×10^4) were incubated at 37°C for 2 h with a range of concentrations of a rabbit polyclonal antibody (0-5.3 µg/ml) directed against the C-terminus, including the cytoplasmic domain to the EGF-4 domain (amino acids 579-799) of $\beta 1$ integrin (Fig 6.2). The cells were washed twice with PBS (500 µl) and fluorescein-labelled TF solution (5 µl) was added to the wells and incubated at 37°C for 15 min. The cells were then washed twice with PBS (500 µl) and visualised using a fluorescence microscope.

6.2.3.3. Examination of TF binding to $\beta 1$ integrin by co-precipitation

TF-agarose and BSA agarose-conjugated microbeads (resins) were prepared by attaching recombinant TF or BSA to activated agarose. Recombinant TF (0.5 g) or BSA (0.5 g) were dissolved in 0.1 M sodium bicarbonate buffer, pH 7.2 (4 ml). p-nitrophenyl chloroformate-activated agarose (0.5 ml) was pipetted into separate pre-boiled dialysis tubing and the TF or BSA solutions were added to the agarose, sealed and placed in 0.1 M sodium bicarbonate buffer (1 L). The samples were incubated at 4°C overnight to allow the binding of TF or BSA to the activated agarose. The dialysis tubing was then transferred to 0.1 M ethanolamine (1 L) and incubated at 4°C for 2 days to block the remaining free chloroformate groups. The TF or BSA-conjugated agarose resins were transferred to 15 ml tubes, centrifuged at 400 g for 10 min and the resins washed twice in PBS (10 ml).

MCF-7 cells were cultured in T150 flasks and when at approximately 80 % confluency, were washed three times with PBS (10 ml) and then lysed with cell lysis buffer (20 mM Tris-HCl pH 7.5, 150 mM NaCl, 1 % (v/v) Triton X-100 and protease inhibitor cocktail (1 %)) (2 ml). The cell lysate was sonicated twice on ice, each for 20 s, cleared by centrifugation at 400 g for 5 min and then transferred to a 15 ml tube. The TF and BSA-

conjugated agarose resins were washed three times in cell lysis buffer (2 ml) and transferred to 1.5 ml tubes (0.3 ml of resin/tube). Cell extract (0.5 ml) was added to each resin sample and incubated at 4°C overnight on a rolling platform. The resins were then washed four times with cell lysis buffer (1 ml), 2× Laemmli's buffer (30 µl) added and the samples heated at 99°C for 5 min. The denatured agarose resins were then removed by centrifuging at 6000 rpm for 2 min in a microcentrifuge and the supernatant containing interacting proteins retained. The proteins were separated by 10 % (w/v) SDS-PAGE and membranes were probed using a rabbit anti-human β1 integrin antibody (0.4 µg/ml) and a rabbit anti-human FVIIa antibody (1.4 µg/ml).

6.2.3.4. Visualisation and modification of protein domain structures

Protein structure files from the “Brookhaven protein data bank” (PDB) were downloaded from PubMed and visualised using the Raswin version 6 program. Files were edited using a general text editor to select the domains of interest. The edited protein structure files were uploaded into the Alchemy III program and amino acid side chains altered according to sequences described in the results section. Finally, the amino acids of interest were highlighted and the protein domain structures compared using the Alchemy III program.

6.3. Results

6.3.1. Examination of the role of PARs and coagulation factors in TF mediated signalling in breast cancer cells

6.3.1.1. Examination of the involvement of PARs in TF mediated breast cancer cell proliferation

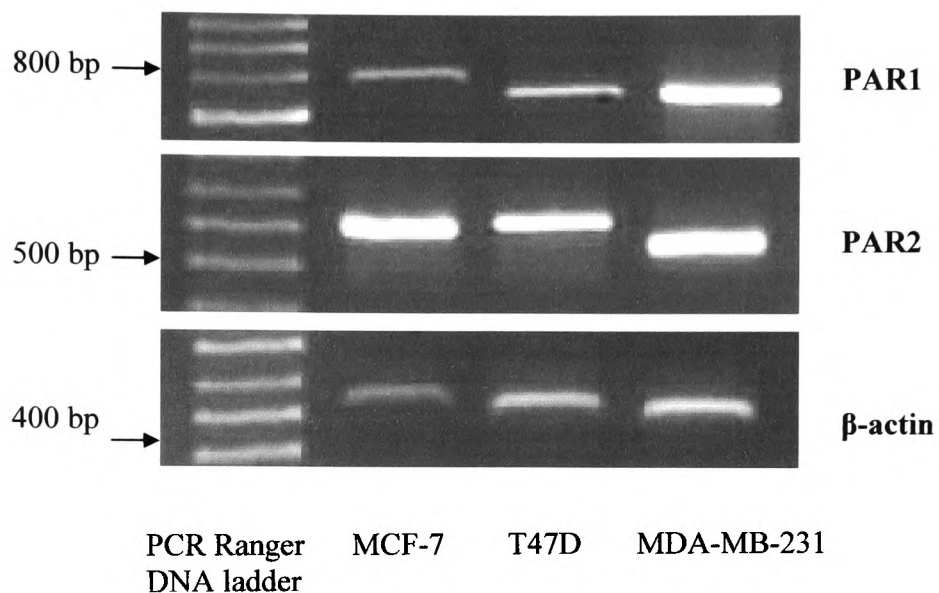
Initially, baseline levels of PAR1 and PAR2 mRNA expression in MCF-7 and T47D cells were examined by RT-PCR. Both MCF-7 and T47D cells expressed low levels of

PAR1, and higher levels of PAR2 (Fig 6.3). MDA-MB-231 cells were used as a positive control as these cells are known to express high levels of both PAR1 and PAR2 (Kamath et al 2001). The PAR1 and PAR2 agonist peptides used in this part of the investigation mimic the cleaved amino-terminus of the tethered ligands of PAR1 and PAR2 and allow activation of PAR1 and 2 individually. In addition, the activation of PAR1 and PAR2 was inhibited using the inhibitory antibodies ATAP2, WEDE15, SAM11 which bind to the N-terminus and prevent activation of PARs (Shi et al 2004). Activation of PAR2 using the agonist peptide was capable of suppressing cell proliferation to a similar extent as that observed with the sample incubated with TF (500 nM) together with oestradiol (250 pM) (Fig 6.4). In addition, the ability of TF (500 nM) to suppress oestradiol-mediated cell proliferation was reversed on incubation of cells with an inhibitory antibody against PAR2 or a polyclonal antibody against TF. The activation of PAR1 in the presence of oestradiol (250 pM) had no influence on rates of proliferation. However, the ability of TF (500 nM) to suppress oestradiol-mediated cell proliferation was reversed on incubation of cells with the PAR1 inhibitory antibodies (Fig 6.4).

6.3.1.2. Examination of the influence of FVIIa and FXa on ER α expression

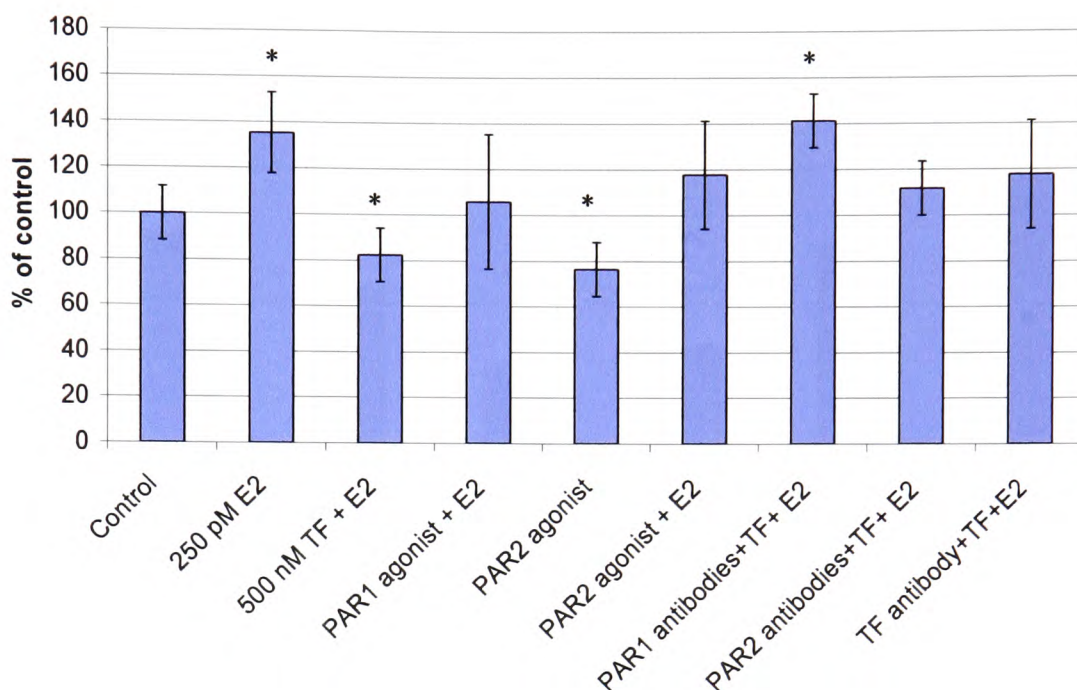
Incubation of MCF-7 cells with recombinant TF (50 nM and 500 nM) in serum-free medium reduced ER α mRNA and protein expression in a concentration dependent manner, with 500 nM TF reducing mRNA expression by 40 % compared to the untreated control (Fig 6.5). Incubation of MCF-7 cells with a combination of FVIIa (5 nM) together with recombinant TF (500 nM) had little additional influence on ER α mRNA expression compared to cells incubated with TF alone. In contrast, the combination of TF and FVIIa appeared to induce increased ER α protein expression (Fig 6.6). The supplementation of TF/FVIIa with FXa (10 nM) restored ER α mRNA and

Figure 6.3. PAR1 and PAR2 mRNA expression in breast cancer cell lines



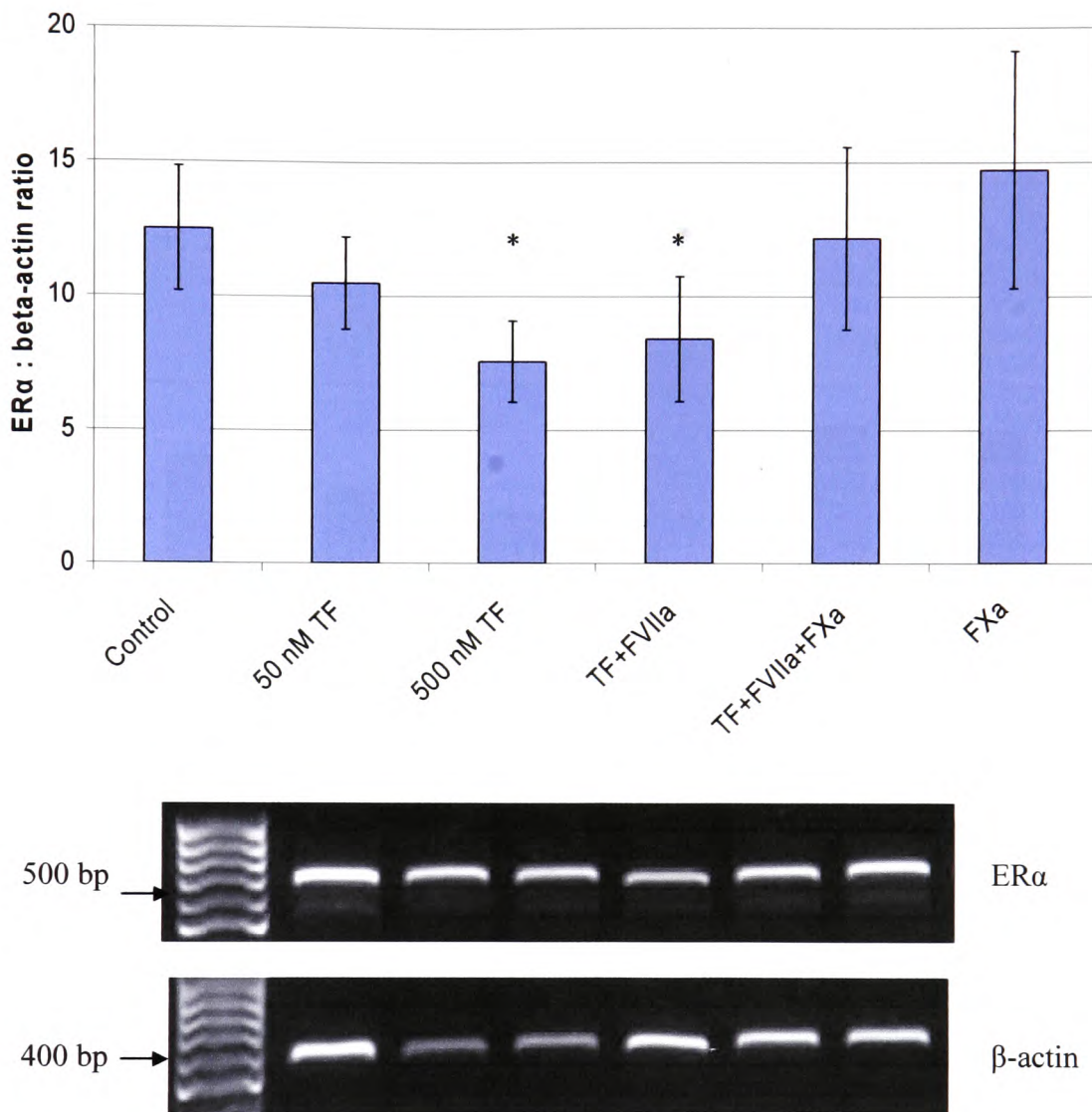
Total RNA was isolated from MCF-7, T47D and MDA-MB-231 cells (10^6) and used for RT-PCR of PAR1, PAR2 and β -actin. DNA products were analysed by 2 % (w/v) agarose gel electrophoresis and viewed under UV light. Images were recorded using the GeneSnap program.

Figure 6.4. The involvement of PAR1 and PAR2 in breast cancer cell proliferation



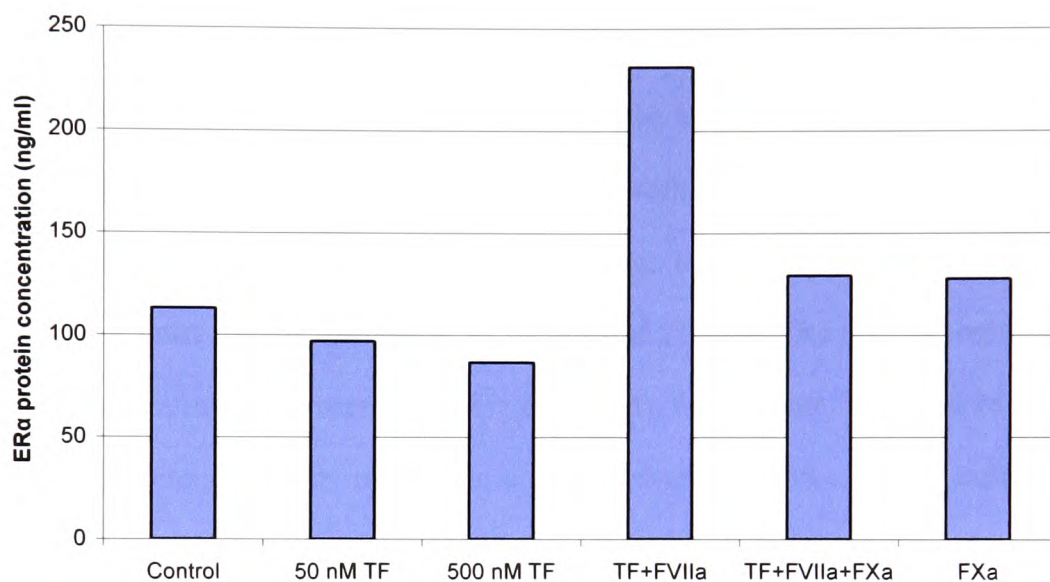
MCF-7 cells (2.5×10^4) were seeded out into 24 well plates and adapted to phenol red-free medium containing 1 % (v/v) FCS. The cells were treated with combinations of recombinant TF (500 nM), oestradiol (250 pM), PAR1 and PAR2 agonist peptides (20 μ M each), the PAR1 inhibitory antibodies ATAP2 and WEDE15 (25 μ g/ml each), the PAR2 inhibitory antibody SAM11 (25 μ g/ml) and a polyclonal anti-TF antibody (100 μ g/ml). The cells were incubated at 37°C for 24 h and rates of cell proliferation determined using the MTS-based assay. Data are representative of four independent experiments, each in duplicate \pm SD. * $p < 0.05$ vs. the untreated control.

Figure 6.5. Examination of the influence of FVIIa and FXa on ER α mRNA expression



MCF-7 cells were seeded out into 12 well plates and adapted to medium containing 2 % (v/v) serum replacement medium. The cells were treated with TF (50 and 500 nM), and combinations of TF (500 nM), FVIIa (5 nM) and FXa (10 nM). Cells were incubated at 37°C for 24 h, RNA isolated and used for RT-PCR. Images were recorded using the GeneSnap program and ER α expression compared to β -actin using the GeneTool program. Data represent the average of five independent experiments \pm SD. * $p < 0.05$ vs. the untreated control.

Figure 6.6. Examination of the influence of FVIIa and FXa on ER α protein expression



MCF-7 cells were seeded out into 12 well plates and adapted to medium containing 2 % (v/v) serum replacement medium. The cells were treated with combinations of recombinant TF (0-500 nM), FVIIa (5 nM) and FXa (10 nM). The cells were incubated at 37°C for 24 h, harvested and whole cell extracts prepared. 10 μ g of protein for each sample was placed into the wells of an ER α ELISA. Absorption values were converted to ER α protein concentrations using a standard curve prepared with recombinant ER α . Data are from one experiment.

protein expression to that of the untreated controls (Fig 6.5 and 6.6). Furthermore, the addition of FXa alone increased ER α mRNA expression above that of the untreated control by 18 %.

6.3.1.3. Examination of the involvement of PAR1 and PAR2 in ER α expression

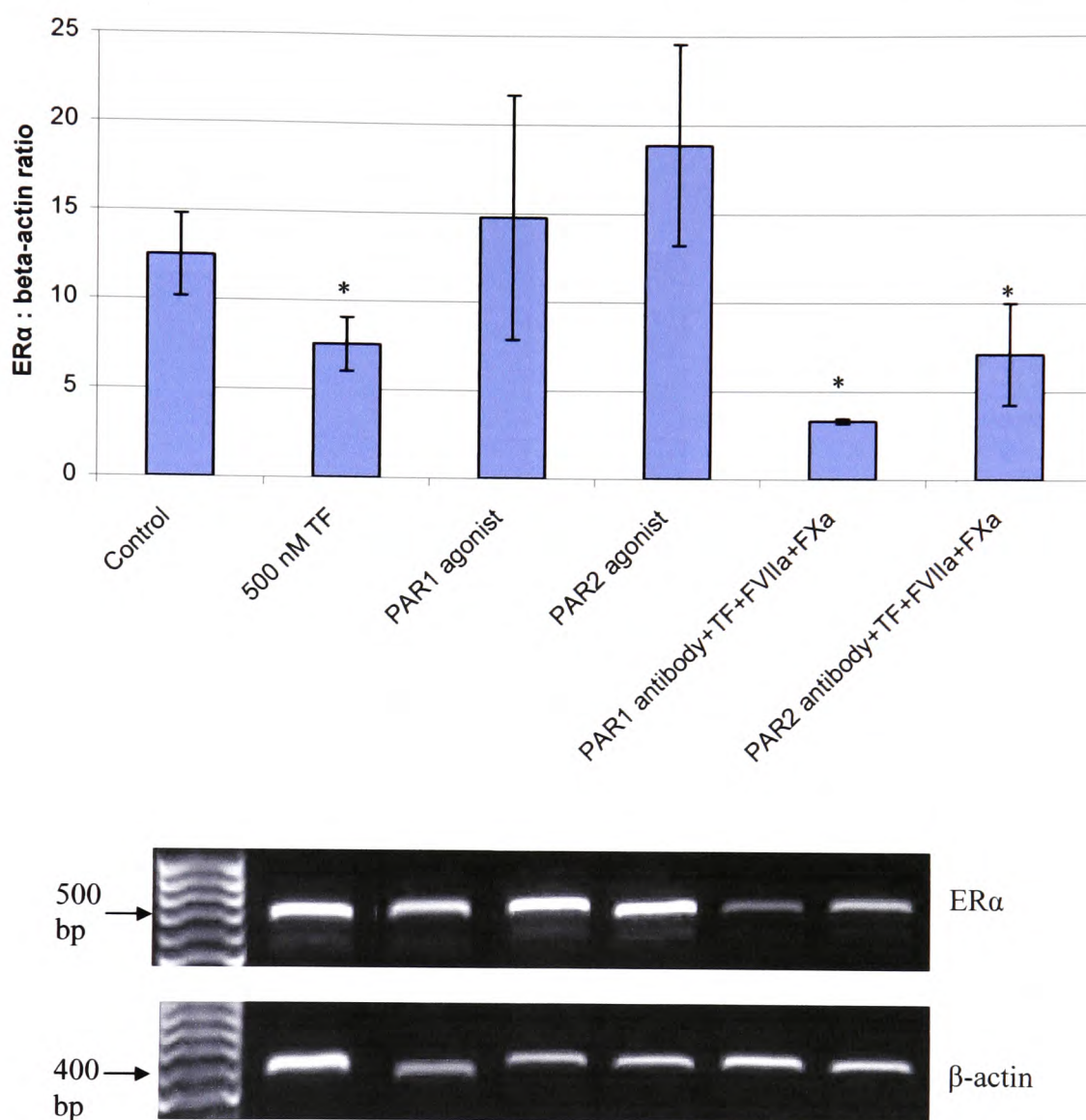
Incubation of MCF-7 cells with the PAR1 agonist peptide resulted in an 18 % increase in ER α mRNA expression, which was reflected in the ER α protein expression (Fig 6.7 & 6.8). Furthermore, pre-incubation of cells with PAR1 inhibitory antibodies suppressed both ER α mRNA and protein expression. Incubation of MCF-7 cells with the PAR2 agonist peptide resulted in an increase of 51 % in ER α mRNA, but only a modest increase in protein expression (Fig 6.7 & 6.8). Furthermore, inhibition of PAR2 using an inhibitory antibody resulted in a 43 % reduction in ER α mRNA expression below that of the untreated control, and suppressed ER α protein expression.

6.3.2. Examination of the binding of exogenous TF to the surface of breast cancer cells

6.3.2.1. Analysis of fluorescein-labelled TF

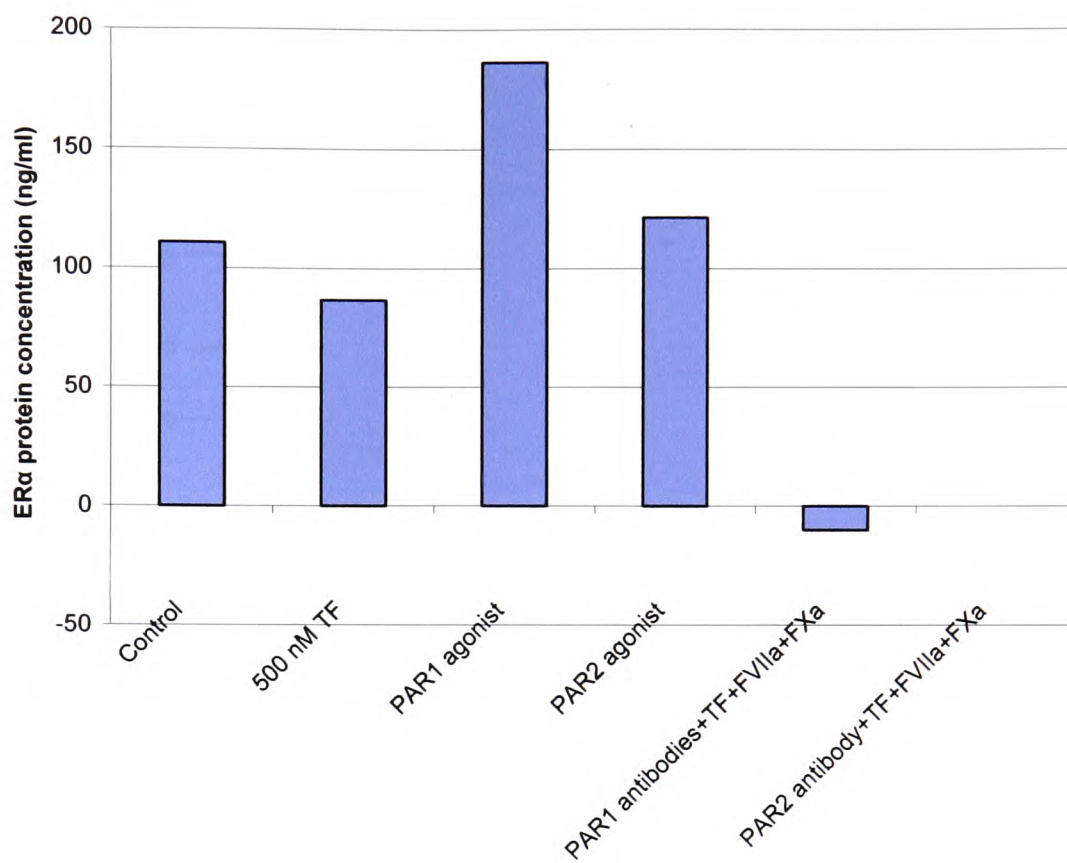
Recombinant TF was labelled with fluorescein using the reagents HBTU and DIPEA, which catalyse the formation of carboxamide bonds between fluorescein and TF molecules. Following labelling, the concentration of fluorescein-labelled TF was determined using the Bradford assay and calculated as 1.8 mg/ml compared to 2.3 mg/ml for the unlabelled TF. Furthermore, the stock solution of fluorescein-labelled TF had a clotting time of 27 s, compared to 13 s for the unlabelled TF. Analysis of the fluorescein-labelled and unlabelled TF by SDS-PAGE produced a single band at approximately 30 kDa (Fig 6.9). However, the band for the fluorescein-labelled TF was weaker, indicating that some recombinant TF was lost during the labelling process. The recombinant TF used in this investigation lacks the cytoplasmic domain and is not

Figure 6.7. Examination of the involvement of PARs in ER α mRNA expression



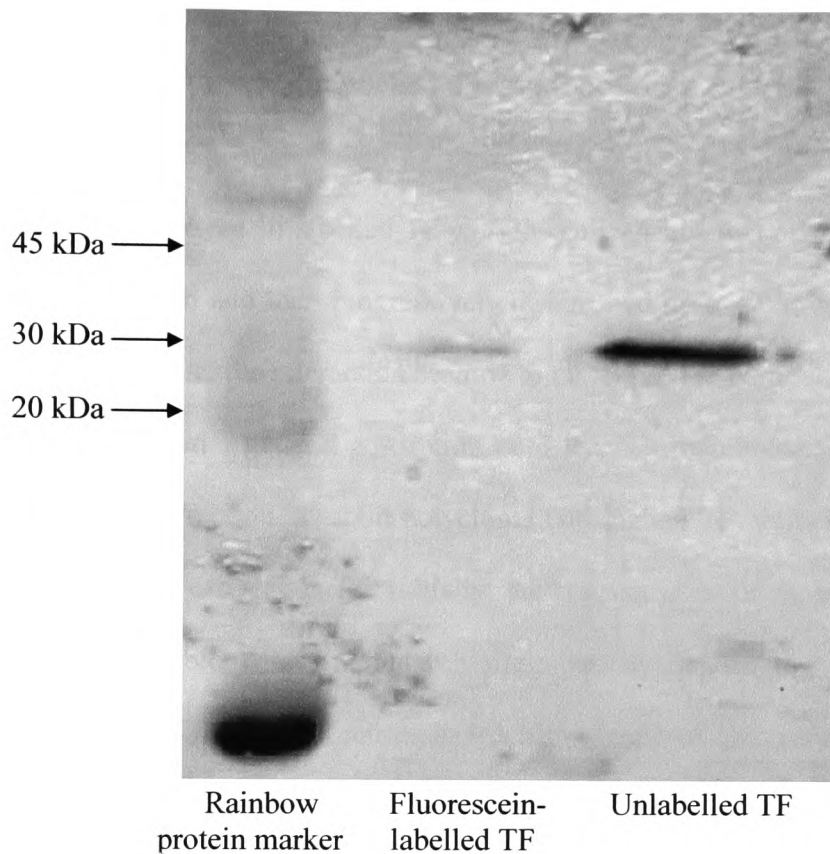
MCF-7 cells were seeded out into 12 well plates and adapted to medium containing 2 % (v/v) serum replacement medium. The cells were treated with recombinant TF (500 nM), PAR1 and PAR2 agonist peptides (20 μ M), PAR1 or PAR2 inhibitory antibodies (25 μ g/ml) with recombinant FVIIa (5 nM) and recombinant FXa (10 nM). Cells were incubated at 37°C for 24 h and RNA isolated and used for RT-PCR. Images were recorded using the GeneSnap program and ER α expression compared to β -actin using the GeneTool program. Data represent the average of five independent experiments \pm SD. * $p < 0.05$ vs. the untreated control.

Figure 6.8. Examination of the involvement of PARs in ER α protein expression



MCF-7 cells were seeded out into 12 well plates and adapted to medium containing 2 % (v/v) serum replacement medium. The cells were treated with combinations of recombinant TF (500 nM), PAR1 and PAR2 agonist peptides (20 μ M), and PAR1 inhibitory antibodies ATAP2 and WEDE15 (25 μ g/ml each), or PAR2 inhibitory antibody SAM11 (25 μ g/ml) with TF (500 nM), FVIIa (5 nM) and FXa (10 nM). The cells were incubated at 37°C for 24 h, harvested and whole cell extracts prepared. 10 μ g of protein for each sample was placed into the wells of an ER α ELISA. Absorption values were converted to ER α protein concentrations using a standard curve prepared with recombinant ER α . Data are from one experiment.

Figure 6.9. Western blot analysis of fluorescein-labelled TF



Aliquots (5 μ l) of fluorescein-labelled TF and unlabelled TF were separated by 12 % (w/v) SDS-PAGE and the proteins transferred onto nitrocellulose membrane. The membrane was probed with a mouse monoclonal anti-human TF antibody (0.5 μ g/ml) followed by an anti-mouse alkaline phosphatase-conjugated antibody (0.1 μ g/ml). The membrane was developed using Western Blue stabilised substrate for alkaline phosphatase and images recorded using the GeneSnap program.

glycosylated, which accounts for the lower molecular weight of 30 kDa compared to full length TF, which has a molecular weight of 42 kDa.

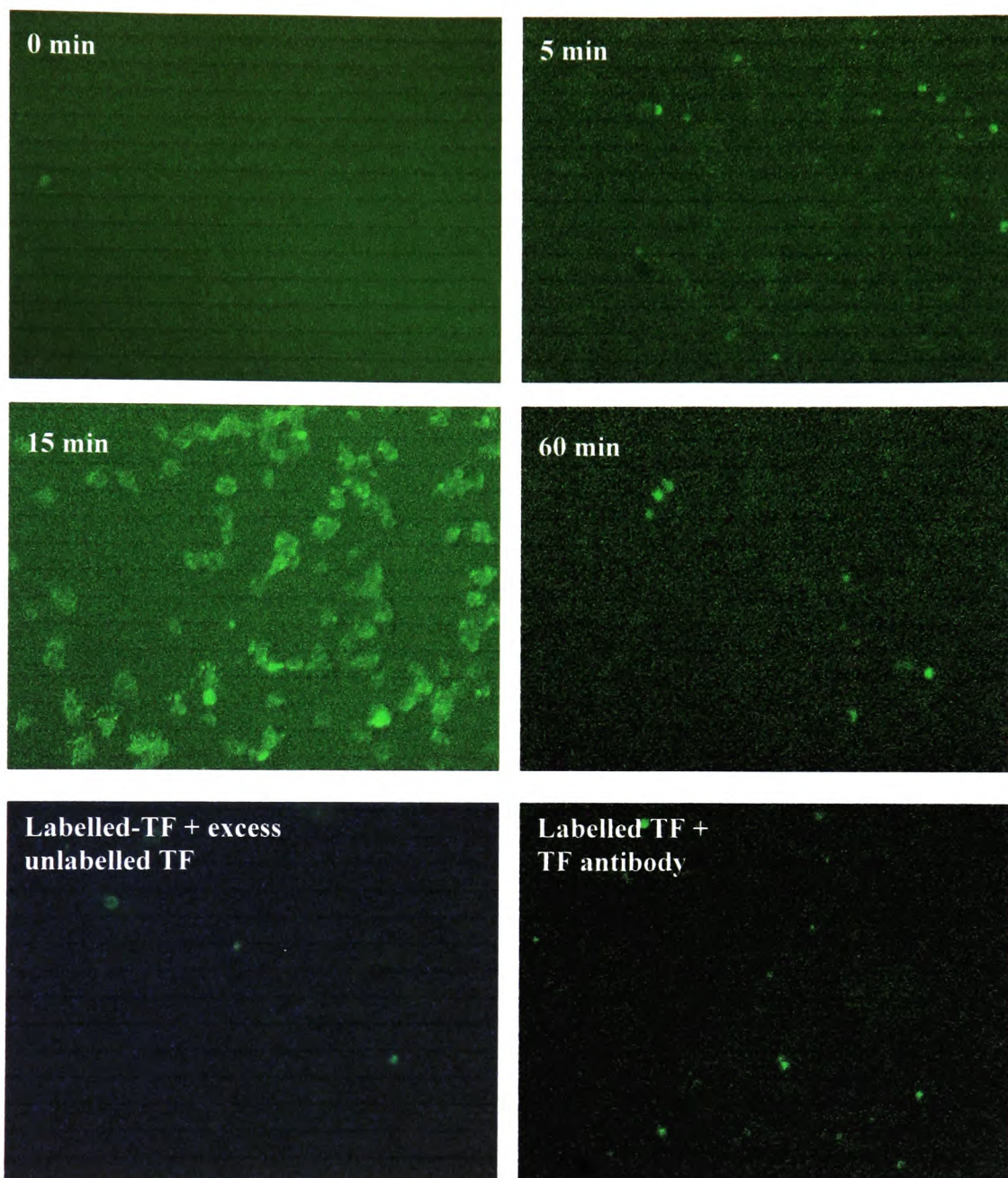
6.3.2.2. Analysis of fluorescein-labelled TF binding to cell surface by fluorescence microscopy

The interaction of fluorescein-labelled TF with the cell surface was observable within 5 min, peaked at 15 min and then progressively diminished up to 60 min post-treatment (Fig 6.10). Furthermore, the interaction seemed to be focused at particular points on the cell surface rather than a general adsorption onto the cell membrane. To confirm the specificity of this interaction, a rabbit polyclonal anti-human TF antibody was used to inhibit the binding of exogenous TF. Initially, the concentration of the polyclonal anti-TF antibody used to block TF binding was optimised by incubating recombinant TF (500 nM) with a range of concentrations (0-100 µg/ml) of the polyclonal anti-TF antibody for 1.5 h and then measuring the procoagulant activity of the samples using the PT assay. The activity of TF in the samples was calculated as described in section 2.9 and the percentage of inhibition of TF activity calculated as follows.

$$\frac{(\text{Initial TF activity} - \text{Residual TF activity})}{(\text{Initial TF activity})} \times 100$$

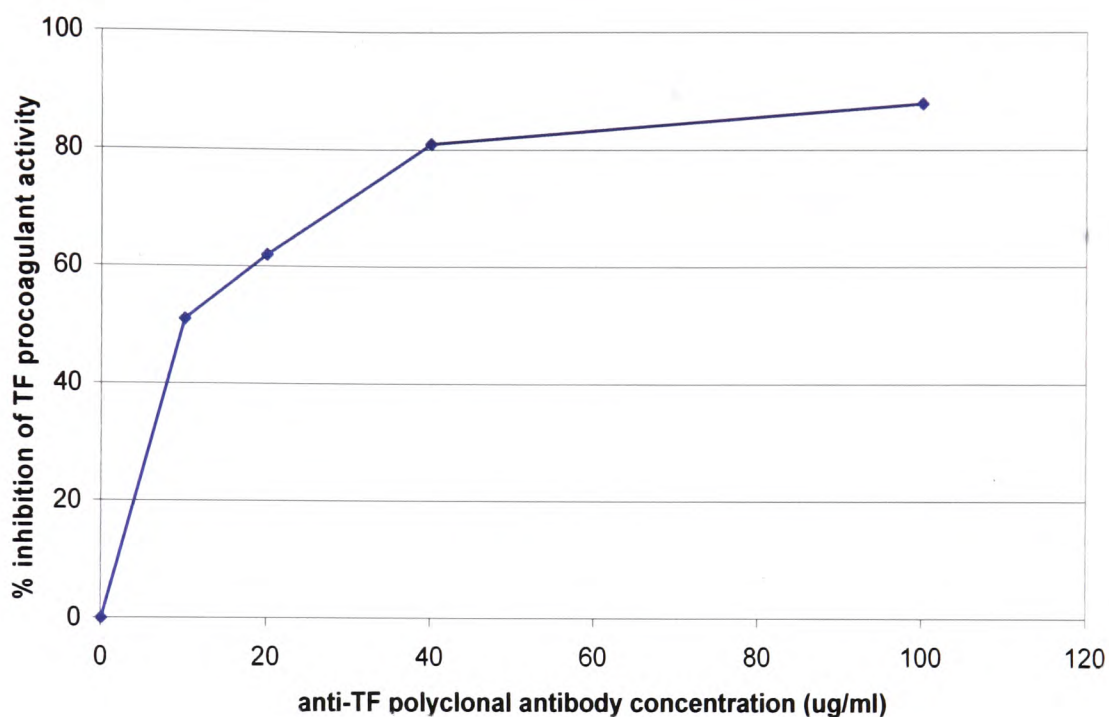
Residual TF activity is TF activity following addition of the anti-TF antibody. The anti-TF antibody was shown to inhibit the procoagulant activity of TF by 88 % at a concentration of 100 µg/ml (Fig 6.11). Pre-incubation of fluorescein-labelled TF with the polyclonal anti-TF antibody (100 µg/ml) reduced the binding of fluorescein-labelled TF to the cell surface at 15 min (Fig 6.10). Furthermore, inclusion of a 10-fold excess of unlabelled TF diminished the binding of fluorescein-labelled TF to the cell surface (Fig 6.10).

Figure 6.10. Interaction of fluorescein-labelled TF with MCF-7 cells



MCF-7 cells (5×10^4) were seeded out into 8 well cultureslides and incubated with fluorescein-labelled TF solution ($5 \mu\text{l}$) for 0-60 min. In addition, labelled TF was pre-incubated with an anti-TF antibody, or cells were pre-incubated with unlabelled TF and fluorescein-labelled TF then added for 15 min. The cells were washed with PBS, fixed with 3 % (v/v) glutaraldehyde and visualised using a CoolSnap Pro camera attached to a Leitz Laborlux S fluorescence microscope. Images were processed using the Image-Pro Plus Version 5.1.2. Data are representative of three independent experiments. (Magnification $\times 10$).

Figure 6.11. Optimisation of anti-TF polyclonal antibody concentration to inhibit TF procoagulant activity



Samples of recombinant TF (500 nM) were incubated with a range of concentrations of the polyclonal anti-human TF antibody (0-100 $\mu\text{g/ml}$) for 1.5 h. The procoagulant activity of each sample was measured using the PT assay and the clotting times were recorded using a Cascade M coagulometer. Clotting times were converted to percentage inhibition of TF activity and the percentage inhibition calculated. Data are from one experiment.

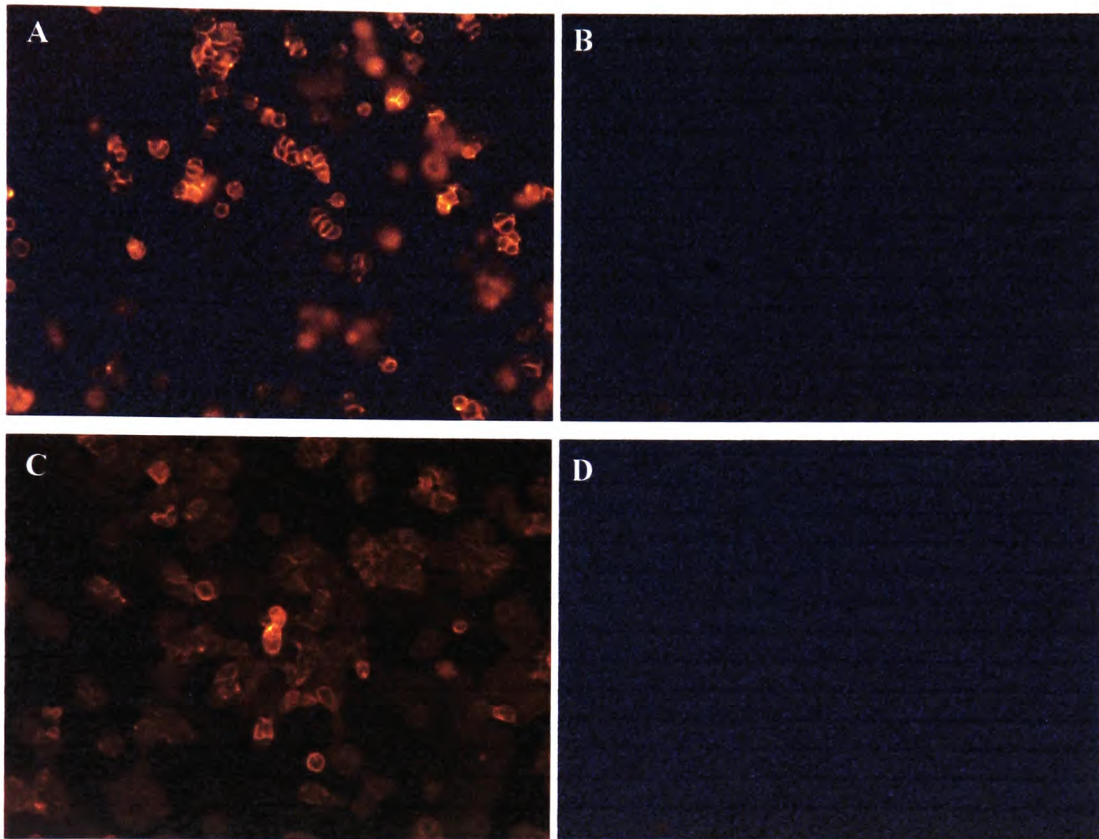
6.3.3. Identification of the receptors involved in the interaction of TF with the cell surface

6.3.3.1. Co-localisation of TF with β 1 integrin by fluorescence microscopy

Initially, the cell surface expression of the β 1 and β 3 integrins in breast cancer cells was examined. MCF-7 and T47D cells both expressed cell surface β 1 integrin but had no detectable surface β 3 integrin as determined by fluorescence microscopy (Fig 6.12). Next, the level of co-localisation between the bound exogenous TF and cell surface β 1 integrin was examined using fluorescence microscopy. The proteins were detected at different wavelengths by the fluorescein-label of TF (green fluorescence) and a PE-conjugated antibody against β 1 integrin (red fluorescence). Overlaying of the images produced orange/yellow points where the two proteins co-localised. A partial co-localisation between fluorescein-labelled TF and β 1 integrin was observed in MCF-7 cells following 15 min incubation with fluorescein-labelled TF (Fig 6.13) as determined using the colour-pair function in ImagePro-Plus program. Furthermore, the Pearson correlation coefficient was calculated to be 0.936, where a value of 1 is a 100 % match.

In a separate experiment, an anti- β 1 integrin polyclonal antibody, raised against the C-terminus amino acids 579-799 of β 1 integrin, including the β TD and EGF-4 domains of β 1 integrin (Fig 6.2), was used to examine whether TF binds to β 1 integrin on the cell surface. MCF-7 cells were incubated with a range of concentrations of the polyclonal β 1 integrin antibody (0-5.3 μ g/ml). While low concentrations of antibody (0.7, 1.3 and 2.6 μ g/ml) had no significant effect on TF binding, cells incubated with a higher concentration (5.3 μ g/ml) had lower fluorescence intensity, indicating that binding of exogenous TF to the surface of MCF-7 cells was partially blocked by the β 1 integrin antibody (Fig 6.14).

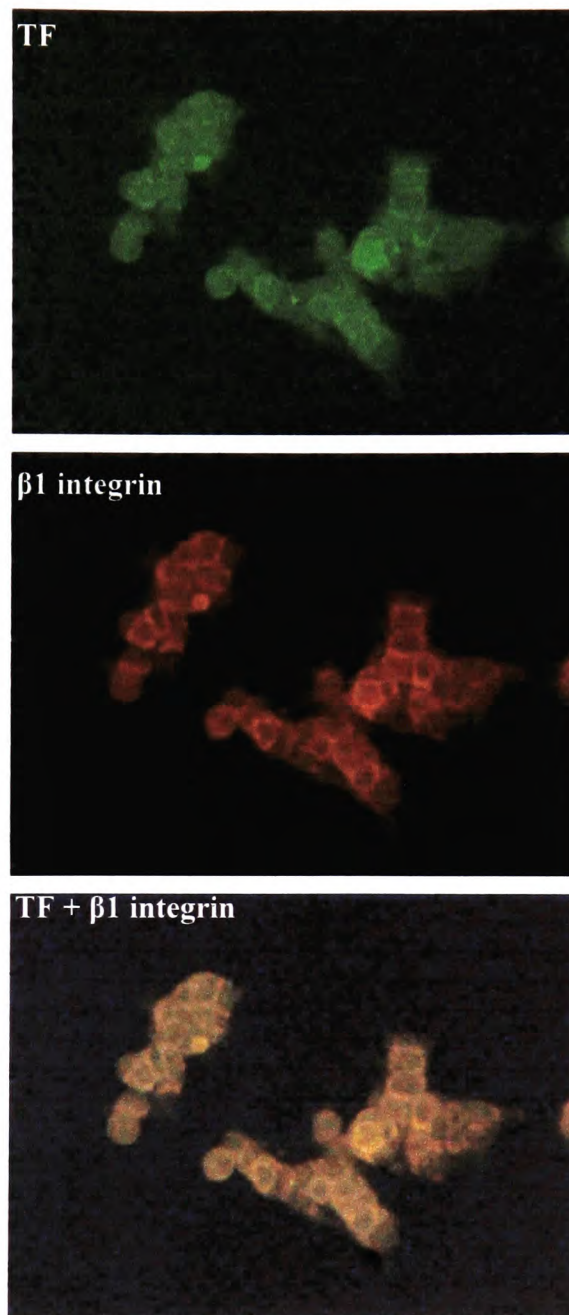
Figure 6.12. Cell surface expression of $\beta 1$ and $\beta 3$ integrins in breast cancer cells



MCF-7 and T47D cells (5×10^4) were seeded out into 8 well cultureslides and incubated at 37°C overnight. The cells were washed three times with PBS, fixed with glutaraldehyde (3 % (v/v)) and incubated with anti-human $\beta 1$ integrin or $\beta 3$ integrin PE-conjugated antibodies (0.1 $\mu\text{g}/\text{ml}$) for 1 h in the dark. The cells were washed with PBS and visualised using a CoolSnap Pro camera attached to a Leitz Laborlux S fluorescence microscope. Images were processed using the Image-Pro Plus Version 5.1.2. Data are from one experiment. (Magnification $\times 10$).

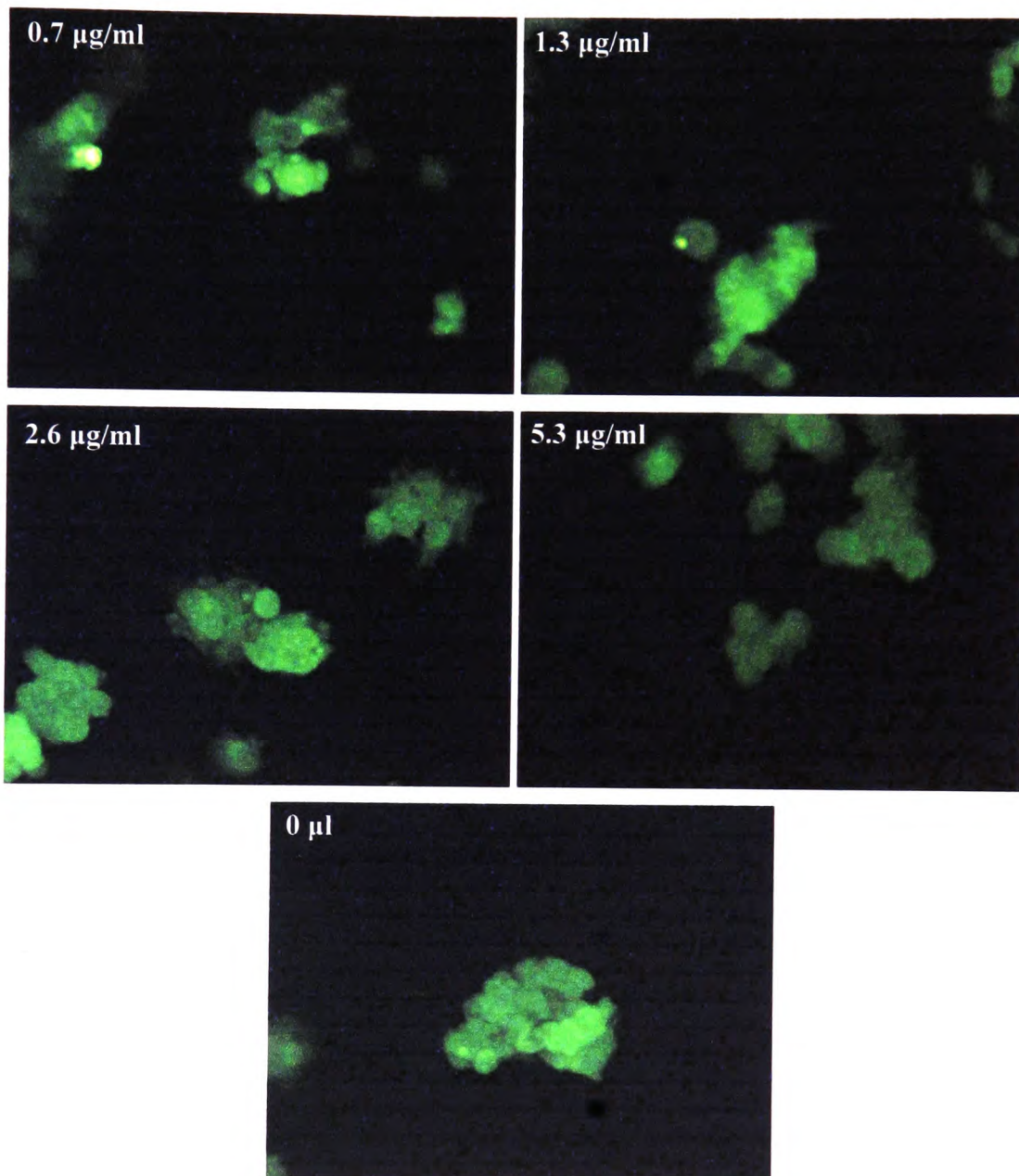
A = $\beta 1$ integrin expression in MCF-7 cells, B = $\beta 3$ integrin expression in MCF-7 cells,
C = $\beta 1$ integrin expression in T47D cells, D = $\beta 3$ integrin expression in T47D cells.

Figure 6.13. Co-localisation of exogenous TF with β 1 integrin in MCF-7 cells



MCF-7 cells (5×10^4) were seeded out into 8 well cultureslides and incubated with fluorescein-labelled TF solution (5 μ l) at 37°C for 15 min. The cells were then washed twice with PBS, fixed with glutaraldehyde (3 % (v/v)) and incubated with an anti- β 1 integrin PE-conjugated antibody (0.1 μ g/ml) for 1 h. The cells were washed three times with PBS and visualised using a fluorescence microscope. The first two images were overlaid to produce the last image using the Image Pro Plus program. Data are representative of two independent experiments. (Magnification \times 25).

Figure 6.14. Examination of the binding of exogenous TF in the presence of an anti- β 1 integrin antibody



MCF-7 cells (5×10^4) were seeded out into 8 well culture slides and incubated with a range of concentrations of a rabbit polyclonal anti-human β 1 integrin antibody (0-5.3 $\mu\text{g/ml}$) at 37°C for 2 h. The cells were washed twice with PBS (500 μl) and fluorescein-labelled TF (5 μl) was added to the wells and incubated at 37°C for 15 min. The cells were then washed twice with PBS (500 μl) and visualised using a fluorescence microscope. Data are representative of two experiments. (Magnification $\times 25$).

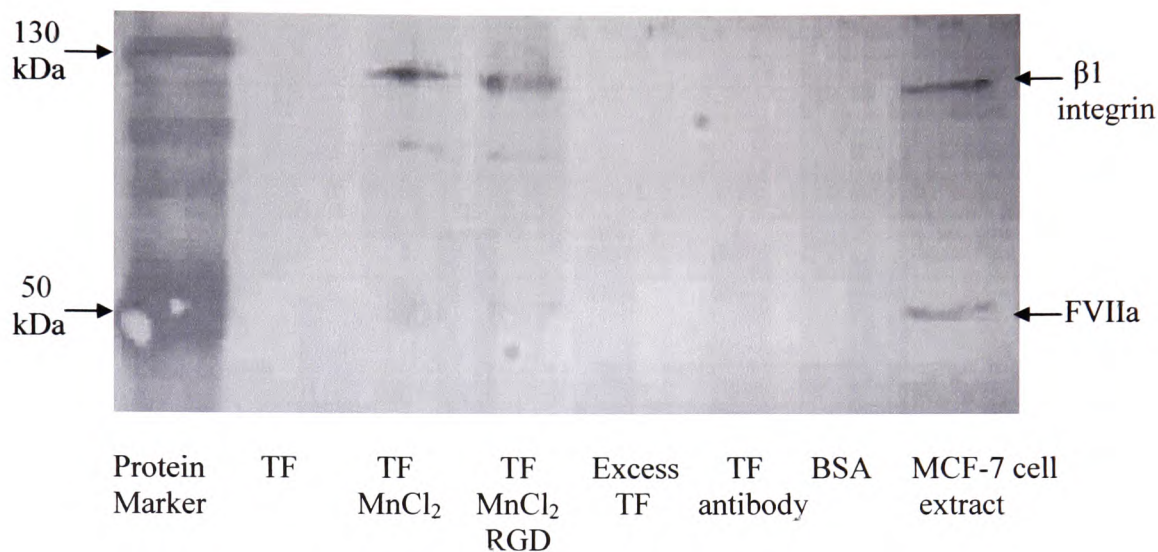
6.3.3.2. Analysis of TF binding to β 1 integrin by co-precipitation

The direct interaction between exogenous TF and β 1 integrin was further examined by co-precipitation of TF with proteins from MCF-7 cell extract. On probing of the samples pulled-down by TF with an anti- β 1 integrin antibody, a single band with a molecular mass of approximately 130 kDa, corresponding to β 1 integrin, was detected. This band was observable in the samples incubated in the presence of MnCl_2 (5 mM) as well as in the total cell extract sample (Fig 6.15). Furthermore, addition of the RGD peptide (400 μM) had no further influence on the binding of TF to β 1 integrin. Pre-incubation of the TF-conjugated agarose beads with a rabbit polyclonal anti-TF antibody (100 $\mu\text{g/ml}$), or a 10-fold excess of recombinant TF (5 μM) prevented the co-precipitation of β 1 integrin with TF. Furthermore, β 1 integrin was not present in the sample incubated with the BSA-conjugated agarose beads, discounting non-specific protein binding. Examination using an anti-human FVIIa antibody excluded the presence of FVIIa in all co-precipitated samples, but was present in the total cell extract.

6.3.3.3. Examination of the involvement of β 1 integrin and the MAPK pathway in TF mediated ER α expression

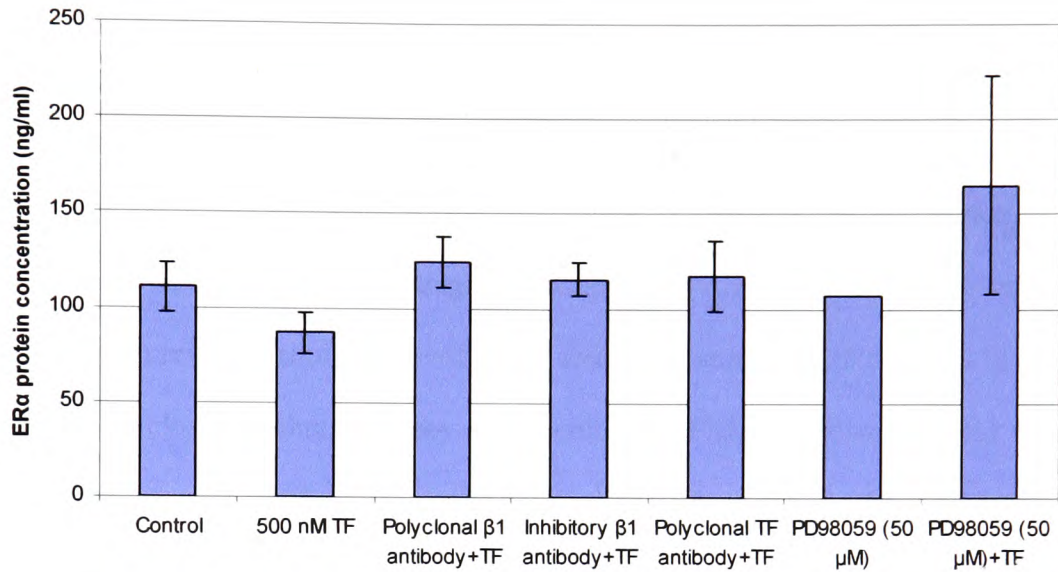
Incubation of MCF-7 cells with either a polyclonal antibody against the C-terminus of β 1 integrin or an inhibitory anti- β 1 integrin antibody in the presence of TF (500 nM) appeared to interfere with the TF-mediated downregulation of ER α protein expression observed with TF (500 nM) alone (Fig 6.16). Furthermore, a polyclonal antibody against TF prevented the downregulation of ER α protein expression by exogenous TF (500 nM). Inclusion of the MAPK inhibitor PD98059 (50 μM) seemed to have little influence on ER α expression (Fig 6.16). However, incubation of cells with the MAPK inhibitor PD98059 (50 μM) in the presence of TF (500 nM) appeared to interfere with the downregulation of ER α protein expression by TF.

Figure 6.15. Co-precipitation of TF and β 1 integrin



MCF-7 cells were lysed in cell lysis buffer and sonicated. The cell lysate was cleared by centrifugation and incubated with the TF and BSA-conjugated beads in the presence of MnCl₂ (5 mM), RGD peptide (400 μ M), 10-fold excess recombinant TF, or a rabbit polyclonal anti-TF antibody (100 μ g/ml) at 4°C overnight. The resins were then washed with lysis buffer and proteins denatured by heating at 99°C in 2 \times Laemmli's buffer. The proteins were separated by 10 % (w/v) SDS-PAGE and membranes were probed using a rabbit anti-human β 1 integrin antibody (0.4 μ g/ml) and a rabbit anti-human FVIIa antibody (1.4 μ g/ml) and images recorded using the GeneSnap program. Data are representative of three independent experiments.

Figure 6.16. The role of $\beta 1$ integrin and the MAPK pathway in TF-mediated downregulation of ER α expression

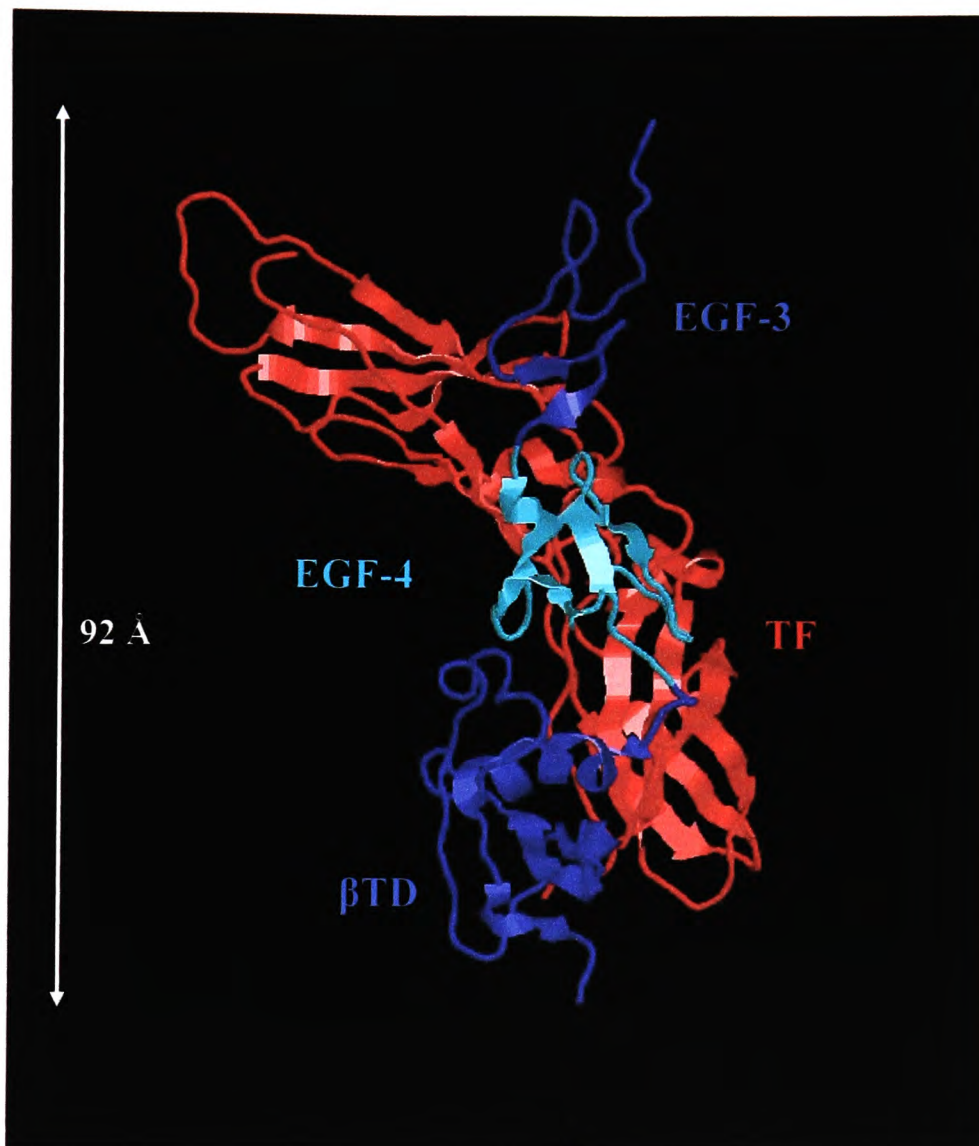


MCF-7 cells were seeded out into 12 well plates and adapted to medium containing 2 % (v/v) serum replacement medium. The cells were pre-incubated with a rabbit polyclonal anti- $\beta 1$ integrin antibody (5.3 μ g/ml), an inhibitory anti- $\beta 1$ integrin antibody (AIIB2) (50 μ g/ml) or a polyclonal anti-TF antibody (100 μ g/ml) and then treated with recombinant TF (500 nM) or the ERK1/2 MAPK inhibitor PD98059 (50 μ M). The cells were incubated at 37°C for 24 h, harvested and whole cell extracts prepared. 10 μ g of protein for each sample was placed into the wells of an ER α ELISA. Absorption values were converted to ER α protein concentrations using a standard curve prepared with recombinant ER α . Data are representative of two independent experiments \pm SD.

6.3.3.4. Examination of the structure of TF and β 1 integrin using Raswin and Alchemy programs

In the previous section it was shown that exogenous TF co-localised with cell surface β 1 integrin and a direct interaction between TF and β 1 integrin was observed, indicating that exogenous TF can bind to cell surface β 1 integrin. Furthermore, a polyclonal antibody directed against the C-terminus of β 1 integrin partially blocked the binding of exogenous TF to the cell surface, and therefore it is possible that this region of β 1 integrin may be capable of interacting with exogenous TF. Examination of the structure of β 1 integrin revealed similarities with FXa, since both contain EGF domains in the C-terminus in close proximity to the cell membrane. FXa is known to bind to the extracellular domain of TF via particular residues (Asp48, Glu51, Ser52, Asn57, Phe76, Asn80 and Glu82) within the EGF-1 domain of FXa (Fig 6.1) (Zhong et al 2002). Therefore, it is feasible that a similar EGF domain within β 1 integrin may be capable of interacting with exogenous TF. The amino acid sequences for the EGF-1 domain of FXa and the EGF-4 domain of β 1 integrin were aligned using the Align program (Pearson et al 1997), to reveal a 29 % sequence identity and a 56 % similarity between these domains of the two proteins. Next, the structure of the β 1 integrin molecule was visualised using the Raswin version 6 program (Fig 6.17). Since the crystal structure of β 1 integrin has not been determined, the crystal structure of β 3 integrin (Xiong et al 2001) was used as a template. For clarity, the sequence for β 3 integrin was edited to leave the C-terminus β TD, EGF-4 and EGF-3 domains. The edited structure for β 3 integrin was then uploaded into the Raswin program and placed next to the extracellular domain of TF (Harlos et al 1994) (Fig 6.17) to demonstrate that the size of the two molecules was compatible.

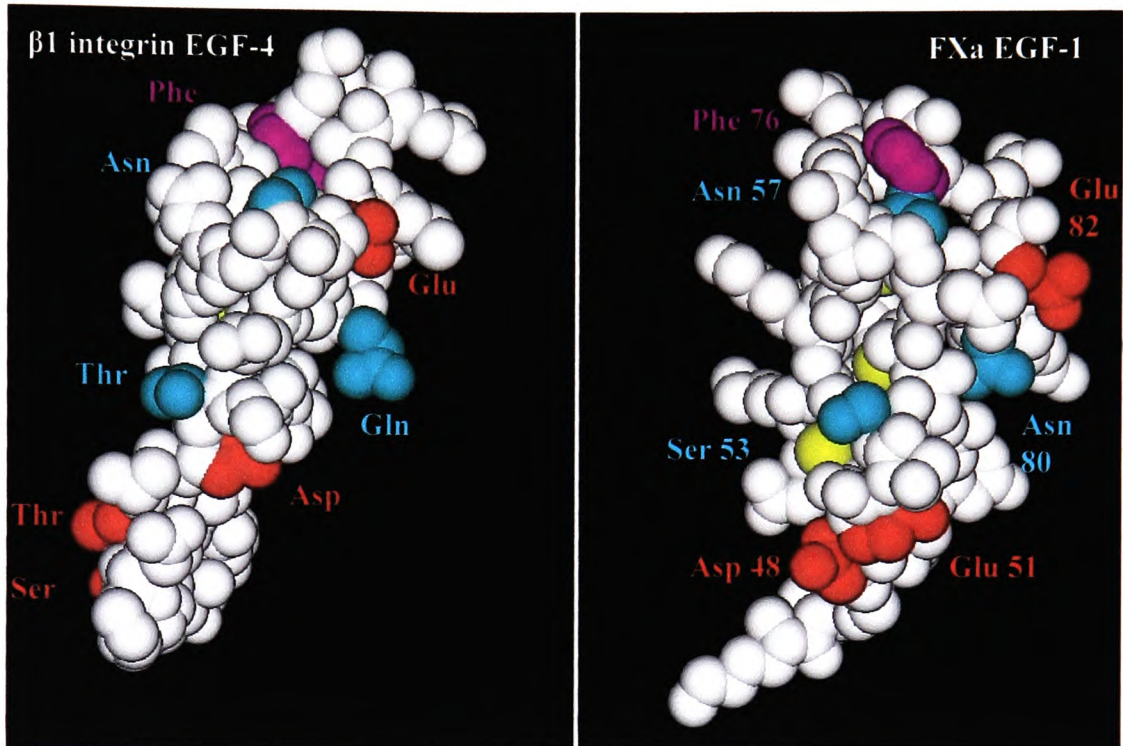
Figure 6.17. Arrangement of the extracellular domain of TF with the C-terminus of $\beta 3$ integrin



PDB files for the structures of $\beta 3$ integrin (blue) (Xiong et al 2001) and the extracellular domain of TF (red) (Harlos et al 1994) were downloaded from PubMed. The C-terminus of $\beta 3$ integrin was arranged next to the extracellular domain of TF in a similar place to where FXa binds and the size of the molecules measured using the Raswin version 6 program.

Next, the structural similarities between the EGF-1 domain of FXa and the EGF-4 domain of β 1 integrin were explored. Since the crystal structures of the FXa EGF-1 domain and β 1 integrin have not been determined, the structure of the EGF-1 domain of FVIIa (Banner et al 1996) and the EGF-4 domain of β 3 integrin (Xiong et al 2001) were used as templates. The structural files were uploaded into the Alchemy III program and the side chains of the amino acids in the EGF-4 domain of β 3 integrin that differed from those in the EGF-4 domain of β 1 integrin were replaced with those in β 1 integrin. Similarly, the amino acids in the EGF-1 domain of FVIIa were replaced with the respective residues found in the EGF-1 domain of FXa. The amino acids within the EGF-1 domain of FXa that are known to participate in the interaction with TF were highlighted. The structure of the EGF-4 domain of β 1 integrin was then superimposed and the equivalent residues highlighted (Fig 6.18). The amino acids are represented as red = negatively charged, blue = hydrophilic, purple = aromatic (the disulphide bridges were also highlighted in yellow). The space-fill diagrams (Fig 6.18) show that the EGF-4 domain of β 1 integrin and EGF-1 domain of FXa do not have identical structures. However, the amino acids within the EGF-1 domain of FXa that are involved in the interaction with TF are conserved between the two structures. Asn57, Phe76 and Glu82 are identical between the two while Glu51, Ser53 and Asn80 are conservative substitutions. Finally, the oxygen molecules present in the side chain of Asp48 in FXa are provided by Ser and Thr residues within β 1 integrin. Moreover, although the length of the loop sections within these EGF domains vary, the position of the interacting amino acids and the disulphide bridges are similar.

Figure 6.18. Comparison of the structures of $\beta 1$ integrin EGF-4 and FXa EGF-1



The PDB files for the EGF-4 domain of $\beta 3$ integrin (Xiong et al 2001) and the EGF-1 domain of FVIIa (Banner et al 1996) were opened in the Alchemy III program and amino acids changed to those in $\beta 1$ integrin EGF-4 and FXa EGF-1. Amino acids within the EGF-1 domain of FXa that interact with the extracellular domain of TF were highlighted as: blue = hydrophilic amino acids, red = negatively charged amino acids, purple = aromatic amino acids. The corresponding amino acids in the EGF-4 domain of $\beta 1$ integrin were similarly highlighted. (Yellow = the position of disulphide bridges).

6.4. Discussion

This part of the investigation initially examined the mechanisms by which exogenous TF induces changes in breast cancer cell proliferation and ER α expression. The activation of PARs by FVIIa and FXa downstream of TF in the coagulation cascade is one of the main mechanisms by which TF initiates cell signalling. Activation of PARs has been shown to result in the activation of cell signalling pathways and lead to changes in gene expression (Morris et al 2006, Liu & Mueller 2006). Initially, the involvement of PAR1 and PAR2 activation in TF-mediated proliferation was examined. Activation of PAR2 using an agonist peptide resulted in reduced rates of MCF-7 cell proliferation to a similar extent of exogenous TF (500 nM) with oestradiol (250 pM) (Fig 6.4). However, addition of oestradiol (250 pM) reversed this inhibition. This is in contrast to the observation with TF (500 nM) which suppressed breast cancer cell proliferation in the presence or absence of oestradiol (250 pM) and indicates that the ability of TF to inhibit proliferation may involve a second pathway in conjunction with PAR2 activation. In contrast, PAR1 activation was shown to have little influence on oestradiol-mediated cell proliferation.

ER α expression is known to be downregulated by the activation of the ERK1/2 MAPK pathway (Kronblad et al 2005, Oh et al 2001). Furthermore, activation of PARs has been shown to activate the ERK1/2 pathway (Riewald & Ruf 2001). In this study, the activation of PAR2 appeared to result in increases in the expression of ER α mRNA and protein (Fig 6.7 & 6.8) whereas inhibition of PAR2 suppressed ER α expression. This indicates that PAR2 activation may positively regulate ER α expression. In serum-free medium, exogenous TF (500 nM) alone downregulated ER α expression and the addition of FVIIa (5 nM) had no additional influence on mRNA expression (Fig 6.5 & 6.6). These results seem contradictory since FVIIa activates PAR2 (Camerer et al 2000b) and

activation of PAR2 using the agonist peptide resulted in the upregulation of ER α expression. A possible explanation for this observation is that the TF:FVIIa complex may activate separate pathways that interfere with signalling downstream of PAR2, preventing the upregulation of ER α . Furthermore, the incubation of MCF-7 cells with TF:FVIIa in the presence of FXa (10 nM) appeared to restore ER α mRNA expression back to control levels, and FXa alone resulted in increased expression above that of the untreated control. This is in agreement with the data showing that the PAR1 and PAR2 agonist peptides increased ER α expression, since FXa activates both PAR1 and PAR2 (Riewald et al 2001). Furthermore, the addition of exogenous TF (500 nM) alone, in the absence of any coagulation factors, resulted in decreases in ER α mRNA and protein expression which indicates that the influence of exogenous TF on ER α expression probably does not require coagulation factors and is not mediated through the activation of either PAR1 or PAR2.

Integrins are known to transduce signals across the cell membrane and induce cell signalling pathways including the MAPK and PI3K pathways (Schwartz 2001). Since the influence of exogenous TF on ER α expression did not appear to involve the activation of PARs by exogenous TF, and exogenous TF was shown to be capable of binding to β 1 integrin, the possibility that the interaction between exogenous TF and β 1 integrin induces the activation cell signalling pathways was explored. Pre-incubation of MCF-7 cells with an inhibitory anti- β 1 integrin antibody or a polyclonal antibody against the C-terminus of β 1 integrin seemed to prevent the downregulation of ER α protein expression by exogenous TF (Fig 6.16). This indicates that the binding of exogenous TF to β 1 integrin is capable of inducing cell signalling leading to the downregulation of ER α . Furthermore, incubation of cells with exogenous TF in the presence of the ERK1/2 inhibitor PD98059 appeared to prevent the downregulation of

ER α (Fig 6.16). This in turn suggests that exogenous TF may mediate the downregulation of ER α expression at least partly through the activation of the ERK1/2 pathway (Fig 6.16). Therefore, a possible mechanism could include the activation of the ERK1/2 pathway through β 1 integrin following the binding of TF. The activation of the ERK1/2 pathway by exogenous TF was not examined in this investigation, although is shown elsewhere (Ettelaie et al 2007), and therefore requires further clarification which may be carried out using reporter assays for the ERK1/2 signalling pathway.

In the next part of the investigation, the interaction of exogenous TF with the surface of breast cancer cells and the signalling mechanisms by which exogenous TF influences breast cancer cell proliferation and ER α expression were examined. The truncated form of TF incorporated into phospholipid vesicles and used throughout this investigation represented microparticle-derived TF such as that released from stromal cells in the vicinity of tumour cells. The interaction of exogenous TF with the cell surface was examined using fluorescein-labelled recombinant TF which was shown to bind to the surface of MCF-7 cells within 5 min and peaked at 15 min incubation (Fig 6.10). Furthermore, the TF was localised to particular points on the cell surface. The binding of exogenous TF to the surface of endothelial cells has been shown previously (Ettelaie et al 2007). Furthermore, localisation of endogenous TF specific sites on the surface of epithelial cells has been previously demonstrated (Muller et al 1999). The level of fluorescein-labelled TF binding to the cell surface diminished after 60 min incubation which may be as a result of internalisation of the TF by the cells.

The exogenous TF used in this investigation was reconstituted in phospholipid vesicles which may fuse with the cell membrane, incorporating TF into the cell membrane. However, since TF was localised to points on the cell surface, this indicates that the TF

was interacting with specific proteins rather than random incorporation into the cell membrane. Moreover, although studies have shown that TF can form homodimers (Roy et al 1991), the lack of TF expression by MCF-7 cells implies that this interaction can be excluded. Another putative target set of proteins that TF may bind to is the integrin family of adhesion receptors. Recently, a direct interaction between cell surface TF and the $\beta 1$ integrin was demonstrated (Versteeg et al 2008). Examination of β integrin expression on breast cancer cells revealed that both MCF-7 cells and T47D cells expressed $\beta 1$ integrin but not $\beta 3$ integrin (Fig 6.12). A partial co-localisation between exogenous TF and cell surface $\beta 1$ integrin was observed in MCF-7 cells (Fig 6.13). Since the integrin family consists of eight types of β integrins, it is possible that exogenous TF can also bind to other β integrins present on the surface of MCF-7 cells as well as $\beta 1$ integrin, although these were not examined here. Furthermore, a polyclonal antibody against the membrane proximal region of $\beta 1$ integrin appeared to partially block the binding of fluorescein-labelled TF to the cell surface (Fig 6.14), possibly by disrupting the binding of exogenous TF to $\beta 1$ integrin. This indicates that the binding of exogenous TF to the cell surface may depend on forming a complex with $\beta 1$ integrin. Therefore, the direct interaction between exogenous TF and $\beta 1$ integrin was examined next using agarose-conjugated TF to “pull-down” proteins from whole cell extract. The interaction of exogenous TF and $\beta 1$ integrin was dependent on the presence of Mn^{2+} but not FVIIa, or the integrin-activating peptide RGD (Fig 6.15). This requirement for Mn^{2+} may be due to the role of divalent cations in inducing conformational changes within integrin molecules (Humphries 1996) and suggests that exogenous TF may bind to integrins that are in the activated conformation. An interaction between cell surface TF and $\beta 1$ integrin has been recently reported (Versteeg et al 2008). However, the interaction between exogenous truncated TF and $\beta 1$ integrin

has not previously been shown and suggests a mechanism by which exogenous microparticle-derived TF may directly bind to tumour cells.

While TF has been shown to bind to $\beta 1$ integrin, the mechanism by which these proteins interact has not been previously examined. The polyclonal anti- $\beta 1$ integrin antibody that partially blocked the binding of exogenous TF to the cell surface was directed against the C-terminus of $\beta 1$ integrin, including the β TD and EGF-4 domain (Fig 6.2), indicating the participation of this region of $\beta 1$ integrin in binding to TF. Further examination of this region of $\beta 1$ integrin revealed similarities with the C-terminus of FXa, since both contain an EGF domain close to the cell membrane. Furthermore, in FXa, the EGF-1 domain is known to interact with the extracellular domain of TF (Fig 6.1). Alignment of the protein sequence of the EGF-1 domain of FXa with the EGF-4 domain of $\beta 1$ integrin revealed a 29 % sequence identity and a considerable similarity (56 %) between the sequences. Furthermore, alignment of the extracellular domain of TF with the C-terminus of $\beta 3$ integrin in a similar configuration as TF/FXa using the Raswin program showed that the scale of the molecules made this interaction feasible (Fig 6.17). The amino acids Asp48, Glu51, Ser52, Asn57, Phe76, Asn80 and Glu82 within the EGF-1 domain of FXa are known to participate in the interaction of FXa with the extracellular domain of TF (Zhong et al 2002). Comparison of the structures of the EGF-4 domain of $\beta 1$ integrin and EGF-1 domain of FXa revealed that these amino acids were conserved between the two molecules (Fig 6.18). This part of the investigation has identified a domain within $\beta 1$ integrin which may be a putative binding site for TF due to its structural and sequence similarities to the EGF-1 domain of FXa. However, further studies using mutagenesis and protein-protein interaction studies may confirm the role of this domain of $\beta 1$ integrin as a TF binding site.

In conclusion, exogenous TF was shown to be capable of interacting with the cell surface of MCF-7 cells by directly binding to cell surface $\beta 1$ integrin. Moreover, a putative binding site for this interaction was identified. Furthermore, it was demonstrated that TF-mediated cell proliferation involves the activation of PAR2 but not PAR1, and is likely to include other unknown pathways. Furthermore, TF-mediated downregulation of ER α did not require either PAR1 or PAR2 activation but did appear to require $\beta 1$ integrin and the activation of the ERK1/2 pathway.

CHAPTER 7

General Discussion

7. General discussion

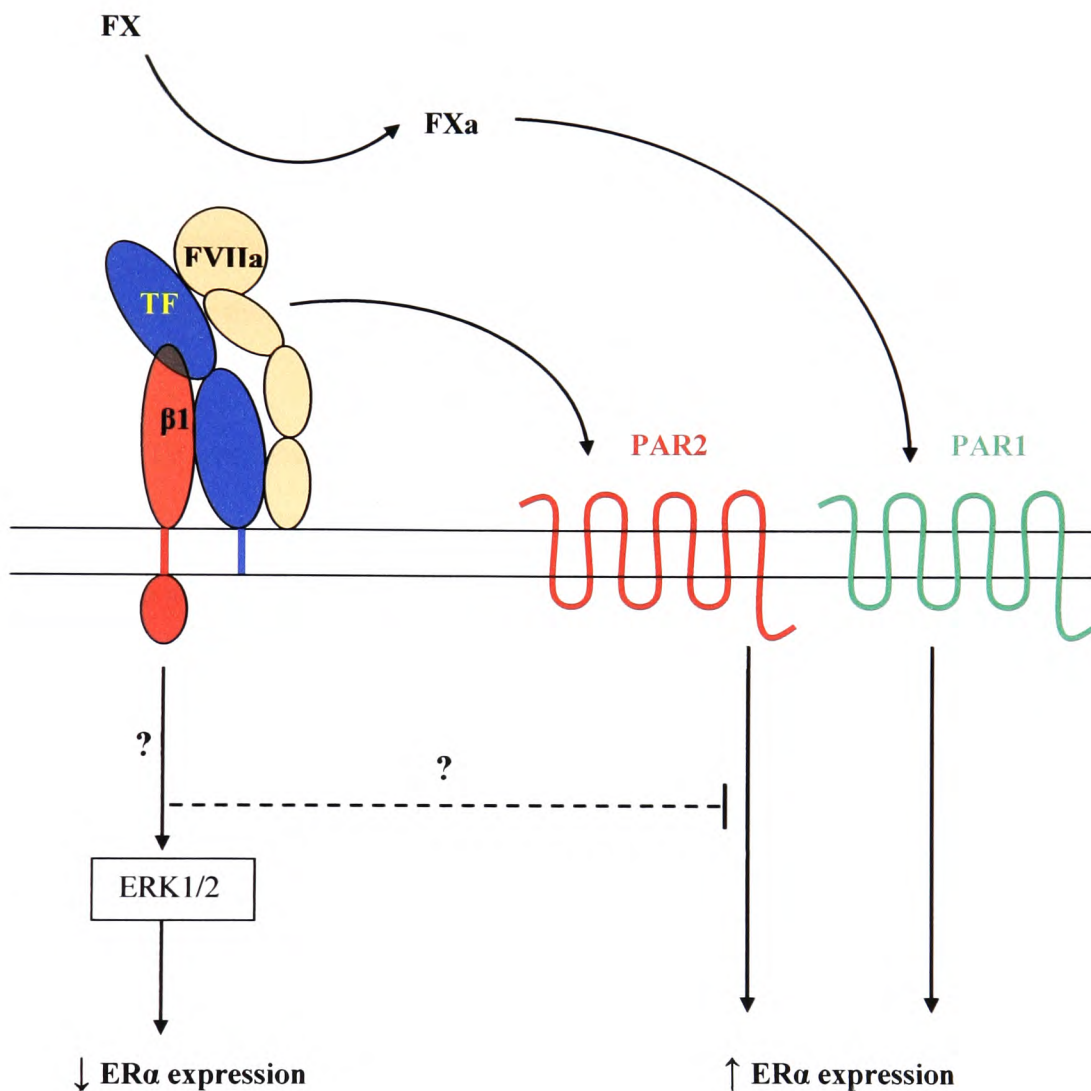
A number of studies have reported increased expression of TF in aggressive/invasive breast tumours (Kato et al 2005, Hu et al 1994). Furthermore, increased expression of TF by stromal cells such as macrophages and fibroblasts within breast tumours has been associated with the progression to invasive breast cancers (Lwaleed et al 1999, Vrana et al 1996). Conversely, the expression of ER α in breast cancer cells is associated with well differentiated, less invasive tumours which respond to oestradiol and anti-hormone therapies. As well as controlling breast cancer cell proliferation (Prall et al 1998), ER α has an anti-invasive role (Rocheffort et al 1998, Garcia et al 1992) and the loss of ER α expression often results in the progression of breast tumours to invasive forms (Thompson et al 1992). Factors involved in regulating ER α expression and activity are therefore crucial in understanding the mechanisms involved in breast cancer progression to invasive forms. Inflammation at the site of breast tumours is associated with more invasive tumours with a poor prognosis (Blot et al 2003). TF is a proinflammatory protein that can be released from cells in microparticles and transferred to different cell types. Therefore, can exogenous TF, such as that released from stromal cells in an inflammatory response within the tumour, influence breast cancer cells through altering ER α function?

Initially, the influence of exogenous TF on the expression of ER α in breast cancer cell lines was investigated. Exogenous TF (50 and 500 nM) resulted in the downregulation of ER α mRNA and protein expression over 24 h. Furthermore, the long-term treatment of cells with exogenous TF resulted in a progressive decrease in ER α expression. Exogenous TF also appeared to suppress oestradiol-mediated cell proliferation and reverse the anti-inhibitory influence of oestradiol on cell invasion. In the second part of the study, the

influence of exogenous TF on ER α activity through the ERE pathway was examined. TF alone was shown to have no measurable influence on ER α activity. However, in the presence of oestradiol (250 pM), exogenous TF reduced ER α activity below that of oestradiol alone. TF also appeared to reduce the DNA binding activity of ER α , but this seemed to be independent of changes in the phosphorylation state of serine 118 within ER α . Next, the influence of exogenous TF on ER α activity through the AP-1-dependent pathway was examined. TF alone reduced the transcriptional activity of AP-1 and a high concentration of TF (500 nM) appeared to reduce the DNA binding activity of c-Jun. However, the transcriptional activity of AP-1 did not seem to be altered by the addition of oestradiol (250 pM). Finally, the mechanisms by which exogenous TF interacts with the cell surface and induces changes in breast cancer cell proliferation and ER α expression were examined. Exogenous TF was shown to bind to the surface of MCF-7 cells and directly interact with cell surface β 1 integrin. TF inhibition of oestradiol-induced cell proliferation partly involved the activation of PAR2. Moreover, the downregulation of ER α by exogenous TF seemed to require the interaction with β 1 integrin and activation of the ERK1/2 pathway, but was independent of PAR1 and PAR2 activation. In order to ensure that the influence of exogenous TF on breast cancer cells observed in this study were not limited to one cell line and hence an anomaly, four breast cancer cell lines were selected, of which MCF-7 and T47D cells were found to be suitable since these cells expressed ER α but lacked significant amounts of TF. However, it is necessary to be cautious when interpreting results from cell lines *in vitro* into relevance for breast cancers *in vivo*, and this could be clarified by further investigations using breast tumour samples to determine if the expression of TF on tumour cells themselves and/or TF released by stromal cells, correlates with ER α expression *in vivo*.

This study demonstrated that the incubation of breast cancer cell lines with exogenous TF (50 and 500 nM) results in the downregulation of ER α expression. Since the recombinant TF lacks a cytoplasmic domain, cell signalling through the cytoplasmic domain of TF can be excluded. The activation of PARs by the coagulation factors FVIIa and FXa downstream of TF in the coagulation cascade has been shown to result in changes in gene expression (Morris et al 2006, Hjortoe et al 2004). The source of these coagulation factors in tumours is likely to be from poorly formed blood vessels within the tumour, which allow plasma proteins to escape into the tumour stroma (Knowles & Selby 2005). However, the involvement of PARs in the downregulation of ER α by exogenous TF can be excluded since the activation of PAR1 and 2 resulted in increases in ER α mRNA and protein expression and inhibition of these receptors suppressed ER α expression. Therefore, the activation of PAR1 and PAR2 may positively regulate ER α expression and is probably not responsible for the downregulation of ER α expression by exogenous TF (Fig 7.1). Tumours have been described as wounds that do not heal, since similar processes found in wound healing such as cell migration and proliferation and angiogenesis occur, but in tumours these processes continue and promote tumour growth (Dvorak 1986). During normal physiological wound healing responses, the coagulation cascade is activated and TF is exposed to the bloodstream, resulting in the activation of FVIIa and FXa and subsequent activation of PAR1 and PAR2. Since PAR1 and PAR2 activation resulted in increases in the expression of ER α , this may be a mechanism to promote healing by increasing cell proliferation of breast epithelial cells. Furthermore, although the addition of FVIIa had little additional influence on ER α mRNA expression in the presence of exogenous TF, inclusion of FXa restored ER α expression, indicating that alternative signalling pathways induced by TF may be capable of blocking PAR2 signalling initiated by FVIIa, but not PAR1 signalling by FXa (Fig 7.1). A trend was observed in which the short-term exposure of cells

Figure 7.1. Schematic representation of a proposed mechanism for the control of ER α expression by exogenous TF



It is proposed that the activation of PAR1 and 2 by FXa downstream of TF results in increased expression of ER α . However, exogenous alone TF leads to the downregulation of ER α mRNA expression. The suggested hypothesis is that TF binding to $\beta 1$ integrin results in the activation cell signalling pathways such as the ERK1/2 pathway which counteract the PAR2 activated signalling pathways, and downregulate ER α expression.

to exogenous TF downregulated the expression of ER α over 24 h and then normalised by 72 h. However, long-term treatment of breast cancer cells with exogenous TF appeared to result in a progressive decrease in ER α expression over five weeks. In tumours, long-term exposure of breast cancer cells to exogenous TF released from stromal cells in an inflammatory response, and in the absence of coagulation factors and PAR activation, may result in reduced ER α expression and loss of response to oestradiol. This suggests that chronic inflammation during breast cancer may alter the level of ER α expression in tumour cells by exposing the cells to high levels of TF over a long period of time.

Exogenous TF was shown to interact with the surface of MCF-7 cells and co-localised with cell surface β 1 integrin. Furthermore, a direct interaction between exogenous TF and β 1 integrin was shown and a putative binding site within β 1 integrin that may be involved in binding to TF was identified, although this needs further investigation using mutagenesis and protein-protein interaction studies. The downregulation of ER α by exogenous TF also appeared to require the activation of the ERK1/2 pathway. The activation of integrins is known to initiate cell signalling pathways such as the ERK1/2 and PI3K pathways (Schwartz 2001). Furthermore, activation of the ERK1/2 pathway in breast cancer cells has been shown to result in the downregulation of ER α expression (Creighton et al 2006). It is possible that the binding of exogenous TF to cell surface β 1 integrin results in the activation of ERK1/2 pathway through the integrin molecule and results in the downregulation of ER α expression (Fig 7.1). Further studies are required to identify cell signalling pathways activated as a result of the binding of exogenous TF to β 1 integrin using reporter assays.

A trend was observed in which exogenous TF appeared to suppress oestradiol-mediated increases in breast cancer cell proliferation. Importantly, incubation of MCF-7 cells with the lipids extracted from the Innovin reagent had no measurable influence on cell proliferation, indicating that the influence of the Innovin reagent on cell proliferation was due to the TF apoprotein and not the lipid component. Oestradiol-ER α signalling results in the expression of genes involved in cell proliferation and promotes cells to enter the cell cycle (Prall et al 1998). Since exogenous TF downregulated both ER α expression and ER α activity through the ERE pathway, this may at least partly explain the observed suppression of oestradiol-controlled proliferation by TF. Furthermore, PAR2 activation resulted in similar reductions in rates of cell proliferation. These observed decreases in rates of cell proliferation in response to exogenous TF may therefore involve the activation of PAR2 by FVIIa or FXa downstream of TF in the coagulation cascade. However, PAR2-mediated suppression of cell proliferation appeared to be reversed by the addition of oestradiol (250 pM), while PAR2 activation increased ER α expression. This indicates the participation of other pathways, in addition to PAR2 signalling, in the suppression of oestradiol-mediated cell proliferation by exogenous TF. Alternatively, it is possible that TF induces the apoptosis of breast cancer cells in the presence of oestradiol by inhibiting the progression of cells through the cell cycle, although this requires further investigations employing apoptosis assays.

Oestradiol-ER α signalling inhibits breast cancer cell invasiveness by controlling the expression of genes involved in cell invasion (Nilsson et al 2007, Rochefort et al 2001). In this investigation, exogenous TF (50 and 500 nM) reversed the inhibitory influence of oestradiol (250 pM) on cell invasion. Moreover, since exogenous TF was capable of downregulating ER α expression and activity, this may account for the increased cell

invasiveness of breast cancer cells in the presence of TF. The hypothesis that exogenous TF may suppress oestradiol-induced proliferation and invasion by downregulating ER α expression and/or activity was investigated by attempting to overexpress the wild-type or a constitutively active form of ER α in breast cancer cells to overcome the influence of TF. However, the cloning of ER α was not completed within the permitted time and therefore further work to investigate this mechanism is required.

The ability of cancer cells to invade across the basement membrane is an important step in metastasis since it allows cancer cells to escape into the bloodstream where they can be transported to other organs and form secondary tumours. In this investigation, TF alone increased the invasiveness of breast cancer cells and appeared to induce the formation of lamellipodia and microspikes structures required for cell migration. The formation of the TF:FVIIa complex is known to be capable of inducing changes in cell morphology through the activation of the PI3K pathway and reorganisation of the cytoskeleton (Versteeg et al 2000). Moreover, the activation of PARs can lead to the activation of these cell signalling pathways and promote cell migration (Jiang et al 2004). In addition, cross-talk between TF and the α 3 β 1 integrin complex has been shown to induce cell migration (Dorfleutner et al 2004). In this study exogenous TF was shown to directly bind to β 1 integrin. Therefore, it is conceivable that exogenous TF may induce changes in cell morphology and increase cell invasion by a mechanism mediated either through the activation of PARs or the interaction with β 1 integrin. Further investigation to confirm the role of these mechanisms would include the use of inhibitory antibodies for PARs and β 1 integrin in Boyden chamber-based invasion assays.

In addition to the classical ERE pathway of ER α transcriptional activity, oestradiol-ER α signalling has been shown to increase the transcriptional activity of AP-1 (Philips et al 1993). However, in this investigation oestradiol (250 pM) had no influence on the transcriptional activity of AP-1. In contrast, exogenous TF alone was shown to be capable of downregulating the transcriptional activity of AP-1 in breast cancer cells. Furthermore, a low concentration of TF (50 nM) seemed to increase the DNA binding activity of c-Jun whereas a high concentration of TF (500 nM) appeared to reduce the DNA binding activity of c-Jun. AP-1 controls many cellular functions including proliferation, differentiation and invasion (Ludes-Meyers et al 2001, Bamberger et al 1999), and TF may influence cellular processes through changes in AP-1. Furthermore, since TF seemed to reduce the DNA binding activity of c-Jun, it is possible that TF may indirectly suppress ER α activity through the AP-1 pathway (Fig 5.14). Further investigations of this process may be carried out using an immuno-precipitation procedure to examine the influence of exogenous TF on the binding of ER α to c-Jun.

Sporadic forms of breast cancer account for the major proportion of the incidence of this disease. In addition to genetic mutations, environmental factors within the breast tissue constitute a principle risk factor in the formation of breast cancer, and can also promote progression to an invasive phenotype. Such environmental factors include those released during inflammatory responses towards the tumour and include the expression and release of factors such as TF. In conclusion, continuous long-term exposure of breast cancer cells to high levels of exogenous TF such as that released from infiltrating macrophages and fibroblasts within tumours in an inflammatory response, may directly interact with breast cancer cells through binding to β 1 integrin, leading to the downregulation of ER α expression and activity, and resulting in breast cancer cells that are unable to respond to

oestradiol. This may in turn result in the suppression of oestradiol-mediated cell proliferation and increased cell invasiveness, contributing to the progression of breast cancers to an ER α -negative, oestradiol-independent and invasive phenotype.

References

Abe K, Shoji M, Chen J, Bierhaus A, Danave I, Micko C, Casper K, Dillehay DL, Nawroth PP, Rickles FR. (1999) Regulation of vascular endothelial growth factor production and angiogenesis by the cytoplasmic tail of tissue factor. *Proc Natl Acad Sci U S A.* **96**, 8663-8668.

Adler V, Franklin CC, Kraft AS. (1992) Phorbol esters stimulate the phosphorylation of c-Jun but not v-Jun: regulation by the N-terminal delta domain. *Proc Natl Acad Sci U S A.* **89**, 5341-5345.

Ahamed J, Niessen F, Kurokawa T, Lee YK, Bhattacharjee G, Morrissey JH, Ruf W. (2007) Regulation of macrophage procoagulant responses by the tissue factor cytoplasmic domain in endotoxemia. *Blood.* **109**, 5251-5259.

Ahamed J, Ruf W. (2004) Protease-activated receptor 2-dependent phosphorylation of the tissue factor cytoplasmic domain. *J Biol Chem.* **279**, 23038-23044.

Albanito L, Madeo A, Lappano R, Vivacqua A, Rago V, Carpino A, Oprea TI, Prossnitz ER, Musti AM, Andò S, Maggiolini M. (2007) G protein-coupled receptor 30 (GPR30) mediates gene expression changes and growth response to 17beta-estradiol and selective GPR30 ligand G-1 in ovarian cancer cells. *Cancer Res.* **67**, 1859-1866.

Ali S, Metzger D, Bornert JM, Chambon P. (1993) Modulation of transcriptional activation by ligand-dependent phosphorylation of the human oestrogen receptor A/B region. *EMBO J.* **12**, 1153-1160.

Anderson E, Clarke RB, Howell A. (1998) Estrogen responsiveness and control of normal human breast proliferation. *J Mammary Gland Biol Neoplasia.* **3**, 23-35.

Bach RR. (2006) Tissue factor encryption. *Arterioscler Thromb Vasc Biol.* **26**, 456-461.

Balfe PJ, McCann AH, Welch HM, Kerin MJ. (2004) Estrogen receptor beta and breast cancer. *Eur J Surg Oncol.* **30**, 1043-1050.

Bamberger AM, Methner C, Lisboa BW, Städtler C, Schulte HM, Löning T, Milde-Langosch K. (1999) Expression pattern of the AP-1 family in breast cancer: association of fosB expression with a well-differentiated, receptor-positive tumor phenotype. *Int J Cancer.* **84**, 533-538.

Banner DW, D'Arcy A, Chène C, Winkler FK, Guha A, Konigsberg WH, Nemerson Y, Kirchhofer D. (1996) The crystal structure of the complex of blood coagulation factor VIIa with soluble tissue factor. *Nature.* **380**, 41-46.

Bazan JF. (1990) Structural design and molecular evolution of a cytokine receptor superfamily. *Proc Natl Acad Sci U S A.* **87**, 6934-6938.

Beatson GT. (1896) On the treatment of inoperable cases of carcinogen of the mamma: suggestions for a new method of treatment with illustrative cases. *Lancet.* **2**, 104-107.

Behl C. (2001) Estrogen - Mystery drug for the brain? : The neuroprotective activities of the female sex hormone. 1st edition. Springer Wein, New York.

Belguise K, Kersual N, Galtier F, Chalbos D. (2005) FRA-1 expression level regulates proliferation and invasiveness of breast cancer cells. *Oncogene.* **24**, 1434-1444.

Ben-Baruch A. (2003) Host microenvironment in breast cancer development: inflammatory cells, cytokines and chemokines in breast cancer progression: reciprocal tumor-microenvironment interactions. *Breast Cancer Res.* **5**, 31-36.

Berry M, Nunez AM, Chambon P. (1989) Estrogen-responsive element of the human pS2 gene is an imperfectly palindromic sequence. *Proc Natl Acad Sci U S A.* **86**, 1218-1222.

Berthois Y, Katzenellenbogen JA, Katzenellenbogen BS. (1986) Phenol red in tissue culture media is a weak estrogen: implications concerning the study of estrogen-responsive cells in culture. *Proc Natl Acad Sci U S A.* **83**, 2496-2500.

Blot E, Chen W, Vasse M, Paysant J, Denoyelle C, Pille J-C, Vincent L, Vannier J-P, Soria J, Soria C. (2003) Cooperation between monocytes and breast cancer cells promotes factors involved in cancer aggressiveness. *British J Cancer.* **88**, 1207-1212.

Bogdanov VY, Balasubramanian V, Hathcock J, Vele O, Lieb M, Nemerson Y. (2003) Alternatively spliced human tissue factor: a circulating, soluble, thrombogenic protein. *Nat Med.* **9**, 458-462.

Brakebusch C, Fässler R. (2005) beta 1 integrin function in vivo: adhesion, migration and more. *Cancer Metastasis Rev.* **24**, 403-411.

Breast cancer.org. Pictures of types of breast cancer. (2007) www.breastcancer.org. [Accessed 15 August 2007].

Bromberg ME, Bailly MA, Konigsberg WH. (2001) Role of protease-activated receptor I in tumor metastasis promoted by tissue factor. *Thromb Haemost.* **86**, 1210-1214.

Bromberg ME, Konigsberg WH, Madison JF, Pawashe A, Garen A. (1995) Tissue factor promotes melanoma metastasis by a pathway independent of blood coagulation. *Proc Natl Acad Sci U S A.* **92**, 8205-8209.

Brown EJ. (2002) Integrin-associated proteins. *Curr Opin Cell Biol.* **14**, 603-607.

Broze GJ. (1995) Tissue factor pathway inhibitor. *Thromb Haemost.* **74**, 90-93.

Broze GJ, Majerus PW. (1980) Purification and properties of human coagulation factor VII. *J Biol Chem.* **255**, 1242-1247.

Callander NS, Varki N, Rao LV. (1992) Immunohistochemical identification of tissue factor in solid tumors. *Cancer*. **70**, 1194-1201.

Camerer E, Gjernes E, Wiiger M, Pringle S, Prydz H. (2000a) Binding of factor VIIa to tissue factor on keratinocytes induces gene expression. *J Biol Chem*. **275**, 6580-6585.

Camerer E, Huang W, Coughlin SR. (2000b) Tissue factor- and factor X-dependent activation of protease-activated receptor 2 by factor VIIa. *Proc Natl Acad Sci U S A*. **97**, 5255-5260

Camerer E, Rottingen JA, Gjernes E, Larsen K, Skartlien AH, Iversen JG, Prydz H. (1999) Coagulation factors VIIa and Xa induce cell signaling leading to up-regulation of the *egr-1* gene. *J Biol Chem*. **274**, 32225-32233.

Camerer E, Rottingen JA, Iversen JG, Prydz H. (1996) Coagulation factors VII and X induce Ca²⁺ oscillations in Madin-Darby canine kidney cells only when proteolytically active. *J Biol Chem*. **271**, 29034-29042.

Campbell RA, Bhat-Nakshatri P, Patel NM, Constantinidou D, Ali S, Nakshatri H. (2001) Phosphatidylinositol 3-kinase/AKT-mediated activation of estrogen receptor alpha: a new model for anti-estrogen resistance. *J Biol Chem*. **276**, 9817-9824.

Carmeliet P, Mackman N, Moons L, Luther T, Gressens P, Van Vlaenderen I, Demunck H, Kasper M, Breier G, Evrard P, Müller M, Risau W, Edgington T, Collen D. (1996) Role of tissue factor in embryonic blood vessel development. *Nature*. **383**, 73-75.

Cassidy J, Bissett D, Spence RAJ. (2004) Oxford Handbook of Oncology. 1st edition. Oxford University Press, Oxford.

Censarek P, Bobbe A, Grandoch M, Schrör K, Weber AA. (2007) Alternatively spliced human tissue factor (asHTF) is not pro-coagulant. *Thromb Haemost*. **97**, 11-14.

Chabbert-Buffet N, Djakoure C, Maitre SC, Bouchard P. (1998) Regulation of the human menstrual cycle. *Front Neuroendocrinol.* **19**, 151-186.

Chen D, Washbrook E, Sarwar N, Bates GJ, Pace PE, Thirunuvakkarasu V, Taylor J, Epstein RJ, Fuller-Pace FV, Egly JM, Coombes RC, Ali S. (2002) Phosphorylation of human estrogen receptor alpha at serine 118 by two distinct signal transduction pathways revealed by phosphorylation-specific antisera. *Oncogene.* **21**, 4921-4931.

Chen D, Riedl T, Washbrook E, Pace PE, Coombes RC, Egly JM, Ali S. (2000) Activation of estrogen receptor alpha by S118 phosphorylation involves a ligand-dependent interaction with TFIID and participation of CDK7. *Mol Cell.* **6**, 127-137.

Chen D, Pace PE, Coombes RC, Ali S. (1999) Phosphorylation of human estrogen receptor alpha by protein kinase A regulates dimerization. *Mol Cell Biol.* **19**, 1002-1015.

Chen J, Kasper M, Heck T, Nakagawa K, Humpert PM, Bai L, Wu G, Zhang Y, Luther T, Andrassy M, Schiekofer S, Hamann A, Morcos M, Chen B, Stern DM, Nawroth PP, Bierhaus A. (2005) Tissue factor as a link between wounding and tissue repair. *Diabetes.* **54**, 2143-2154.

Chen TK, Smith LM, Gebhardt DK, Birrer MJ, Brown PH. (1996) Activation and inhibition of the AP-1 complex in human breast cancer cells. *Mol Carcinog.* **15**, 215-226.

Clarke RB, Howell A, Potten CS, Anderson E. (1997) Dissociation between steroid receptor expression and cell proliferation in the human breast. *Cancer Res.* **57**, 4987-4991.

Contrino J, Hair G, Kreutzer DL, Rickles FR. (1996) In situ detection of tissue factor in vascular endothelial cells: correlation with the malignant phenotype of human breast disease. *Nat Med.* **2**, 209-215.

Creighton CJ, Hilger AM, Murthy S, Rae JM, Chinnaiyan AM, El-Ashry D. (2006) Activation of mitogen-activated protein kinase in estrogen receptor alpha-positive breast cancer cells in vitro induces an in vivo molecular phenotype of estrogen receptor alpha-negative human breast tumors. *Cancer Res.* **66**, 3903-3911.

Crowe DL, Brown TN. (1999) Transcriptional inhibition of matrix metalloproteinase 9 (MMP-9) activity by a c-fos/estrogen receptor fusion protein is mediated by the proximal AP-1 site of the MMP-9 promoter and correlates with reduced tumor cell invasion. *Neoplasia.* **1**, 368-372.

Cunningham MA, Romas P, Hutchinson P, Holdsworth SR, Tipping PG. (1999) Tissue factor and factor VIIa receptor/ligand interactions induce proinflammatory effects in macrophages. *Blood.* **94**, 3413-3420.

Deroo BJ, Korach KS. (2006) Estrogen receptors and human disease. *J Clin Invest.* **116**, 561-570.

Desombre ER. (1984) Steroid receptors in breast cancer. *Monogr Pathol.* **25**, 149-174.

Dorfleutner A, Hintermann E, Tarui T, Takada Y, Ruf W. (2004) Cross-talk of integrin alpha3beta1 and tissue factor in cell migration. *Mol Biol Cell.* **15**, 4416-4425.

Drake TA, Morrissey JH, Edgington TS. (1989) Selective cellular expression of tissue factor in human tissues. Implications for disorders of hemostasis and thrombosis. *Am J Pathol.* **134**, 1087-1097.

Dubik D, Shiu RP. (1992) Mechanism of estrogen activation of c-myc oncogene expression. *Oncogene.* **7**, 1587-1594.

Dunn C, Wiltshire C, MacLaren A, Gillespie DA. (2002) Molecular mechanism and biological functions of c-Jun N-terminal kinase signalling via the c-Jun transcription factor. *Cell Signal.* **14**, 585-593.

Dutertre M, Smith CL. (2003) Ligand-independent interactions of p160/steroid receptor coactivators and CREB-binding protein (CBP) with estrogen receptor-alpha: regulation by phosphorylation sites in the A/B region depends on other receptor domains. *Mol Endocrinol.* **17**, 1296-1314.

Dvorak HF. (1986) Tumors: wounds that do not heal. Similarities between tumor stroma generation and wound healing. *N Engl J Med.* **315**, 1650-1659.

El-Ashry D, Chrysogelos SA, Lippman ME, Kern FG. (1996) Estrogen induction of TGF-alpha is mediated by an estrogen response element composed of two imperfect palindromes. *J Steroid Biochem Mol Biol.* **59**, 261-269.

Ettelaie C, Li C, Collier ME, Pradier A, Frentzou GA, Wood CG, Chetter IC, McCollum PT, Bruckdorfer KR, James NJ. (2007) Differential functions of tissue factor in the trans-activation of cellular signalling pathways. *Atherosclerosis.* **194**, 88-101.

Ferro P, Forlani A, Muselli M, Pfeffer U. (2003) Alternative splicing of the human estrogen receptor alpha primary transcript: mechanisms of exon skipping. *Int J Mol Med.* **12**, 355-363.

Flössel C, Luther T, Albrecht S, Kotsch M, Müller M. (1992) Constitutive tissue factor expression of human breast cancer cell line MCF-7 is modulated by growth factors. *Eur J Cancer.* **28**, 1999-2002.

Foster JS, Henley DC, Bukovsky A, Seth P, Wimalasena J. (2001) Multifaceted regulation of cell cycle progression by estrogen: regulation of Cdk inhibitors and Cdc25A independent of cyclin D1-Cdk4 function. *Mol Cell Biol.* **21**, 794-810.

Futreal PA, Liu Q, Shattuck-Eidens D, Cochran C, Harshman K, Tavtigian S, Bennett LM, Haugen-Strano A, Swensen J, Miki Y. (1994) BRCA1 mutations in primary breast and ovarian carcinomas. *Science.* **266**, 120-122.

Garcia M, Derocq D, Freiss G, Rochefort H. (1992) Activation of estrogen receptor transfected into a receptor-negative breast cancer cell line decreases the metastatic and invasive potential of the cells. *Proc Natl Acad Sci U S A.* **89**, 11538-11542.

Garrett RH, Grisham CM. (2005) *Biochemistry*. 3rd edition. Thomson Learning Inc, Belmont.

Germain P, Harbrioux G. (1993) Modulation of the estradiol-17 beta mitogenic effect on human breast cancer MCF-7 cells by serum albumin in defined medium. *Anticancer Res.* **13**, 1581-1585.

Godolphin W, Elwood JM, Spinelli JJ. (1981) Estrogen receptor quantitation and staging as complementary prognostic indicators in breast cancer: a study of 583 patients. *Int J Cancer.* **28**, 677-683.

Green S, Walter P, Kumar V, Krust A, Bornert JM, Argos P, Chambon P. (1986) Human oestrogen receptor cDNA: sequence, expression and homology to v-erb-A. *Nature.* **320**, 134-139.

Grignani G, Maiolo A. (2000) Cytokines and hemostasis. *Haematologica.* **85**, 967-972.

Gross JM, Yee D. (2002) How does the estrogen receptor work? *Breast Cancer Res.* **4**, 62-64.

Gruber CJ, Gruber DM, Gruber IM, Wieser F, Huber JC. (2004) Anatomy of the estrogen response element. *Trends Endocrinol Metab.* **15**, 73-78.

Gustafsson JA. (1999) Estrogen receptor beta - a new dimension in estrogen mechanism of action. *J Endocrinol.* **163**, 379-383.

Harlos K, Martin DM, O'Brien DP, Jones EY, Stuart DI, Polikarpov I, Miller A, Tuddenham EG, Boys CW. (1994) Crystal structure of the extracellular region of human tissue factor. *Nature.* **370**, 662-666.

- Higashimoto K, Kuhn P, Desai D, Cheng X, Xu W. (2007) Phosphorylation-mediated inactivation of coactivator-associated arginine methyltransferase 1. *Proc Natl Acad Sci U S A.* **104**, 12318-12323.
- Hjortoe GM, Petersen LC, Albrechtsen T, Sorensen BB, Norby PL, Mandal SK, Pendurthi UR, Rao LV. (2004) Tissue factor-factor VIIa-specific up-regulation of IL-8 expression in MDA-MB-231 cells is mediated by PAR-2 and results in increased cell migration. *Blood.* **103**, 3029-3037.
- Holloway JN, Murthy S, El-Ashry D. (2004) A cytoplasmic substrate of mitogen-activated protein kinase is responsible for estrogen receptor-alpha down-regulation in breast cancer cells: the role of nuclear factor-kappaB. *Mol Endocrinol.* **18**, 1396-1410.
- Hu T, Bach RR, Horton R, Konigsberg WH, Todd MB. (1994) Procoagulant activity in cancer cells is dependent on tissue factor expression. *Oncol Res.* **6**, 321-327.
- Huang Y, Keen JC, Pledge A, Marton LJ, Zhu T, Sukumar S, Park BH, Blair B, Brenner K, Casero RA Jr, Davidson NE. (2006) Polyamine analogues down-regulate estrogen receptor alpha expression in human breast cancer cells. *J Biol Chem.* **281**, 19055-19063.
- Humphries MJ. (1996) Integrin activation: the link between ligand binding and signal transduction. *Curr Opin Cell Biol.* **8**, 632-640.
- Ito S, Takeyama K, Yamamoto A, Sawatsubashi S, Shirode Y, Kouzmenko A, Tabata T, Kato S. (2004) In vivo potentiation of human oestrogen receptor alpha by Cdk7-mediated phosphorylation. *Genes Cells.* **9**, 983-992.
- Jakacka M, Ito M, Weiss J, Chien PY, Gehm BD, Jameson JL. (2001) Estrogen receptor binding to DNA is not required for its activity through the nonclassical AP1 pathway. *J Biol Chem.* **276**, 13615-13621.

Janowska-Wieczorek A, Marquez-Curtis LA, Wysoczynski M, Ratajczak MZ. (2006) Enhancing effect of platelet-derived microvesicles on the invasive potential of breast cancer cells. *Transfusion*. **46**, 1199-1209.

Janowska-Wieczorek A, Wysoczynski M, Kijowski J, Marquez-Curtis L, Machalinski B, Ratajczak J, Ratajczak MZ. (2005) Microvesicles derived from activated platelets induce metastasis and angiogenesis in lung cancer. *Int J Cancer*. **113**, 752-760.

Jiang X, Bailly MA, Panetti TS, Cappello M, Konigsberg WH, Bromberg ME. (2004) Formation of the tissue factor-factor VIIa-factor Xa complex promotes cellular signalling and migration of human breast cancer cells. *J Thromb Haemost*. **2**, 93-101.

Joel PB, Smith J, Sturgill TW, Fisher TL, Blenis J, Lannigan DA. (1998) pp90^{src}1 regulates estrogen receptor-mediated transcription through phosphorylation of Ser-167. *Mol Cell Biol*. **18**, 1978-1984.

Johnson DG, Walker CL. (1999) Cyclins and cell cycle checkpoints. *Annu Rev Pharmacol Toxicol*. **39**, 295-312.

Johnston CL, Cox HC, Gomm JJ, Coombes RC. (1995) bFGF and aFGF induce membrane ruffling in breast cancer cells but not in normal breast epithelial cells: FGFR-4 involvement. *Biochem J*. **306**, 609-616.

Kamath L, Meydani A, Foss F, Kuliopulos A. (2001) Signaling from protease-activated receptor-1 inhibits migration and invasion of breast cancer cells. *Cancer Res*. **61**, 5933-5940.

Karin M, Liu Z, Zandi E. (1997) AP-1 function and regulation. *Curr Opin Cell Biol*. **9**, 240-246.

Kato S, Pinto M, Carvajal A, Espinoza N, Monso C, Sadarangani A, Villalon M, Brosens JJ, White JO, Richer JK, Horwitz KB, Owen GI. (2005) Progesterone increases tissue factor gene expression, procoagulant activity, and invasion in the breast cancer cell line ZR-75-1. *J Clin Endocrinol Metab*. **90**, 1181-1188.

Kato S, Endoh H, Masuhiro Y, Kitamoto T, Uchiyama S, Sasaki H, Masushige S, Gotoh Y, Nishida E, Kawashima H, Metzger D, Chambon P. (1995) Activation of the estrogen receptor through phosphorylation by mitogen-activated protein kinase. *Science*. **270**, 1491-1494.

Klein-Hitpass L, Ryffel GU, Heitlinger E, Cato AC. (1988) A 13 bp palindrome is a functional estrogen responsive element and interacts specifically with estrogen receptor. *Nucleic Acids Res*. **16**, 647-663.

Knowles M, Selby P. (2005) Introduction to the cellular and molecular biology of cancer. 4th edition. Oxford University Press, Oxford.

Koide A, Zhao C, Naganuma M, Abrams J, Deighton-Collins S, Skafar DF, Koide S. (2007) Identification of regions within the F domain of the human estrogen receptor alpha that are important for modulating transactivation and protein-protein interactions. *Mol Endocrinol*. **21**, 829-842.

Kong EH, Pike AC, Hubbard RE. (2003) Structure and mechanism of the oestrogen receptor. *Biochem Soc Trans*. **31**, 56-59.

Korach KS. (1994) Insights from the study of animals lacking functional estrogen receptor. *Science*. **266**, 1524-1547.

Krege JH, Hodgin JB, Couse JF, Enmark E, Warner M, Mahler JF, Sar M, Korach KS, Gustafsson JA, Smithies O. (1998) Generation and reproductive phenotypes of mice lacking estrogen receptor beta. *Proc Natl Acad Sci U S A*. **95**, 15677-15682.

Kronblad A, Hedenfalk I, Nilsson E, Pählman S, Landberg G. (2005) ERK1/2 inhibition increases antiestrogen treatment efficacy by interfering with hypoxia-induced downregulation of ERalpha: a combination therapy potentially targeting hypoxic and dormant tumor cells. *Oncogene*. **24**, 6835-6841.

Kurebayashi J, Otsuki T, Kunisue H, Tanaka K, Yamamoto S, Sorvoo H. (2000) Expression levels of estrogen receptor-alpha, estrogen receptor-beta, coactivators and corepressors in breast cancer. *Clin Cancer Res.* **6**, 512-518.

Laidlaw IJ, Clarke RB, Howell A, Owen AW, Potten CS, Anderson E. (1995) The proliferation of normal human breast tissue implanted into athymic nude mice is stimulated by estrogen but not progesterone. *Endocrinology.* **136**, 164-171.

Lannigan DA. (2003) Estrogen receptor phosphorylation. *Steroids.* **68**, 1-9.

Lapidus RG, Nass SJ, Davidson NE. (1998) The loss of estrogen and progesterone receptor gene expression in human breast cancer. *J Mammary Gland Biol Neoplasia.* **3**, 85-94.

Latchman DS. (1998) Eukaryotic transcription factors. 3rd edition. Academic Press, London.

Leygue E, Dotzlaw H, Watson PH, Murphy LC. (2000) Altered expression of estrogen receptor-alpha variant messenger RNAs between adjacent normal breast and breast tumor tissues. *Breast Cancer Res.* **2**, 64-72.

Liu Y, Mueller BM. (2006) Protease-activated receptor-2 regulates vascular endothelial growth factor expression in MDA-MB-231 cells via MAPK pathways. *Biochem Biophys Res Commun.* **344**, 1263-1270.

Liu Y, Ludes-Meyers J, Zhang Y, Munoz-Medellin D, Kim HT, Lu C, Ge G, Schiff R, Hilsenbeck SG, Osborne CK, Brown PH. (2002) Inhibition of AP-1 transcription factor causes blockade of multiple signal transduction pathways and inhibits breast cancer growth. *Oncogene.* **21**, 7680-7689.

Lu T, Achari Y, Sciore P, Hart DA. (2006) Estrogen receptor alpha regulates matrix metalloproteinase-13 promoter activity primarily through the AP-1 transcriptional regulatory site. *Biochim Biophys Acta.* **1762**, 719-731.

Ludes-Meyers JH, Liu Y, Muñoz-Medellin D, Hilsenbeck SG, Brown PH. (2001) AP-1 blockade inhibits the growth of normal and malignant breast cells. *Oncogene*. **20**, 2771-2780.

Luo BH, Carman CV, Springer TA. (2007) Structural basis of integrin regulation and signaling. *Annu Rev Immunol*. **25**, 619-647.

Lwaleed BA, Chisholm M, Francis JL. (1999) The significance of measuring monocyte tissue factor activity in patients with breast and colorectal cancer. *Br J Cancer*. **80**, 279-285.

Macdonald F, Ford CHJ, Casson AG. (2004) *Molecular Biology of Cancer*. 2nd edition. BIOS Scientific Publishers, London.

Mackman N, Sawdey MS, Keeton MR, Loskutoff DJ. (1993) Murine tissue factor gene expression in vivo. Tissue and cell specificity and regulation by lipopolysaccharide. *Am J Pathol*. **143**, 76-84.

Mackman N, Morrissey JH, Fowler B, Edgington TS. (1989) Complete sequence of the human tissue factor gene, a highly regulated cellular receptor that initiates the coagulation protease cascade. *Biochemistry*. **28**, 1755-1762.

Manithody C, Yang L, Rezaie AR. (2007) Identification of a basic region on tissue factor that interacts with the first epidermal growth factor-like domain of factor X. *Biochemistry*. **46**, 3193-3199.

Marshall WJ. (1995) *Clinical chemistry*. 3rd edition. Mosby, London.

Masuda M, Nakamura S, Murakami T, Komiyama Y, Takahashi H. (1996) Association of tissue factor with a gamma chain homodimer of the IgE receptor type I in cultured human monocytes. *Eur J Immunol*. **26**, 2529-2532.

Morel O, Toti F, Hugel B, Freyssinet JM. (2004) Cellular microparticles: a disseminated storage pool of bioactive vascular effectors. *Curr Opin Hematol.* **11**, 156-164.

Morris DR, Ding Y, Ricks TK, Gullapalli A, Wolfe BL, Trejo J. (2006) Protease-activated receptor-2 is essential for factor VIIa and Xa-induced signaling, migration, and invasion of breast cancer cells. *Cancer Res.* **66**, 307-314.

Morrissey JH, Fakhrai H, Edgington TS. (1987) Molecular cloning of the cDNA for tissue factor, the cellular receptor for the initiation of the coagulation protease cascade. *Cell.* **50**, 129-135.

Mosselman S, Polman J, Dijkema R. (1996) ER beta: identification and characterization of a novel human estrogen receptor. *FEBS Lett.* **392**, 49-53.

Mueller BM, Ruf W. (1998) Requirement for binding of catalytically active factor VIIa in tissue factor-dependent experimental metastasis. *J Clin Invest.* **101**, 1372-1378.

Mueller MD, Vigne JL, Minchenko A, Lebovic DI, Leitman DC, Taylor RN. (2000) Regulation of vascular endothelial growth factor (VEGF) gene transcription by estrogen receptors alpha and beta. *Proc Natl Acad Sci U S A.* **97**, 10972-10977.

Müller M, Albrecht S, Gölfert F, Hofer A, Funk RH, Magdolen V, Flössel C, Luther T. (1999) Localization of tissue factor in actin-filament-rich membrane areas of epithelial cells. *Exp Cell Res.* **248**, 136-147.

Murphy L, Cherlet T, Adeyinka A, Niu Y, Snell L, Watson P. (2004) Phospho-serine-118 estrogen receptor-alpha detection in human breast tumors in vivo. *Clin Cancer Res.* **10**, 1354-1359.

Ngo CV, Picha K, McCabe F, Millar H, Tawadros R, Tam SH, Nakada MT, Anderson GM. (2007) CNTO 859, a humanized anti-tissue factor monoclonal

antibody, is a potent inhibitor of breast cancer metastasis and tumor growth in xenograft models. *Int J Cancer*. **120**, 1261-1267.

Nilsson UW, Garvin S, Dabrosin C. (2007) MMP-2 and MMP-9 activity is regulated by estradiol and tamoxifen in cultured human breast cancer cells. *Breast Cancer Res Treat*. **102**, 253-261.

Oh AS, Lorant LA, Holloway JN, Miller DL, Kern FG, El-Ashry D. (2001) Hyperactivation of MAPK induces loss of ERalpha expression in breast cancer cells. *Mol Endocrinol*. **15**, 1344-1359.

Ollivier V, Bentolila S, Chabbat J, Hakim J, de Prost D. (1998) Tissue factor-dependent vascular endothelial growth factor production by human fibroblasts in response to activated factor VII. *Blood*. **91**, 2698-2703.

Ott I, Fischer EG, Miyagi Y, Mueller BM, Ruf W. (1998) A role for tissue factor in cell adhesion and migration mediated by interaction with actin-binding protein 280. *J Cell Biol*. **140**, 1241-1253.

Paborsky LR, Caras IW, Fisher KL, Gorman CM. (1991) Lipid association, but not the transmembrane domain, is required for tissue factor activity. Substitution of the transmembrane domain with a phosphatidylinositol anchor. *J Biol Chem*. **266**, 21911-21916.

Paborsky LR, Tate KM, Harris RJ, Yansura DG, Band L, McCray G, Gorman CM, O'Brien DP, Chang JY, Swartz JR. (1989) Purification of recombinant human tissue factor. *Biochemistry*. **28**, 8072-8077.

Pearson WR, Wood T, Zhang Z, Miller W. (1997) Comparison of DNA sequences with protein sequences. *Genomics*. **46**, 24-36.

Pendurthi UR, Alok D, Rao LV. (1997) Binding of factor VIIa to tissue factor induces alterations in gene expression in human fibroblast cells: up-regulation of poly(A) polymerase. *Proc Natl Acad Sci U S A*. **94**, 12598-12603.

Petz LN, Nardulli AM. (2000) Sp1 binding sites and an estrogen response element half-site are involved in regulation of the human progesterone receptor A promoter. *Mol Endocrinol.* **14**, 972-985.

Philips A, Chalbos D, Rochefort H. (1993) Estradiol increases and anti-estrogens antagonize the growth factor-induced activator protein-1 activity in MCF7 breast cancer cells without affecting c-fos and c-jun synthesis. *J Biol Chem.* **268**, 14103-14108.

Platet N, Cathiard AM, Gleizes M, Garcia M. (2004) Estrogens and their receptors in breast cancer progression: a dual role in cancer proliferation and invasion. *Crit Rev Oncol Hematol.* **51**, 55-67.

Platet N, Cunat S, Chalbos D, Rochefort H, Garcia M. (2000) Unliganded and liganded estrogen receptors protect against cancer invasion via different mechanisms. *Mol Endocrinol.* **14**, 999-1009.

Ponglikitmongkol M, Green S, Chambon P. (1988) Genomic organization of the human oestrogen receptor gene. *EMBO J.* **7**, 3385-3388.

Porter W, Saville B, Hoivik D, Safe S. (1997) Functional synergy between the transcription factor Sp1 and the estrogen receptor. *Mol Endocrinol.* **11**, 1569-1580.

Poulsen LK, Jacobsen N, Sorensen BB, Bergenhem NC, Kelly JD, Foster DC, Thastrup O, Ezban M, Petersen LC. (1998) Signal transduction via the mitogen-activated protein kinase pathway induced by binding of coagulation factor VIIa to tissue factor. *J Biol Chem.* **273**, 6228-6232.

Pradier A, Ettelaie C. (2007) The influence of exogenous tissue factor on the regulators of proliferation and apoptosis in endothelial cells. *J Vasc Res.* **45**, 19-32.

Prall OW, Rogan EM, Sutherland RL. (1998) Estrogen regulation of cell cycle progression in breast cancer cells. *J Steroid Biochem Mol Biol.* **65**, 169-174.

Price JE. (1990) The biology of metastatic breast cancer. *Cancer*. **66**, 1313-1320.

Rauch U, Bonderman D, Bohrmann B, Badimon JJ, Himber J, Riederer MA, Nemerson Y. (2000) Transfer of tissue factor from leukocytes to platelets is mediated by CD15 and tissue factor. *Blood*. **96**, 170-175.

Reid G, Hübner MR, Métivier R, Brand H, Denger S, Manu D, Beaudouin J, Ellenberg J, Gannon F. (2003) Cyclic, proteasome-mediated turnover of unliganded and liganded ERalpha on responsive promoters is an integral feature of estrogen signaling. *Mol Cell*. **11**, 695-707.

Rickles FR, Falanga A. (2001) Molecular basis for the relationship between thrombosis and cancer. *Thromb Res*. **102**, 215-224.

Riewald M, Kravchenko VV, Petrovan RJ, O'Brien PJ, Brass LF, Ulevitch RJ, Ruf W. (2001) Gene induction by coagulation factor Xa is mediated by activation of protease-activated receptor 1. *Blood*. **97**, 3109-3116.

Riewald M, Ruf W. (2001) Mechanistic coupling of protease signaling and initiation of coagulation by tissue factor. *Proc Natl Acad Sci U S A*. **98**, 7742-7747.

Rochefort H, Chalbos D, Cunat S, Lucas A, Platet N, Garcia M. (2001) Estrogen regulated proteases and antiproteases in ovarian and breast cancer cells. *J Steroid Biochem Mol Biol*. **76**, 119-124.

Rochefort H, Platet N, Hayashido Y, Derocq D, Lucas A, Cunat S, Garcia M. (1998) Estrogen receptor mediated inhibition of cancer cell invasion and motility: an overview. *J Steroid Biochem Mol Biol*. **65**, 163-168.

Rogatsky I, Trowbridge JM, Garabedian MJ. (1999) Potentiation of human estrogen receptor alpha transcriptional activation through phosphorylation of serines 104 and 106 by the cyclin A-CDK2 complex. *J Biol Chem*. **274**, 22296-22302.

Rottingen JA, Enden T, Camerer E, Iversen JG, Prydz H. (1995) Binding of human factor VIIa to tissue factor induces cytosolic Ca²⁺ signals in J82 cells, transfected COS-1 cells, Madin-Darby canine kidney cells and in human endothelial cells induced to synthesize tissue factor. *J Biol Chem.* **270**, 4650-4660.

Roy S, Paborsky LR, Vehar GA. (1991) Self-association of tissue factor as revealed by chemical crosslinking. *J Biol Chem.* **266**, 4665-4668.

Ruedl C, Cappelletti V, Coradini D, Granata G, Di Fronzo G. (1990) Influence of culture conditions on the estrogenic cell growth stimulation of human breast cancer cells. *J Steroid Biochem Mol Biol.* **37**, 195-200.

Ruf W, Dorfleutner A, Riewald M. (2003) Specificity of coagulation factor signaling. *J Thromb Haemost.* **1**, 1495-1503.

Ruf W, Edgington TS. (1994) Structural biology of tissue factor, the initiator of thrombogenesis in vivo. *FASEB J.* **8**, 385-390.

Santini D, Ceccarelli C, Taffurelli M, Pileri S, Marrano D. (1996) Differentiation pathways in primary invasive breast carcinoma as suggested by intermediate filament and biopathological marker expression. *J Pathol.* **179**, 386-391.

Sarwar N, Kim JS, Jiang J, Peston D, Sinnott HD, Madden P, Gee JM, Nicholson RI, Lykkesfeldt AE, Shousha S, Coombes RC, Ali S. (2006) Phosphorylation of ERalpha at serine 118 in primary breast cancer and in tamoxifen-resistant tumours is indicative of a complex role for ERalpha phosphorylation in breast cancer progression. *Endocr Relat Cancer.* **13**, 851-861.

Sato Y, Asada Y, Marutsuka K, Hatakeyama K, Sumiyoshi A. (1996) Tissue factor induces migration of cultured aortic smooth muscle cells. *Thromb Haemost.* **75**, 389-392.

Schechter AD, Spirn B, Rossikhina M, Giesen PL, Bogdanov V, Fallon JT, Fisher EA, Schnapp LM, Nemerson Y, Taubman MB. (2000) Release of active tissue factor by human arterial smooth muscle cells. *Circ Res.* **87**, 126-132.

Schiemann S, Schwirzke M, Br nner N, Weidle UH. (1998) Molecular analysis of two mammary carcinoma cell lines at the transcriptional level as a model system for progression of breast cancer. *Clin Exp Metastasis.* **16**, 129-139.

Scholz T, Temmler U, Krause S, Heptinstall S, L sche W. (2002) Transfer of tissue factor from platelets to monocytes: role of platelet-derived microvesicles and CD62P. *Thromb Haemost.* **88**, 1033-1038.

Schwartz MA. (2001) Integrin signaling revisited. *Trends Cell Biol.* **11**, 466-470.

Shi X, Gangadharan B, Brass LF, Ruf W, Mueller BM. (2004) Protease-activated receptors (PAR1 and PAR2) contribute to tumor cell motility and metastasis. *Mol Cancer Res.* **2**, 395-402.

Siegbahn A, Johnell M, Sorensen BB, Petersen LC, Heldin CH. (2005) Regulation of chemotaxis by the cytoplasmic domain of tissue factor. *Thromb Haemost.* **93**, 27-34.

Smith LM, Wise SC, Hendricks DT, Sabichi AL, Bos T, Reddy P, Brown PH, Birrer MJ. (1999) cJun overexpression in MCF-7 breast cancer cells produces a tumorigenic, invasive and hormone resistant phenotype. *Oncogene.* **18**, 6063-6070.

Smith DF, Toft DO. (1993) Steroid receptors and their associated proteins. *Mol Endocrinol.* **7**, 4-11.

S rensen BB, Freskg rd PO, Nielsen LS, Rao LV, Ezban M, Petersen LC. (1999) Factor VIIa-induced p44/42 mitogen-activated protein kinase activation requires the proteolytic activity of factor VIIa and is independent of the tissue factor cytoplasmic domain. *J Biol Chem.* **274**, 21349-21354.

Spicer EK, Horton R, Bloem L, Bach R, Williams KR, Guha A, Kraus J, Lin TC, Nemerson Y, Konigsberg WH. (1987) Isolation of cDNA clones coding for human tissue factor: primary structure of the protein and cDNA. *Proc Natl Acad Sci U S A*. **84**, 5148-5152.

Szotowski B, Antoniak S, Poller W, Schultheiss HP, Rauch U. (2005) Procoagulant soluble tissue factor is released from endothelial cells in response to inflammatory cytokines. *Circ Res*. **96**, 1233-1239.

Tang Z, Treilleux I, Brown M. (1997) A transcriptional enhancer required for the differential expression of the human estrogen receptor in breast cancers. *Mol Cell Biol*. **17**, 1274-1280.

Taubman MB, Fallon JT, Schechter AD, Giesen P, Mendlowitz M, Fyfe BS, Marmur JD, Nemerson Y. (1997) Tissue factor in the pathogenesis of atherosclerosis. *Thromb Haemost*. **78**, 200-204.

Taylor AH, Al-Azzawi F. (2000) Immunolocalisation of oestrogen receptor beta in human tissues. *J Mol Endocrinol*. **24**, 45-455.

Tesselaar ME, Romijn FP, Van Der Linden IK, Prins FA, Bertina RM, Osanto S. (2007) Microparticle-associated tissue factor activity: a link between cancer and thrombosis? *J Thromb Haemost*. **5**, 520-527.

Teyssier C, Belguise K, Galtier F, Chalbos D. (2001) Characterization of the physical interaction between estrogen receptor alpha and JUN proteins. *J Biol Chem*. **276**, 36361-36369.

Thompson EW, Paik S, Brünner N, Sommers CL, Zugmaier G, Clarke R, Shima TB, Torri J, Donahue S, Lippman ME. (1992) Association of increased basement membrane invasiveness with absence of estrogen receptor and expression of vimentin in human breast cancer cell lines. *J Cell Physiol*. **150**, 534-544.

Ueno T, Toi M, Koike M, Nakamura S, Tominaga T. (2000) Tissue factor expression in breast cancer tissues: its correlation with prognosis and plasma concentration. *Br J Cancer*. **83**, 164-170.

Umayahara Y, Kawamori R, Watada H, Imano E, Iwama N, Morishima T, Yamasaki Y, Kajimoto Y, Kamada T. (1994) Estrogen regulation of the insulin-like growth factor I gene transcription involves an AP-1 enhancer. *J Biol Chem*. **269**, 16433-16442.

Valley CC, Metivier R, Solodin NM, Fowler AM, Mashek MT, Hill L, Alarid ET. (2005) Differential regulation of estrogen-inducible proteolysis and transcription by the estrogen receptor alpha N terminus. *Mol Cell Biol*. **25**, 5417-5428.

Versteeg HH, Schaffner F, Kerver M, Petersen HH, Ahamed J, Felding-Habermann B, Takada Y, Mueller BM, Ruf W. (2008) Inhibition of tissue factor signaling suppresses tumor growth. *Blood*. **111**, 190-199.

Versteeg HH, Hoedemaeker I, Diks SH, Stam JC, Spaargaren M, van Bergen En Henegouwen PM, van Deventer SJ, Peppelenbosch MP. (2000) Factor VIIa/tissue factor-induced signaling via activation of Src-like kinases, phosphatidylinositol 3-kinase, and Rac. *J Biol Chem*. **275**, 28750-28756.

Vrana JA, Stang MT, Grande JP, Getz MJ. (1996) Expression of tissue factor in tumor stroma correlates with progression to invasive human breast cancer: paracrine regulation by carcinoma cell-derived members of the transforming growth factor beta family. *Cancer Res*. **56**, 5063-5070.

Wang X, Gjernes E, Prydz H. (2002) Factor VIIa induces tissue factor-dependent up-regulation of interleukin-8 in a human keratinocyte line. *J Biol Chem*. **277**, 23620-23626.

Watanabe T, Yasuda M, Yamamoto T. (1999) Angiogenesis induced by tissue factor in vitro and in vivo. *Thromb Res*. **96**, 183-189.

Weisz A, Rosales R. (1990) Identification of an estrogen response element upstream of the human c-fos gene that binds the estrogen receptor and the AP-1 transcription factor. *Nucleic Acids Res.* **18**, 5097-5106.

Woodside DG, Liu S, Ginsberg MH. (2001) Integrin activation. *Thromb Haemost.* **86**, 316-323.

Xiong JP, Stehle T, Diefenbach B, Zhang R, Dunker R, Scott DL, Joachimiak A, Goodman SL, Arnaout MA. (2001) Crystal structure of the extracellular segment of integrin alpha Vbeta3. *Science.* **294**, 339-345.

Yamaguchi H, Wyckoff J, Condeelis J. (2005) Cell migration in tumors. *Curr Opin Cell Biol.* **17**, 559-564.

Yin YJ, Salah Z, Grisar-Granovsky S, Cohen I, Even-Ram SC, Maoz M, Uziely B, Peretz T, Bar-Shavit R. (2003) Human protease-activated receptor 1 expression in malignant epithelia: a role in invasiveness. *Arterioscler Thromb Vasc Biol.* **23**, 940-944.

Yoshioka K, Deng T, Cavigelli M, Karin M. (1995) Antitumor promotion by phenolic antioxidants: inhibition of AP-1 activity through induction of Fra expression. *Proc Natl Acad Sci U S A.* **92**, 4972-4976.

Yu JL, Rak JW. (2004) Shedding of tissue factor (TF)-containing microparticles rather than alternatively spliced TF is the main source of TF activity released from human cancer cells. *J Thromb Haemost.* **2**, 2065-2067.

Zhang Z, Maier B, Santen RJ, Song RX. (2002) Membrane association of estrogen receptor alpha mediates estrogen effect on MAPK activation. *Biochem Biophys Res Commun.* **294**, 926-933.

Zhong D, Bajaj MS, Schmidt AE, Bajaj SP. (2002) The N-terminal epidermal growth factor-like domain in factor IX and factor X represents an important recognition motif for binding to tissue factor. *J Biol Chem.* **277**, 3622-3631.

Zioncheck TF, Roy S, Vehar GA. (1992) The cytoplasmic domain of tissue factor is phosphorylated by a protein kinase C-dependent mechanism. *J Biol Chem.* **267**, 3561-3564.

Zwicker JJ, Furie BC, Furie B. (2007) Cancer-associated thrombosis. *Crit Rev Oncol Hematol.* **62**, 126-136.